Characteristics and biological considerations of newly developed bioactive NanoFA-based dental composite.

Widad Al-Omairi

Supervisors

Dr Andreas Werner and Dr Matthew German

September 2022

Abstract

Amalgam use will be phased out in restorative dentistry. The introduction of the Minamata convention offers the perspective of dental composite becoming the main direct restorative material. The currently available tooth-coloured restorative materials are satisfactory with regards to mechanical and optical properties. Moreover, significant innovation has improved the clinical performance of the material, reduced the polymerization shrinkage and enabled conservation of the tooth structure.

Most of the available composite materials contain Bis-GMA, which is toxic due to Bisphenol A content. Additionally, they lack bioactive properties. Bioactive composites are materials with bacteriostatic and remineralising potential due to fluoride release. Alternative, Bis-GMA free composite materials that release fluoride are expected to significantly decrease restoration failure caused by secondary caries. Newly developed materials need to be thoroughly tested for cytocompatibility. In addtion, the effect of adding bioactive compounds on the mechanical properties should be investigated.

In this project prototypes of novel restorative materials were developed, and their mechanical properties were tested. These were based on UDMA (urethane dimethacrylate) and HEMA (2-hydroxyethyl methacrylate) and silica glass fillers ($SiO_{2)}$. The remineralizing properties were provided by adding nanofluorapatite ($NanoF_A$) nanoparticles as secondary fillers. The degree of polymerization was measured by infra-red spectroscopy (FTIR). The amount of residual monomer after polymerization was quantified by HPLC. The mechanical properties were examined by three-point bending test. Fluoride release was measured using an ion selective electrode. The effect of storage in distilled water, artificial saliva and acidified artificial saliva on composite specimen was monitored and examined under a scanning electron microscope (SEM). The toxicity was assessed by different parameters. The toxicity of individual dental resin monomers to oral gingival fibroblasts (HGF) was assessed by XTT viability assay and RT-qPCR. Finally, the effect of the final material on gingival fibroblasts was characterized by RNA Seq transcriptome analysis.

The novel NanoFA filled material achieved a mean degree of conversion of 84.61%. Additionally, the fluoride release of the novel material was significant compared to the NanoFA-free control. The material's mechanical properties were compromised by storage in

aqueous environment. Dental resin monomer toxicity was revealed by a significant reduction ($P<0.05$) in the cell viability at 2 mM of HEMA, while for UDMA a reduction in viability to 60% was found at 1 mM ($P<0.05$). RT-qPCR expression analysis of DNA repair genes showed a dose-dependent expression increase in HGF treated with HEMA. A statistically significant expression change ($P<0.001$) of four genes (*DDX11*, *IPPK*, *XRCC2* and *RAD50*) was noted with 10 mM and 40 mM of HEMA. In contrast, UDMA increased the expression of stress response genes (*Cox-2*, *CES2* and *HO-1*) at 4 mM ($P<0.001$). The amount of residual resin monomers quantified by HPLC were below the toxic concentrations. However, RNA Seq analysis revealed signs of toxicity to oral gingival fibroblasts after 24 hours exposure to dental composite materials as manifested by an increased expression of cellular signalling pathways such as oxidoreductase activity, NADPH activity and ferroptosis.

To conclude, novel dental composite materials were successfully designed. The new materials have promising performance with regards to high degree of conversion and fluoride release, though mechanical properties need to be improved. The release of residual monomers from the polymerized materials were below the detected toxic concentrations. Nevertheless, further research may improve the material formula with the aim of reducing chemical toxicity to oral gingival fibroblasts.

Dedication

This work is dedicated to my beloved father General Habeeb Al-Omairi for your braveness, service, devotion, and true love for your country.

Acknowledgement

I would like to express my genuine gratitude to my supervisors Dr A. Werner and Dr Matt German for their unlimited support, encouragement, and guidance. This work would not have been achieved without their consistent help, time, and advice. In addition, I am highly appreciative of their support and kindness during the difficult times of the pandemic. I will always be grateful to be blessed by the opportunity they have provided me to study for a research degree in a subject area that I am truly enthusiastic about.

I would like to express my gratefulness to my sponsors, the Iraqi ministry of higher education and scientific research, the Iraqi cultural attaché in London and Waset University/School of dental sciences. More specifically, for funding, guidance and facilitating different phases of my studies.

I would like to thank my PhD panel members Dr Alison Howard and Dr Ruth Valentine for their time, guidance, and advice during my research project. I appreciate their valuable opinions, fruitful discussions they provided, and time they spent to correct my progression reports.

I would like to thank Prof Caroline Austin and Dr Ian Cowell for their significant help during the early stage of my research project. I hold true appreciation and admiration for both of them for providing me with valuable advice. Additionally, and more specifically, for providing me with the opportunity to train in their lab to perform the immunocytochemistry assays during the first year of my PhD and for the generous support.

I would like to express my gratefulness to the members of the Biosciences institute/School of medical sciences. Starting with Dr Tim Cheek for all his support during my studies. Ms Louise Campbell for facilitating all the paperwork for students. Ms Helen Glenwright, the technical manager for the tissue culture lab, for her kindness and help during my research time. I would like to thank the Bioimaging unit staff members and Bioinformatic unit staff members. Finally, I am grateful to Mr Kyle Stanforth and Dr Peter Chater for their help with the HLPC experiments. I am truly grateful to Dr Kim Pearce to for all her support with statistical analysis.

I would like to thank Dr German's research group, starting with the technical lab manger, Mr Anthony Townshend, for all the help provided during my research time. Moreover, I would like to thank my colleagues and friends Dr Bryan Murchie, Dr Saleh Al-Qahtani, Dr Farah Elfakhri, Aziz Algadhi and Benjarat Kornphot.

I would like to thank the dental school coordinator Ms Magdalena Grainger and all members for organising the school postgraduate research events and keynote lectures. I would like to thank Ms Helen Lewis, the English language teacher, the students services team members of Newcastle University and many other staff members.

Finally, my endless gratitude goes to the most important people in my life. My wonderful parents for their support, patience, care, and unconditional love. For being a source of inspiration to me and my brothers and sister. For their countless sacrifices to raise a wonderful family of three dentists, pharmacist, and a doctor. My beloved, dear and wonderful mother for being the light that brightens my life through the dark and difficult times.

Contents

List of abbreviations

ATR:	Attenuated total reflection
Bis-EMA:	2,2-bis(4-(2-Methacryloxyethoxy) phenylpropane
Bis-GMA:	Bis-phenol –A-glycidyl dimethacrylate
BSA:	Bovine serum albumin
CQ:	Camphorquinone
DC:	Degree of Conversion
DNA:	Deoxyribonucleic acid
EDAB:	4-ethyl dimethyl aminobenzoate
FTIR:	Fourier-transform infrared spectroscopy
GICs:	Glass ionomer cements
HEMA:	2-hydroxyethyl methacrylate
HPLC:	High performance liquid chromatography
KCL:	Potassium Chloride
LED:	Light-emitting diode
MMA:	Methylmethacrylate
NaCl:	Sodium chloride
PBS:	Phosphate buffered saline
PMMA:	Polymethylmethacrylate
QTH:	Quartz-tungsten-halogen
RBCs:	Resin-based composites
RMGIC:	Resin-modified glass ionomer cements
ROS:	Reactive oxygen species
RT-qPCR:	Quantitative reverse transcriptase polymerase chain reaction
TEGDMA:	Tri-ethylene glycol dimethacrylate
UDMA:	Urethane dimethacrylate
UV:	Ultraviolet
XTT:	2, 3-bis (2-methoxy-4-nitro-5-sulfophenyl)-2H-tetrazolium-5-carboxanilide
γ-MPTS:	$_{\gamma}$-methacryloxypropyltriethoxysilane

Chapter 1: Introduction

1.1 History of restorative materials in dentistry

The history of restorative materials in dentistry dates back to the fourth millennium (BC) where gold was first used as a restorative option by the Babylonians, Assyrians and Egyptians 4000-4500 BC [1]. Bone, ivory, mastic and waxes were used to restore teeth cavities during ancient times; in addition, gold crowns had been applied as restorations by the Etruscans and Phoenicians 2700 BC [2]. Advancements and innovations continued, countless attempts to use direct restorative materials that are comfortable to patients were made. In the 18th century initial basic material formulation for amalgam restorative materials were used in attempts to treat teeth in an easy and low-cost manner. In 1826 amalgam was used as restorative material for the first time, based on a mixture of five-franc shavings with mercury by August Taveau in Paris [3]. This material had poor properties and was considered to be of inferior standard, hence, when it was introduced to the United States in 1833 a controversy regarding its use unfolded between advocates and opponents, known as the ''amalgam war'' [4]. An organised movement known as the ''new departure'' supporting the use of amalgam started in the late 1870 [5]. This lead to amalgam being the main direct restorative material used in the late 1880s [6]. Eventually, the use of amalgam was established with the introduction of a more balanced formula of amalgam to the profession by Greene Vardiman Black, the so-called father of dentistry in the 1895 [7]. The material and its derivatives were the main class of materials used to directly restore teeth until the 1960s when dental composite formulas were introduced and related materials are still being used in dentistry today [8].

The first semi-aesthetic restorative materials were developed around 1908, silicate cement was used in an attempt to create a restorative material that matches tooth colour [9]. These materials were mainly used to treat anterior teeth and had the advantage of fluoride release. However, they stain rapidly, cause irritation to the pulp tissue and dissolve in the oral environment [10]. An improved resin-based formula was first used in dentistry in 1936. These findings inspired the development of new restorative materials, for example, the use of polymethylmethacrylate (PMMA) in fabricating denture bases [11]. The material consisted of polymethylmethacrylate powder with pigments and chemical initiator in addition to liquid methacrylate monomers and activator. The resin-based material had good restorative properties such as the ability to be tinted, shaped and moulded easily and cured by chemical

reaction [12]. Dr Michael Buonocore made a major discovery in 1955 that revolutionised the field of restorative aesthetic dentistry and resin bonding [13]. His discovery, based on the application of a phosphoric acid solution to the enamel surface of the teeth, enabled mechanical bonding of polymeric materials to the teeth. Finally, resin-based composites were developed and the use of dental composites expanded after the synthesis of Bis-GMA monomer in 1956 by Dr. Rafael Bowen [14]. Bis-GMA synthesis and bonding of composite material to the tooth structure were a significant breakthrough in dentistry [15].

1.2 Resin-based composite materials

The term composite in general refers to a material containing two or more different constituents, insoluble in each other, constituting a material with better characteristics than the individual components alone [16]. In dentistry, dental composites are widely used to restore cavities in primary and permanent dentition and consist of organic resin monomers, inorganic filler particles, silane coupling agents and an initiator-coinitiator system [17]. Organic resins add the advantage that they can be moulded at ambient temperature and set by polymerization. While the reinforcing fillers contribute to good mechanical properties such as strength, hardness and reduced setting contraction or polymerization shrinkage [18]. The use of composite restorations exceeded amalgam in several countries with roughly 800 million restorations performed worldwide in 2015, 80% of which are posterior restorations [19] [20] [21]. The increased popularity of composites as direct restorative materials is due to their aesthetic properties and the improved adhesives that can be used with them, that allows for conservation during tooth preparation when compared to amalgam materials [22].

Currently available materials have been improved significantly compared to earlier types of composites due to optimisation of filler content and size. Nano particles in the nanometre range (0.1-100nm) can be incorporated to enhance mechanical and optical properties of dental composites [23]. Enhanced aesthetics and mechanical properties are seen with the newer materials with smaller filler size compared to traditionally available tooth-coloured materials such as silicate and acrylic materials [24]. The benefits include strength, rigidity, low dimensional changes during setting, low coefficient of thermal expansion and less

susceptibility to wear in areas of masticatory forces and these have significantly contributed to their popularity in dentistry [25].

1.3 The composition of dental composite

1.3.1 Resin phase

Methylmethacrylate or MMA is considered a major component in polymeric-based acrylic resin industry. The monomer is also known as methacrylic acid methyl ester [26]. The monomer is used for polymethylmethacrylate or PMMA polymer synthesis (figure 1). PMMA was the successful polymer used for denture bases, artificial teeth and temporary crowns [27]. In addition, PMMA or acrylic resin was also used as restorative filling material [28]. However, the mono-methacrylate resin had the tendency to generate linear polymer chains with poor characteristics with respect to rigidity and degradation [29]. At present, dimethacrylate monomers are extensively employed in dental composite synthesis due to their ability to create crossed linked polymers as compared to linear polymers with MMA [30]. Polymers produced from methyl methacrylate by addition reaction were associated with higher polymerization shrinkage, high coefficient of thermal expansion and damage to dental tissues. On the other hand, difunctional methacrylate has a larger molecular structure, less volatility, lower polymerization shrinkage, and the ability to form stiffer crossed linked polymers [29].

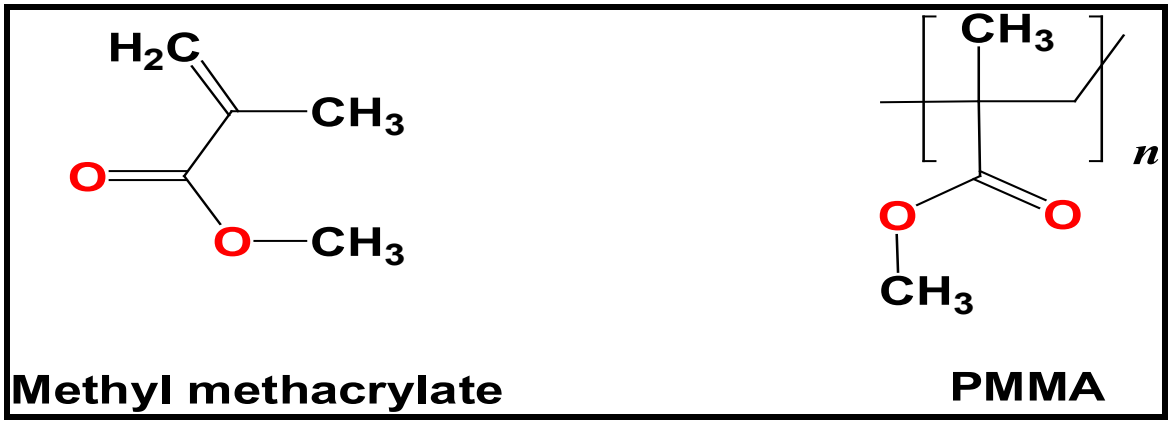

Figure 1: Chemical structure of methylmethacrylate and polymethylmethacrylate, drawn with Chemdraw.

The characteristics of a dental composite depends on the structure of monomers used to make the final polymer network [31]. The resin phase of dental composite consists commonly of a blend of dimethacrylate compounds. Most commonly used is the monomer Bis-GMA (bis-phenol –A-glycidyl dimethacrylate), a derivative of bisphenol A diglycidyl ether

and methacrylic acid that contains two functional methacrylate groups [32]. The monomer is commonly used in dental composites, fissure sealants, and cement [33]. It has a high molecular weight and limited flexibility upon polymerization due to its molecular structure with an aromatic core and hydroxyl groups, as shown in figure 2. The use of Bis-GMA offers the advantage of improved mechanical properties, i.e. reduced polymerization shrinkage compared to methyl methacrylate resin [34]. The higher viscosity of Bis-GMA compared to other dimethacrylate monomers is considered a disadvantage that precludes higher filler loading in the polymer network of the final material [35]. Due to the higher molecular structure, Bis-GMA is a bulky monomer, less volatile and offers rapid hardening [29]. Therefore, its viscosity should be reduced by mixing it with other dimethacrylate monomers such as TEGDMA to obtain suitable viscosity for filler loading [36].

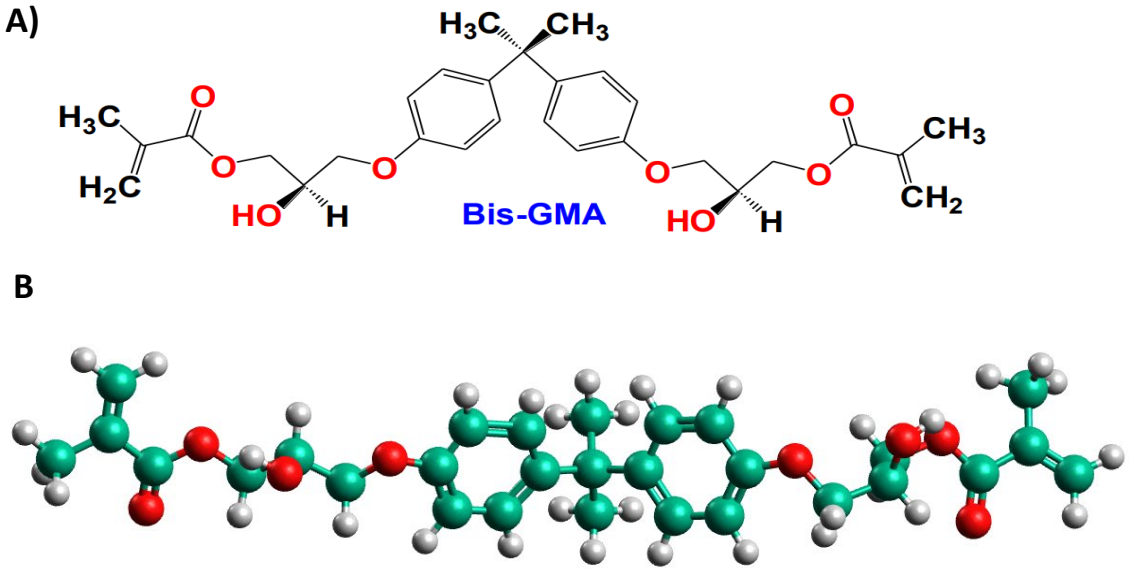

Figure 2: Chemical Structure of Bis-GMA (Bisphenol A-glycidyl methacrylate), a dimethacrylate monomer most commonly used in dental resin composites. A) 2D structure drawn with Chemdraw. B) 3D Structure drawn with Avogadro, free available software (https://sourceforge.net/projects/avogadro).

Urethane dimethacrylate (UDMA) contains peripheral carbon-carbon double bonds, as shown in figure 3, that contribute to the polymerization reaction by free radical formation. When compared to Bis-GMA, UDMA has lower viscosity and higher flexibility that can improve the mechanical properties of the dental composite [37]. The monomer has a flexible aliphatic core and the dual urethane linkage facilitates hydrogen bonding and therefore higher reactivity and double bond concentration [38]. Therefore, UDMA-based composites are better candidates to substitute Bis-GMA, as UDMA allows more filler to be added to the polymer network [39].

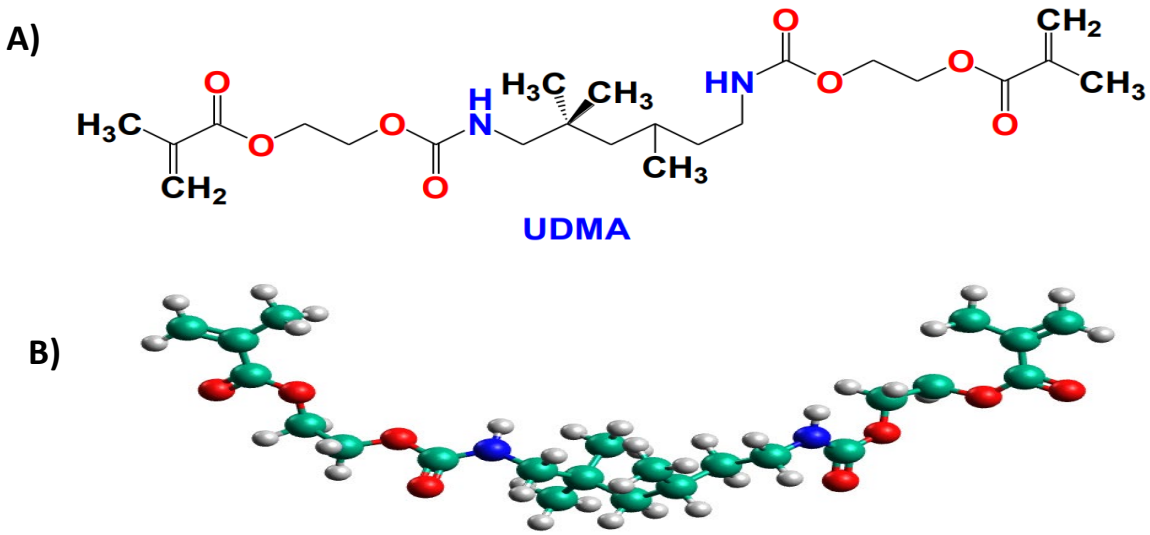

Figure 3: Chemical Structure of UDMA (Urethane methacrylate), a dimethacrylate monomer. A) 2D structure drawn with Chemdraw. B) 3D Structure drawn with Avogadro.

Other dimethacrylate monomers such as tri-ethylene glycol dimethacrylate (TEGDMA) are used as a diluent co-monomer with Bis-GMA blends to control the high viscosity of Bis-GMA, improve polymer handling properties and increase filler loading [40]. TEGDMA contains ethylene oxide groups (C_2H_4O) at the end of the monomer chain, as shown in figure 4. The presence of ethylene groups enhances monomer reactivity. However, this enhances its hydrophilicity and compromises mechanical properties due to increased water uptake and polymerization stress [41]. Bis-EMA, figure 5, is another monomer that is extensively used in resin-based composite materials as a diluent monomer. It has a structure that is similar to Bis-GMA, with two aromatic groups but without hydroxyl groups. Therefore, it can improve viscosity, flexibility, polymerization and results in an increased degree of conversion [42].

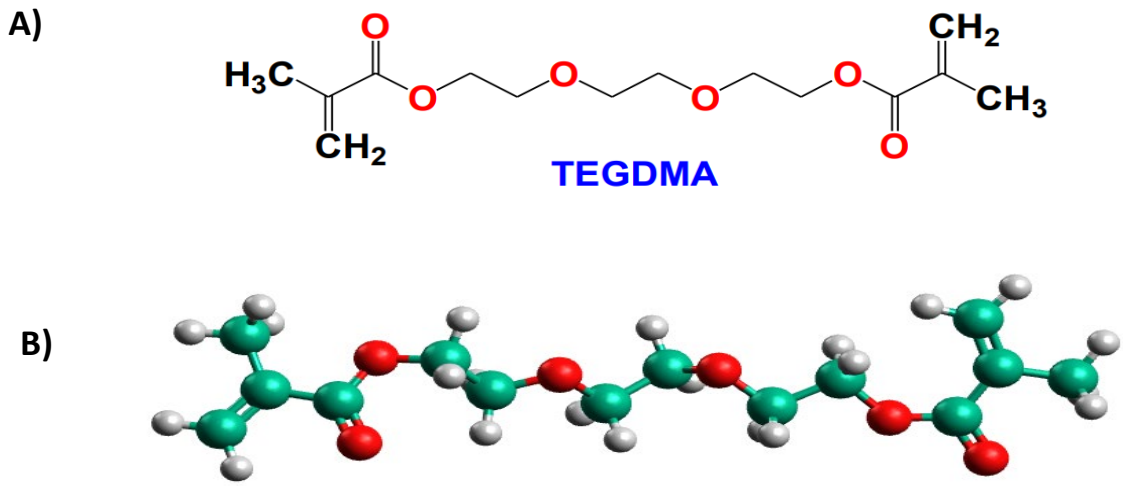

Figure 4: Molecular Structure of TEGDMA (Tri-ethylene glycol dimethacrylate). A) 2D structure drawn with Chemdraw. B) 3D Structure drawn with Avogadro.

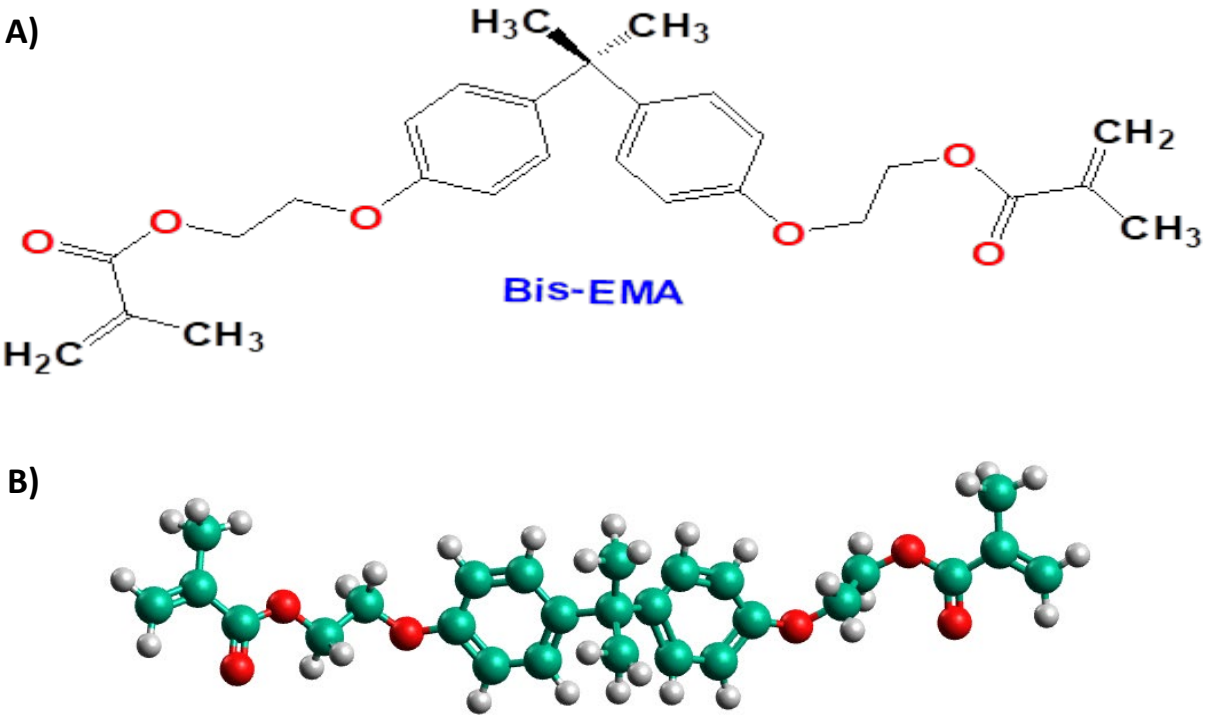

Figure 5: Molecular Structure of Bis-EMA (2,2-bis(4-(2-Methacryloxyethoxy) phenylpropane). A) 2D structure drawn with Chemdraw. B) 3D Structure drawn with Avogadro.

The monofunctional monomer 2-hydroxyethyl methacrylate or HEMA, figure 6, has many applications and is most frequently used due to its hydrophilic nature in dental adhesives, resin-modified glass ionomer cements and luting cements [43] [44]. In adhesive dentistry, HEMA has several advantages. The dentine adhesive systems can be classified into total-etch (TEAs) and self-etch adhesives (SEAs). The TEAs system is based on the application of phosphoric acid gel to demineralize dental hard tissues prior to the use of an adhesive, in these systems HEMA is added to the primer to enhance adhesive infiltration and improve dentine adhesion [45]. On the other hand, in SEAs systems, demineralization of the dental hard tissue and infiltration can be achieved in one step due to the aqueous formulation of this system [46]. This formulation contains hydrophilic and hydrophobic monomers comonomers, the advantage of HEMA is to improve the miscibility between these monomers to prevent phase separation and thereby improves adhesion [46].

HEMA is not normally used in dental composite formulation; some researchers have attempted to use it in experimental composites to study its effect on the properties of the material or to design chlorhexidine releasing dental composites [47] [48]. Therefore, incorporation of HEMA into dental composite formulation can facilitate the release of certain ions such as fluoride. One of the drawbacks associated with the use of HEMA in dental materials is that it can increase water sorption. Increased water uptake can lead to decreased mechanical properties, subsequently results in degradation of the polymer network [48].

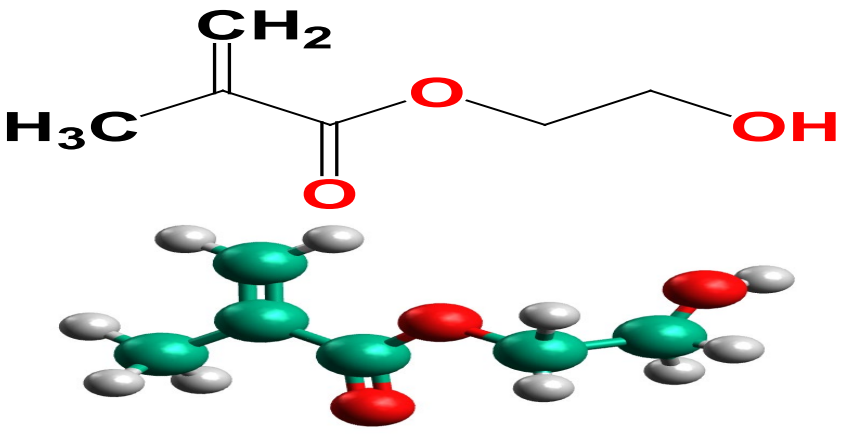

Figure 6: Molecular structure of HEMA (2-hydroxyethyl methacrylate), 2D structure drawn with Chemdraw. B) 3D Structure drawn with Avogadro.

1.3.2 Fillers

Fillers used in dental composites are quartz, silica glass including borosilicate and aluminosilicate glass as well as zirconia particles. The filler type significantly affects the properties of the composite materials with respect to strength, hardness, polymerization shrinkage, elasticity and thermal expansion [18] [25]. Fillers also influence the physical and mechanical properties of the materials, and the current resin-based composites have significantly enhanced clinical performance due to improved technology in grinding and dispersing fillers and increased filler loading into the material's formulation [49]. The latest developments include composite materials with nanofillers. Due to their small size, shape and content the material has better optical properties such as colour match to the surrounding teeth and radiopacity, in addition to better strength and abrasion resistance [23].

Initially, macrofilled composites used quartz and glass fillers such as borosilicate glass and aluminosilicate glass, due to their low cost and optical properties [17]. Filler size could reach up to 100 µm and a loading of 70-80 %, by weight. These fillers have a large size, hard surface and could become exposed after resin matrix wear resulting in restorations with a rough and dull appearance. In addition, these fillers are not radiopaque which is an important property for posterior restoration [50]. Composite resins' radiopacity allow radiographic identification of the existing restoration and secondary caries underneath the restoration that has a radiolucent appearance, i.e. transparent in X-ray in comparison to the radiopaque restoration appearance [51]. As a consequence, quartz, and glass macrofillers were replaced and are no longer available.

Microfilled composites were developed that incorporate silica particles with an average size of 0.04 µm. The small filler diameter provides materials with smooth, polishable surfaces to be used as restoration for anterior teeth. However, the reduced filler size increases the surface area of filler, and thus more resin is required to coat these fillers which leads to decreased loading of fillers (30%-60% by weight). As a consequence, these composites show reduced mechanical properties and lower thermal expansion coefficients compared to macrofilled composites [52] [53] [54] [55]. To increase the filler content, and thereby improve mechanical properties, the addition of microfilled complexes of either pre-polymerized silica particles produced by milling blocks of pre-polymerized microfilled

composite (1-200 µm) or by adding silica microfillers to pre-polymerized particles of 20-30 µm [14]. Although fillers load was increased to 60 wt %, these pre-polymerized fillers cannot covalently bond to resin matrix and the materials have low wear resistance under load bearing areas [56]. An overview of different filler types is given in figure 7.

Hybrid composites were developed in the 1980s to combine the properties of macrofilled and microfilled composites. Materials were produced with 60-70 wt % filler loading and two filler sizes of about 5 µm and 0.04 µm, respectively, suitable for restorations in areas of high occlusal load [57]. The incorporation of smaller particles resulted in a reduction of interparticle distance that allowed the improvement of mechanical properties and wear resistance [14]. These materials have good surface polish, enhanced filler packing, and improved handling properties (reduced stickiness) as compared to macrofilled composites. Conversely, the hybrid composites lose their surface polish and become rough with time [24]. Roughness can also result from clinical polishing procedures [58]. Polishing of the final restoration is necessary to produce clinically acceptable and stain resisting restoration that reduce plaque retention [59]. Excessive degradation and decomposition of composite resin restoration can result from the effect of consumed food and beverages such as tea, coffee and cola which can also contribute to roughness and colour change of the final restoration [60].

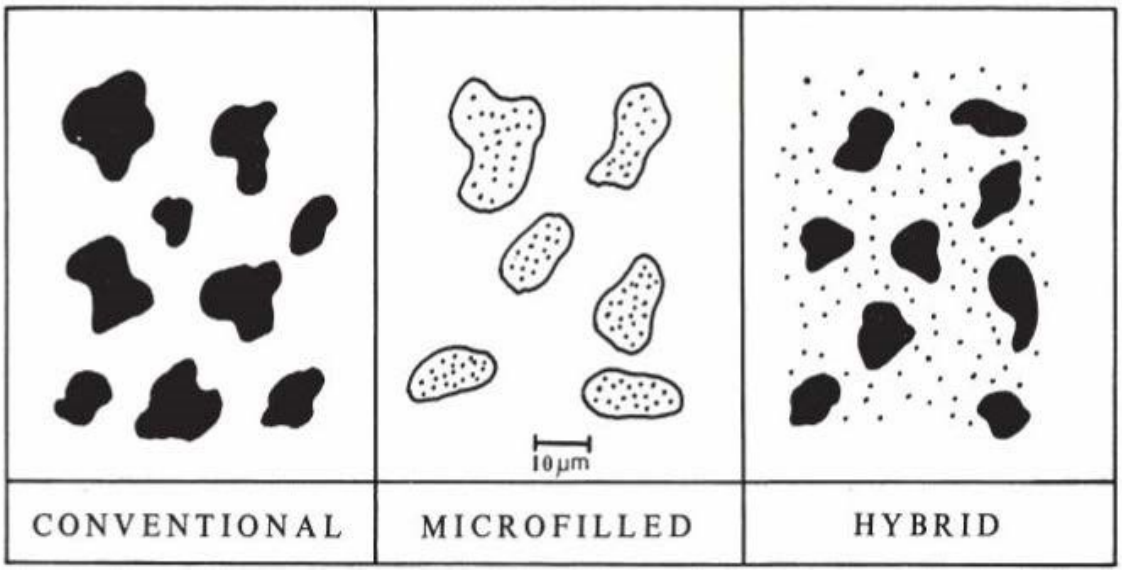

Figure 7: Filler particles used in the three main groups of composite resins (McCabe and Walls, 2008).

A next generation of dental composites has been developed using nanotechnology. Nanocomposites are materials with high polish retention, in addition to the excellent mechanical properties of hybrid composites allowing their application in restoring of anterior and posterior dentition. The fillers include nanoparticles of silica and zirconia silica in the range 1-100nm [23].

1.3.3 Coupling Agents

Silane coupling agents are responsible for the formation of chemical bonds between the resin matrix and filler particles as shown in figure 8. This bridge between resin and filler enhances the mechanical properties of the composite material and contributes to even stress distribution between resin and filler and reduced plucking of the fillers from the polymer matrix. Moreover, the hydrophobic properties of the coupling agents help to reduce swelling of the polymer due to water sorption [24]. The most commonly used coupling agent is γ-methacryloxypropyltriethoxysilane (γ-MPTS). The hydroxyl group binds to the hydroxyl group of the silica filler and at the other end, the methacrylate group interacts with the methacrylate group of the monomer. Silane coupling agents are essential for even stress distribution between the resin phase and silica glass fillers. The absence of silane bonds result in stress to the resin which can cause cracks, excessive creep and fracture of the restoration [14].

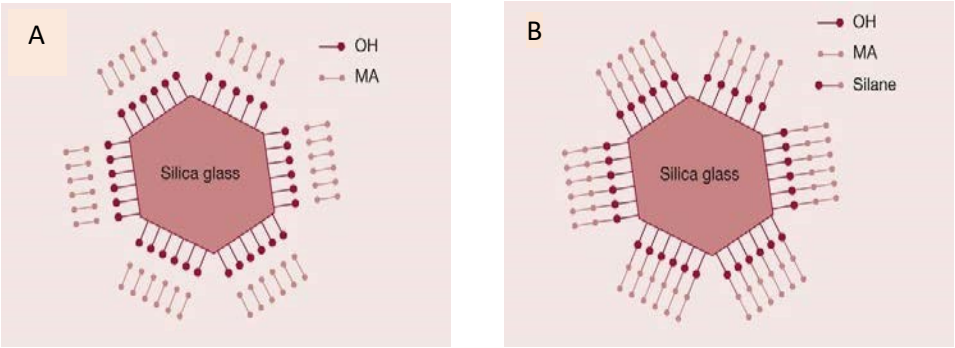

Figure 8: A) Resin molecules are repelled from glass fillers. B) Silane coupling agent forming bonds between filler and resin molecule [61]. MA=methacrylate group.

1.4 Initiators of polymerization

Polymerization of dental composite is a chain reaction that requires a radical donor to initiate the reaction. Traditionally chemically activated dental composites contained benzoyl peroxide (BPO) and aromatic tertiary amines such as N, N' dimethyl-p-toluidine or p-tolyl diethanolamine as free radical donors to start polymerization at ambient temperature [62]. The polymerization reaction was initiated when mixing a two paste system, with one paste containing the peroxide initiator and the other paste containing the amine activator as shown in figure9 [18].

Figure 9: Dental composite initiator/activator system based on two pastes, one containing the initiator and the other containing the activator. Polymerization is initiated upon mixing of the two components. (McCabe and Walls, 2008).

Light activated dental composites are supplied as a single paste system and can be polymerized by either ultraviolet (UV) or visible light. The potential hazards of long-term exposure to ultraviolet radiation has reduced the use of UV-activated composite materials [63]. Visible light activated systems use either type I or type II Norrish photointiators. Type I Norrish photointiators absorb light in the lower visible light range at a maximum of 400 nm. Phosphine oxides such as phenylbis (2,4,6-trimethylbenzoyl) phosphine oxide known as TPO or germanium-based initiators such as the commercial Ivocerin^{TM} are examples of type I photoinitiator. TPO has a white colour and therefore, will mitigate the problem of yellowish

discolouration and can be used in combination with Camphorquinone (CQ) [64]. CQ is a type II photoinitiator, which is the most commonly used in commercial dental composite materials today [52]. The irradiation time is usually less than 20 seconds for CQ to produce free radicals and initiate polymerization when used in combination with a co-initiator such as tertiary amines. CQ absorbs light in the range of 400-500 nm with a maximum at 470 nm, and is characterized by a yellowish colour, figure 10 [65]. For optimal polymerization, an electron donor such as dimethylaminoethylmethacrylate (DMAEMA) is usually used as a reducing agent in combination with CQ [66].

Figure 10: Initiators used for dental composite polymerization.

Increasing the photoinitiator concentration can improve the degree of polymerization and mechanical properties [67] [68] [69], the ratio of photoinitiator should not exceed a certain threshold, commonly ranging from 0.1%-1 wt% [70]. Aesthetic properties of the material can be compromised due to CQ yellowish discoloration [71]. Depth of cure of light activated dental composite is one of the important parameters for the clinical success of the restoration, it can be defined as the maximum thickness of the material that can be polymerized under light curing condition [72]. The depth of cure can be determined by simple scrape test according to ISO 4049 by filling a cylindrical mould with the material, then one end is cured for an amount of time that is specified by the manufacturer. After that, a plastic spatula is used to remove uncured, soft material as soon as it has finished curing, the depth of cure represents the height of the remaining hard, cured material [18]. Unreacted CQ and co-initiator lead to reduced depth of cure of composite material and hence reduced formation of free radicals deeper in the material [71] [73]. Low curing depth increases the degradation, bulk fracture and marginal discoloration of the final restoration since shallow depth of cure affect the final degree of conversion which directly affects the mechanical properties [74].

Therefore, nature and concentration of photoinitiator system has been extensively studied to improve the polymerization of resin-based composites [71] [64] [66] [75].

1.5 Mechanism of polymerization

Polymerization is the process by which monomers are converted to crossed linked polymers by a free-radical assisted reaction. The free radicals are generated by heat, light or chemical activation [15]. Understanding the polymer chemistry and polymerization kinetics is essential to help researchers develop novel materials and to enable dentists to achieve best performance of the final set composite material. Additionally, the kinetics of polymerization will influence the mechanical and physical properties of materials [76]. In general, polymers can be classified according to their composition into addition and condensation polymers, the chain configuration into linear, branched and crosslinked and finally the polymerization mechanism into step-growth and chain-growth polymers [52].

An addition polymer is formed by joining monomers without the formation of by-products and the resultant polymer has a similar chemical composition as the original monomer. An example of an addition polymer is polyethylene:

$$nCH2 = CH2 \rightarrow -(CH2 - CH2 -)n$$

Ethylene Polyethylene [77]

Condensation polymers are formed by step-growth polymerization where monomers react to form dimers, trimers, longer oligomers, and finally the polymer network [78]. Each reacting monomer has a functional group, the reaction produces a product with a further reactive group. For example, two monomers X-M1-X and Y-M2-Y with reactive functional groups undergo a condensation reaction as follows:

$$X - M1 - X + Y - M2 - Y \xrightarrow{yields} X - M1 - M2 - Y + XY$$

$$X - M1 - M2 - Y + X - M1 - X \xrightarrow{yields} X - M1 - M2 - M1 - X + XY$$

$$X - M1 - M2 - M1 - X + Y - M2 - Y \xrightarrow{yields} X - M1 - M2 - M1 - M2 - Y + XY, \quad \text{etc.}$$

[18]

In condensation polymerization, the molecular weight of polymers builds up slowly until later in conversion process [79]. Condensation polymerization occurs in a stepwise fashion also termed step-growth. In general, condensation polymers form at a slower rate than addition polymers, but both reactions form polymers at a faster rate when heat is applied. The molecular weight of the final polymers is generally lower than the one of polymers formed by an addition reaction, due to the one-to-one ratio of functional groups and the high conversion rate required to produce polymers of high molecular weight [14] [80]. In addition, slow build-up and shorter chain formation delays gelation and vitrification to a later stage in conversion and hence influence stress resistance [14]. Generally, at the beginning of polymerization the reaction is chemically controlled. The sufficient supply of monomer molecules and free radicals contribute to the similar rate of propagation and termination [52]. When the reaction continues, the reaction becomes diffusion controlled and viscosity will increase due to the growth of high molecular weight species. As the mobility of the molecules become difficult, the termination events decrease due to the reduction in disproportionation and bimolecular termination. Consequently, this reduction of termination event will favour the propagation of the reaction. This is termed as autoacceleration, figure 11 [81]. At some point, one macromolecule during the polymerization reaction will span the whole specimen. This point is called the gelation point [52]. The reaction continues with favoured propagation until the maximum polymerization rate is reached. The gelation accounts for 5% of the methacrylate polymerization and is observed before maximum polymerization rate is reached. Therefore, it will influence the conversion and stress development [82]. As the polymerization procedure continues, the diffusion of even small molecules will also become restricted. Eventually, propagation will become diffusion controlled. Autodeceleration coincides with vitrification, figure 11, and is defined as the degree of conversion following the maximum polymerization rate where the reaction rate decreases sharply and is accompanied by a sharp increase in stress [83]. For those reasons, gelation and vitrification of methacrylate monomers have gained increasing attention by research to develop low stress dental polymers [84] [85] [86].

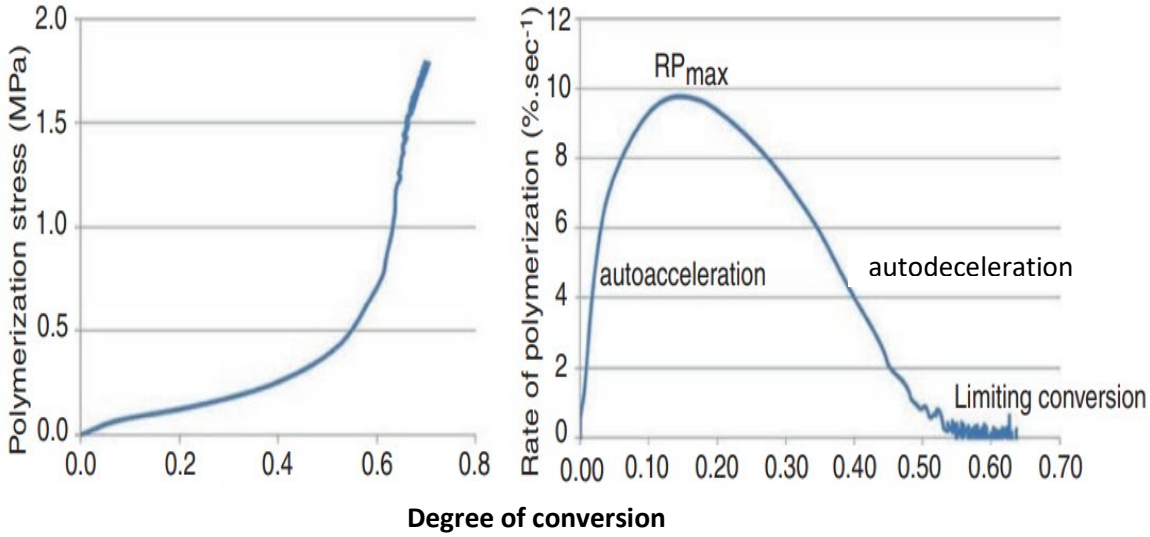

Figure 11: The figure demonstrates the polymerization stress of multifunctional methacrylate, in addition to the polymerization rate as function of conversion. The conversion was followed on a specimen to investigate the development of stress and the degree of conversion. From the polymerization rate vs conversion curve, it shows that stress start to build up at conversion coincides with the end of autodeceleration, Fugolin et al., 2018.

Additionally, in practice incremental placement techniques i.e., placement of the material in multiple layers rather than bulk placement of the restorative material is usually advised to reduce the polymerization stress. The reduced volume of the material will reduce the polymerization stress [87].

During dental composite polymerization, the material turns from a paste-like texture to its final set form, by either chemical or light activation. The degree of conversion is a measure of polymerization which is defined as the ratio of the carbon=carbon double bonds converted to single bonds [88]. The degree of conversion for multi-methacrylate dental polymers ranges reach up to 75%, leaving a significant percentage of unreacted residual monomers [89]. A high degree of conversion is essential for good mechanical and physical properties, colour stability, and biocompatibility [90].

The polymerization reaction of composite materials occurs in four stages: activation, initiation, propagation and termination, figure 12 [14]. At the start, initiator molecules such as benzoyl peroxide (chemically activated composites) or camphorquinone (light activated composites) are activated by heat or blue light of around 465 nm to form free radicals. Organic amines are added to the monomer mixture as accelerators [15]. The free radicals

attack the carbon- carbon double bond of the methacrylate monomer to form a reactive centre, which continues to build up a network of cross-linked polymers (propagation stage). The chain continues to grow by adding single molecules to the polymer network until the process is terminated by disproportionation or combination reaction [24].

A high degree of monomer to polymer conversion results in favourable mechanical properties [91]. Resistance to degradation and wear has been reported to be associated with increased extent of cure [92]. High degree of conversion also results in increased strength and hardness of dental composites [74] [91]. However, full conversion cannot be achieved, and a variable percentage of residual monomers will remain unreacted [93]. The presence of the residual monomers can be explained by trapped individual monomers during the polymerization reaction [94]. When free radicals collide with monomer molecules, they react to form covalent bonds. The polymer chain continues to grow with more molecules added like beads on a string. The growing chains with crosslinks result in increased viscosity and rigidity and thus some unreacted monomers will become trapped within the polymer network [95]. The release of these residual monomers into the oral cavity is critical due to their toxic and genotoxic effects [96]. In addition, leaching of monomers alters the structure of the composite material and results in voids in the polymer network. Factors that influence the residual monomer release include diffusion and swelling [97]. Diffusion depends on the network characteristics; hydrophobic polymer networks are affected by organic solvents while hydrophilic monomers attract aqueous solvents. Consequently, solvent diffusion, depending on the degree of cross linking and rigidity of the polymer network, results in swelling and pores [98]. Eventually the release of residual monomers from the network is determined by the molecular structure and its flexibility. For instance, the release of residual monomer molecules of bulky monomers such as Bis-GMA and Bis-EMA is less than the release of the smaller molecular weight monomer TEGDMA [97]. The amount of unreacted residual monomer is affected by the degree of conversion. Higher degree of polymerization means a more cross-linked network, higher rigidity and less residual monomers [99]. In addition, mechanical properties are affected by the degree of conversion.

The degree of the methacrylate double bond conversion ranges between 43%-75% [100] [101] [102]. Many factors affect the degree of polymerization such as the size and amount of fillers, the intensity of light, the distance of the light source and the irradiance time [103]. An

increase in filler content will reduce the monomers and determines important properties such as strength, occlusal load resistance, translucency and radiopacity. Additionally, fillers translucency affects the degree of polymerization as the depth of cure is determined by fillers translucency. One approach is to increase the fillers size and decrease their content to ensure light penetrates to deep layers [104]. Efficient polymerization of 2mm thickness of dental composite, requires irradiance energy ranging from 16-24 J/cm^2 [105] [106] [90]. This energy is calculated by multiplying the duration of curing time (T) by the irradiance level of the light curing unit (mW/ cm^2). Therefore, the higher the irradiance the shorter the curing time required [15].

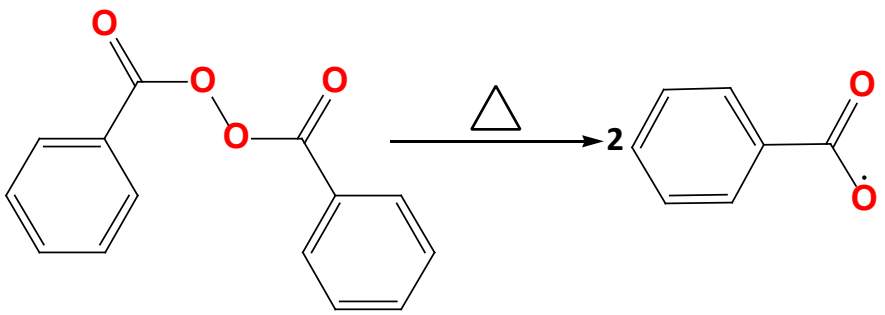

Initiation step: The initiator is activated by energy to form free radicals.

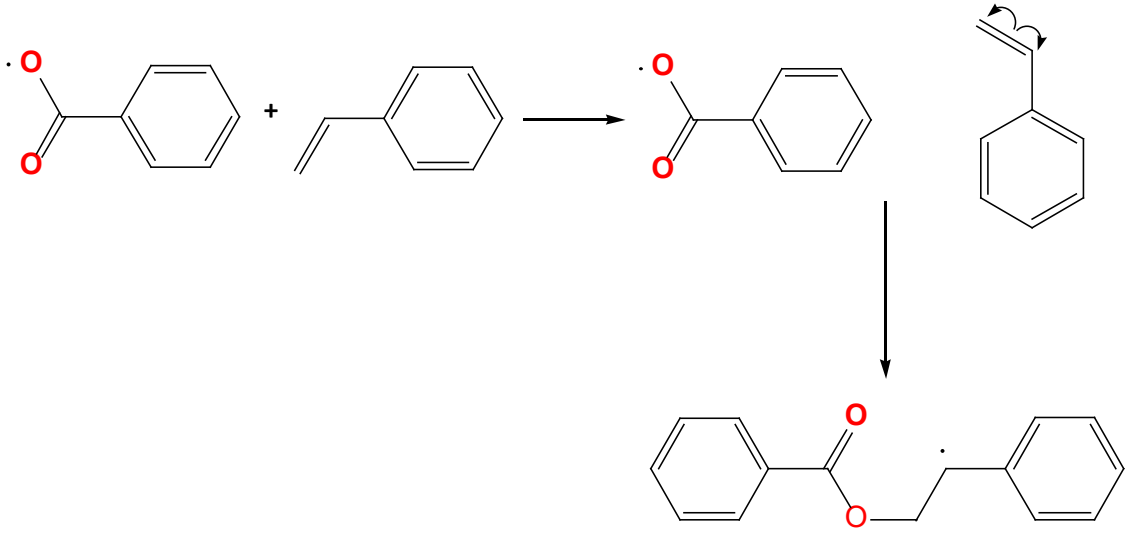

Free radicals attack the carbon-carbon double bond of the monomer.

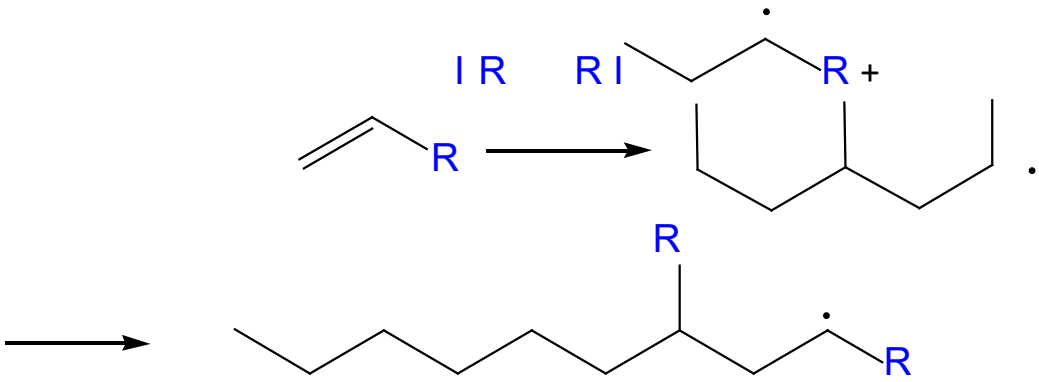

Propagation step: Free radicals react with monomers, macroradicals or reactive centres continue to react with monomers (addition reaction).

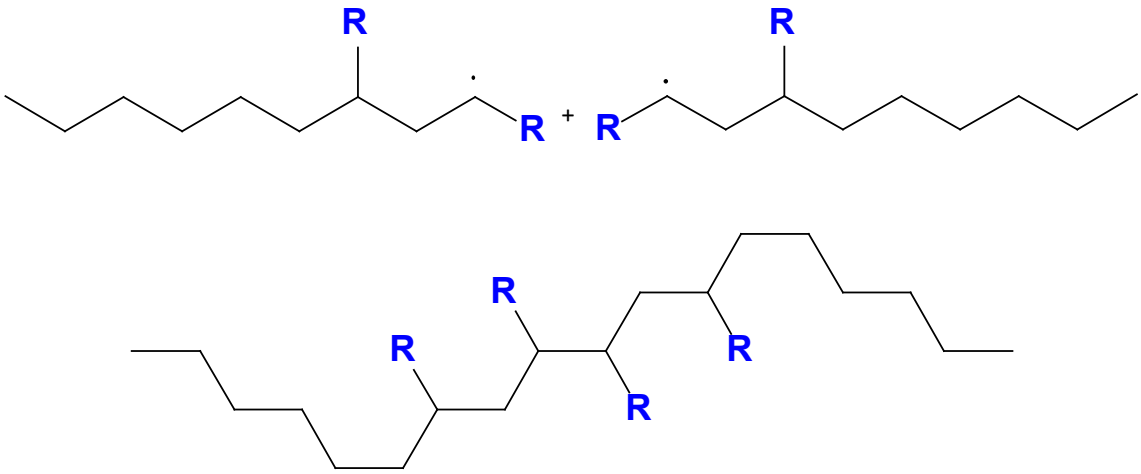

Termination step: The reaction is terminated by either disproportionation or combination reaction. The combination reaction involves two free radicals to react and combine, while disproportionation includes the transfer of a hydrogen atom from one free radical to another.

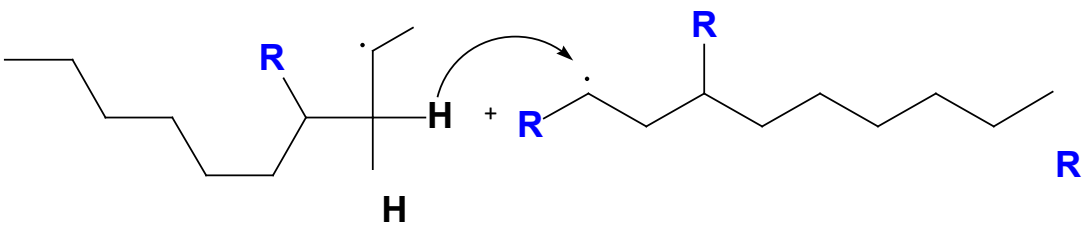

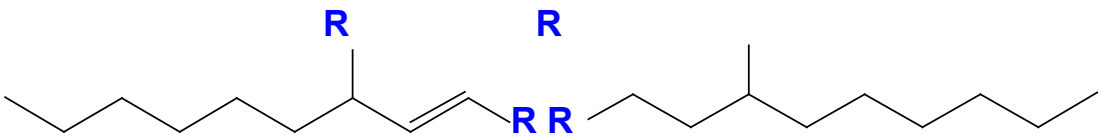

Combination reaction

Figure 12: Steps of the polymerization reaction of resin based composite materials. Drawn with Chemdraw, modified from (Fugolin et al., 2018).

1.6 Curing of dental composites

Early types of composite materials were supplied as two paste systems, as mentioned earlier with one paste containing an initiator and the other paste containing the chemical activator. Polymerization was achieved by mixing the two pastes, figure 9 [18]. These are now termed chemically activated composites or traditional composites. Critically, hand mixing could introduce air bubbles which affected the mechanical properties of the final set material [107]. In the 1970s, light activated materials were developed. These materials were supplied as single paste systems and were activated by ultraviolet light at a wavelength range of 360-400 nm [52]. UV curing units were designed based on light emission from a source containing high pressure mercury through quartz rod. This photocuring unit had the advantage of curing on demand compared to the chemically activated materials. Curing time of 20 seconds was sufficient for polymerization, however 60 seconds resulted in enhanced polymerization [108]. Polymerization with UV light had a number of drawbacks, firstly, limited curing depth due to limited light penetration [109]. Secondly, UV-inflicted tissue damage have been reported such corneal burn and cataract formation in addition to changes of the oral microflora [110] [111]. For these reasons, improved materials were developed in the late 1970s that could be cured by visible wavelengths, eliminating the need for the hazardous UV light. Camphorquinone was introduced as a photoinitiator and tertiary amines as coinitiator. The novel light activated composites showed higher degrees of conversion than chemically activated types [112]. The light activating unit was a quartz-tungsten-halogen (QTH) source, consisting of a heat absorbing glass with a bandpass filter emitting light with a wavelength of 400-550 nm that is sufficient to activate the photoinitiator camphorquinone [113]. These units provided the advantage of curing a 2mm layer of the material by visible light with elimination of the potential hazard associated with the UV lights. However, the light required to initiate the system was within the frequencies that results in retinal burning. Therefore,

practitioners were advised to use blue-blocker to prevent ocular damage while curing [114]. Additionally, the light produced by the bulb increases the operating temperature which limits its lifetime to 100 h and requires fans to mitigate the rising temperature [106]. The newest light curing system introduced in dentistry is the light-emitting diode (LED) [90]. LED technology uses a junction of doped semi-conductors instead of lightbulbs, and therefore less heat is generated, and no fans or filters are required. The life span of an LED unit is around 10,000 h and produces light in the wavelength range of 400-500 nm which is suitable to polymerize CQ [115].

1.7 Drawbacks of resin-based materials

Resin based materials yield favourable mechanical properties if high degrees of monomer to polymer conversion are achieved [116]. Efficient conversion ensures chemical stability of the polymer network and minimizes the release of monomers into the surrounding environment [117]. However, complete conversion of resin-based material is not achievable, the common range of conversion is typically between 55%-75% [118]. Increased viscosity and rigidity of the composite during polymerization is one of the main reasons for the presence of trapped residual monomer molecules in the final cross-linked network [95]. An additional contributing factor to the low degree of conversion are unreacted methacrylate groups that associate with the silane coupling agents [119]. A low degree of conversion results in a significant amount of unreacted monomer that will be released, affecting the surrounding tissue [120]. In addition, the aqueous oral environment impacts on the resin-based polymer and subjects it to volumetric changes and triggers the release of by-products into the neighbouring oral tissue [117]. Biodegradation of resin polymer into smaller oligomers and monomers that can leach out of the polymer network can occur by two ways: (i) the release of the small unbound monomers/additive molecules from the polymer due to the effect of solvents or (ii) by hydrolytic degradation of polymer or enzymatic degradation by salivary esterases [121].

The elution process is affected by several factors but is most prominently related to the degree of conversion which directly relates to the amount of the released substances [122]. The degree of double bond conversion can be significantly affected by the type of light source used for polymerizing the material. A light source with higher energy (incident light

intensity) will be typically associated with a higher degree of conversion than a light source with lower energy [14]. Higher energy of light will activate more photoinitiator molecules and thus result in more free radicals required for the polymerization process. This will also reduce the irradiation time due to higher free radical termination [123]. Secondly, leaching depends on the chemical nature of the solvent: For example, elution is enhanced in artificial saliva as compared to water and elution in solvents such as ethanol was found to be even higher and persist up to three months [97]. Thirdly, the size and chemical structure of the released monomers or additives influences release [124]. Bulky monomers such as Bis-GMA and UDMA elute less than smaller, lower molecular weight monomers such as HEMA and TEGDMA [125]. In addition, the presence of additives such as bioactive glass in the structure of the polymer network increases the monomer elution. This can be due to poor crosslinking in the final polymer network in the presence of bioactive glass [126].

1.8 Measuring the degree of conversion

One of the most commonly used techniques to measure the degree of conversion (DC) in composite materials is infrared (IR) spectroscopy [14]. The DC can be calculated by comparing the concentration of the remaining aliphatic C=C double bonds in the cured material relative to the uncured material as shown in the schematic representation, figure 13 [88]. The samples are exposed to infrared light, some wavelengths that pass through the specimen are absorbed and some are reflected, the remaining wavelengths can be recorded to produce a spectrum, figure 14 [127]. Infrared spectroscopy is used in conjunction with the attenuated total reflection technique (ATR), which is a sampling technique where solid or liquid samples can be examined without further preparation [128]. ATR is based on the total internal reflection of an infrared light within the sample. The sample is placed in direct contact with an ATR crystal. After that, a beam of light is sent through the ATR crystal in a certain angle known as the critical angle, the light bounces through the crystal resulting in an evanescent wave, as in figure 14. This evanescent wave is extending into the sample and can be used to collect information about the specimen. The remaining light that exits through the crystal is then collected by a detector. The penetration depth of the evanescent wave is typically between 0.5-2 micrometres. This depth is dependent on the wavelength of the light, the incidence angle and the refractive index of the crystal and the sample [129]. The infrared spectrum is divided into three regions (with reference to visible light): near

region IR (14,000-4000 cm^{-1}), mid region IR (4000-400 cm^{-1}) and far IR (400-25 cm^{-1}). For most dental resins the changes in double bond formation that occur during polymerization and are detected by IR spectroscopy lie in the mid region [130].

Calculating the amount of converted double bonds for dental composite is based on the presence of a linear relationship between the vibrational band intensity measured by FTIR spectroscopy and the aliphatic C=C concentration [16]. Information can be collected by comparing the band intensity in polymerized and unpolymerized samples using a reference band. For Bis-GMA or Bis-EMA dental composite, the aromatic C=C bond is most commonly used as an internal standard which is represented at 1610cm^{-1} absorption, as shown in Figure12. However, for UDMA containing composites an aromatic core is missing, therefore an alternative reference is used [131] [132]. The degree of conversion can be calculated by using the equation:

$$DC = 1 - \frac{\left(\frac{I_{C=C}}{I_{\text{reference}}}\right) polymerized}{\left(\frac{I_{C=C}}{I_{\text{reference}}}\right) unpolymerized} \qquad [14].$$

Where $I_{C=C}$ represents the vibrational stretching of the aliphatic C=C at 1640cm^{-1} and $I_{reference}$ represents the vibrational stretching of the internal standard or reference band. The expression in the fraction indicates the proportion of the residual aliphatic C=C bonds, the degree of conversion is the percentage obtained from subtracting this amount from unity [133].

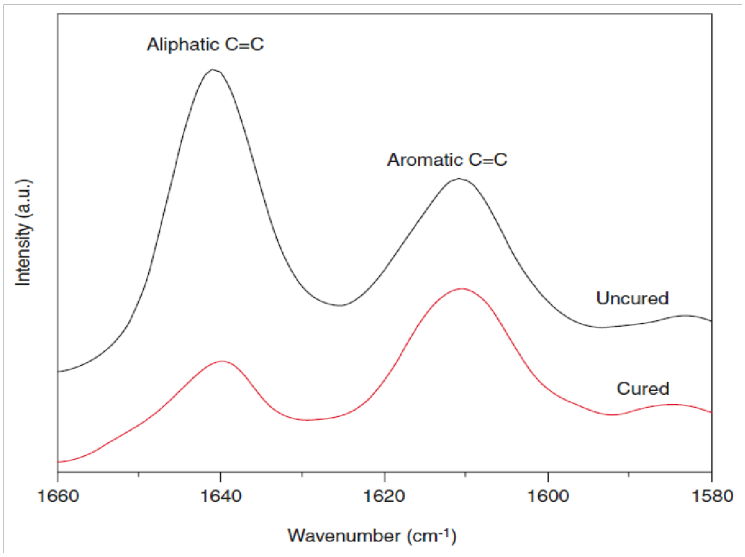

Figure 13: Part of an IR spectrum used to calculate the DC for dental composite materials. The aromatic C=C double bond is used as internal standard, DC is reflected by the decrease in the aliphatic C=C double bond, Tarle et al., 2018.

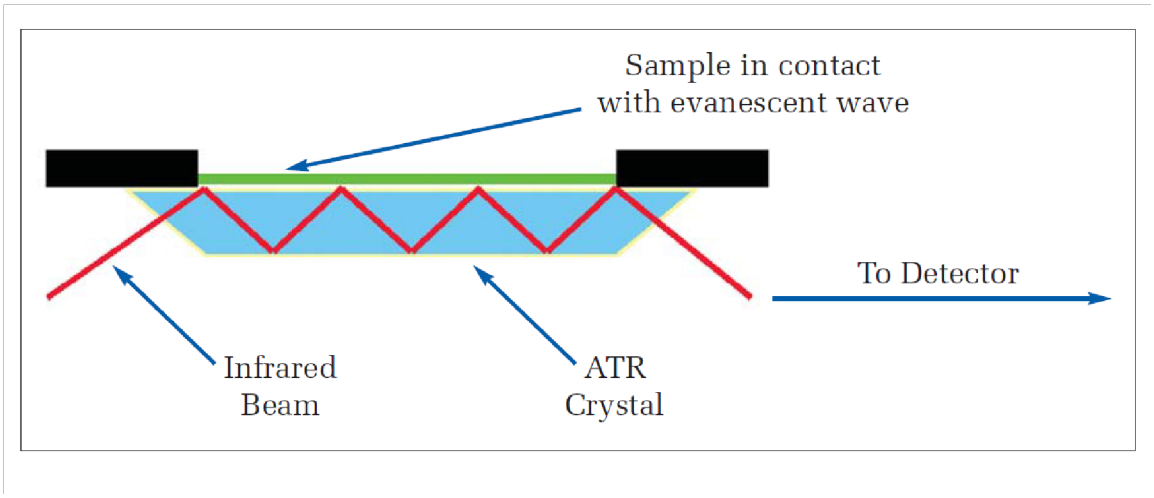

Figure 14: Mechanism of total attenuated reflection in FTIR spectroscopy [134].

1.9 Bioactive and fluoride releasing materials in restorative dentistry.

Bioactive materials can be defined as materials that can induce biological activity within cells or tissues. In dentistry, bioactive restorative materials can induce tooth remineralization and enhance hydroxyapatite formation, pulp regeneration and reparative dentine formation [135].

Calcium hydroxide, $Ca(OH)_2$, was the first bioactive material used in dentistry, introduced in 1920 [136]. $Ca(OH)_2$ is a white odourless powder, as a chemical it is classified as strong base with a pH of 12.5-12.8 that has low solubility in tissues [137]. The main therapeutic action of $Ca(OH)_2$ arises from its antibacterial characteristics due to the high alkaline pH, the dissociation of calcium and hydroxyl ions in tissues and the ability to aid in reparative dentine formation [138]. Therefore, it was used for many clinical applications such as pulp capping, stimulation of root resorption repair by reducing osteoclastic activity [139], apexogenesis, i.e. vital pulp therapy of immature teeth by enhancing the growth and development of root apices, induction of calcified barrier formation in open apex of non-vital teeth (apexification) [140] and finally as intracanal medicament [136].

Fluoride is a well-known anti-cariogenic agent that reduces secondary caries in tooth tissue including enamel and dentine. The observation of reduced caries incidence associated with fluoride-containing silicate cement contributed to the increased effort for a development of various fluoride containing dental products such as lining cements, fissure sealants, orthodontic adhesives and cement [141]. The mechanism underlying the fluoride anticarcinogenic effect involves reduced demineralization, an increase in remineralization, an interference with plaque formation, and inhibition of bacterial growth and metabolism [142] [143]. Fluoridated dental restorative products available on the market today include glass ionomer cements (GICs), resin-modified glass ionomer cements RMGICs, polyacid-modified composites (compomers), and amalgams. All contain different matrices and setting reactions which influence fluoride release. The amount of the fluoride released from these products is dependent on the formulation of the materials which affect the cariostatic and antibacterial properties of these restoratives [141, 144]. However, these restoratives, except amalgam, are not suitable as permanent filling materials under stress bearing areas because of their poor mechanical properties [145].

Glass ionomer materials are adhesive cements used for their therapeutic action offered by the fluoride release of the material [146]. GICs consist of powder of fluoride containing glass such as aluminofluorosilicate and polyalkenoic acid [147]. The liquid part consists of an acrylic acid/itaconic acid copolymer, a solution of maleic acid polymer or a maleic/acrylic copolymer [18]. GICs can also be supplied in anhydrous form, where the powder contains the sodium aluminosilicate glass and vacuum-dried polyacids with setting achieved by mixing this powder

with ultrapure water. Both forms set by the same acid-base reaction [148]. During the setting reaction, fluoride ions in the glass powder are released into the aqueous acid phase and become trapped in the hardening cement matrix [149]. Therefore, the cement shows long-term fluoride release for several years [150] [151]. Fluoride release from glass ionomer cement into the surrounding aqueous environment has been explained by two mechanisms. The first process involves a short-term fluoride release due to dissolution of ions from the material's outer surface, while the second process consists of sustained long-term ion release from the bulk material [147]. These processes are explained by the following equation which represents the kinetics of fluoride release:

$$[F]_C = [F]_1 \, t/\left(t + t_{1/2}\right) + \beta\sqrt{t}$$

Where $[F]_c$ is the cumulative fluoride release and $[F]_1$ is the total fluoride available. The parameter $t_{1/2}$ is the so-called ''half-life'' that is defined as the time required for fluoride release to reach half of its maximum value of the process that is given by $[F]_1$. The driving force for fluoride release in the 2nd process is $\beta\sqrt{t}$ which is a material dependant parameter; the greater value of this parameter, the higher and faster is fluoride release [152]. The process of fluoride release for most conventional and resin modified GICs and some high fluoride-containing compomers follows square root dependency, this suggests that the elution process is driven by the concentration gradient in some way [150] [153].

The interest in increased clinical use of GICs is mainly due to their adhesive bioactive properties and their therapeutic potential. The extended fluoride release by GICs has been shown by many studies [154] [155] [156]. The rate and amount of fluoride release is dependent on the different formulations of GICs [147]. GICS are commonly used for crowns and bridge cementation, cavity lining materials under restorations, dentine replacement and as restoration of primary dentition [157]. They can also be used as restoration of small cavities such as erosion and abrasion, small class V and class III lesions. As filling materials, when compared to resin-based composite materials, GICs are less technique demanding as the adhesion to the tooth surface does not require extra provision of retentive features and humidity control [157]. Composite restorations require multiple steps including tissue conditioning and acid etching and adhesive application, steps have to be done in optimum dryness. GICs cannot be used as permanent filling material in areas where toughness and

resistance to wear from enamel is a requirement due to inferior mechanical properties such as fast wear due to surface degradation under occlusal load [158].

Resin modified glass ionomer cements or RMGICs, also known as light cured GICs, are a modification of the conventional glass ionomer cements. The replacement of polyacids with modified polyacids that contain unsaturated groups and hydrophilic, polymerizable monomers such as HEMA improves the polymerization reaction [159]. RMGIC set by a dual reaction, the first one is an acid-base reaction like with conventional GIC, the second is an addition polymerization reaction. The initiator for the polymerization reaction is CQ. Due to the combined products of those two reactions, the structure of the resultant material is complex [44] . The combination of those setting processes in the material may compromise the reliability of the set material. Therefore, attention to the manufacturer's instructions with regards to the irradiation phase is necessary to generate a material with optimal qualities. The kinetics of fluoride release by RMGICs is comparable to conventional GIC-mediated fluoride release by a two phase-process: an initial burst phase release followed by prolonged or sustained release [152]. The RMGIC was introduced in dentistry in 1991. They have been used for multiple clinical applications including use as a liner or base, orthodontic brackets bonding and primary dentition restoration of class I, class II and class III restorations [160] [161] [162].

Compomers are polyacid-modified composites. These materials are a further development of the resin modified GICs and are similar to composite and GIC in some areas [163]. Their polymeric matrix consists of modified Bis-GMA, UDMA and bifunctional monomers. The bifunctional monomers contain two double bonds and two carboxylic groups. Therefore, the bifunctional monomer can react with methacrylate through a radical polymerization reaction in addition to the acid-base neutralization reaction that liberate cations from glass particles after water diffusion [164]. Moreover, the matrix contains ion leachable glass such as calcium aluminium fluorosilicate glass. The particles are partially silanized to allow direct bonds with the resin matrix [165]. The mechanical properties are inferior to composite materials and are recommended for clinical applications where low stress would be produced such as primary teeth restorations [166].

Conventional amalgam alloys contain mercury triturated with silver, tin, and copper in addition to small quantities of other metals. Subsequent developments introduced high copper amalgam alloy with 30% copper particles that had better mechanical properties and clinical performance. Both of these formulas are considered inert and do not contain fluoride [141]. Fluoride releasing amalgams were developed in an attempt to overcome restoration failure; 50% of cases due to secondary caries [167]. Follow up clinical trials showed marginally improved integrity of mandibular molars in children restored with 1 % SnF_2 containing amalgam alloy compared to conventional alloy [168]. Additionally, *in vitro* studies with artificial caries models concluded that fluoridated amalgams inhibited secondary caries compared to conventional material [169]. While these materials are considered inexpensive and suitable as restoration options, several disadvantages have to be considered. First, microleakage was shown to be associated with all amalgam restorations due to contraction after setting. Although corrosion products form and fill the space between the enamel and the restoration interface, this process takes a few months and pulp inflammation may result in the meantime [170]. Amalgam restoration requires mechanical and micro-retentive features and therefore are not conservative to the tooth structure [171]. There is also a concern that 60 % of amalgam waste can enter the food chain; during restoration replacement, the material escapes to wastewater and can affect people who consume fish [172]. Therefore, there are governmental recommendations that ban the use of materials in Scandinavia or limits their use in children and pregnant women in the UK [173] [174] [21].

A potentially bioactive resin-based dental composite can be developed from the incorporation of fillers such as ceramics or bioactive glasses that have shown to release remineralising ions when exposed to aqueous environment [175]. These fillers include calcium phosphates, calcium fluoride, fluorapatite and bioactive glasses that include reagents such as: SiO_2, Na_2O, CaO and P_2O_5.

Hydroxyapatite is a calcium phosphate with formula $Ca_{10}(PO_4)_{10}OH$, which has good biocompatibility and bioactivity [176]. Dentine is a natural composite the inorganic part of which is made of hydroxyapatite crystals in 1-100nm [177]. Therefore, researchers attempted to add synthetic hydroxyapatite crystals to restorative composites to produce restoratives with favourable properties. The characteristics of hydroxyapatite such as radio-opacity, enhanced wear performance, polishability and hardness values comparable to that of the

natural teeth are considered advantageous to use them as additives in composite materials [178]. It has been reported that the use of micro-size, rather than nano-sized hydroxyapatite, in a composite results in better mechanical properties [178]. This was attributed to water diffusion when nano range hydroxyapatite was used with hydrophilic monomers such as HEMA to add the advantage of good interaction with fillers. The hydrolytic stability and mechanical properties of experimental materials loaded with nanosized hydroxyapatite has also been investigated, they have been reported to be not suitable for clinical application due to their high solubility in a wet environment and poor mechanical properties [179]. On the other hand, when the experimental composite was loaded with hydroxyapatite in the micro range size of filler particles and coated with either citric, acrylic or methacrylic acid an improvement in mechanical properties have been noted, with the mechanical properties being similar to composites containing hydroxyapatite coated with a silane coupling agent [179]. In general, nanohydroxyapatite is a new material to be applied in dentistry and further investigations regarding the physical and mechanical properties in addition to the effects of silane coating on their bioactivity is needed.

Fluorapatite is a bioceramic material with the formula $Ca_{10}(PO_4)_6\ F_2$ the pure material exists as colourless crystalline solid in nature [180]. Fluorapatite has attractive characteristics to be used in clinical applications such as hardness, stability in an aqueous environment, bioactivity, biocompatibility and bacteriostatic properties [181, 182]. Several studies aimed to use fluorapatite to develop novel experimental prototypes of dental composites. Fluorapatite was used as a potential filler in designing experimental bioactive dental composites [183] [184]. Fluorapatite crystals were shown to be a suitable additive to produce anti-caries materials due to their chemically stable and ability to release fluoride in an acidic environment below pH 5.5 [183].It has been shown that incorporating powdered fluorapatite crystals (0.6-1 μm) into a BisGMA/TEGDMA monomer system resulted in fluoride release [185]. These materials showed no cytotoxicity to pulp stem cells and resulted in significant reduction of bacterial biofilm and mass colony formation of cariogenic bacteria. Fluorapatite addition did not reduce the degree of conversion, hardness, or wear rate of composites but did reduce the strength and stiffness of the material.

Bioactive glasses were first developed in 1969 by Hench *et al*. They are degradable upon contact with bodily-fluids and can produce hydroxycarbonated apatite (HCA), therefore have

been considered for use as bone substitutes [186]. They were applied as additives in remineralising and desensitising tooth pastes to treat teeth hypersensitivity in the past fifteen years [187] [188] [189]. Bioactive glasses have been considered as additives to resin-based composites to produce remineralisation. The bioactive behavior is due to their ability to release calcium, phosphate, and fluoride ions and because they raise the pH as they dissolve and form apatite [186]. Most studies on their mechanical properties, used dry samples. Therefore, it was recommended that materials containing these fillers should be investigated in physiological fluids and for longer immersion time points of the samples to replicate oral environment [190].

1.10 Measurement of fluoride release

Fluoride release from dental restoratives has been extensively reported in the literature, though, no standard protocol for testing is available. Fluoride release in an experimental set-up is affected by experimental factors, material preparation and formulation [141]. Different sizes and shapes of specimens were used during the many investigations. It was concluded that the exposed surface area of the specimen has a more pronounced effect on fluoride release than the weight of the specimen [191]. Additional factors influencing fluoride release include filler type, storage media, pH and frequency of storage media renewal [192] [193] [194] [195]. Moreover, factors related to material formulation are powder-liquid ratio, mixing procedure and curing time [196] [197] [198].

A variety of storage solutions including saline, distilled water, human saliva, artificial saliva and acidic solutions have been used in fluoride release studies [199] [200] [201]. The pattern of fluoride release was similar in distilled water, artificial saliva and acidified media, however variations in the daily and cumulative release were found [199] [201]. The lack of ions in distilled water makes it a good option as a storage solution. Many studies provided an accurate estimation of fluoride ion released from dental restorative materials kept in water [202] [203] [204]. The highest amount of fluoride was released in acidic media and artificial saliva models or in a model based on alternating demineralization and remineralization, also termed pH-cycling, to mimic the oral situation [205] [206] [207]. The high fluoride release was explained by enhanced dissolution of fluoridated compounds in acidic media. In contrast, in artificial saliva, fluoride release is generally 17-25% less compared to water [208]. The

concentration of ions is higher in artificial saliva and thereby may affect fluoride diffusion from the restorative material into the storage solution. Moreover, it was suggested that the release was affected by the formation of salivary pellicle around the surface of the restorative material when immersed in artificial saliva [209] [199] [155].

One of the most common methods to measure fluoride release is an ion selective electrode (ISE), a widely used technique in electrochemistry. Conventional electrodes used to measure hydrogen ion concentrations in pH meters can be adapted for specific analytical applications to measure the concentration of different ions such as sodium, calcium, chloride and fluoride [210]. ISEs measure total fluoride i.e. free fluoride ions and fluoride complexes in solution [211]. Therefore, the use of a total ionic strength adjustment buffer, TISAB buffer is required to prevent the formation of fluoride-complexes and to control the pH of the solution [212]. The ISE method is widely used due to its simplicity, reliability, and suitability for measuring a wide concentration range of fluoride [213]. Another method suitable for fluoride ion measurement is ion chromatography (IC), a method with wide application in analytical chemistry [214]. IC has the advantage of improved accuracy when measuring low concentrations of fluoride down to 0.001 ppm [211]; although IC is more expensive than ISE. A comparison of fluoride release from glass ionomer cements measured by ISE and IC gave nearly identical measurements and detected no statistically significant difference between the two methods [145].

1.11 Evaluation of fluoride release in clinical studies

An anticariogenic effect has been noted in number of clinical studies associated with increased salivary fluoride concentrations after topical application and release from dental restoratives [215] [216]. A constant slow supply of low levels of fluoride can be beneficial to health. Increasing the salivary fluoride concentration from 0.001 to 0.005-0.010 mmol/L may be effective in caries prevention [217]. Therefore, a number of *in vivo* studies measured the salivary fluoride concentration after topical fluoride application as in mouthwashes and toothpaste and compared it to fluoride release from dental restorative materials [218] [219] [141]. After 5-10 minutes of fluoride containing toothpaste application (1250 ppm), salivary fluoride levels elevated to 1-3 ppm [220] [221] [218]. When comparing the salivary fluoride levels from fluoridated toothpaste use, the concentrations were lower than from fluoride-

releasing restoratives [219]. It has been demonstrated that after the application of glass ionomer restoration, salivary fluoride concentration levels increased from 0.04 to 0.8-1.2 ppm. Furthermore, it was noted that these concentrations decreased to 0.5-0.8 and to 0.3-0.4 ppm, respectively 3-4 weeks later. When fluoride concentrations were measured one year after restoration, a concentration of 0.2-0.3 ppm of fluoride was found. It is worth mentioning that in these *in vivo* studies, patients were allowed to continue using fluoridated toothpastes [222] [223]. This is important to be taken into account as the regular use of fluoridated mouthwashes and toothpaste might change the baseline of salivary fluoride levels [141]. However, the clinical studies demonstrated that the anticariogenic effect of fluoridated dental materials is highly likely due to the increased fluoridation around the restoration site rather than an elevated salivary concentration. It has been shown that fluoride concentrations are increased in dental plaques [215] [216] particularly adjacent to fluoride releasing cement [219, 224, 225] . The concentrations were significantly higher in comparison to 1-5 μg/F^-/g plaque fluoride content following the use of fluoridated mouthwash [219].

According to Duckworth and Morgan [219], there are two phases of salivary fluoride clearance after toothbrushing: the first phase involves rapid drop of salivary fluoride concentration due to the removal of the topical fluoride and this phase lasts for 40-80 minutes. The second phase, during which the fluoride concentration gradually declines, reflects fluoride release from oral reservoirs such as tongue, mucosa, and surfaces of the teeth. Therefore, it is possible to speculate that the primary purpose of fluoridated restoratives is not to temporarily increase the salivary fluoride levels, which are in the fluoride range 15 minutes after topical application of mouthwashes and dentifrices. They act as fluoride reservoirs in the second phase of the fluoride clearance [141].

The mechanism of caries prevention by fluoride involves antimicrobial effects and increasing tooth surface remineralization [141] as fluoride increases tooth enamel remineralization and reduces demineralization. The fluoride antimicrobial effect is explained by inhibition of the bacterial metabolism, reduced colonization and enhanced competition and thereby reducing the overall dental plaque acidogenicity. The effects are mainly caused by inhibition of enzymes such as glycolytic enolase, proton-extruding ATPase, acid phosphatase, pyrophosphatase, peroxidase and catalase [226].

The mechanism of remineralization can be explained by the ability of fluoride to shift the demineralization process by increasing the resistance of dentine and enamel to the cariogenic micro-organisms and acid attack challenges. Fluoride absorption into crystal surfaces of the teeth promote remineralization and inhibition of the minerals dissolution due to the formation of fluorapatite [227]. The tooth enamel surface consists of 85% inorganic matrix and 3% organic material, i.e. proteins and lipids and 12 % water [228]. The inorganic matrix is carbonated-calcium hydroxyapatite [$Ca_{10}(PO_4)_6(OH)_2$]. These hydroxyapatite crystals are organised as rods, which are clusters of smaller crystallites. The spaces between the rods are filled with organic material which leaves a pathway for the diffusion of acids, minerals, and fluoride [229]. The acids produced from bacterial metabolism diffuse from the dental plaques to the adjacent tooth surface. Demineralization occurs, when the inorganic enamel matrix is broken down and ions are removed from the tooth surface [230].

The dissolution of the enamel surface depends on the processes at the tooth enamel interface. The enamel surface is covered by dental plaque and therefore subjected to cariogenic challenges. Both dental plaque and saliva contain concentrations of calcium and phosphate in lower ratio than the apatite in the enamel. The caries consists of two independent processes, the first one demineralization from the acids formed in the dental plaque and the second process is a repair process which involves remineralization near neutral pH. These processes are determined by the solubility of hydroxyapatite [229]. The role of fluoride in the remineralization process lies in its ability to increase calcium-phosphate precipitation. This will increase enamel crystal growth and was observed at fluoride concentrations as low as 0.05 ppm (=2.5 µmol/L) [231]. These events will lead to fluorapatite formation [$Ca_{10}(PO_4)_6F_2$]. Due to the lower solubility product of fluorapatite in comparison to hydroxyapatite, the enamel crystal growth will occur rapidly [232].

1.12 Flexural strength of dental composite

Mechanical integrity of dental restoratives is of clinical importance since restorations are placed under occlusal forces; ultimately these forces result in a reaction within the material network leading to deformation [233]. The durability of restorative materials can be compromised eventually. Therefore, dental restoratives have a minimal requirement of mechanical properties to withstand forces of occlusion without fracture and to have sufficient

rigidity to maintain shape under load [18]. This is specifically important since fracture is the most common cause for restoration failure [234].

Dental composites are subjected to forces of occlusion with the stress-strain relationship being the defining characteristic of their mechanical properties. Stress is defined as the internal force created within a test specimen, characterized as being opposite in direction and equal in magnitude to the external force applied [18].

$$s=F/A$$

F equals the force applied and A is the cross-sectional area. The unit for stress is Pascal (Pa). Stress applied to restorations within the mouth can be simple stresses such as compressive, tensile or shear or more commonly more complex situations in which combinations of the simple stresses are experienced [233]. These stresses result in alteration of restoration dimensions. The changes are dependent on the characteristics of the applied stress and the ratio of the dimension changes to the original dimension is defined as strain [235].

The mechanical behaviour of a material is related to its stress-strain ratio. The stress-strain curve is established based on the proportional relationship of stress-stain [233] [235]. A linear slope indicates a rigid material that can resist the stress applied with no deformation and return to its original shape when the stress is removed. While shallow stress-strain slope indicates a flexible material which undergoes deformation when stress is applied. The material's stiffness can be assessed by the elastic modulus or Young's modulus of elasticity, which is defined as the proportional limit of the stress-strain ratio that a material can withstand deformation within the elastic limit [236]. When the applied stress results in the permanent deformation of the material it is defined as plastic, as shown in figure 16 below.

Testing dental composite flexural strength is the standard method for strength evaluation according to the ISO 4049 [237]. Flexural strength can be defined as the maximum stress that a material can resist without failure under bending load. The required flexural strength for restorative material depends on the clinical application [238]. According to the ISO 4049 standard classification of dental composites, type 1 materials are indicated for occlusal restorations with flexural strength values of greater than 80 MPa, while type 2 materials are those indicated for other clinical applications and are of flexural strength of greater than 50 MPa [239]. The three point-bending tests, as shown in figure15, is one of the most common

tests to assess flexural strength [240]. The ISO standard recommends a specimen beam of $25\times2\times2mm^3$ and for the specimen to be polymerized in an overlapping curing pattern due to the large specimen size [237].

Generally, the mechanical properties of RBCs are affected by different factors. Good mechanical properties are essentially dependant on the degree of conversion. Two important aspects are to be considered here. Since the resin monomers are weaker than the polymers a higher degree of polymerization will increase the material strength. An optimal combination of resins will increase the degree of conversion and thereby the mechanical properties [16]. Secondly, the amount of residual monomer left after polymerization reaction will significantly affect the mechanical properties [52]. The residual monomers act as plasticiser that reduce the material mechanical properties and elastic modulus. A plasticiser is a substance that increases the flexibility/plasticity and decrease the viscosity when added to a material. The unreacted residual monomers are extractable and can increase the swelling and allow diffusion of water and fluids [81]. Therefore, an increased ratio of residual monomers will contribute to reduction of the material mass and subsequently decrease the mechanical properties.

Another factor that influences the mechanical properties of RBCs is the filler loading and the geometry of the filler particles. For example, composites with round filler particles and irregularly shaped fillers or mixture of both had higher flexural strength and flexural modulus, while composites with pre-polymerized fillers had lower flexural strength and flexural modulus [241]. The morphology of the fillers will affect the filler loading. The fillers are considered as the reinforcing phase of resin-based composite and in order to increase the mechanical properties of these materials, filler particles should be optimally loaded and dispersed. One strategy to control the morphology is grinding the filler particles to obtain maximum loading [14]. Since RBCs are bimodal, i.e., have more than one size distribution of fillers, smaller particles fill the spaces between the larger particles resulting in efficient packing. This will additionally reduce the volumetric shrinkage and stresses generated within the materials during the polymerization reaction [242] [243].

Finally, mechanical properties are affected by the resin monomer molecular architecture which is an important determinant of the mechanical properties [16]. The monomer

composition affects the mobility of the reactive groups during polymerization, and thereby primarily determines the degree of conversion. However, improved DC will not necessarily guarantee improved mechanical properties. For example, increasing the diluent monomer concentration such as TEDGMA in a Bis-GMA/TEGDMA copolymer improved the degree of conversion but lowered the strength [29] [244]. On the other hand, increasing the Bis-GMA ratio did not lower the strength but reduced the final degree of conversion [245] [246].

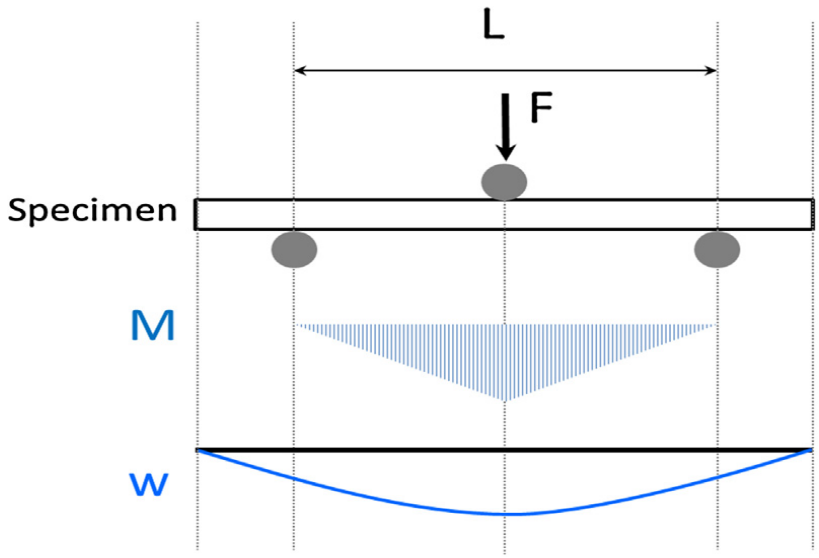

Figure 15: Schematic representation of the three point-bending test. M=bending moment, W=deflection. A beam shaped specimen placed horizontally on two supports, with loading point in the middle. L represents the distance between the two supports (span length of the beam specimen). F is the force applied on the specimen (in Newtons). The mechanical properties are calculated from the load displacement curve created due to the deflection at the midpoint from the load applied.

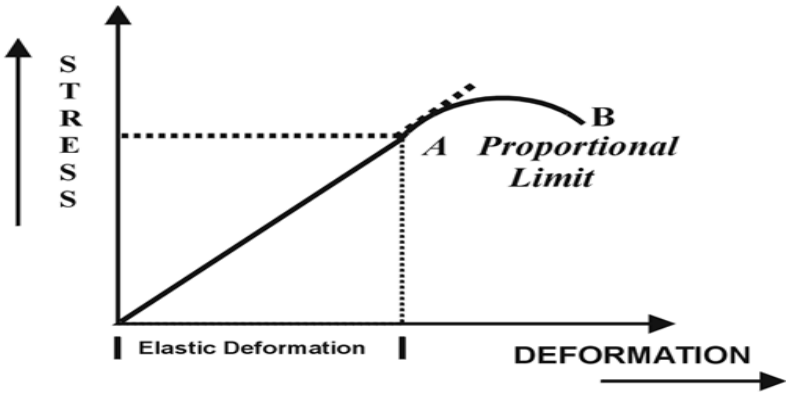

Figure 16: Representation of a stress-strain curve, where point A represent elastic deformation. Between A and B plastic deformation takes place while point B indicates failure of the material to resist stress and rupture. J. F. McCabe et al,.2008.

1.13 Water sorption of dental composite

All dental composites undergo degradation when exposed to the oral environment. Sorption and solubility are physical properties that reflect degradation and they depend on the degree of conversion [247]. The monomer's hydrophilicity and the filler ratio significantly affect the amount of water absorbed. Despite being generally hydrophobic, resin monomers contain certain functional groups or bonds such as hydroxyl groups as well as ether and ester bonds that show affinity to water [117]. When composites are in an aqueous environment, water will penetrate through the polymeric network and interact with the hydrophobic environment with two main consequences of the water absorption. Firstly, hygroscopic expansion and subsequent swelling of the polymeric network that will manifest through weight gain [248]. Secondly, since the degree of conversion is never complete, water diffusion will leach out unreacted monomers leading to weight loss of the material [249]. Therefore, water sorption and monomer solubility are dependent on the degree of conversion [250].

Water infiltration enhances the hydrolysis of siloxane bridges of the coupling agents that are responsible for the bridge formation between the silica fillers and resin monomers [25]. Once the bonds are broken, accelerated filler debonding, erosion and dissolution of the material matrix can result [251]. Degradation of the filler/resin matrix interface has been investigated by SEM imaging and shown to be the leading cause for the formation of interfacial microcracks in composites after storage in water [252].

Water sorption and hydrolysis can also be enhanced by chemical or biodegradation of the dental material [253]. Biodegradation of dental composite in the oral cavity has been shown to be associated with several mechanisms. Hydrolytic and proteolytic enzymes of either bacterial origin or inflammatory processes, in addition to bacterial metabolic by-products, have significant interaction potential with composite restorations in the mouth [254]. On the other hand, chemical hydrolysis is correlated with pH changes, saliva formulation and oxidation [255]. Both events, chemical degradation and biodegradation compromise the resin-based composite structural integrity and lead to the release of unreacted monomers from the restorative materials [256].

Overall, the degree of conversion is considered the primary factor determining dental composite water sorption and solubility. However, many factors affect the final degree of

conversion, for example, the method of curing different composites [257]. To make matters more complex, different degrees of degradation and solubility have been demonstrated in the same material cured to the same degree of conversion [258] suggesting that structural complexity of the material has a significant influence on sorption. Hence water sorption is clearly linked to the degree of conversion but cannot be correlated with double bond conversion only [257] [259].

1.14 Cytotoxicity of Dental Resin Monomers

The toxicity of dental resin monomers has been extensively studied over the last decades and a variety of adverse reactions have been reported. Examples include postoperative sensitivity [260], inflammatory reaction of the dental pulp tissue [261], immunological reactions [262], oral lichenoid reactions as shown in figure 17 [263] and apoptosis [264]. Moreover, allergic reactions have been described in patients, dentists and dental care professionals such as occupational asthma, contact dermatitis and rhinoconjunctivitis [265] [266]. Resin monomer toxicity has been ranked using various cell lines and primary cells including 3T3 mouse fibroblasts, Hela S3, human gingival fibroblasts and HaCat keratinocytes by different researchers as follows: Bis-GMA> UDMA> TEGDMA> HEMA [267-271].

In vitro studies have shown that different cells respond differently to specific monomers and the reported concentrations responsible for reducing cell viability by 50% (TC_{50}) varied among different cell types and donors [272]. TC_{50} values range from 0.06 to > 5 mM for different resin monomers, co-monomers, photointiators, inhibitors and other additives in composite materials tested. In addition, these studies were investigated in different primary human cells such as periodontal and pulp fibroblasts and mouse gingival fibroblasts [273].

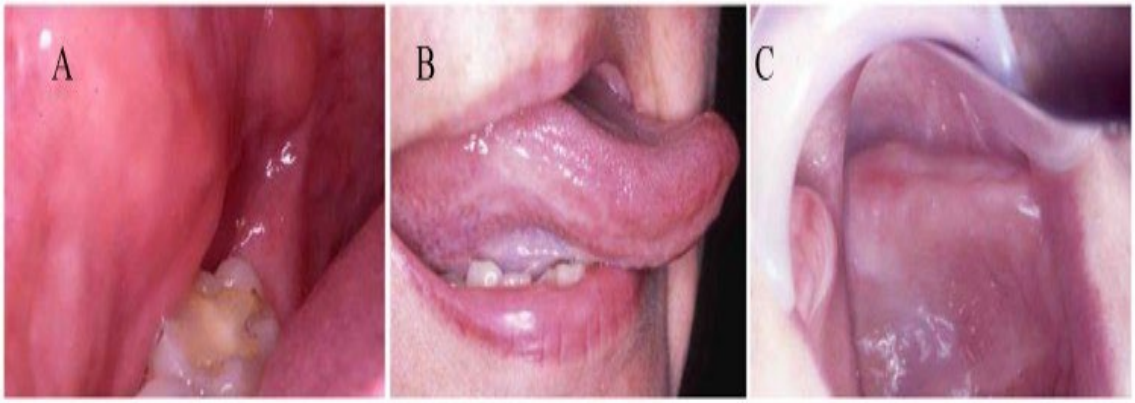

Figure 17: Adverse lichenoid reactions in response to resin based composite materials. A) Buccal mucosa with lichenoid lesion opposed to occlusal restoration. B) Lichenoid lesion on the lateral aspect of the tongue opposed to anterior restoration. C) Allergic reaction due to resin denture material in palatal tissue and alveolar ridge (Moharamzadeh et al., 2009).

Different viability assays have been used in testing the cytotoxicity of resins. Quantification of the released lactate dehydrogenase enzyme (LDH) is an effective parameter for determining cellular injury [274]. For example, TEGDMA (2 mM) and HEMA (4 mM) increased LDH release significantly in L2 rat, alveolar epithelial cells after 8 hours incubation. Interestingly, the amount of the released LDH from these cells was 3-15-fold higher than the amount released from malignant human lung cells (A549), again, indicating a cell type specific response [275]. Colorimetric viability assays were also used to assess the cytotoxicity of resin monomers. MTT (3-(4,5-dimethylthiazol-2-yi)-2,5-diphenyltetrazolium bromide) and XTT (2, 3-bis (2-methoxy-4-nitro-5-sulfophenyl)-2H-tetrazolium-5-carboxanilide) assays were used as quantitative methods to detect viable cells and proliferation rate [276]. Issa reported that lower concentrations of monomers can penetrate the cell membrane without lysis and result in disturbing mitochondrial functions; the consequences are cell lysis and death [277].

Urcan *et al.* used the XTT viability assay to test toxicity of dental monomers in human gingival fibroblasts after incubation with monomers for 24 hours. The results were in accordance with previous studies, I. e. Bis-GMA>UDMA>TEGDMA>HEMA [262].

Table 1: Monomer toxicity tested by Urcan and colleagues showing the half maximal concentrations of resin monomer in mmol/L. [262].

Substance	EC_{50}	Relative toxicity
HEMA	11.20	1
TEGDMA	3.60	3
UDMA	0.10	112
BisGMA	0.09	124

Many *in vitro* studies investigated the toxicity of monomers at relatively high concentrations that resulted in cell death and do not reflect the situation of tooth restoration *in vivo*. Mechanisms by which lower concentrations of monomers affect the dental mucosa are considered to be clinically more relevant. More emphasis should be given to cellular events that occur prior to severe cell damage or even cell death. Events including changes in protein expression, redox oxidative stress and DNA damage may be considered [278]. Lower concentrations of HEMA (1 mM or 2 mM) triggered certain adaptive responses such as increased levels of protective proteins [279]. These experiments concur with estimated HEMA concentrations in pulp tissue between 0.6 and 3.6 mM [280]. Low concentrations of HEMA (3 mM) also showed a general, chronic effect on protein expression in human gingival fibroblasts. For example, the expression of procollagen α1 protein was significantly reduced [281]. In addition, the hydrophilic co-monomer TEGDMA resulted in a significant reduction of the glutathione pool at subtoxic concentrations, again these early events were noted after a short incubation (2-6 hours) with resin monomers [282] .

The generation of excessive reactive oxygen species (ROS), depletion of intracellular glutathione and covalent binding to cellular proteins has been suggested as a potential consequence of resin monomer toxicity. ROS as a result of oxidative stress can lead to cell damage and reduced viability by activation of signalling pathways that lead to apoptosis. Reactive oxygen species are natural by-products generated in cells under physiological and pathological conditions. ROS derive from oxygen metabolism and generate cellular oxidative stress by damaging the plasma membrane, proteins, and DNA. In addition, ROS can be generated in response to stress such as heat, UV and ionizing radiation [283]. Depletion of

intracellular antioxidants such as glutathione result in a disturbed cellular redox balance which can lead to impaired cell growth and death [279].

The mechanism how TEGDMA affects ROS levels is well established. TEGDMA is considered as one of the main components that leach from restorative materials and accounts for 30-50% of dental composite materials [284] [29]. The unsaturated ester of TEGDMA interacts directly with the -SH group of glutathione, hence reducing ROS buffering capacity [285]. Likewise, binding of HEMA to serum proteins such as albumin by the formation of covalent bonds between the methacrylate group and lysine residues results in a modified immune response and autoantibody production [286].

The resin monomer's DNA damaging potential has been emphasized in the literature. Cells respond to DNA damage by activation of numerous mechanisms: 1) Cell cycle arrest via the activation of checkpoint proteins that prevent further cycle progression. 2) Change of the transcriptional profile, 3) Repair and removal of the damaged DNA and 4) Apoptosis [287]. Upon DNA damage the ATM protein kinase (ataxia telangiectasia, mutated) is activated. ATM is a member of the phosphatidylinositol 2 kinase (PIK3) protein family and displays serine/threonine kinase activity. ATM becomes phosphorylated as an early response to DNA damage. Interestingly, ATM mutations lead to the genome instability syndrome known as Ataxia Telangiectasia Syndrome [288]. DNA double-strand break formation associated with ATM activation in response to exposure to resin monomers (TEGDMA) was reported by Eckhardt and colleagues [289]. Moreover, p53 (tumour suppressor protein) activation as a consequence of ATM phosphorylation induced by HEMA was shown by Samuelsen [290] . ATM activation causes serine phosphorylation of histone H2AX, a member of the H2A protein family, to produce gamma H2AX. Specific antibodies against this modification can be used to quantify the number of double strand breaks in the area of damage [291]. Gamma H2AX foci in human gingival fibroblasts in response to short exposure to resin monomers have been quantified by various groups. The induced DNA double strand breaks by Bis-GMA at 0.09 mM (half maximum concentration) was 5 foci per cell. A concentration of 0.1 mM UDMA resulted in 3 foci/cell, while 11.2 mM of HEMA resulted in an average 2 foci/cell [292].

In general, the number of induced double-strand breaks in human gingival fibroblasts reflects the toxicity of the monomers, i.e., Bis-GMA>UDMA>TEGDMA>HEMA. Bis-GMA is

more lipophilic than other monomers which could explain the high toxicity of Bis-GMA. Bis-GMA and UDMA are used in dental composite material at a percentage of 70 %-75 % and potentially contribute to the material's cytotoxicity. Both monomers are relatively hydrophobic and leach in much lower concentrations than HEMA and TEGDMA in an aqueous environment. However, Bis-GMA and UDMA show toxic effects at lower concentrations compared to hydrophilic monomers such as HEMA. The reported toxicity mechanism seems to be similar and affect cell growth and disrupt redox balance and immunological reactions [293].

Most common resin monomers have been tested by genotoxicological assays such as micronuclei formation and increased DNA migration in comet assays [294] [295]. Moreover, microarray analysis of transcriptome changes induced by low concentrations of HEMA showed overexpression of transcripts involved in maintaining genome stability and DNA repair. Long term exposure to HEMA (greater than 24 h) revealed overexpression of genes responsible for cell cycle arrest in response to chronic damage [296] .

To conclude, the severity of the adverse reactions caused by resin material should be investigated with sensitive methods to gain an overall comprehensive understanding of its toxicity. The choice of the method to study toxicity will depend on the endpoint information required, cell viability, inflammatory markers, or genomic changes. In addition, considerations regarding costs and time to perform the assays may influence the choice of the assay [297].

1.15 RNA (ribonucleic acid) Seq Technology

The identification of tumour markers and characterisation of inflammatory diseases and chronic infections requires the ability to comprehensively catalogue and measure the variety of RNA molecules that are expressed over a wide range level. The study of transcriptomic changes, discovery and analysis of novel transcripts has changed in the recent years due to the emergence of the RNA seq technology [298]. Since then, RNA seq has become the gold standard for transcriptome analysis for its high dynamic range of detection, small variability and high resolution [299]. For example, transcriptome analysis by RNA seq allows exploring disease mechanisms by comparison between healthy and disease conditions.

Currently a variety of RNA seq and bioinformatic tools are available including platforms such as Illumina, Roche 454, Helicos BioSciences, and Oxford Nanopore. They all display significant sequencing capabilities for RNA and DNA and are characterised by high throughput, read length, low error rate, and ability to produce paired reads [299]. The protocol for sequencing includes many steps. Initially, RNA is isolated from tissues, treated with DNase to ensure no contamination with genomic DNA occurs and checked for RNA quality and purity. Then, the RNA is reverse transcribed to complementary DNA (cDNA) to allow for amplification and sequencing through DNA polymerases. The massive parallel RNA seq process then results in a huge number of reads that can be analysed bioinformatically.

The large expansion and use of RNA seq technology by scientists in transcriptomic studies has resulted in established methods and algorithms to monitor differential gene expression. These pipelines are well established, though there is a lack of general consensus on the best method for data analysis [300]. The generation of vast amounts of RNA seq data and their availability through public repositories such as NCBI gene expression Omnibus (GEO) facilitated systematic reviews and meta-analyses [301].

Applications of RNA seq are widespread across different biological disciplines for the identification of differentially expressed genes (DEGs) to detect disease markers in autoimmune diseases, tumours, neurological disorders and infectious diseases [302]. With relevance to this work transcriptomic studies have been performed to characterize mutations and DNA double strand breaks in genotoxic lesions periodontal and gingival tissues post-irradiation to investigate the risk of developing oral cancers [303]. Moreover, RNA seq has informed diagnosis and staging of oral squamous cell carcinoma to allow for early detection, since 60-70% of those cases are diagnosed after the lesion has become locally advanced [304].

The cytotoxicity of resin monomers *in vitro* to different cell lines has been studied in detail. However, comprehensive knowledge is missing of the underlying transcriptomic changes associated with cytotoxicity and oral tissue inflammatory reactions to unreacted resin monomers of dental composite. The identification of these inflammatory markers in gingival/epithelial tissues will inform strategies to mitigate tissue destruction and resultant

inflammation. Moreover, it will serve to improve dental material formulation by replacement of potential cytotoxic monomers with more cytocompatible resins.

1.16 Evaluation of dental materials

With an increasing number of dental products on the market, it is crucial for patients, dentists, and dental care professionals to be protected from potentially hazardous side effects of the materials. Therefore, manufacturers should thoroughly test new materials and follow extensive quality assurance procedures [305]. The quality of a new material is subjected to a number of specifications and general regulations. These specifications include information on how a new product should be tested and how minimal acceptable results are determined. However, the overall suitability of new materials should not be considered only according to those standards, as for instance, most restorative materials fail due to fatigue, and fatigue testing is not defined in current specifications [18].

The first legal regulation for dental material safety was established in the United States in 1970, the so-called medical device directive (MDD) which included the classification of dental materials as medical devices. The MDD was adopted by the EU in 1993 and tightly revised and amended to produce the Medical Device Regulations (MDR) in 2017. The safety and performance of medical devices including dental materials before being released to general practitioners are determined within those regulations. For a material to be marketed, compliance with the MDD or MDR general requirements for safety and performance must be demonstrated by the manufacturer [306]. Additionally, standard specifications of the international standards organization for evaluating the safety of dental materials (ISO 7405) have been developed. These consider the anatomical and physiological conditions within the oral environment to evaluate dental materials and establish a test strategy for evaluating novel materials including nanomaterials. This aspect has attracted increasing attention due to a potential release of nanoparticles and associated health concerns [307].

1.17 Aim of the study

The overall aim of this project is to develop novel bioactive dental composite materials and test their cytotoxicity. To achieve this goal, a model composite was developed based on UDMA (urethane dimethacrylate) and HEMA (2-hydroxyethyl methacrylate) and silica glass particles such as SiO_2. The bioactivity of this material is dependent on fluoride ion release to enhance tooth tissue remineralization and thereby reduce the occurrence of secondary caries. Therefore, nanofluorapatite ($NanoF_A$) was incorporated as a secondary filler.

The underlying cellular changes in response to the resin monomers used in the composite formulation was tested to consider the putative adverse effects from the resins. Cellular viability and gene expression changes in human gingival fibroblasts cells were evaluated.

The new composite material was characterised by measuring the mechanical properties, flexural strength, and elastic modulus in comparison to a commercially available composite. In addition, fluoride release was measured under three different storage conditions such as distilled water, artificial saliva, and acidified artificial saliva. The degree of composite polymerization was measured using infra-red spectroscopy, in addition, the released components from the set composite system were quantified by HPLC.

Finally, overall oral gingival tissue reaction to the novel composite materials was investigated. Dental composite specimens were incubated with oral gingival fibroblasts and their transcriptome changes characterised by RNA seq.

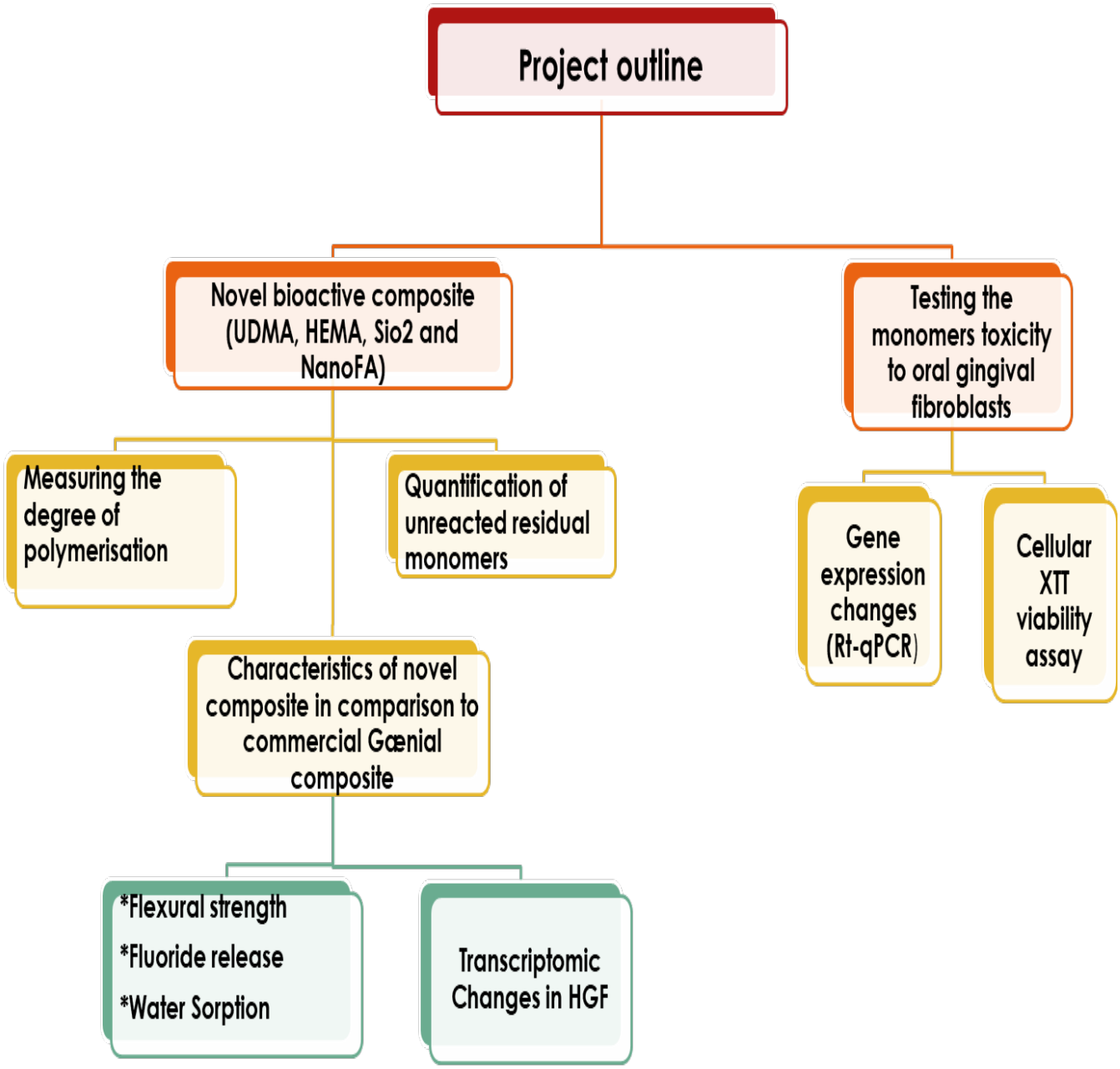

Figure 18: The outline and different stages of the research project.

Chapter 2: The effect of resin monomers on human oral gingival fibroblast viability and gene expression

2.1 Introduction

The improved aesthetic properties of resin-based composite material have contributed to their wide application in dentistry. The research on dental restorative materials mainly focuses on the improvement of mechanical and physical properties of the filler fraction of these materials. Little considerations are given to the monomer fraction. The monomers used in this project were UDMA (urethane dimethacrylate) and HEMA (hydroxyethylmethacrylate). UDMA is a resin dental material used in the composition of dental composites with reinforcing fillers. The higher polymerization rate and degree of conversion makes it a widely used monomer in commercial dental materials. [308]. On the other hand, HEMA is used in the composition of most adhesives in dentistry. The lower viscosity of HEMA qualifies it as diluent monomer in combination with UDMA in dental composite formula.

It has been shown that methacrylic monomers can be released from dental composites into the oral environment. The amount of released monomer depends on the degree of conversion and the type of monomers used in the material [309]. Hence, the biocompatibility of the materials is dependent on the degree of conversion. A higher degree of conversion of the materials will result in less unpolymerized monomers in the final polymer network. Therefore, a reduction of residual monomers that can leach out will limit the toxic effect on pulpal and oral mucosal tissues [310].

Studies on methacrylic resin monomer toxicity mainly focused on Bis-GMA toxicity [311] [312] [313] and reported significant adverse effects. Consequently, recent calls demand Bis-GMA free composites and UDMA based composites have become commercially available. However, research on UDMA toxicity is limited. Chang et al. investigated the toxic effect of UDMA in human dental pulp cells. Their findings showed morphological changes in the cells, reduced viability, and expression of chemical toxicity biomarkers [314]. Research addressing UDMA and HEMA toxic effects on human gingival fibroblasts are still scarce and further investigations are needed.

The oral mucosa is the oral gingival connective tissue that forms the lining of the mouth. It functions as a physical barrier protecting the underlying tissues against mechanical forces, toxins, and microbes. Oral mucosa consists of gingival fibroblasts that have an essential role

in oral wound healing [315]. Therefore, in this chapter, the effect of resin monomers UDMA and HEMA on oral gingival fibroblasts will be investigated.

2.2 Aims

To explore the toxic effects of the resin monomers UDMA and HEMA on oral gingival fibroblasts (HGF). A range of UDMA concentrations was examined to determine the toxic concentrations for the cells. In addition, the mechanism underlying monomer toxicity was studied by measuring the expression levels of various stress response genes. Cell viability assay (XTT) and real-time quantitative polymerase chain reaction (RT-qPCR) techniques were used in these investigations.

The expression of four genes involved in maintaining genome stability in oral gingival fibroblasts was assessed after 24-hour exposure to the dental resin monomers UDMA and HEMA. The four tested genes are:

- Dead box helicase (DDX11, NM_030653.4): A member of a family of RNA helicases involved in various functions depending on their location in the cell. They are important during embryogenesis, spermatogenesis and cellular growth and division, in addition to maintaining genome stability.
- Inositol-pentakisphosphate 2-kinase (IPPK, NM_022755.6): The protein encoded by this gene is a kinase that phosphorylates position 2 of inositol-1,3,4,5 pentakisphosphate to inositol-1,2,3,4,5,6 hexakisphosphate (IP-6). IP-6 induces a variety of functions including stimulation of DNA repair, endocytosis, and RNA export.
- X-ray Repair cross complementing2 (XRCC2, NM_005431.2): This gene is involved in the repair of DNA double-strand breaks by homologous recombination. XRCC1 functionally complements Irs1 in repair-deficient CHO cells (Chinese hamster ovary cells) that exhibit hypersensitivity to several different DNA-damaging agents.
- Double strand repair (RAD50, NM_005732.4): A protein involved in DNA double-strand repair. This protein forms a complex with MRE11 and NBS1 (also known as Xrs2 in yeast). This MRN complex (MRX complex in yeast) binds to broken DNA ends and displays numerous enzymatic activities that are required for double-strand break repair by nonhomologous end-joining or homologous recombination.

Furthermore, the response to oxidative stress in oral gingival fibroblasts exposed to UDMA will be examined. The overexpression of genes involved in impaired redox balance, reactive oxygen species (ROS) and inflammation will be explored. These genes are:

- Hemeoxygenase-1 (HO-1, NM_002133.3): The expression of this gene is provoked by inflammation, ROS production and glutathione depletion. For example, H_2O_2 has been shown to be a potent inducer of HO-1 overexpression. HO-1 functions to mitigate impaired redox-balance, to dampen inflammation, promote cell survival and maintain cellular integrity.
- Cyclooxygenase-2 (COX-2, NM_000963.4): Also known as prostaglandin endoperoxide (PTGS), is a proinflammatory mediator involved in prostanoids biosynthesis and functions as dioxygenase and peroxidase.
- Carboxylesterase2 (CES2, NM_001365405.1): The carboxylesterase gene family encodes for proteins involved in the detoxification of chemical toxins and hydrolysis of xenobiotics. These proteins play a role in lipid metabolism and are differentially expressed in human tissues, most abundantly in liver.

2.3 Methods and materials

2.3.1 Cell Culture

Cells were obtained from ATCC. (Primary Gingival Fibroblasts; Normal, Human, Adult (HGF) (ATCC® PCS201018, lot number: 64440682), these were isolated from the gingival tissue of the jaw of 60 year old Caucasian female. Cells (passage 4-8) were grown in T175 and T75 flasks in fibroblast basal medium (ATCC®PCS-201-030™). The medium was supplemented with fibroblast growth kit- low serum (ATCC®PCS201-041™). The growth kit contains the following components added to final concentrations as follows: Recombinant human basic FGF (5 ng/ml), L-glutamine (7.5 mM), ascorbic acid (50 µg/mL), hydrocortisone hemisuccinate (1 µg/mL), recombinant human insulin (5 µg/mL) and fetal bovine serum (2 %). When reaching 70-80% confluency, cells were passaged and seeded in 6-well plates with a density of 5×10^5 cells per well.

Cell exposure to dental resin monomers: The monomers 2-Hydroxyethyl methacrylate (HEMA; CAS-NO 868-77-9) and Urethane Dimethacrylate (UDMA; CAS-NO 72869-68-4) were obtained from Sigma Aldrich, UK. HEMA was dissolved in fibroblast basal medium, while UDMA was first dissolved in DMSO and then diluted in medium (final DMSO concentration

<1%). For gene expression analysis, cells received dental resin monomers at the following concentrations: HEMA 40 mM, 10 mM, 5 mM, and 1 mM, and UDMA 10 mM, 5 mM, and 1 mM. Cells were incubated with resins for 24 hours. For the analysis of stress response genes, cells received UDMA at the following concentrations: 0.5 mM, 1 mM, 2 mM, 3 mM, and 4 mM.

2.3.2 XTT Viability Assay:

Human gingival fibroblasts (ATCC PCS -201-018) were grown in T175 or T75 flasks. After they reached 75%-80% confluency, cells were washed with PBS and trypsinized. Cells used for these experiments were passage 6-8. Cells were then seeded in 96 well plates at a density of 20,000 cells per well and incubated for 24 hours. After that, cells were exposed to fibroblast basal medium containing various concentrations of UDMA and HEMA. UDMA of the following concentrations were used (first test series): 0.02 mM, 0.05 mM, 0.1 mM, 0.2 mM, and 0.3 mM. In the second test series the following concentrations were tested: 0.5 mM, 1 mM, 2 mM, 3 mM, 4 mM, and 5 mM. HEMA was first tested at 1 mM, 5 mM, 10 mM, and 40 mM, the second concentration series contained 1 mM, 2 mM, 3 mM, 4 mM and 5 mM of HEMA. The cells were incubated for 24 hours. Next, 100 µl of activated XTT reagent was added. The formazan quantification was performed spectrophotometrically at 450 nm (FLUOstar Omega Microplate Reader, BMG LABTECH).

2.3.3 RNA Extraction & Reverse Transcription:

After incubating oral gingival fibroblasts with dental resin monomers, cell lysis and RNA extraction were performed using the RNeasy Kit (Qiagen, 163029675) according to Qiagen's protocol. RNA integrity and the absence of genomic DNA was tested by 2 % agarose gel electrophoresis. The RNA concentration was measured by Nano drop (Thermo Fisher Scientific, NANODROP1000). Samples contained degraded or low RNA concentrations (<2µg) were excluded. For the cDNA synthesis, a total reaction of at least 2 µg of total RNA in nuclease free water up to 13 µl was used.

For cDNA synthesis, 2 µg of RNA was diluted in RNase free water up to 13 µl, then the Ominiscript cDNA kit (Qiagen, # 205111) was used. Components of the kit (2 µl of each random hexamers (0.4 µg/ml), dNTP mix (10mM), and 10x RT buffer) were added followed by

1 µl of Ominscript reverse transcriptase(200U). Reactions were incubated at 37 ^{o}C for an hour and then stored at -20 ^{o}C.

2.3.4 Polymerase chain reaction (PCR) and primer design

Primers were designed using the Ensembl genome browser (https://www.ensembl.org/index.html) and a primer design web tool (https://eu.idtdna.com/pages). In a first step, the whole transcript sequence was identified using the Ensembl genome browser. Then a region of 600 bp (this is an arbitrary number chosen to span intron/exon boundaries, the maximum capacity is 1000bp) containing multiple exons was selected ensuring these were protein coding areas and fed into the primer design program. The primers were then tested by BLAST using the Ensembl browser. Primer specifications are shown in table 2.

Table 2: Primer sequences.

Gene name	Gene Symbol	Primer Sequence 5' -3'	Annealing temperature	Product length
DEAD/H-box helicase11, Synonyms: CHL1, ChIR1	DDX11	Forward: ACCTGGAGGAAGAACACATAAC Reverse: CTTCTTCACCTCATGCACAAAC	58°C	86bp
Inositol-Pentakisphosphate 2-Kinase Synonyms: INSP5K2, IP5K	IPPK	Forward: CCGATTCTGTGTGTAGAGATTAAG Reverse: ATGCAGTATCGACAGACCTTATG	58°C	99bp
X-ray Repair cross Complementing2 Synonyms: FANCU, POF17	XRCC2	Forward: TCACCTGTGCATGGTGACTC Reverse: TTCCAGGCCACCTTCTGATTTG	58°C	148bp
Double strand break repair gene Synonyms: RAD502, hRad50	RAD50	Forward: AATTTGGCATT AGGGCGACAG Reverse: TCCTCAGCAT CCCGAAATTG	58°C	92bp
Prostaglandin-endoperoxide synthase 2 Synonyms: PTGS2, PHS-2	COX-2	Forward: GAAGAAAGTTCATCCCTGATC Reverse: CCAGAGTTTCACCGTAAATATG	55°C	165bp
Synonyms: HMOX-1	HO-1	Forward: GGCAGAGGGTGATAGAAGAG Reverse: GCAGAATCTTGCACTTTGTTG	55°C	157bp
Carboxylesterase2 Synonyms: CE-2, CES2A1	CES2	Forward: TCTCTGTCCATTTCCTTCTG Reverse: GTCAACAACAATGAATTCGG	55°C	166bp
B-Actin, housekeeping gene (reference gene)	β-Actin	Forward: AGAGCTACGAGCTGCCTGAC Reverse: AGCACTGTGTTGGCGTACAG	58°C	148bp

End point polymerase chain reaction was done to optimize the annealing temperature of the primers. A reaction of 10 µl contained 1 µl of cDNA, 0.5 µl of each forward and reverse primer (10 µM), 3 µl of RNase-free water and 5 µl of LightCycler® 480 SYBR® Green I master mix (Roche, 27584120). Amplifications were run at the following cycling conditions: Activation 94 ^{o}C for 5 minutes, denaturation 95 ^{o}C for 12 seconds, annealing 55 ^{o}C for 30 seconds, and elongation 72 ^{o}C for 10 seconds, 35 cycles and final extension at 72 ^{o}C for 10 minutes. A Multigene Optimax PCR machine (Appleton Woods) was used to run the reactions. The identity of PCR products was confirmed by sequencing.

RT-qPCR light cycler **(**LightCycler® 480, Roche) was used to determine the expression profile of the gene sets. A reaction was conducted in 96 well plate in three replicates, each well contained 0.5 µl of forward and reverse primers (10 µM), 1 µl of cDNA (1:5 diluted), 5µl of Syber Green mix, and 3 µl of nuclease free water. Negative control samples were included in the experiment and β-Actin was used a reference gene. The cycling condition for each primer pair are shown in table 3. Afterward, a melting curve analysis was conducted to verify the amplification of the desired product.

Table 3: qPCR conditions for each primer pair.

Target Gene	**Primer's pair**	**Amplification condition**
DEAD/H-box helicase11	DDX11-F DDX11-R	Hot start at 95^{o}C. Then 45 cycle of 10 seconds at 95^{o}C, 20 seconds at 58^{o}C and finally 5 seconds at 72^{o}C
Inositol-Pentakisphosphate 2-Kinase	IPPK-F IPPK-R	Hot start at 95^{o}C. Then 45 cycle of 10 seconds at 95^{o}C, 20 seconds at 58^{o}C and finally 5 seconds at 72^{o}C
X-ray Repair cross Complementing2	XRCC2-F XRCC2-R	Hot start at 95^{o}C. Then 45 cycle of 10 seconds at 95^{o}C, 20 seconds at 58^{o}C and finally 5 seconds at 72^{o}C
Double strand break repair gene	RAD50-F RADF-R	Hot start at 95^{o}C. Then 45 cycle of 10 seconds at 95^{o}C, 20 seconds at 58^{o}C and finally 5 seconds at 72^{o}C
Prostaglandin-endoperoxide synthase2	COX-2-F COX-2-R	Hot start at 95^{o}C. Then 45 cycle of 10 seconds at 95^{o}C, 20 seconds at 55^{o}C and finally 5 seconds at 72^{o}C
Heme oxygenase 1	HO-1-F HO-1-R	Hot start at 95^{o}C. Then 45 cycle of 10 seconds at 95^{o}C, 20 seconds at 55^{o}C and finally 5 seconds at 72^{o}C
Carboxylesterase2	CES2-F CES2-R	Hot start at 95^{o}C. Then 45 cycle of 10 seconds at 95^{o}C, 20 seconds at 55^{o}C and finally 5 seconds at 72^{o}C

2.4 Statistical analysis

A one-way *ANOVA* was performed to compare the effect of the different concentrations of HEMA and UDMA monomers on cell viability and gene expression of gingival fibroblasts. Tukey's HSD test for multiple comparisons was used to compare the mean of each monomer concentration on cell viability and the expression of selected genes.

2.5 Results

2.5.1 Viability Assay

The results of the cell viability assay are displayed graphically in the figures 19-22. The XTT viability assay was used to determine the toxic concentrations of the dental resin monomers. Human gingival fibroblasts were seeded at a density of 20,000 cells in 96 well plates in 100 µl of fibroblasts basal medium. After 24-hour incubation the medium was removed, and cells were treated with medium containing HEMA of the following concentrations, 1 mM, 5 mM, 10 mM, and 40 mM. Control cells received medium without monomers. After 24 hours, cells were treated with medium containing activated XTT reagent for 30 minutes before photometric analysis.

The results of the XTT assay for cells treated with the resin monomer HEMA, show significant reduction of human gingival fibroblast viability ($P<0.05$). The concentrations of 40 mM, 10 mM and 5 mM of HEMA resulted in death of all cells (figure 19). In contrast, 1 mM of HEMA resulted in an apparent increase in viability. An interesting finding was that the percentage of the HGF viability fell sharply between treatment with 1 mM and 5 mM of HEMA. Therefore, additional concentrations were tested within that interval.

For the second experimental series, the tested concentrations of HEMA were 1 mM, 2 mM, 3 mM, 4 mM, and 5 mM. Interestingly, 1 mM HEMA appeared to increase cell viability again suggesting that defensive mechanisms successfully mitigated the stress induced by 1 mM of HEMA (figure 20). The monomer concentrations 2 mM, 3 mM, 4 mM and 5mM resulted in a significant reduction in viability of HGF ($P<0.05$) as shown in the figure 20.

Cell treatment with UDMA concentrations of 0.02 mM, 0.05 mM, 0.1 mM, 0.2 mM, and 0.3 mM resulted in no significant reduction in the cell viability (figure 21). Cells were able to cope with these concentrations of UDMA. A slight increase in cell viability at the tested concentrations indicate an activation of cell protective mechanisms in response to the resin

monomer. These findings necessitated another set of experiments with higher monomer concentrations to determine toxic concentrations.

For the second experimental series with UDMA, the cells were exposed to UDMA at the concentrations of 0.5 mM, 1 mM, 2 mM, 3 mM, 4 mM, and 5 mM. The findings of the viability assay showed a 6 % decrease in the cell viability at 0.5 mM UDMA. At 1 mM UDMA, cell viability significantly decreased to 60 % ($P < 0.05$). The remaining concentrations were extremely damaging to the cells and resulted in very low viability rates indicating death of most cells, as shown in figure 22.

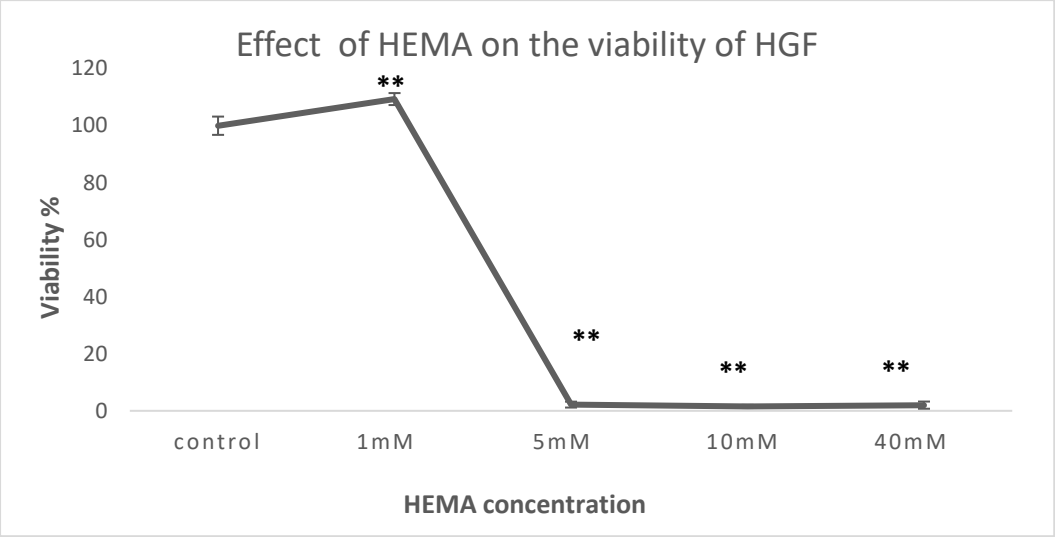

Figure 19: Effect of HEMA on the viability of human gingival fibroblasts after 24 hours incubation. Statistical significance was established using *ANOVA* and Tuckey's test for multiple comparisons; * $P<0.05$, ** $P<0.01$. The results are shown as mean ± SD of three individual experiments compared with the control. (n=3).

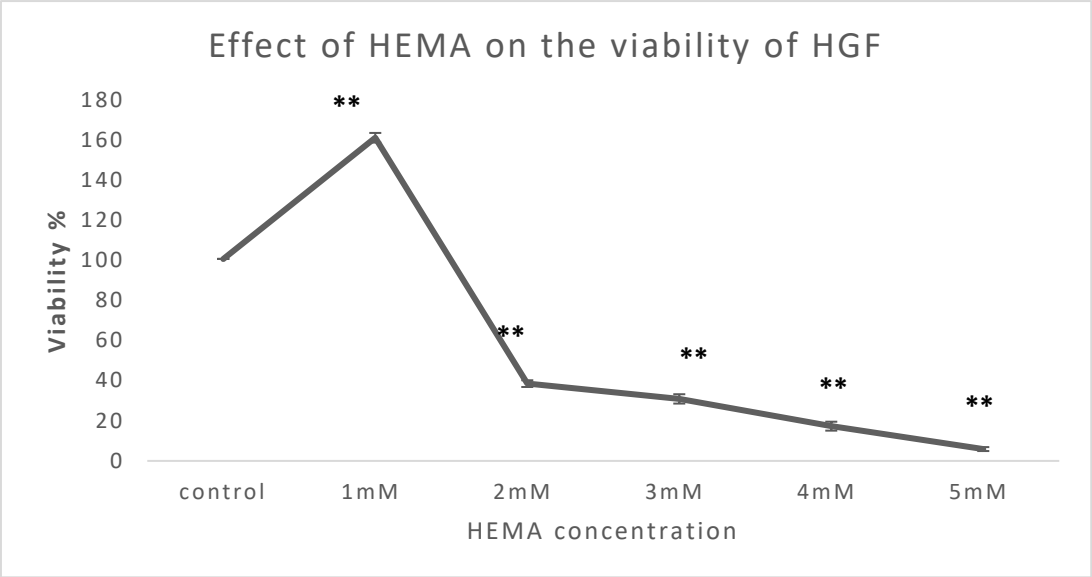

Figure 20: Effect of HEMA on the viability of human gingival fibroblasts after 24 hours incubation. Statistical significance was established using *ANOVA* and Tuckey's test for multiple comparisons; * P<0.05, **=P<0.01. The results are shown as mean ± SD of three individual experiments compared with the control. (n=3).

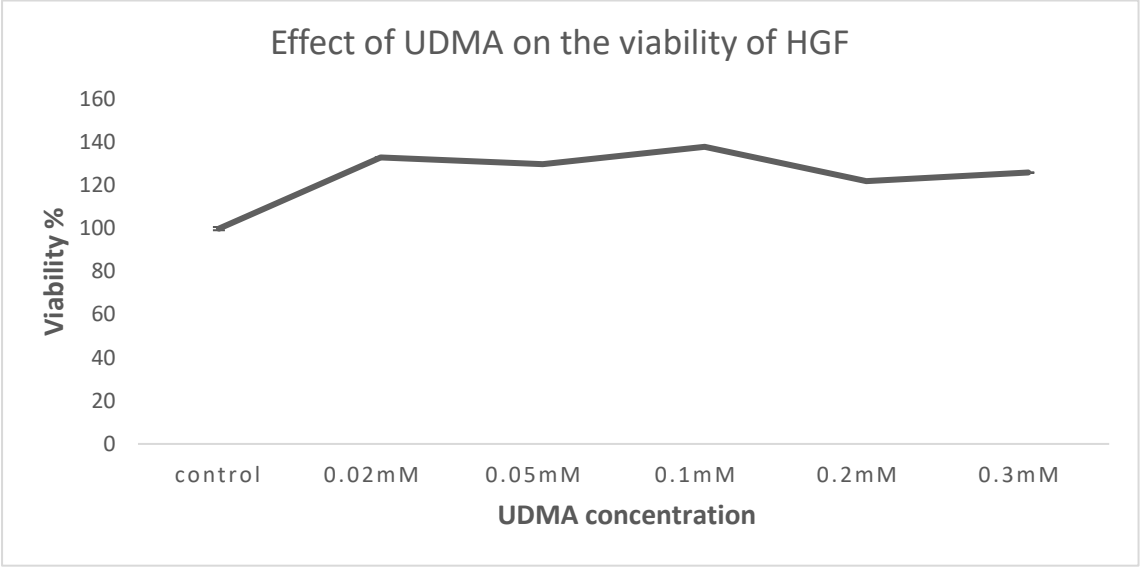

Figure 21: Effect of UDMA on the viability of human gingival fibroblasts after 24 hours incubation. Statistical significance was established using *ANOVA* and Tuckey's test for multiple comparisons. The results are shown as mean ± SD of three individual experiments compared with the control. (n=3).

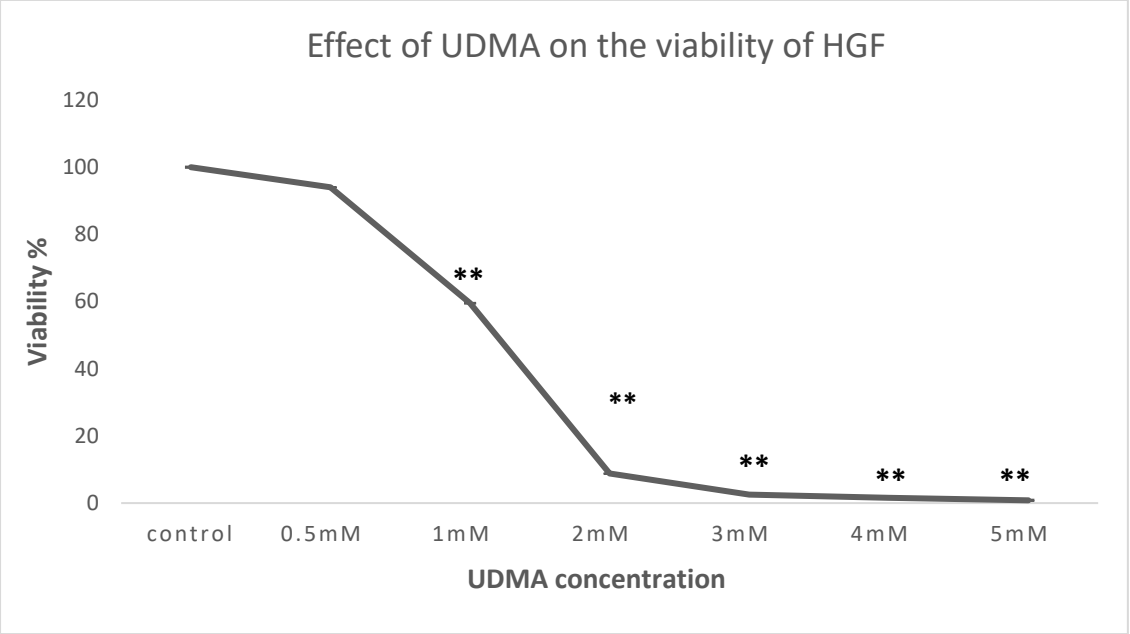

Figure 22: Effect of UDMA on the viability of human gingival fibroblasts after 24 hours incubation. Statistical significance was established using *ANOVA* and Tuckey's test for multiple comparisons; * P<0.05, **=P<0.01. The results are shown as mean ± SD of three individual experiments compared with the control. (n=3).

2.5.2 Results of RT-qPCR

The results of RT-qPCR are represented in the figures 23, 24 & 25. Overall, the dental resin monomer HEMA induced overexpression of transcripts involved in maintaining genome stability and DNA repair. While the resin monomer UDMA inhibited the expression of those genes. On the other hand, higher concentrations of UDMA resulted in upregulation of genes involved in inflammation and stress response.

RNA was extracted from human gingival fibroblasts cultured with the following concentrations of HEMA, 1, 5, 10, and 40 mM. RT-qPCR expression analysis showed a dose dependent expression increase of DNA repair genes as shown in figure 23. A slight upregulation of DDX11, IPPK, XRCC2 and RAD50 was shown in response to 1 mM HEMA. A statistically significant increase of IPPK ($P<0.05$) and RAD50 ($P<0.001$) was measured with 5 mM of HEMA. A 1.8-fold increase was detected for DDX11 and an up to 7-fold increase in XRCC2 transcript levels. A statistically significant expression change ($P<0.001$) of all four genes (DDX11, IPPK, XRCC2 and RAD50) was noted with 10 mM and 40 mM of HEMA.

After a 24-hour treatment of gingival fibroblasts with UDMA (1 mM, 5 mM, and 10 mM), qPCR data showed a down regulation of the four genes tested. Figure 24 shows the average of three experiments with a similar pattern of gene expression. The data obtained from qPCR analysis indicates that UDMA reduced rather than stimulated DNA repair gene expression.

The RT-qPCR data measuring the effect of UDMA on the expression of stress response genes showed that concentrations of 0.5 mM, 1 mM, and 2 mM of UDMA inhibited the expression of COX-2, HO-1 and CES2. Significant upregulation ($P<0.05$) of CES2 and HO-1 was found at 3 mM of UDMA. Moreover, the three genes (COX-2, HO-1 and CES2) were significantly increased at 4 mM of HEMA compared to other concentrations, figure 25.

Apparently, these significant gene expression changes in response to both monomers were seen at high toxic concentrations as measured in the previous section (viability assay). It is worth mentioning that RNA yields were significantly lower for these toxic concentrations compared to the control. Despite that majority of cells were dying at these concentrations few cells were surviving and produced sufficient RNA to be quantified by RT-qPCR. For example, with 40 mM of HEMA amount of RNA was 1.3 µg eluted in 30 µl RNase free water compared to 4.4 µg RNA for the control cells.

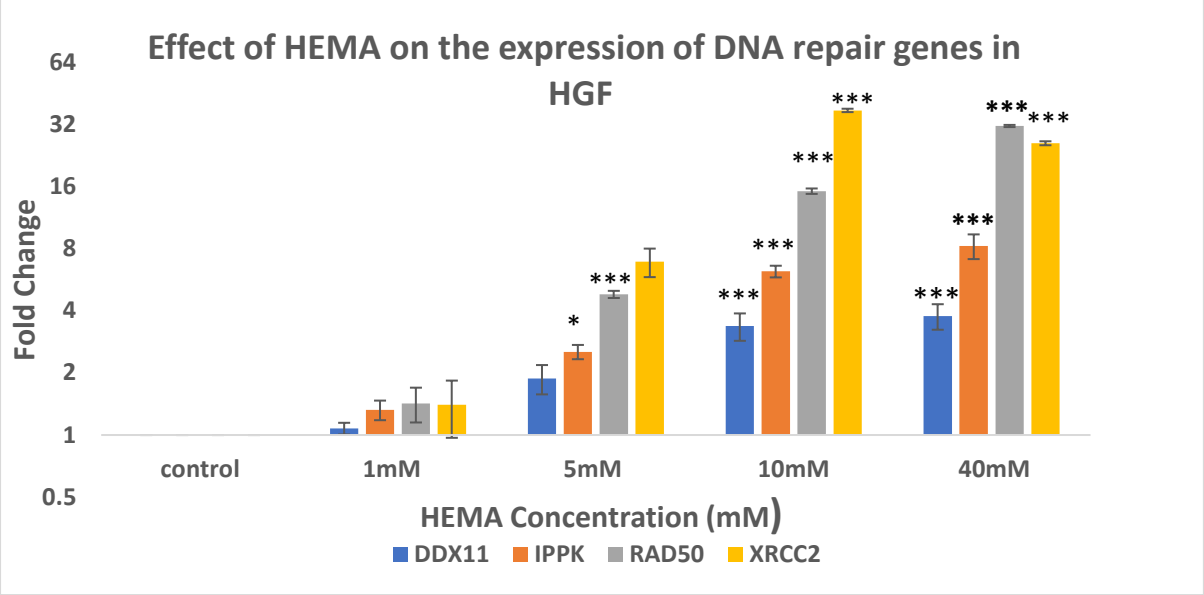

Figure 23: Effect of HEMA on the expression of DNA repair genes. Statistical significance is indicated ($P<0.05$=*, $P<0.05$, $P<0.0001$=***). The bars represent the fold change in relation to untreated cells.

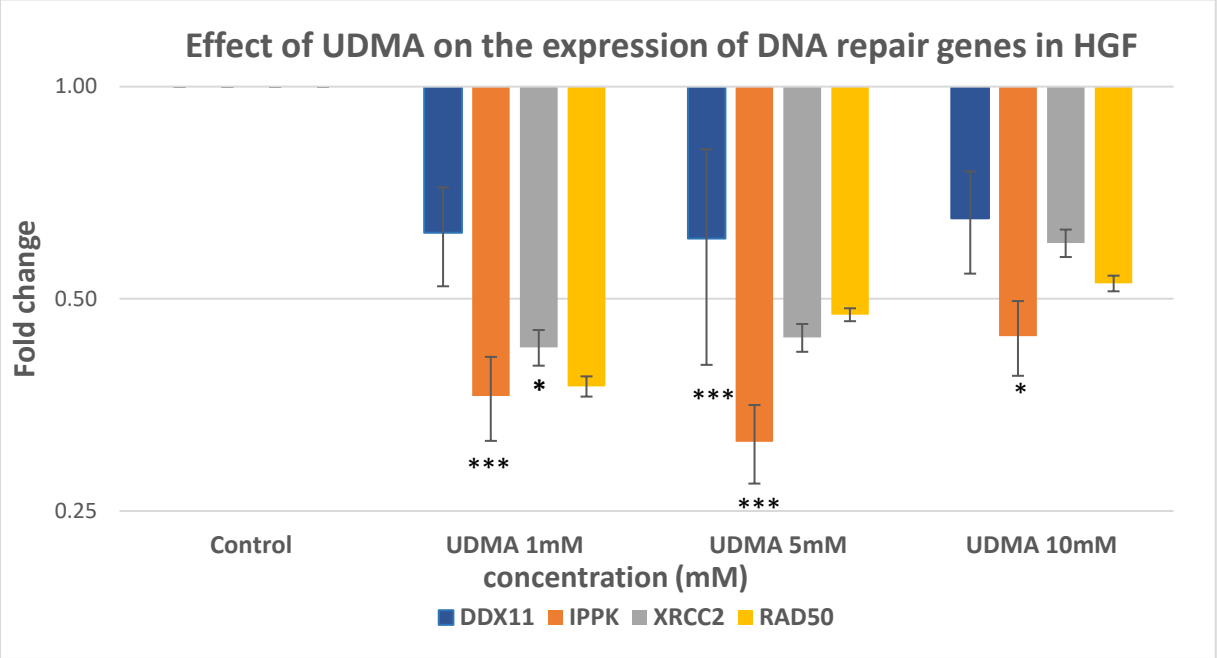

Figure24: Effect of UDMA on the expression of DNA repair genes. Statistical significance is indicated (P<0.05=*, P<0.05, P<0.0001=***). The bars represent the fold change in relation to untreated cells.

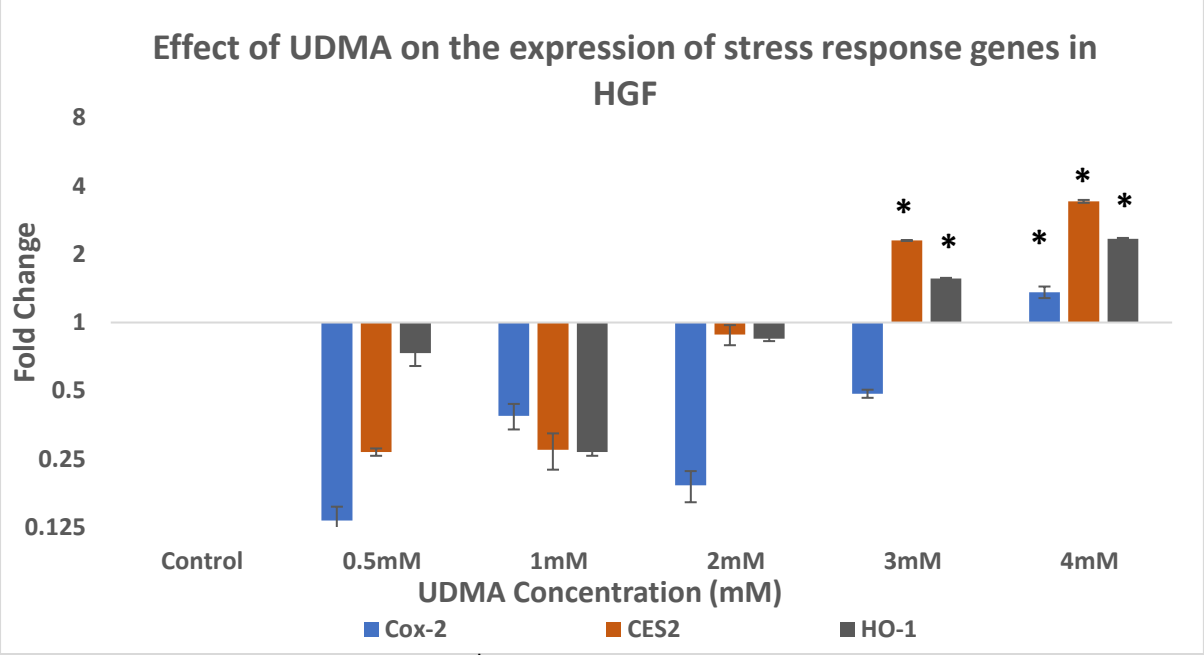

Figure25: Effect of UDMA on the expression of stress response genes. Statistical significance is indicated (P<0.05=*). The bars represent the fold change in relation to unchallenged cells.

2.6 Discussion

The aim of this part of the study was to investigate the effect of the resin monomers on oral tissues. UDMA and HEMA are the resin components that were used to develop the bioactive dental composite as will be described in the following chapter. Hence, characterizing the impact of these materials on the oral environment is essential. UDMA was chosen as the main monomer in the material formula as an alternative to BPA (Bisphenol A) to reduce the potential cytotoxicity of the final product. The other monomer in the formula was chosen for its hydrophilicity due to the presence of an additional hydroxyl group in the monomer chain. This will facilitate fluoride release from the bioactive composite material. On the other hand, adding HEMA to the final polymer network might result in the material absorbing water which then contributes to degradation or release of unreacted residual monomers. Therefore, evaluation and testing potential cytotoxic effects of these monomers is essential.

Cytotoxicity assays are useful testing methods to evaluate the biocompatibility of dental materials. Here, the XTT viability assay were chosen for this purpose in addition to gene expression analysis by RT-qPCR. The colorimetric XTT assay is a rapid and inexpensive method that measures the activity of mitochondrial enzymes which convert colourless XTT into formazan which absorbs light between 550 and 600 nm. The respiratory activity of mitochondria gives an indication of cell viability [316].

The XTT viability assay results showed 60 % cell viability of HGF at 1 mM UDMA compared to 1mM HEMA which caused no reduction of cell viability. On the contrary there was an apparent increase in cell viability in response to 1 mM of HEMA. Cell viability was 40 % at 2 mM of HEMA compared to 8 % at 2 mM UDMA. These results indicate that UDMA is more toxic to human gingival fibroblasts than HEMA at the same concentrations. These findings may be explained by the difference in the molecular mass between the two resin monomers. UDMA's molecular weight is 470.6 g/mol compared to 130.14 g/mol for HEMA. A direct relationship between molecular mass of a monomer and its cytotoxicity was suggested by Geurtsen et al., and Szep et al., [317] [273] . Accordingly, the higher the molecular mass of a dental resin monomer the greater the likelihood of cytotoxicity. The increased cell viability of HGF indicates that at low concentrations (up to 1 mM), HEMA may act as a signalling molecule to promote growth and development rather than being cytotoxic. This can be interpreted by

increased superoxide activity in cell culture exposed to monomers. Accordingly, it has been revealed that in response to oxidative stress reactive oxygen species (ROS) such as superoxides and hydrogen peroxide have a dual action either inducing a stress response or signal cell growth [318]. The XTT viability assay showed that 3 mM HEMA resulted in significant (70% $P<0.01$) cell viability reduction of oral gingival fibroblasts. The same concentration of HEMA examined by MTT after 24-hour exposure was shown to be non-toxic [281]. Moharamzaadeh hypothesised that there were variations in the response to toxic resin monomers among the same type of primary cells obtained from different donors. These variations were attributed to differences in intrinsic cell susceptibility to the monomers [272]. Additionally, it has been shown that the XTT viability assay can overestimate the cell viability results in cell cultures when superoxide ions are generated as these ions can convert the XTT salt to formazan and hence might overrate the cell viability [319]. Therefore, results can vary depending on the test assay and cell type.

In order to assess resin monomer interaction with oral mucosal tissues in more detail quantitative polymerase reaction was considered. Previous research into dental restorative genotoxicity has found that substances containing bisphenol A resulted in DNA damage in human cells as shown by comet assay [320]. In addition, exposure to some methyl methacrylate monomers such as TEGMA increased the number of micro-nucleated cells in bone morrow and DNA strand breaks in macrophages [321]. Therefore, RT-qPCR was used to assess the expression of DNA repair genes after HEMA and UDMA exposure to HGF cells.

The RT-qPCR findings suggest that a 24-hour incubation period with HEMA causes dose-dependent upregulation of DNA repair genes. Transcriptome changes of HGF after exposure to 3 mM HEMA for 24 and 96 hours has been assessed previously [296]. The findings were suggestive of triggering DNA repair mechanisms, specifically those genes involved in maintaining chromosomes and genome stability were found to be upregulated after 24 hours exposure and down regulated after 96 hours of exposure. The HEMA concentrations that were found to diffuse through dentin layer from dental restoratives are in the range of 1.5- 8 mmol/l [322]. Exposure time is important to consider when evaluating resin monomer toxicity as initially released resin in a nanomolar range might not have a toxic effect [323]. Long term elution of resin monomers should be considered when assessing the risk to human health. Restorative materials are exposed to erosion and degradation inside the mouth. Moreover,

they are liable to the effect of different solvents and salivary enzymes that facilitate the long term release of unbound resins [324] [325].

The qPCR results showed inhibition of DNA repair genes in response to the tested concentrations of UDMA. Of note, at these concentrations UDMA was shown to be non-mutagenic by Schweikl and co-workers as UDMA did not induce the formation of micronuclei in V79 cells [326]. Moreover, no point mutations were induced by UDMA as tested in Ames assays [327]. However, the role of UDMA in DNA damage cannot be ruled out as the inhibition of DNA repair mechanism may contribute to DNA damage. For example , the decreased expression of DNA repair proteins in response to UDMA might lead to higher mutation frequency, and as result increase the risk of genotoxicity due to oxidative stress inducing agents [328]. Moreover, one of the limitations of the RT-qPCR assay is its inability to detect DNA lesions that stop DNA polymerase. DNA lesions formed due to oxidative stress outside the amplified region are not detected by the assay [329]. Therefore, to further investigate UDMA toxicity, the expression of genes involved in inflammation such as COX-2 and antioxidant such as HO-1 and CES2 was considered.

To assess cellular cytotoxicity in response to dental resin monomers three biological systems have been used: Established cell lines, oral human gingival fibroblasts, and human keratinocytes. Cell lines are easy to grow, and reproducible results can be expected in repeated experiments. Though, established cell lines are not ideal model systems for the oral cavity, human oral gingival fibroblasts or oral keratinocytes are more relevant models and are preferably used to test for changes in gene expression. Oral fibroblasts are in direct contact with dental material, they are a major component of periodontal soft tissue and play an important role in the integrity of the tissue and its regenerative capacity. Therefore, primary gingival fibroblasts were chosen to investigate the expression of differentiation markers in response to dental material induced changes in the transcriptome.

Investigating whether the exposure to dental resin monomers induce oxidative stress in the cells of oral tissues and establish chemical toxicity is one of the main aims of this project. The expression of HO-1 protein, an antioxidant enzyme that catalyses the degradation of heme, helps to maintain cell viability, cellular integrity and reduce inflammation [330]. While cyclooxygenase (COX) isoenzymes such as COX-2 function during inflammation to enhance

prostaglandin synthesis [331]. Carboxylesterases play important roles in detoxification and drug metabolism and therefore they are abundant in GIT tract, liver and lung [332]. The upregulation of HO-1, COX-2 and CES2 in HGF was confirmed at 4 mM UDMA by RT-qPCR assay. These findings help to understand the response of HGF to UDMA exposure. The gene expression changes in gingival fibroblasts as a result of UDMA exposure give an indication that UDMA toxicity resulted from ROS production.

2.7 Conclusion

The viability assays and RT-qPCR results highlight that apoptosis, DNA damage and inflammation are potentially induced by HEMA and UDMA. These findings reflect toxicity by resin monomers to HGF. Whether these compounds result in toxicity in their polymeric state needs further investigations. In the following steps of the project dental composite materials were designed and their degree of polymerization measured by FTIR. Then the amount of residual monomers in the polymerized composite was measured. The effect of these residual monomers on gene expression changes in HGF was investigated by RNA Seq to give a detailed account of the potential toxic effects of dental composite materials on HGF.

Chapter 3: Development of experimental dental composites and testing their properties

3.1 Aims

- To prepare three monomer mixtures: Polymer 1, 100% UDMA, polymer 2 UDMA: HEMA 90%: 10% and polymer 3, UDMA: HEMA 80%: 20% and measure their degree of conversion.
- To specify the most suitable curing time for the three polymers.
- To test a potential difference in the degree of conversion between different surfaces of composite samples.
- To design model dental composites, by incorporating silica fillers and measure the degree of conversion for the filled composites.
- To develop novel bioactive dental composites by incorporation of $NanoF_A$ as secondary fillers.
- To quantify the residual unreacted monomers in the polymerized composite by HPLC.

3.2 Method and materials

3.2.1 Preparation of the monomer mixtures

The monomers 2-hydroxyethyl methacrylate (HEMA; CAS-NO868-77-9) and urethane dimethacrylate (UDMA; CAS-NO 72869-68-4) were obtained from Sigma Aldrich, UK. Bottles of amber glass were used to prepare the polymers. HEMA and UDMA were mixed for 30 minutes using a magnetic stirrer at 70°C. The photosensitizer camphorquinone (CQ) and accelerator 4- ethyl dimethyl aminobenzoate EDAB (Sigma –Aldrich Company Ltd., Dorest UK) were added after obtaining a homogenous mixture, at a weight ratio of 1 % wt. Mixtures were stored in containers made of amber glass to prevent light penetration, and covered with aluminium foil and stored at 4 °C.

Table 4: Concentration of monomers used to prepare the three dental composites.

UDMA-HEMA percentage	UDMA(g)	HEMA(ml)	CQ 1% (g)	EDAB 1%(g)
100 %	20 g	0	0.2 g	0.2 g
90 %-10 %	18 g	2 ml	0.2 g	0.2 g
80 %-20 %	16 g	4 ml	0.2 g	0.2 g

3.2.2 Designing experimental dental composite materials

Three model dental composites were synthesized from chemicals listed in table 4. These were based on three monomer ratios, composite 1: 100 % UDMA (no HEMA), composite 2: UDMA: HEMA 90 %: 10 % and composite 3: UDMA: HEMA 80 %: 20 %. The photo-initiator system used was CQ: EDAB, at a weight ratio of 1 % of the monomer weight. The filler was silanised silica glass (First Scientific Dental Materials - GmbH -Elmshorn, Germany) used at 63 vol %. Dental composites were prepared in a two-step procedure. First, the monomer blends were prepared as described earlier in the monomer mixture preparation. In a second step the fillers were gradually added (table 5). A centrifugal mixer, shown in figure 25 (Speed-Mixer™, DAC 150.1 FVZ, Hauschild Engineering, Germany) was used to mix the composites at a speed of 2000 rpm for 2 minutes for each portion. For composite 1, a visibly homogenous mixture was obtained. For composites 2 and 3 solvent was added (acetone, Sigma Aldrich 20% of monomer weight) to obtain a homogenous mixture.

Table 5: Composition of silica filled experimental composites.

Material	Filler size	UDMA:HEMA ratio	Silica filler	Monomer +EDAB& CQ
Composite 1 (63%vol filler)	0.75 µm	100 %	19.25 g	5.75 g
Composite 2 (63% vol filler)	0.75 µm	90: 10	19.25 g	5.75 g
Composite 3 (63 % vol filler)	0.75 µm	80: 20	19.25 g	5.75 g

3.2.3 Preparation of bioactive NanoFA containing Dental Composite

Novel composite materials were produced using chemicals listed in table 6. The following monomer weight ratio UDMA:100 and UDMA: HEMA 80: 20 were used. The photo-initiator system used was CQ: EDAB, at a weight ratio of 1 % of the monomer weight. The filler was silanised silica glass (First Scientific Dental Materials - GmbH -Elmshorn, Germany) used at 42.1 % volume ratio. The secondary filler NanoFA was added at 20 % weight ratio.

In plastic a container, the NanoFA filler (25gram) was added first, then monomers containing the photo-initiator system were added next. The mix was centrifuged using a speed mixer (Speed-Mixer™, DAC 150.1 FVZ, Hauschild Engineering, Germany) for 2 minutes at 2000 rpm. Next the silica fillers were added at incremental ratio after dividing them into four sections. Acetone at 20% of monomer weight was added to obtain homogenous material. Commercial G-ænial Anterior (GC, Europe) was chosen as a comparator, composition in table 7.

Table 6: Final composition of Nano-filled experimental composites**.**

Material	Filler size	UDMA: HEMA	Resin	Silica fillers	NanoFA fillers
1) 42.1 % silica 20 % NanoFA	0.75 µm	100 %: 0	5.60 g	15.52 g	3.88 g
2) 42.1 % silica 20 % NanoFA	0.75 µm	80 %: 20 %	5.56 g	15.55 g	3.89 g

Table 7: Composition of the Gænial Composite.

Gænial Anterior (GC, Europe)	
Resin	Mixture of urethane dimethacrylate monomer (UDMA) and dimethacrylate co-monomer
Fillers	- Pre-polymerized filler (16-17 µm) silica containing: Strontium (400 nm) and Lanthenoid Fluoride (100 nm). - Inorganic filler: inorganic silica > 100 nm + dispersed fumed silica (16nm).

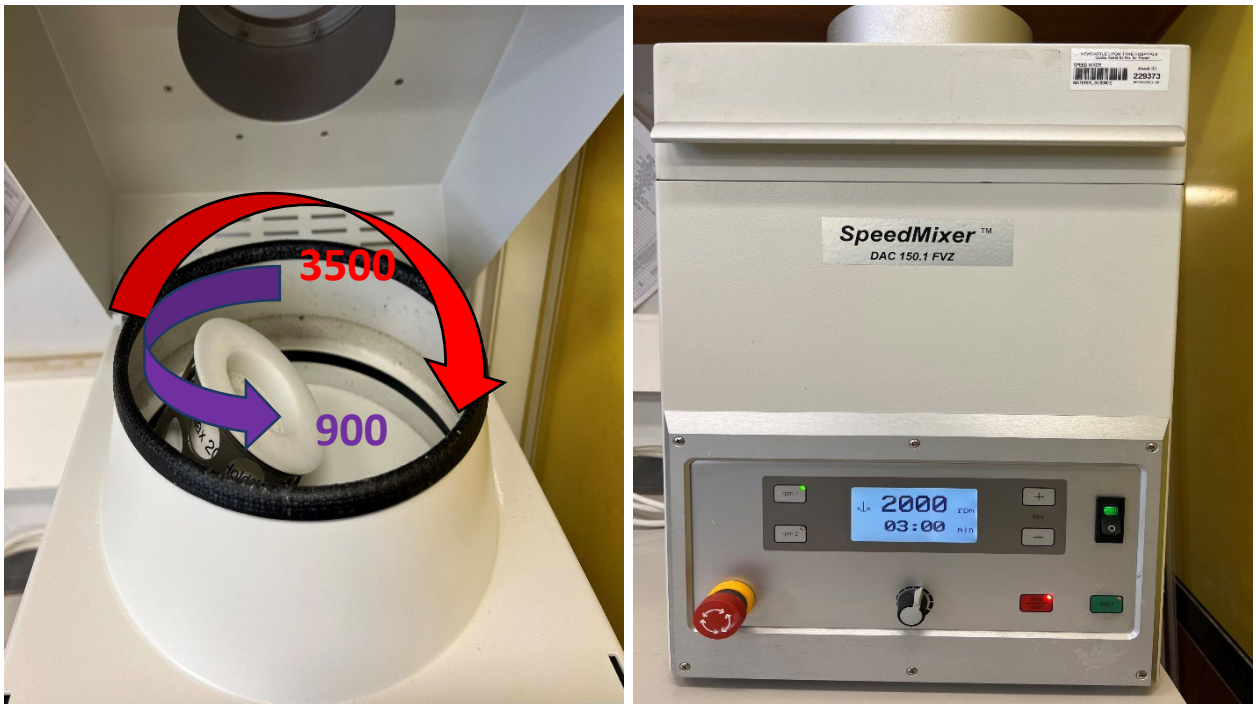

Figure 26: DAC system (Speed-Mixer™, DAC 150.1 FVZ, Hauschild Engineering, Germany). The picture on left demonstrates the two rotations of the speed mixer. The first is in a clockwise direction with a maximum speed of 3500 rpm, while the second is in anticlockwise direction and rotates the sample around its own vertical axis with maximum speed of 900 rpm.

3.2.4 Degree of Conversion

For the three polymers and composite materials, the degree of conversion was recorded by Attenuated Total Reflection Fourier Transform Infrared (ATR- FTIR) Spectroscopy (Spectrum One, PerkinElmer, Inc., Waltham, MA 02451 USA). Five samples were measured for each material. For the polymers, the degree of conversion was recorded for five curing times (5, 10, 20, 40 and 60 seconds). 5 mm metal molds were used to prepare the samples (figure 28). The mold was sandwiched between two Mylar strips (Kent Dental, Gillingham, UK) on a glass slide.

After pouring a small droplet of monomer mixture into the mold another matrix strip was placed on the mold and a small glass slide was slightly pressed to generate a flat surface. (Figure 27).

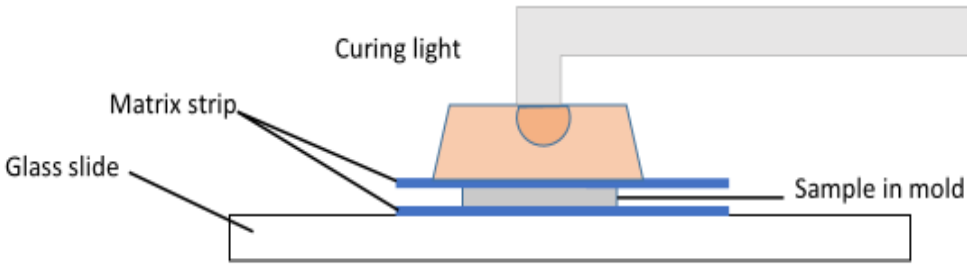

Figure 27: Set-up for the curing of dental composite materials.

Samples were polymerized by blue light using a LED light cure unit (EliparTM DeepCure-S, 3M ESPE, 3M Deutschland GmbH, Germany). Light intensity ranged between 1100-1140 mW/cm^2 as recorded with a Bluephase Meter II lightmeter.

Figure 28: Metal molds used to prepare composite samples.

3.2.5 Recording FTIR Spectra and calculating the degree of conversion

Attenuated Total Reflection Fourier Transform Infrared (ATR- FTIR) Spectroscopy (PerkinElmer, Inc., Waltham, MA 02451 USA), (figure 29) was used to record the degree of conversion for the samples. Unpolymerized monomers of each mixture were recorded first as a reference. The diamond plate of the spectrometer was cleaned with 70% ethanol and a background measurement was recorded first. Then a small droplet of polymer was put on the diamond plate. Absorption peaks for the top and bottom of the polymerized samples (n=4) (figure29) were then measured under the following conditions: 16 scans, wavelength 400-4000 cm^{-1} and a spectral resolution of 4 cm^{-1}.

The changes in peak height which represent the absorption intensities of aliphatic C=C bonds at 1640 cm^{-1} and the internal standard C=O carbonyl group at 1720 cm^{-2} for the polymerized samples were compared to unpolymerized monomer to calculate the degree of conversion. The following equation was applied:

$$(\%\ C{=}C) = \frac{[\boldsymbol{Abs\ (aliphatic)/Abs\ (aromatic)]\ polymer}}{[\boldsymbol{Abs\ (aliphatic)/Abs\ (aromatic)]\ monomer}} \times 100$$

Degree of conversion=100-(% C=C) [333].

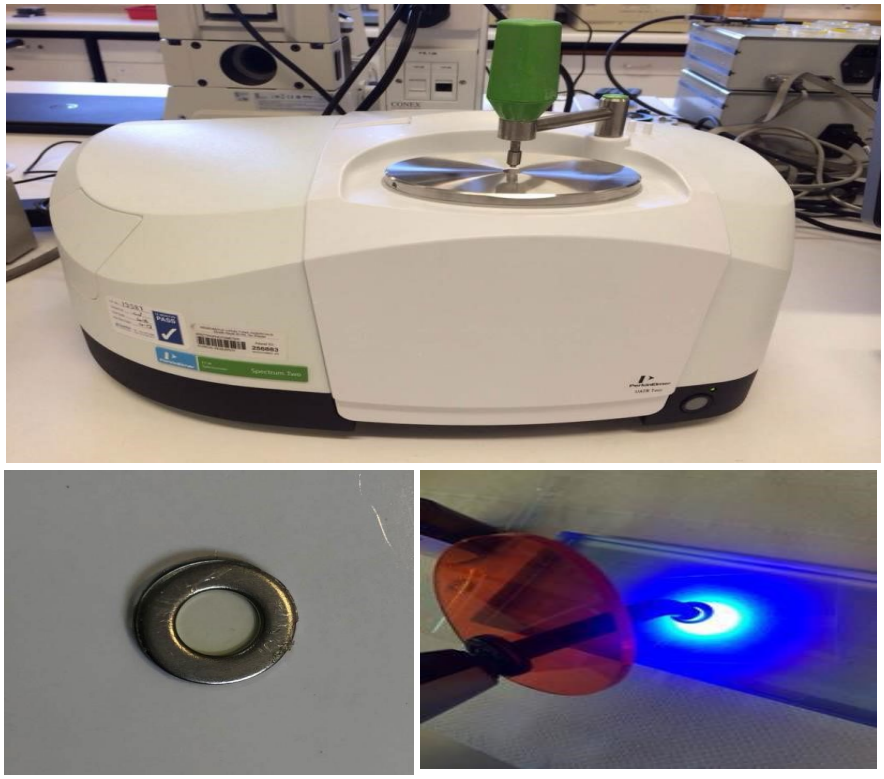

Figure 29: Preparing and curing composite specimens to measure the degree of conversion by FTIR.

3.2.6 Monomer release from dental composites

3.2.6.1 Sample preparation

A plastic teflon mold of 10mm diameter and 1mm thickness was used to prepare composite samples. The samples were polymerized using a blue light LED cure unit (EliparTM DeepCure-S, 3M ESPE, 3M Deutschland GmbH, Germany). After polymerization, each sample was immediately immersed in a glass container with 3 mL of 75 % ethanol in H_2O at 37 ^{o}C. During immersion the containers were shaken for 10 seconds. Thereafter 400 µL samples were taken from each container at 1 hour, 2 hours, 3 hours, 8 hours, and 24 hours. The monomers UDMA and HEMA in the samples were analysed by high performance liquid chromatography (HPLC).

3.2.6.2 HPLC analysis

The samples were analysed using a HPLC system Agilent 1260 Infinity II Multisampler (G7167A), supplied with an Agilent 1290 Infinity II Flexible Pump (G7104A) and a multicolumn thermostat (MCT) (G7116A). The detector was from Agilent, 1290 Infinity II Diode Array Detector (DAD) (G7117B) and the Syncronic C18 column was purchased from Thermo Fisher Scientific.

The mobile phase was a solution of 60 % methanol, 25 % water and 15 % acetonitrile with a flow rate of 1.5 mL/minute. The injection volume was 20 µL. UDMA and HEMA calibration curves of different concentrations were performed to obtain standard chromatograms of the two monomers. The concentration of each monomer was calculated by comparing the obtained peak areas of monomer chromatograms to the standard series.

3.3 Statistical Analysis

Independent samples t-test was conducted for the degree of conversion between the top and bottom surfaces of the samples. A *One-way ANOVA* was used to compare the effect of different curing times on the degree of conversion of composite samples. HPLC data were analysed by *Mixed assumption ANOVA.* The statistical package, IBM SPSS statistics, version27 was used.

3.4 Results

3.4.1 Degree of conversion (DoC%)

Figures 30 and 31 represent the degree of conversion for top and bottom surfaces of the samples for the three polymers. Independent samples t-test suggested little differences between the degree of conversion measured at the top surface and the bottom surface of the samples. Only in a few samples was a significant difference ($P<0.05$) between the degree of conversion at the top and the bottom.

Polymers with the compositions 100 % UDMA and 90 % UDMA: 10 % HEMA had nearly the same degree of conversion. The polymer with 80% UDMA: 20% HEMA had the highest degree of conversion, up to 68 %. For the effect of the curing time on the degree of conversion of the three polymers the *One-way ANOVA* test with multiple comparisons post HOC Tukey test was conducted. Multiple comparison post hoc testing showed no significant difference ($P>0.05$)

between the different curing times (5, 10, 20, 40 and 60 sec) on the degree of conversion of the three polymers.

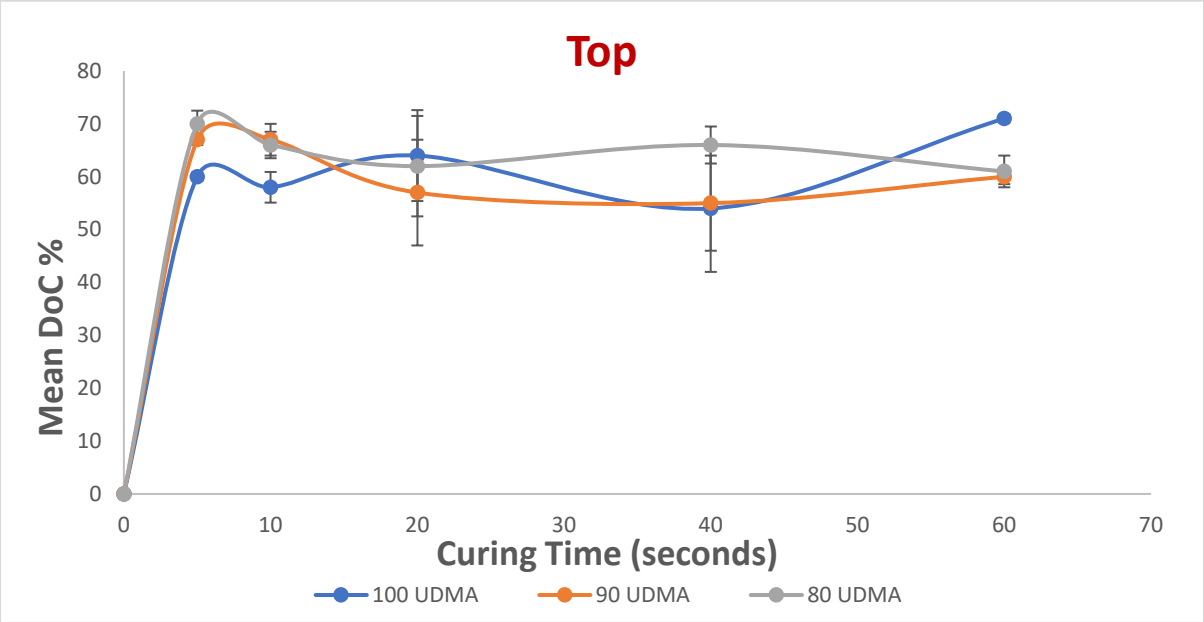

Figure 30: Mean DoC% for the three composite polymers (top surface measurements). Error bars represent standard deviation.

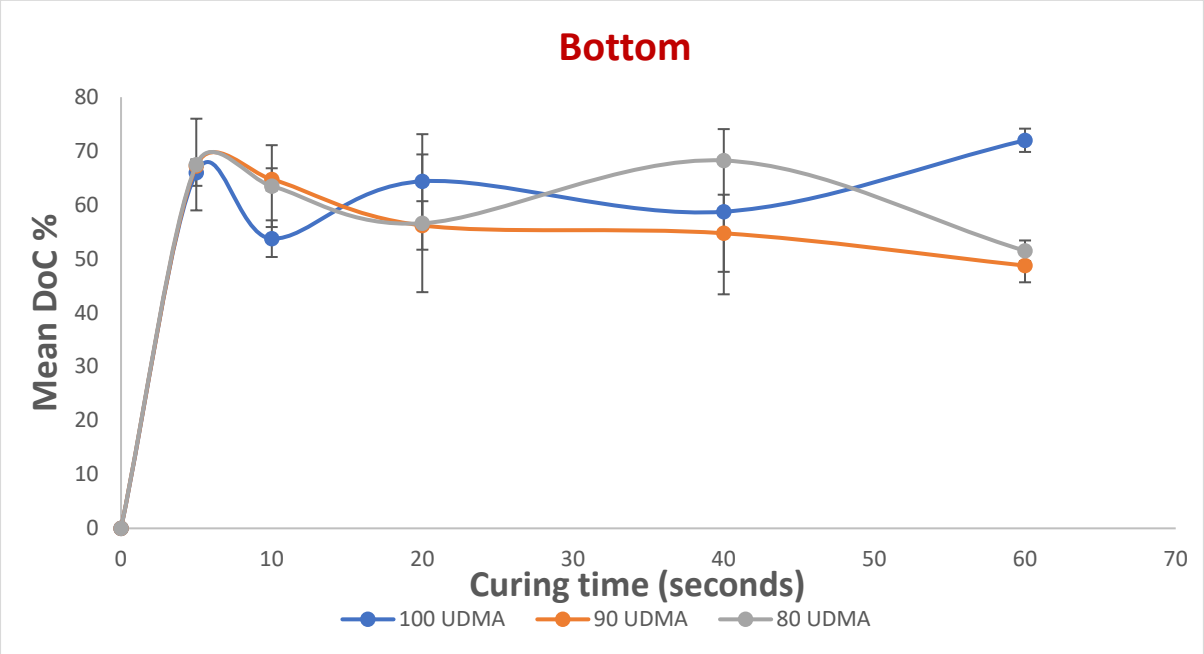

Figure 31: Mean DoC% for three composite polymers (bottom surfaces). Error bars represent standard deviation.

The prepared new materials are shown in the figures 32-34. For composite 1 which is based on 100 % UDMA, a visibly homogenous mixture was obtained after adding the filler. To composites 2 and 3 the fillers were added incrementally. After first and second increment, some fillers were not mixed properly and after the third increment 1.15 g of acetone were added.

The NanoFA filled composite was prepared with 80 % UDMA: 20 % HEMA, silica fillers 63 % volume ratio and NanoFA as secondary filler at 20 % weight ratio, a homogenous mixture was obtained as shown in figure 31. Interestingly, no homogenous composite was attained with 100 % UDMA, silica and NanoFA fillers. The material turned powdery, figure 32, when no HEMA was involved in the formula.

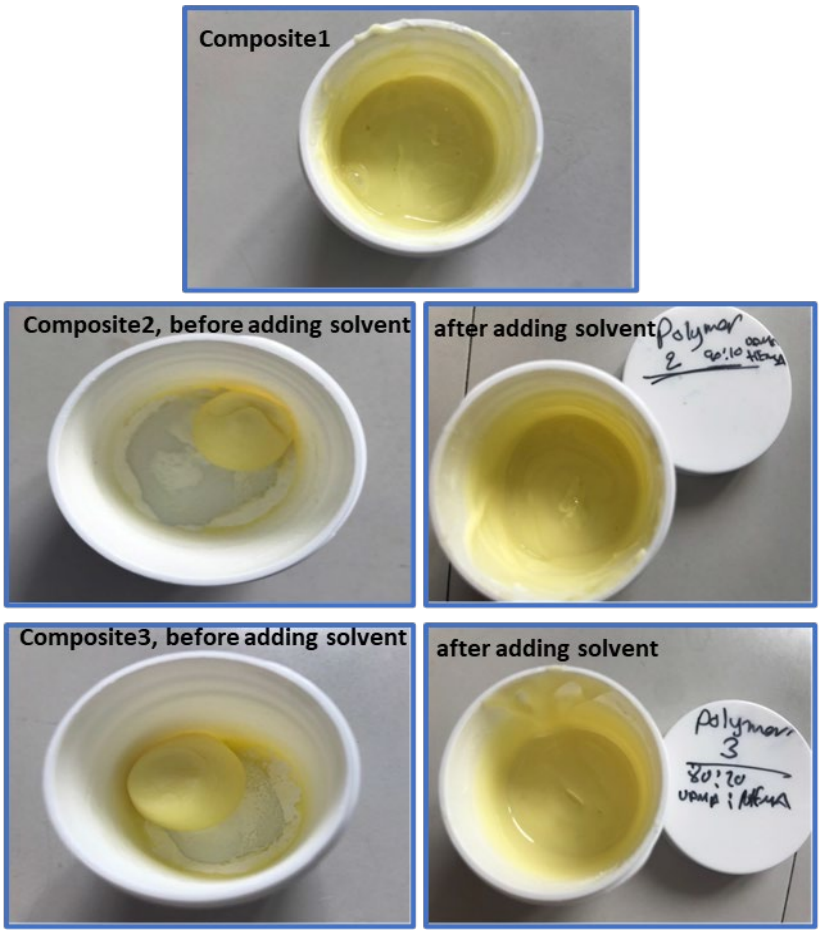

Figure 32: Model dental composites and the effect of acetone. Composite 1: 100 % UDMA, Composite 2: 90 % UDMA: 10 % HEMA and composite 3: 80 % UDMA: 20 % HEMA. The pictures on the left show the materials after mixing the monomer blend with the filler but before adding solvent, while pictures on the right show the materials after adding the solvent.

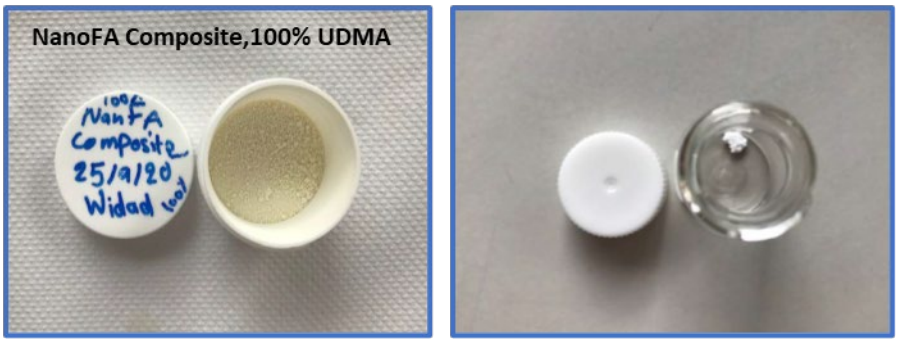

Figure 33: NanoFA composite material with 100% UDMA monomer and no HEMA.

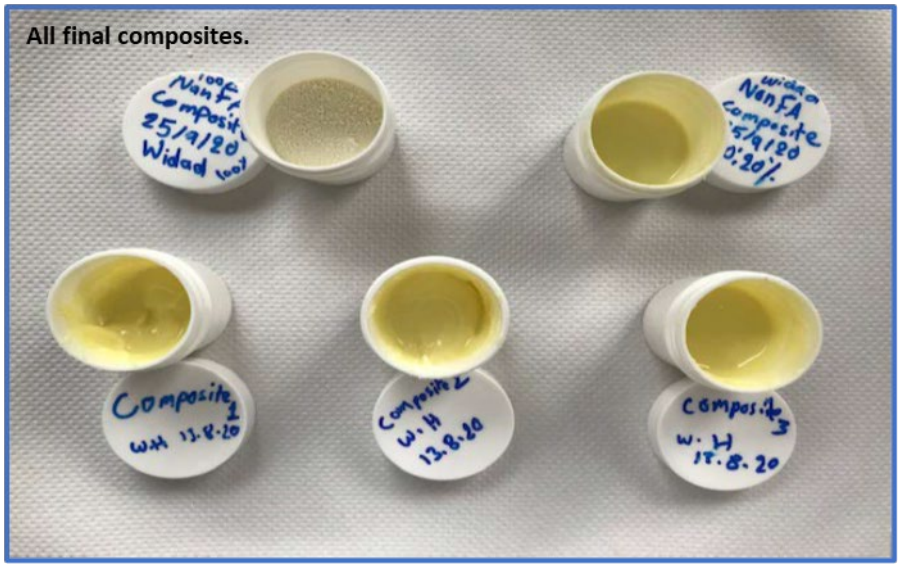

Figure 34: All final experimental dental composites materials designed in the lab.

The results of degree of conversion measurements of filled composite materials are summarized in table 8 and figure 35. The degree of conversion was only measured at the top surface. Curing time was 20 s for each sample. The degree of conversion experiments on the unfilled materials revealed no significant increase after 20 s of light exposure. Consequently, all of the composites were cured for 20 s in this experiment. As shown in table 7 the mean degree of conversion increased with increasing HEMA concentrations. This trend was also noted with the unfilled composites. As discussed, previously for the unfilled composites, the incorporation of HEMA increases the degree of conversion because of a reduction in viscosity of the mixture, thus enhancing the movement of molecules toward polymerisation centres [334].

Table 8: DoC% for model dental composites, CV is the coefficient of variance.

Sample	100 UDMA	90 UDMA	80 UDMA
Mean	74.77	79.38	82.98
SD	1.11	1.59	1.53
CV	1.49	2.00	1.85

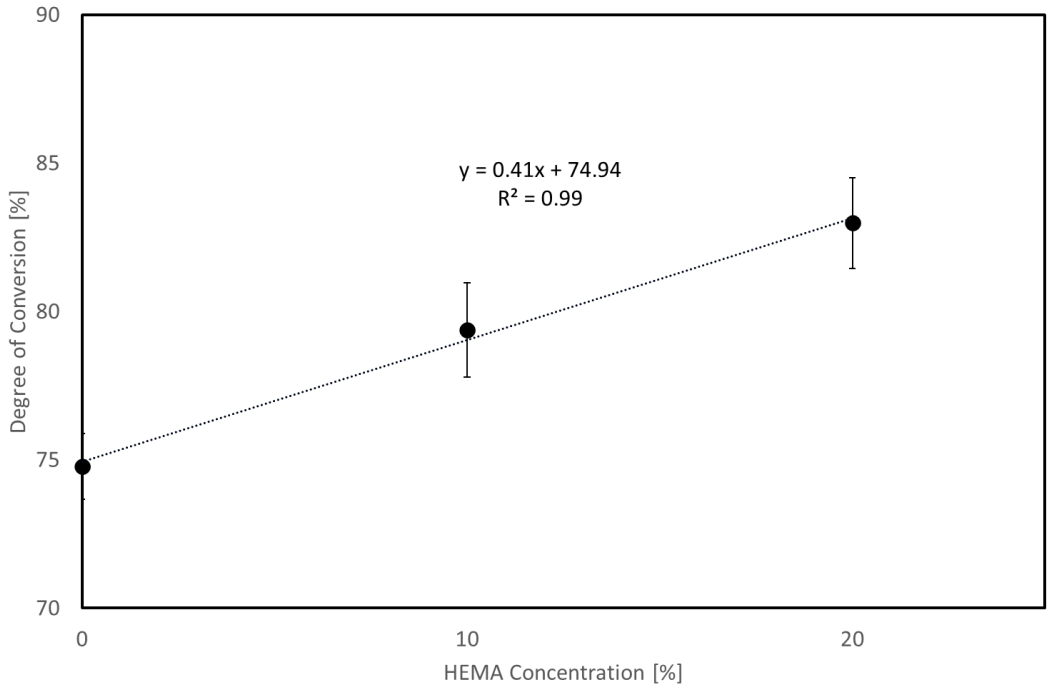

Figure 35: Mean values of DoC% vs HEMA concentration, error bars represent standard deviation.

The results for the degree of conversion (DoC%) of NanoFA composite in comparison to Gænial composite are shown in table 9 below. The degree of conversion of the experimental and NanoFA composites is significantly higher than commercial Gænial composite ($P<0.05$).

Table 9: DoC% for NanoFA and Gænial composites.

Sample	80 UDMA without NanoFA	80 UDMA with NanoFA	Gænial Composite
Mean	82.98	84.61	40.41
CV	1.85	0.98	0.46
SD	1.53	0.83	1.14

3.4.2 Monomer release

UDMA was eluted from all samples of the three polymers as shown in figure 36. HEMA was only eluted from polymers 2 and 3 as polymer 1 does not contain HEMA (figure 37).

Mixed assumption *ANOVA* was used to test the mean difference of the monomers leached from the three different composites, and the difference of the monomer concentration released at each time point (1 hour, 2 hours, 3 hours, 8 hours, and 24 hours).

In general, a significant leakage of monomers was found for UDMA released from composite 1, figure 36. With respect to the different time points, a statistically significant difference ($P<0.05$) in UDMA release was observed between composite 1 and 3, and between composite 2 and 3 at hour 1. However, at 2, 3 and 8 hours no significant difference was found in UDMA release. At 24 hours, there was again a statistically significant ($P<0.05$) release of UDMA from the three composites.

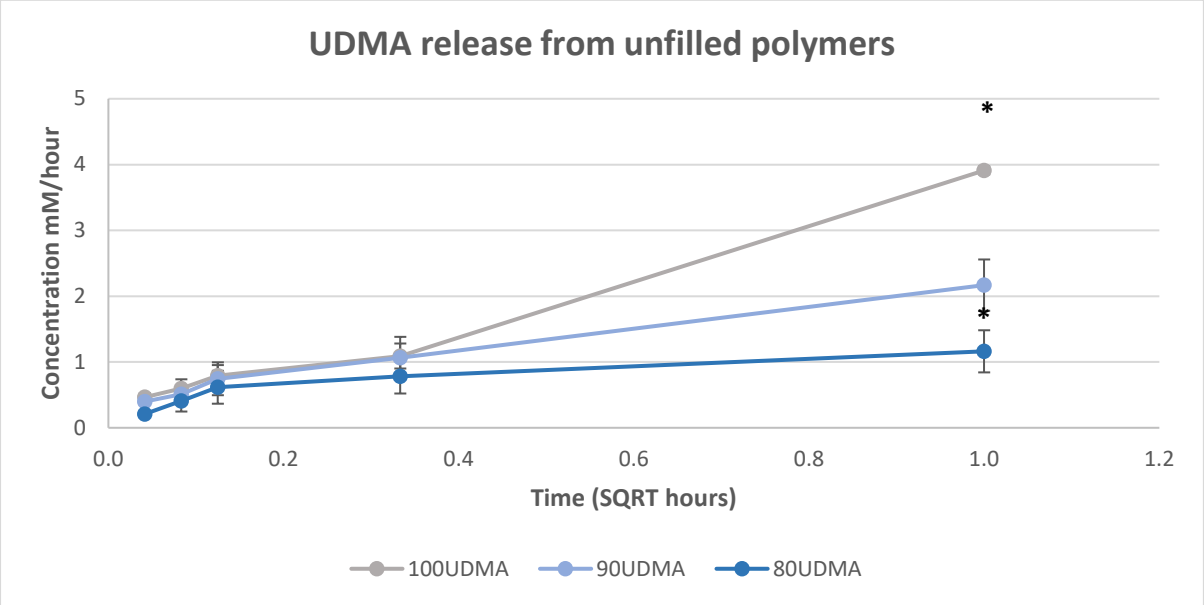

Figure 36: Concentration of UDMA released from three unfilled dental composites (polymers) measured by HPLC. Polymer 1: 100 % UDMA based, polymer 2 UDMA: HEMA 90 %:10 % and polymer 3 UDMA: HEMA 80 %: 20 %. Numbers reflect mM of monomer released per hour (mM/h), in 3ml of 75%ethanol: water solution, size of the specimen 2-2.5 cm2. The x-axis is SQRT of time to compensate for the difference in time intervals (1,2,3,8 & 24 hours).

HEMA concentrations released from polymers 2 and 3 are shown in the figure 37 below. Mixed assumption *ANOVA* revealed no significant differences in HEMA release from the two composites.

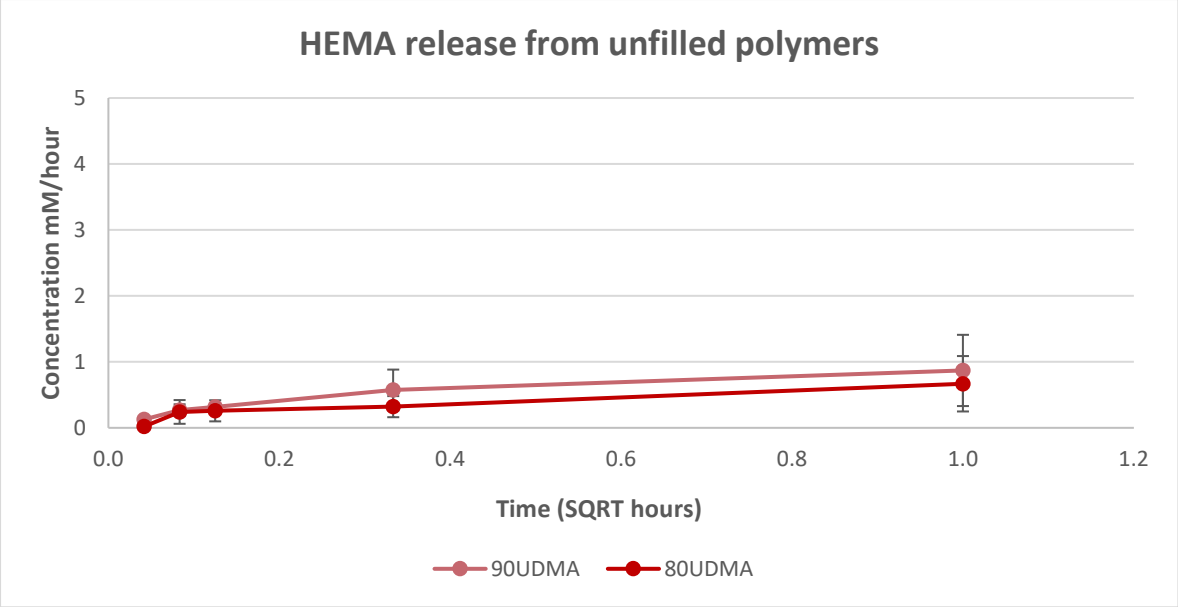

Figure 37 Concentration of HEMA (mM/h) released from two unfilled dental composites (polymers) measured by HPLC (polymer 2: UDMA: HEMA 90 %: 10 % and polymer 3 UDMA: HEMA 80 %: 20 %). The x-axis is SQRT of time to compensate for the difference in time intervals.

The figures 38, 39 and 40 summarize the results of the monomers released from dental composites after the incorporation of fillers. The amount of the released monomers decreased after adding the fillers.

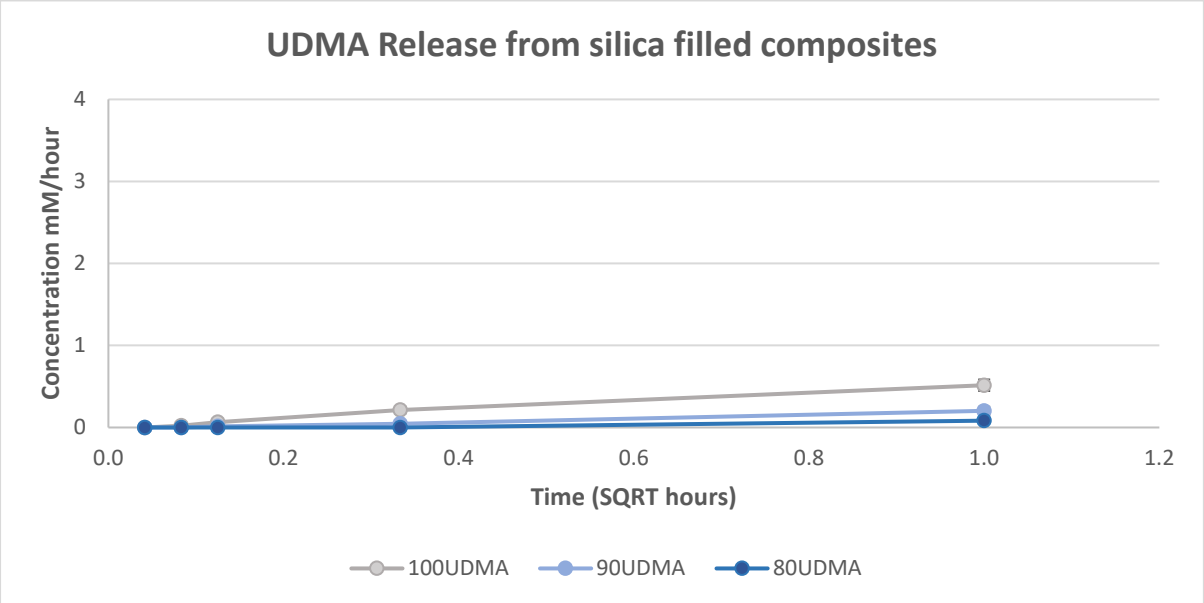

Figure 38: Concentration of UDMA (mM/h) released from silica filled dental composites measured by HPLC.

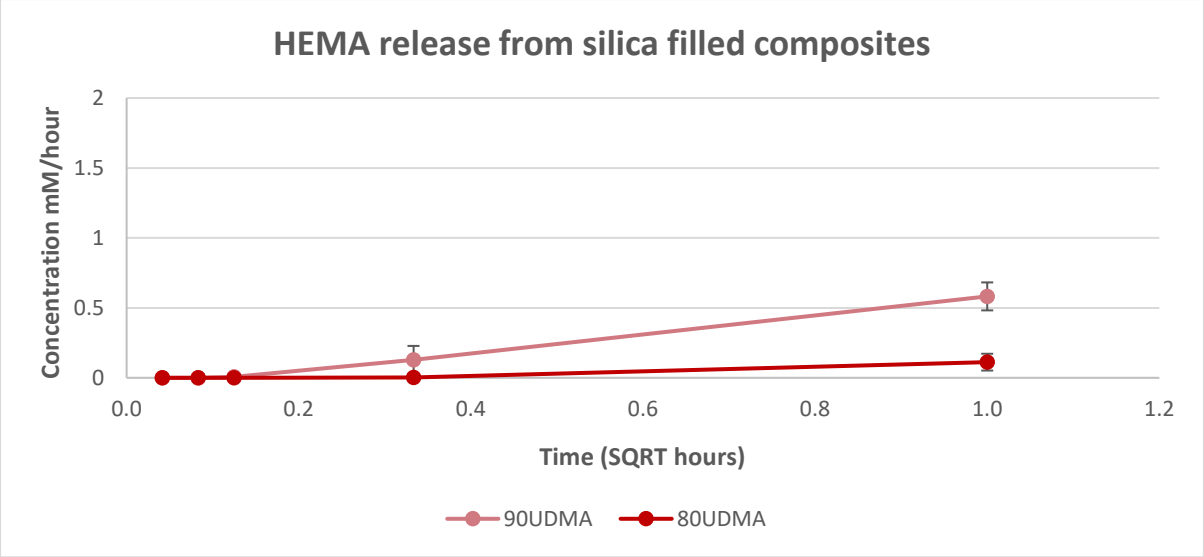

Figure 39: Concentration of HEMA (mM/h) released from silica filled dental composites measured by HPLC.

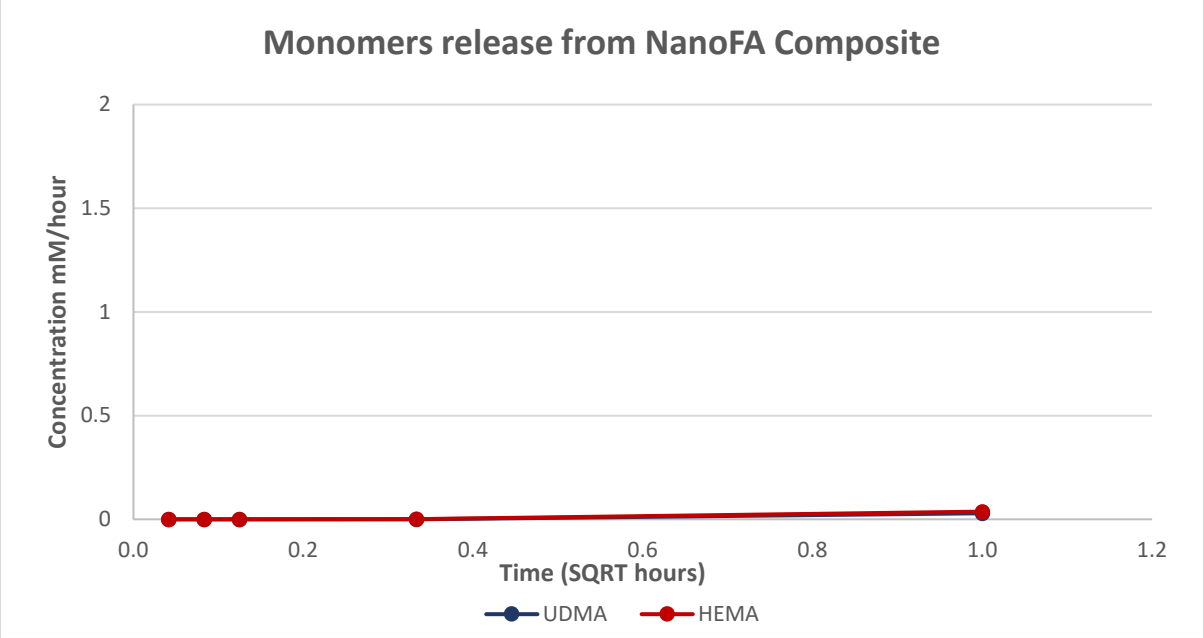

Figure 40: Concentrations of UDMA, HEMA (mM/h) released from NanoFA composite measured by HPLC.

3.5 Discussion

Bis-GMA is the most common resin monomer used as base for the development of dental composites [335]. The monomer's functional reactive group and high viscosity make it suitable to be used in composite formulation, in addition it requires the use of a diluent monomer for optimum reactivity [336]. The resin matrix chosen here for the development of experimental composites was based on UDMA and HEMA. Reports of high cytotoxicity due to the release of Bisphenol A (BPA) has been associated with Bis-GMA based composites [337] [338] [339]. Therefore, Bis-GMA free composites are a better alternative as they might have less detrimental effect on oral tissues. The addition of HEMA to the formula offers better monomer reactivity and hence better degree of conversion. Moreover, HEMA has the ability to interact with hard tissues, it is most commonly used in dental adhesive [340]. The addition of HEMA as comonomer is expected to increase the resin/filler coherence [341]. The hydrophilicity of this monomer is expected to facilitate the release of fluoride from NanoFA containing composite.

As shown in figures 32-34, a visibly homogenous mixture was obtained when HEMA was added as diluent monomer and when a solvent such as acetone was added indicating a decrease in viscosity with increasing HEMA concentration and with the solvent addition. Since a low final degree of conversion has been associated with homopolymerized dimethacrylate resin monomers [342], a diluent monomer is often used to improve conversion, viscosity and reactivity of mixtures containing highly viscous monomers such as UDMA. When 100% UDMA was used, the mixture had a higher viscosity due to the absence of a diluent monomer. HEMA provides better miscibility when added to hydrophobic monomers [46]. Therefore, a more homogenous monomer blend can be obtained. The high viscosity of UDMA affected the monomer flow, integration and spread over the inorganic filler particles [343]. Consequently, the amount of the fillers mixed with resin-monomers was affected by the viscosity of the monomer [344] and changed the final product quality. An additional factor that improved the viscosity was the addition of acetone. Solvent addition improves handling properties and viscosity of resin-based composites and therefore are commonly added during preparation of the materials [345]. Moreover, the solvent will facilitate the polymerization reaction and improve the DoC% [346]. This effect was explained by the favourable growth of polymer

chains due to the solvent facilitating the diffusion of the free radicals throughout the matrix during polymerization [346].

An additional factor that affects the viscosity of composite material is the filler size, content, and chemistry. Composite 1 in figure 32 contains 100 % UDMA and 63 % silica filler vol % ratio and a visibly homogenous mixture was obtained. However, this was not the case when secondary NanoFA fillers were added. When NanoFA was added to 100 % UDMA based silica filled composite, the material turned into a powder after mixing which was an interesting finding, figure 33. Although the overall filler volume was very similar between the nanoFA containing composites (62.1 vol %) and the silica-only filled composites (63 vol %), the smaller sized NanoFA particles increased the number of the particles in the resin matrix for the same filler vol %. Therefore, the effect of the filler was intensified and slightly increased filler concentration as a consequence of the smaller filler size increased the viscosity of the composite [347]. Additionally, when nanofillers were added the interaction between the resin matrix and filler particles was increased due to increased surface area.

The mixing procedure of the composite has affected the viscosity and resulted in the material converting to powder. One reason could be the heterogeneity of the mixture. The addition of the primary silica fillers followed by secondary NanoFA fillers to viscous UDMA monomer contributed to this heterogenous mixture. Thereby, it was difficult to incorporate the fillers by the monomer. Additionally, a dual asymmetric centrifugation DAC system was used for the mixing procedure. The technique by which the DAC system operates, is that it provides two types of rotations within the same cycle, figure 26. The first one is clockwise rotation that moves the material toward the container's periphery and the second rotation is in anticlockwise direction to the container's long axis and hence brings the material back to the centre [348]. Although, it was reported that using DAC mixer at high speed (3000rmp) resulted in a homogenous mixture [349], evaporation of the solvent during the mixing may have affected the viscosity. Moreover, the addition of non silanated nanofillers as secondary fillers potentially affected the flow rate of the mixture and increased viscosity. Accordingly, a previous study has demonstrated that the viscoelasticity of composites was affected by filler silanation [350]. The absence of interfacial bonds between the filler particles and monomers will significantly reduce the integration and adhesion of the matrix and subsequently result in

non-homogenous mixture [351]. Therefore, the mixing procedure may have further increased the viscosity of the mixture and made the composite turn into powder.

The composite material preparation was done at three stages and three polymer compositions were tested to find the polymer with the best performance. Initially polymer preparation and DoC% measurement were performed to obtain the best polymer formula and compare their characteristics. Then silica glass fillers (SiO_2) were added to the three polymers and DoC% was measured. Finally, the secondary NanoFA filler was followed by testing the performance.

Polymers with the compositions 100 UDMA and 90 UDMA had no significant difference in the degree of conversion. The polymer with 80 % UDMA had the highest degree of conversion up to 68 %. This can be interpreted by the effect of HEMA on the DoC%. This enhancement of DoC% can be explained by HEMA contribution to subsequent copolymerization with UDMA that occurs in addition to the vinyl group dependent polymerization of the bifunctional dimethacrylate such as UDMA [352]. Furthermore, the addition of monofunctional monomer to achieve a desired molecular weight and higher degree of polymerization has been applied in industry [353]. The effect of HEMA to increase the degree of conversion is also related to the lower molecular weight of HEMA as compared to UDMA as the monomer molecules can diffuse throughout the polymer network easily [354]. HEMA also has a lower viscosity than UDMA, therefore the mobility and flexibility of the molecules will be facilitated during polymerisation [334]. Further, HEMA contributes to the primary cyclization which leads to better conversion. In a multifunctional monomer system, pendant double bond form on the growing macroradicals during chain polymerization. Primary, secondary cycles and multiple cross links form due to the reaction of the propagating macroradicals with these pendant double bonds [355]. These reactions lead to a more heterogeneous matrix as a consequence of the coexistence of highly crossed linked regions and loosely crossed regions microgels. Therefore, improved conversion results as primary cyclization does not interfere with growing chain mobility in the system compared to cross linking [356].

The effect of the curing time on the degree of conversion of the three polymers was not significant ($P>0.05$) between the different curing times (5, 10, 20, 40 and 60 sec). All samples were cured with the same range of irradiance of the light curing unit (1000-1100 mW/cm^2).

With high irradiance shorter curing times are required to achieve adequate polymerization. Some manufacturers claim that 3 sec curing is sufficient to achieve optimal polymerization with newly developed light curing systems that can deliver up to 5000 mW/cm^2 [357]. This suggestion is also supported by the exposure reciprocity law which predicts a reciprocal relation between radiance level and curing time, accordingly the curing time for dental composites can be reduced if high energy light curing units are used [358] [359] [360]. Additionally, the results showed no significant difference in the degree of conversion measured at the top and bottom surface in the majority of the composite samples. The reason for a difference between the degree of conversion at the top and the bottom could be the time lag between curing process and measuring the sample. Even though the process was standardized for all samples (50 sec), the top was measured first, then sample was flipped to measure the bottom with the possibility to introduce some variability. Therefore, for subsequent experiments the composite specimens were polymerized for 20 sec and the DoC% was only measured at the top surface of the specimen.

The monomers released from unfilled composite materials were higher than silica filled and NanoFA filled composites. Significant amounts of UDMA were released from 100 % UDMA based polymer, 3.9 mM after 24 hours, which is in the toxic range [361] [268] [292]. The UDMA release decreased as the concentration of HEMA increased in the polymer. This is consistent with the increased degree of conversion as a result of HEMA in the composite. Therefore, the residual monomer decreased as the DoC% increased. The higher release from 100 % UDMA polymer can be explained by the higher concentration of monomer. In addition, UDMA is one of the most commonly reported monomers to be released from dental composite materials and has been found to have poor resistance to the effect of solvent [125] [124] [362]. It is important to highlight that the solvent, 75% ethanol/water, represent a worst-case scenario and has been used as extraction solution in many studies [363] [97] [364].

HEMA was the least released monomer from resin polymers and from filled composites, although it was expected that HEMA release would be higher due to the lower molecular weight of 130.14 g/mol compared to UDMA with 470 g/mol [365]. Improved reactivity and increased polymerization of HEMA may have reduced leakage as a higher degree of polymerization means less residual monomer and therefore less release [18].

The incorporation of silica fillers into the composite material resulted in reduced UDMA and HEMA release in ethanol. This can be explained by the fact that adding fillers to the polymer network has a significant effect on solvent absorption and dissolution with an inverse relationship between the proportion of the filler and the volume of solvent absorbed by the polymer network [366]. Accordingly, UDMA and HEMA release decreased further after adding the nanoFA secondary fillers, table 10. Similar findings of lower residual monomer release as filler content was increased from commercial materials has been reported [367].

3.6 Conclusion

Novel NanoFA filled composite was designed. The material achieved high DoC%. The amount of the monomer released from NanoFA composite was below the toxic concentrations. Despite the fact that the released UDMA and HEMA monomers from NanoFA composite were below the detected toxic concentrations for gingival fibroblasts by XTT viability assay (Chapter 2) the effect of the novel composite material on the cells should be investigated with more sensitive techniques. Therefore, the effect of residual monomer and NanoFA fillers was explored by RNA Seq analysis. In addition, the study involved characterization of the composite material, with regard to its mechanical properties and include the comparison with a commercially available composite.

Chapter 4: Fluoride release and mechanical properties of novel composite materials

4.1 Introduction

In this chapter the mechanical properties of the NanoFA composite were investigated to explore whether materials with this formulation have a satisfactory performance in clinical settings, properties such as fluoride release, water sorption, weight changes, flexural strength and elastic modulus were investigated.

Fluoride release from these materials was measured by ion selective electrode (ISE). A composite material without NanoFA filler was used as control. Moreover, commercial G-ænial composite was used as a comparator. Dental composite materials were stored in deionized distilled water, artificial saliva, and acidified artificial saliva. The fluoride release was measured at the following time points: 24 hours, 48 hours, 72 hours, 96 hours, 1 week, 2 weeks, 3 weeks, 4 weeks, and 12 weeks.

Weight changes and sorption of the dental composite after storage in distilled water, artificial saliva, and acidified artificial saliva were measured at the mentioned time points. Initially, artificial, and acidified artificial saliva solutions and the experimental composite materials were prepared. Then experimental and commercial composite specimens were polymerized, finished, and polished. Next, the specimens were stored in distilled water, artificial saliva, and acidified artificial saliva. Finally, fluoride released from composite materials in the above-mentioned solutions were measured and quantified using a standard curve.

Flexural strength was measured after storage in distilled water, artificial saliva, and acidified artificial saliva for the following time points: 24 hours, 1 week and 1 month. Finally, specimens were analysed under a scanning electron microscope (SEM) to examine the effect of storage in different solutions.

4.2 Method and materials

4.2.1 Artificial saliva and acidified artificial saliva preparation method.

Artificial saliva solution pH7 was prepared by using 1.5mM calcium chloride dihydrate ($CaCl_2$), 0.9mM potassium dihydrogen phosphate (KH_2PO_4), 20mM Hepes, and 130mM potassium chloride (KCl), all chemicals were purchased from (Sigma-Aldrich/UK). The chemicals were dissolved in 400 mL of distilled H_2O. The initial pH was measured by pH meter (Orion Star A214 pH/ISE meter, Thermo scientific, Waltham MA, USA) connected to an ion analyser

(Thermo Electron Corporation, Orion 4 star, USA), the pH was adjusted with potassium hydroxide (KOH) to pH 7, the volume was adjusted to 1 L.

Acidified artificial saliva was prepared by using 1.5 mM calcium chloride dihydrate ($CaCl_2$), 0.9mM potassium dihydrogen phosphate (KH_2PO_4), and 2.86 mL of acetic acid. The pH was adjusted to pH 4 with potassium hydroxide (KOH). Before measuring the pH for artificial and acidified artificial saliva, the pH meter was calibrated using standard solutions of pH 4, 7 and 11.

4.2.2 Specimen preparation

Experimental composite materials were prepared as described in chapter 3.2.2 and 3.2.3. The composition of dental composites used is given in table 5 (chapter 3). Specimens of experimental and G-ænial composites were prepared by pouring the mixture into plastic PTFE molds (10mm diameter and 1mm thickness) using a plastic spatula. The plastic mold was placed on transparent polyethylene terephthalate film (PET Goodfellow Cambridge Ltd., Huntingdon, UK) on top of glass slides (Goodfellow Cambridge Ltd., Huntingdon, UK). A second layer of PET strip was placed on top of the material and a glass slide was used to press the sample to a uniform flat surface shaped sample. All samples were polymerized for 20 seconds using a blue light LED cure unit (EliparTM DeepCure-S, 3M ESPE, 3M Deutschland GmbH, Germany). Light curing intensity ranged between 1100-1140 mW/cm^2 recorded with a Bluephase Meter II lightmeter. Each specimen was weighted using a digital balance (Mettler AE 240, 0.01 mg accuracy, Switzerland) and thickness and diameter were measured using digital Vernier callipers (Mitutoyo Digimatic, Japan). Specimens were stored in sealed plastic containers in an incubator (Gallenkamp, Riley Industries Ltd., UK) at 37°C until the day of the experiment. Five specimens were prepared from each material, then specimens were removed, and rough edges were smoothed and polished using 1200-grit silicon carbide paper (Norton, Abrasive Technological Excellence, France).

Figure 41: Specimens of dental composites stored in liquid at 37 °C. In this case, the specimen is stored in distilled water to detect fluoride release.

4.2.3 Calibration of the ISE

Using a fluoride stock solution of 1000ppm (Fluoride ISE standard solution, Reagecon, Switzerland) concentration a serial dilution was used to prepare six solutions with the following concentrations:

- 100ppm
- 10ppm
- 1ppm
- 0.1ppm
- 0.001
- 0.001ppm

The solutions were prepared at the room temperature. Using a magnetic stirrer, solutions were mixed for ten minutes. Then, 5ml of each solution were measured by ISE starting from the lowest concentration, 0.001ppm. After each measurement the electrode was cleaned thoroughly to ensure accurate measurement. Then, these measurements were plotted to create a standard curve. The ISE was calibrated every four hours at the day of the fluoride measurement experiment. Additionally, the samples were allowed to cool to room temperature to ensure the solution used to make the standard curves are of the same room temperature as the measured samples.

4.2.4 Fluoride measurement

On the day of the experiment specimens were taken out and placed in glass vials (15 ml, Fisherbrand, Lot#M600080). Next, 5 mL of storage solution which was either distilled water,

artificial saliva or acidified artificial saliva was added and stored at 37 °C. The glass containers were placed at an angle as shown in figure 41 to enable the storage solution to contact as much of the specimen as possible. The storage solution was changed at each time point of measurement of fluoride, which were: 30 minutes, 1 hour, 4 hours, 24 hours, 48 hours, 72 hours, 96 hours, 1 week, 2 weeks, 3 weeks, 4 weeks, and 12 weeks.

After that, for measuring fluoride concentration first measurement, 30 minutes for instance, the specimen was taken out and dried on paper towel then weight of each specimen measured. Next, the specimen was immediately placed in fresh solution and stored at 37˚C to allow fluoride to be released for the next measurement, i.e. the following time point. Table 10 illustrates the experiment plan followed for measuring the sample during the day of experiment. Fluoride was measured with an ion-selective electrode (Orion Research, Thermo Scientific, Waltham MA, USA). A total ionic strength adjustment buffer, TISAB III (TISAB III concentrate with CDTA, Thermo Fisher science) 0.5 ml was added to each solution. The advantage of TISAB addition is to prevent the formation of fluoride-complexes and to control the pH of the solution A magnetic stirrer (VELP, Scientifica, Italy) was used to mix the solutions for three minutes prior to measurements. The released fluoride ion in the storage solution was measured for 24 hours, 48 hours, 72 hours, 96 hours, 1 week, 2 weeks, 3 weeks, 4 weeks, and 12 weeks.

Table 10: Fluoride experiment plan showing the accurate time points for each sample fluoride measurement.

Samples	**Insert in liquid**	**1st measurement**	**2nd measurement**	**3rd measurement**
Sample1	10:00 am	10:30 am	11:00 am	2:00 pm
Sample 2	10:10 am	10:40am	11:10 am	2:10 pm
Sample3	10:20 am	10:50am	11:20 am	2:20 pm
Sample4	11:30 am	12:00am	12:30 am	3:30 pm
Sample5	11:40 am	12:10am	12:40am	3:40 pm

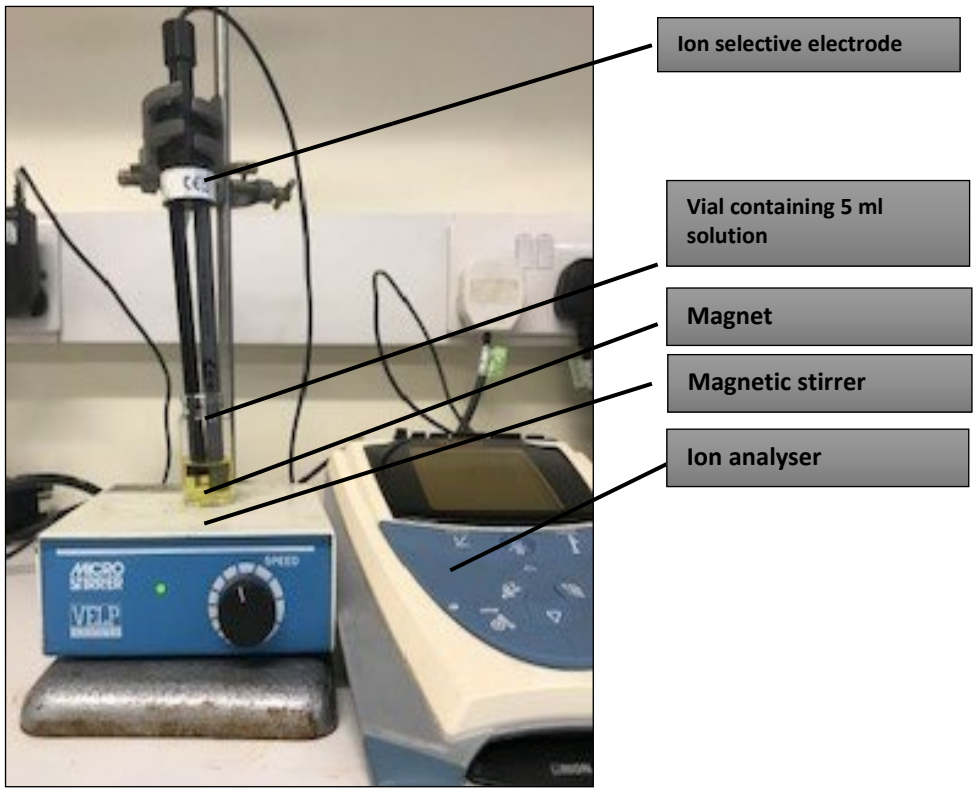

Figure 42: Fluoride measurement set up by Ion selective electrode.

Before testing, the ISE was calibrated using different fluoride concentrations as mentioned earlier. The concentration of each solution was recorded in millivolts (mV) and then, a logarithmic equation was used to convert these reading into ppm according to the following equations:

$$\frac{\mathrm{mV1-mV2}}{\mathrm{logC1-logC2}} = \frac{\mathrm{mVs-mV2}}{\mathrm{logCs-logC2}}$$

$$\frac{logCs - logC2}{loC1 - logC2} = \frac{mVs - mV2}{mV1 - mV2}$$

$$logCs - logC2 = \left(\frac{mVs - mV2}{mV1 - mV2}\right) \times (logC1 - logC2\ )$$

$$logCs = \left(\frac{mVs - mV2}{mV1 - mV2}\right) logC1 - \left(\frac{mVs - mV2}{mV1 - mV2}\right) logC2 + logC2$$

$$Cs = 10^{logCs}$$

Where *mV1* and *mV2* represent *mV* of standard solutions, *C1* and *C2* represent concentrations of standard solutions, *mVs* represents *mV* of the test sample, *Cs* represents the concentration of the test sample, *logCs* represent the concentration of the test sample in ppm, *mV* represents the measured value in milliVolts, ppm stands for parts per million.

4.2.5 Flexural strength measurement

Composite materials were prepared using the same method as described in chapter 3, sections 3.2.2 and 3.2.3 with a custom-made split steel mold shown in Figure 43. The specimen's dimensions were 25×2×2mm. A three-point bending test was performed using a universal test machine (Instron 3365, MA, USA) to calculate the flexural strength and elastic modulus. The specimens were polymerised at five locations along the specimen length, in an overlapping manner for 20 seconds using a blue light LED cure unit (EliparTM DeepCure-S, 3M ESPE, 3M Deutschland GmbH, Germany). Light curing intensity ranged between 1100-1140 mW/cm^2 recorded with a Bluephase Meter II lightmeter. Flexural strength was measured for each composite material (composite without NanoFA, G-ænial and NanoFA composite) after storage under three conditions, namely: distilled water, artificial saliva, and acidified artificial saliva. Three time points of storage were tested, 24 hours, 7 days and 1 month. For all storage condition 10 specimens were prepared. Total number of specimens prepared of each composite material were therefore 90.

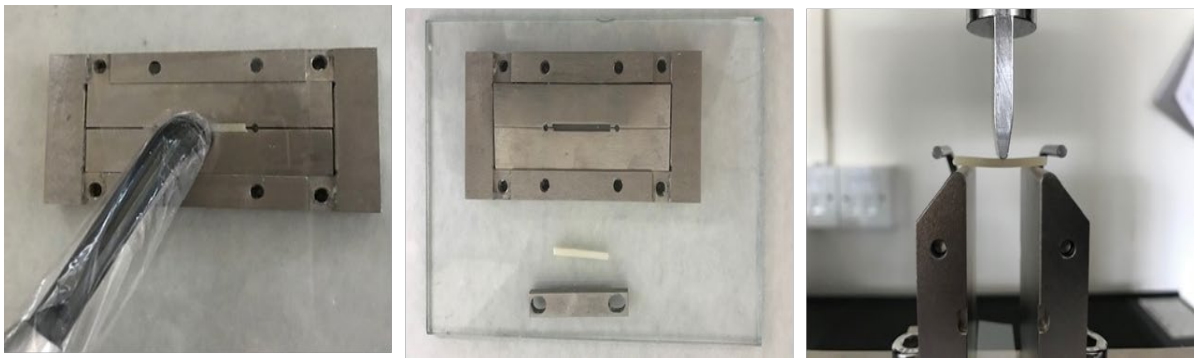

Figure 43: Composite specimen preparation for the three point-bending test.

The formula to calculate the flexural stress (σ) are given below:

$$\sigma_{flex} = MC/I$$

Where σ= flexural stress in (MPa)

M=maximum bending moment

C=distance between the centre and outer surface of the specimen

I= moment of inertia of the specimen's cross section

$$\boldsymbol{M = FL/4}$$

Where F= applied force on the specimen (N)

L= distance between the supports in (mm)

$$c = d/2 \ (mm)$$

Where d= thickness of the specimen

$$I = bd^3/12$$

b= width of specimen (mm)

Therefore, final equation is:

$$\boldsymbol{\sigma_{flex=3FL/2bd^3}}$$

4.2.6 Scanning Electron Microscopy (SEM)

To investigate the effect of storage on the commercial and experimental dental composites, the specimens were visualized under a scanning electron microscope. SEM images were obtained from the EM Research Service, Newcastle University, using a scanning electron Microscope (TESCAN VEGA-3 LMU Scanning Electron Microscope).

Two representative specimens from each dental composite stored under distilled water, artificial saliva and acidified artificial saliva were chosen after the end of the storage period. Then, specimens were coated with gold using a 5-10 nm, Polaron SEM Coating Unit and examined under the microscope using 80 X and 500 X settings and a beam intensity 10-12.

Figure 44: Composite specimens on SEM stubs applied with sticky carbon, ready to be gold coated for SEM images.

4.3 Statistical analysis

The fluoride and water sorption data were analysed by mixed assumption ANOVA and Kruksall-Wallis test (IBM SPSS, version 27.0). The mixed ANOVA was applied due to difference in groups, difference in each time point and difference within each material. Three mixed ANOVA were performed for each solution. Then non-parametric testing (Kruskal Wallis) was applied to establish significance among the materials at each time point. In total, there are three groups with 13 time points (3*13=39 cell) in each cell there were five replicates.

4.4 Results

4.4.1 Fluoride release results

The cumulative fluoride release from NanoFA and G-ænial composites are shown in Figure 45. Figure 46 summarizes the results of daily fluoride release in distilled water, artificial saliva, and acidified artificial saliva.

In general, the novel NanoFA based dental composite showed comparable fluoride release to commercial G-ænial material, as shown in the cumulative fluoride release graph (Figure 45). The highest cumulative fluoride release by both dental composites was seen in acidified artificial saliva. The mixed *ANOVA* results show overall significance of the amount of fluoride released by NanoFA composite compared to the control group ($P<0.001$). The amount of fluoride that the NanoFA composite released was not significantly different compared to G-ænial composite ($P> 0.05$). However, Kruksall-Wallis test results show significance of at least one pair of the groups at each time point. These will be explained specifically in each storage solution. Overall, the trend was initially high fluoride release during days 1 and 2 then a

gradual decline with time (Figure 46) in distilled water and acidified artificial saliva. In artificial saliva, fluoride release increased gradually with time up to week 1 or 2, then the release diminished gradually by week 4.

In the distilled water group (Figure 46), the amount of fluoride released by the NanoFA composite was higher but not significantly different from commercial G-ænial at any point. The release followed a high initial burst pattern followed by a gradual decline with time. $NanoF_A$'s highest release was noted during the first 24 hours. These were significantly higher with NanoFA compared to the control group, which was the composite without NanoFA. The commercial comparator, G-ænial, released significant amounts of fluoride compared to the control during the first 48 hours which was again followed by gradual decline.

In artificial saliva, the composite materials' fluoride release pattern was different. Overall, they were lower as compared to the samples stored in distilled water or acidified artificial saliva. A low amount was released by the $NanoF_A$ composite during the first 24 hours (Figure 46) while, for G-ænial there was no detectable fluoride release during the first 24 hours. The fluoride release by G-ænial and NanoFA increased at week 1 and week 2. Specifically, G-ænial released significant amounts by week 1 ($P=0.001$) and NanoFA composite- mediated release was significant by week 2 ($P=0.001$). Later the release diminished toward the endpoint of the storage.

In acidified artificial saliva, the pattern of fluoride release was similar to the release in distilled water. The higher release was during the first 24 to 48 hours followed by decline in fluoride release with time. For the $NanoF_A$ group, the highest release was during the first 24 hours ($P<0.05$) while for G-ænial the highest release was during the first 48 hours ($P>0.01$). Overall, the G-ænial released more fluoride than the $NanoF_A$ composite in acidified artificial saliva, as demonstrated in the cumulative fluoride release graph (Figure 45). However, by week 1 & 3 of storage G-ænial fluoride release was non-significant, while the $NanoF_A$ composite release was still significant ($P<0.05$).

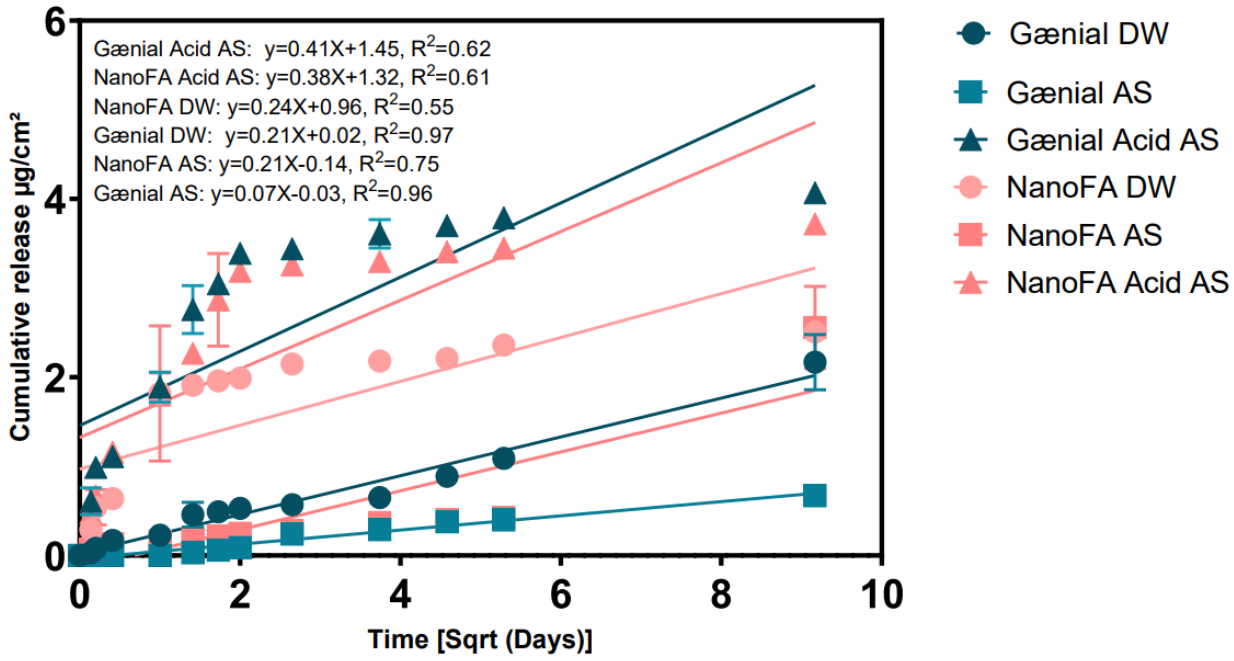

Figure 45: Cumulative fluoride release (µg/cm^2) with standard deviation (error bars) from commercial G-ænial and NanoFA composite measured by ion selective electrode, ISE in three storage solutions. DW: distilled water, AS: artificial saliva and Acid AS: acidified artificial saliva.

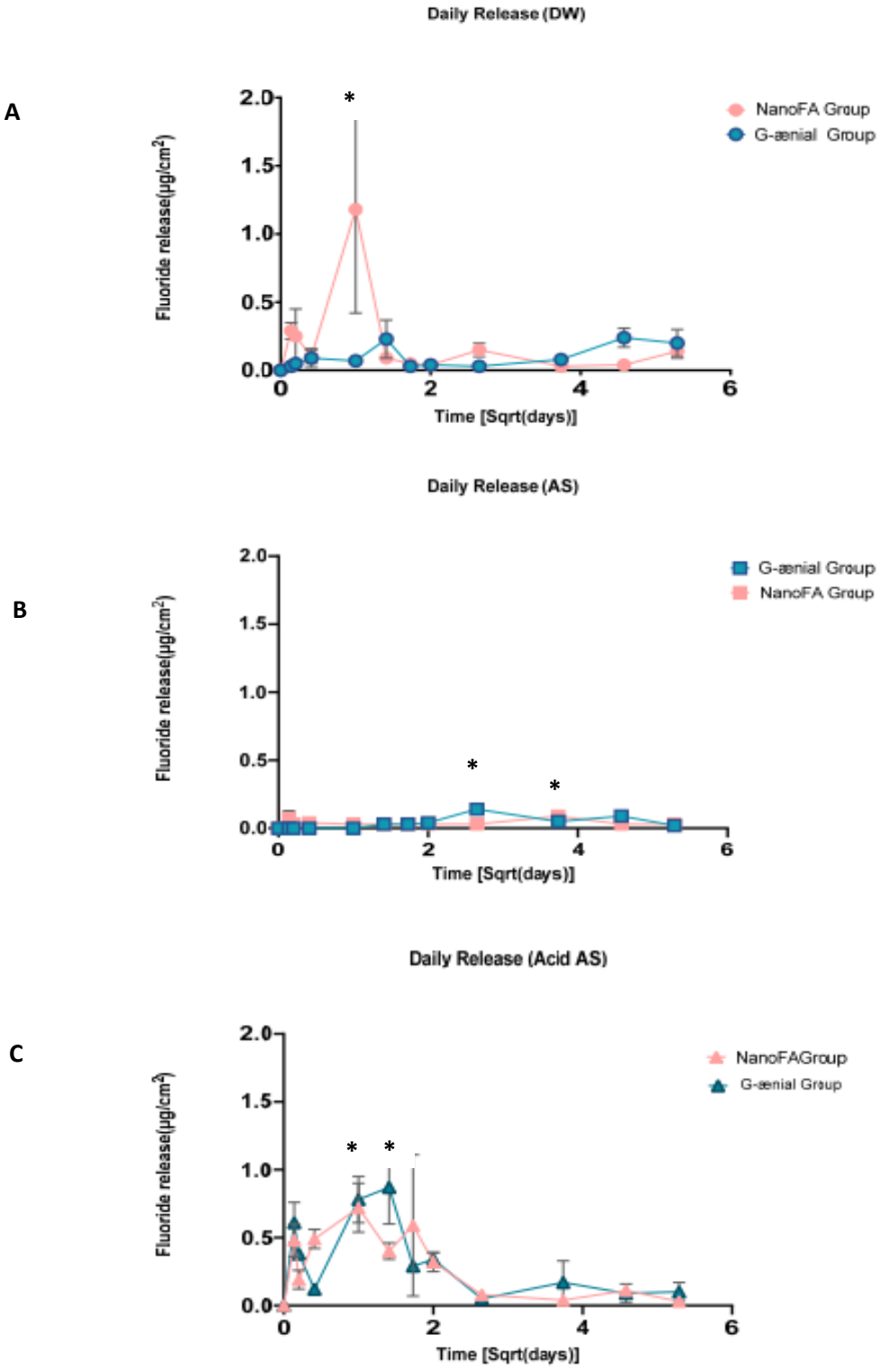

Figure 46: Daily fluoride release from experimental and commercial dental composites measured by ISE in A) distilled water, B) artificial saliva & C) acidified artificial saliva. *= P<0.05.

4.4.2 Weight changes and sorption

The sorption (calculated from weight changes) of the three dental composite materials is displayed graphically in figures 47. In general, all composite material increased in weight in the three storage solutions. The pattern of liquid sorption increased with time then plateaued or decreased after one month of storage. Overall, NanoFA composite showed a higher sorption rate than G-ænial and composite without NanoFA in all three storage solutions.

In distilled water, overall, NanoFA composite showed high water sorption compared to the other two materials figure 47. However, G-ænial showed significantly greater water sorption during the first 30 minutes, 1 hour and 4 hours of storage compared to the NanoFA composite. At day 1 and 2 of storage the three materials' sorption was not significant and comparable to each other's. However, significant water sorption was observed by week 1 of storage by NanoFA compared to other groups. The amount of sorption continued to increase until week 4 but was not significantly differently from G-ænial which showed the highest sorption value at this point. After one month, water sorption decreased in all three dental composite materials toward the end point of storage which was week 12.

In artificial saliva, NanoFA sorption was higher than sorption in distilled water. Moreover, the sorption rate was higher than G-ænial and composite without NanoFA, the difference was significant after the first 30 minutes ($P = 0.01$) and 24 hours (P value < 0.005), respectively. Then significant artificial saliva sorption was observed with NanoFA compared to G-ænial by week 1 ($P < 0.005$) and week 4 ($P < 0.05$). Sorption decreased to nonsignificant amounts by week 12. In acidified artificial saliva, overall, the sorption trend is similar among the three composite materials. The sorption values in acidified artificial saliva were similar for most of the time points and therefore without statistical significance. The only significant sorption values by NanoFA compared to G-ænial were observed at day 1 ($P < 0.05$), day 2 ($P < 0.05$) and day 4 ($P = 0.001$).

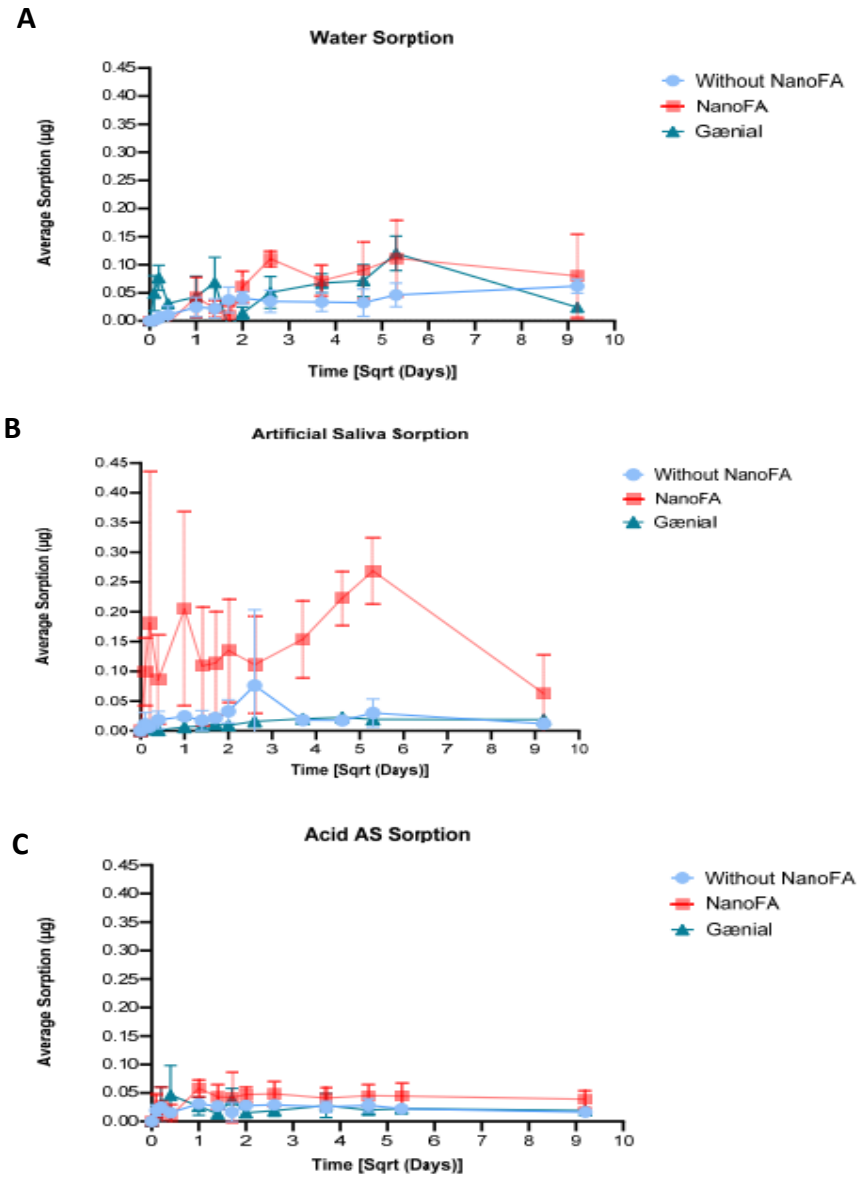

Figure 47: Sorption of experimental and commercial dental composites in A) distilled water, B) artificial saliva and C) acidified artificial saliva.

4.4.3 Flexural strength testing results

The results of the three-point bending test for the experimental and Gænial composites are displayed graphically in figure 48. The results of Analysis of Covariance (ANCOVA) for the data showed flexural strength of G-ænial significantly higher ($P< 0.01$) in any storage solution than experimental composites. In addition, no significant difference in flexural strength was found between NanoFA composite and composite without NanoFA, meaning the addition of NanoFA fillers to the experimental material has not significantly reduced the mechanical properties.

Overall, the ANCOVA results showed that the reduction of the flexural strength of G-ænial composite over time was significant ($P< 0.01$). However, there was no significant effect of the storage medium on the flexural strength. For the experimental composites, coefficient of variation was greater than 50 indicating variability of the data. Moreover, time and storage medium did not significantly affect the flexural strength of experimental composite.

The results indicate that the choice of material is important, and that commercial composite is significantly stronger in any storage solution than the lab produced composites. G-ænial is industrially produced composite, on the other hand the experimental composites NanoFA composite contains 20% non-silanated fillers. For the composite without NanoFA, all silica fillers were silanated. However, both experimental composites contain 20% of the resin monomer HEMA.

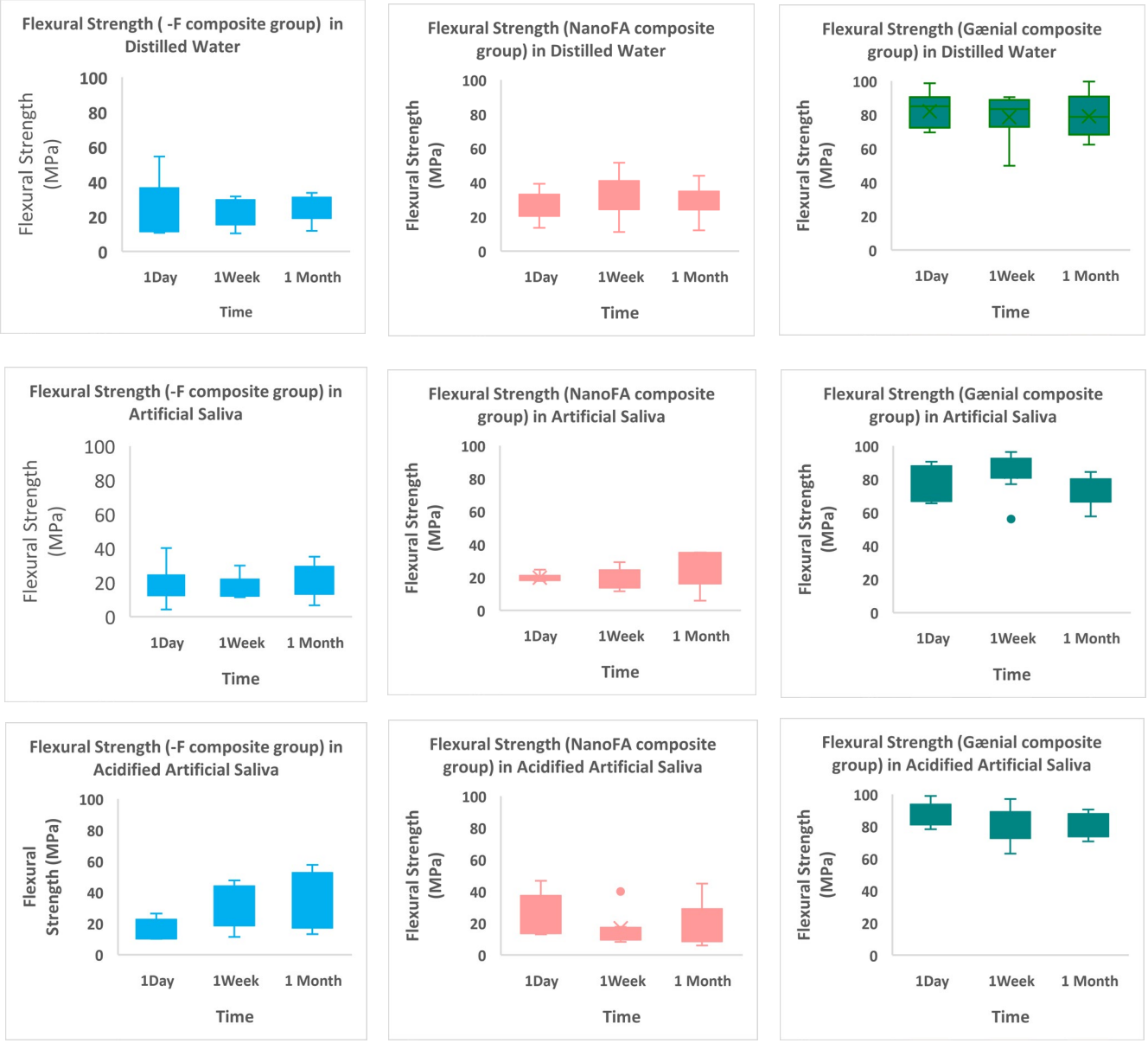

Figure 48: Flexural strength values for experimental and commercial dental composites measured by three point bending test in three storage solutions. DW: distilled water, AS: artificial saliva and Acid AS: acidified artificial saliva.

4.4.4 Scanning Electron microscopy (SEM) results

The figures 49-51 demonstrate the microstructure of the surfaces of the experimental and commercial G-ænial composites. Specimens chosen for two time points, 24 hours and one month, were aged in the three different solutions: distilled water, artificial saliva, and acidified artificial saliva. All specimens showed morphological changes more prominent at the end of storage period. These changes reflect degradation of composite specimens under different storage solutions that affected the polymer matrix, fillers and interfacial bond, appearing as increased number of cracks or irregular shaped voids or pores. The morphology changed according to the type of the material and the storage medium. In distilled water, specimens displayed small multiple cracks. In artificial saliva and acidified artificial saliva, specimens showed increased porosity, voids, and more extensive cracks.

The SEM images showed that microcracks varied in number and extent and were more prominent after one month displaying the effect of the aging process of dental composite in aqueous medium. For example, specimen of the experimental composite (without NanoFA) aged in distilled water for one month, showed small multiple cracks (Figure 49, B), while NanoFA composite specimen aged for one month in acidified artificial saliva showed extensive cracks throughout the specimen (Figure 50, F) due to more severe damage due to acid attack. In comparison commercial G-ænial showed smaller multiple cracks in acidified artificial saliva after one month of storage (Figure 51, F).

The different storage solutions appear to modify composite materials by breakdown of the interfacial bond between the resin-matrix and filler phase, subsequently leading to plucking or loss of filler particles. This is termed plasticising effect [368]; the damage appears as irregular shaped voids. Interfacial bridge failure of the resin matrix-filler phase can be seen in the figures for the G-aenial specimen stored in artificial saliva (Figure 51, D white arrow).

Porosity, black regular-shaped circles, or pores distributed throughout the specimens can be seen in all materials under all storage conditions. These might reflect air bubbles trapped within the materials during composite specimen preparation. In addition, pores might be reflecting stress introduced with composite materials during polymerization (Blue arrows).

Aged specimens showed an increased number of circular areas appearing as floating bubbles being more evident in composite materials after one month of storage. These might represent

spaces left after unreacted residual monomer leached out from the polymeric matrix or, in NanoFA filled composite, could represent the spaces left after fluoride release due to dissolution of fluoride containing particles into the storage solution. These are indicated by yellow arrows.

The SEM micrographs displayed differences of surface texture of the materials. Composite without NanoFA fillers appears to have a smooth surface that might be due to more homogenous filler distribution throughout the polymer matrix. NanoFA composite appears rough with some areas of filler clusters that can be attributed to non-silanated NanoFA fillers. Commercial G-ænial composite, on the other hand also appears to have a more uniform composition or homogenous consistency due even filler dispersion throughout the polymer network.

Composite without NanoFA

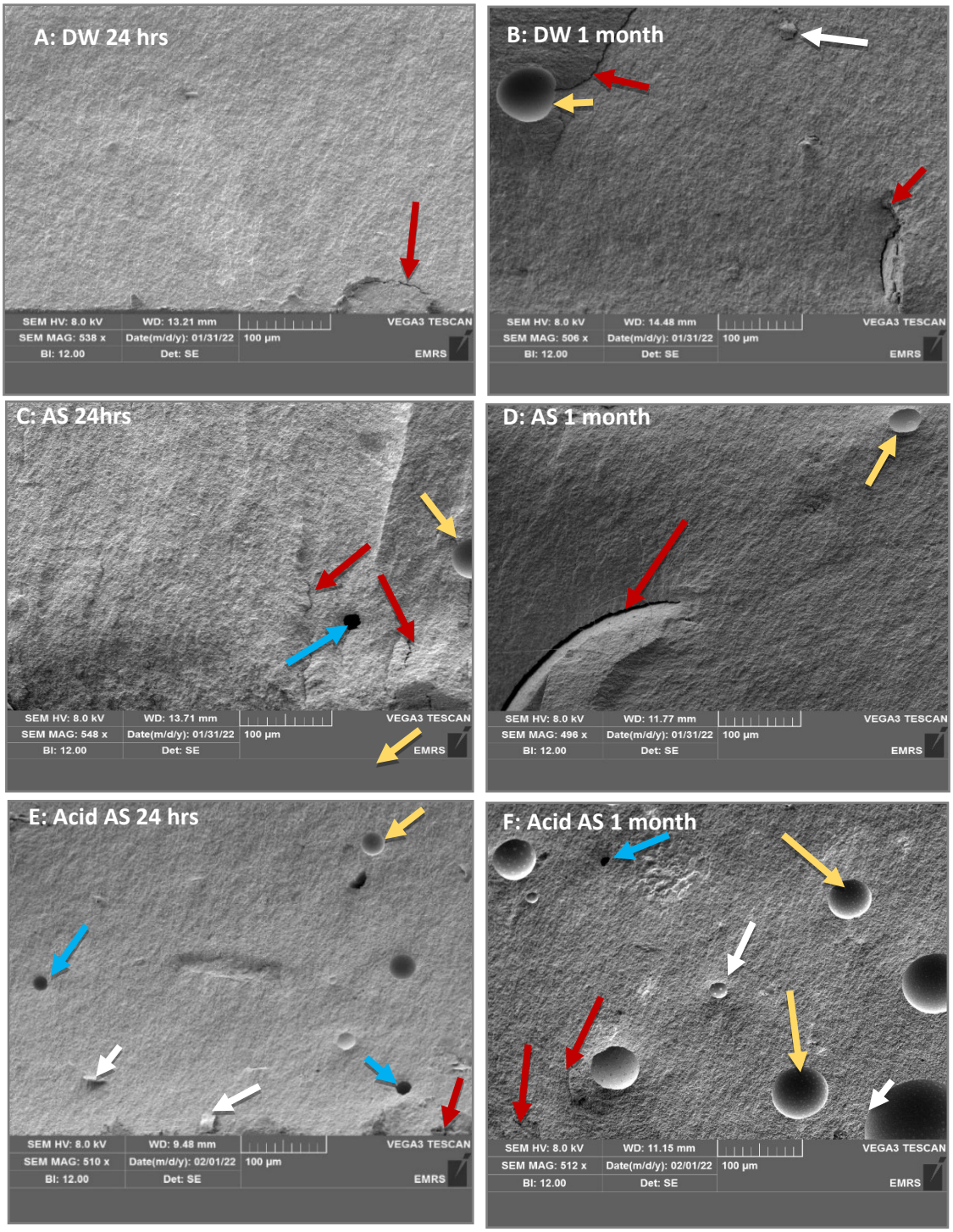

Figure 49: SEM micrographs of composite without NanoFA. Specimen A & B aged in distilled water for 24 hours and one month, C & D aged in artificial saliva and E & F in acidified artificial saliva. The Red arrows display microcracks, blue arrow shows micropores, white arrow filler plucking, or plasticising effect and yellow arrows indicate spaces left after residual monomer leached out.

NanoFA Composite

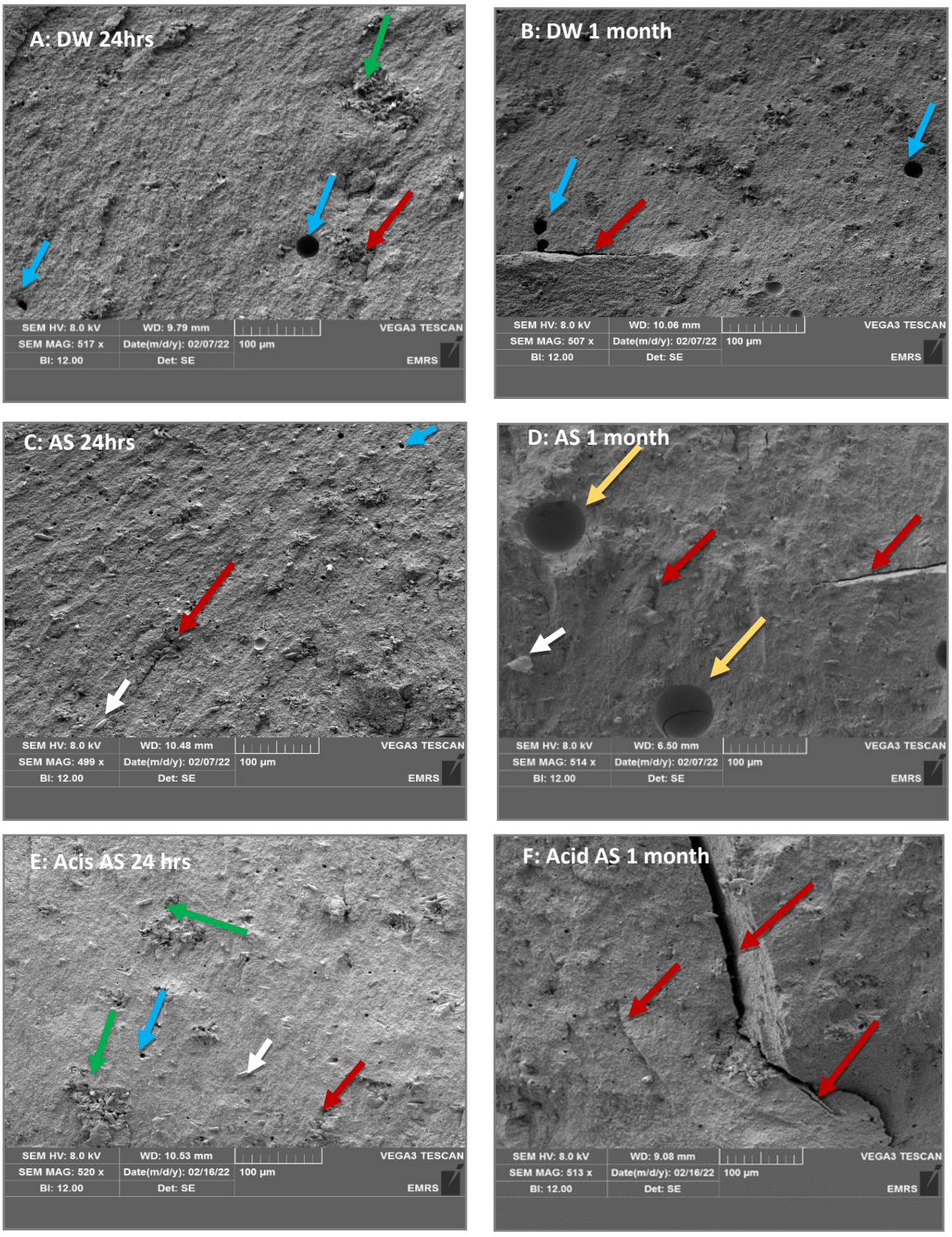

Figure 50: SEM micrographs of NanoFA composite. Specimen A & B aged in distilled water for 24 hours and one month, C & D aged in artificial saliva and E & F in acidified artificial saliva. The Red arrows display microcracks, blue arrows show micropores, white arrow fillers plucking or plasticising effect and yellow arrows indicate spaces left after residual monomer leached out, green arrow, areas of filler clusters.

G-ænial Composite:

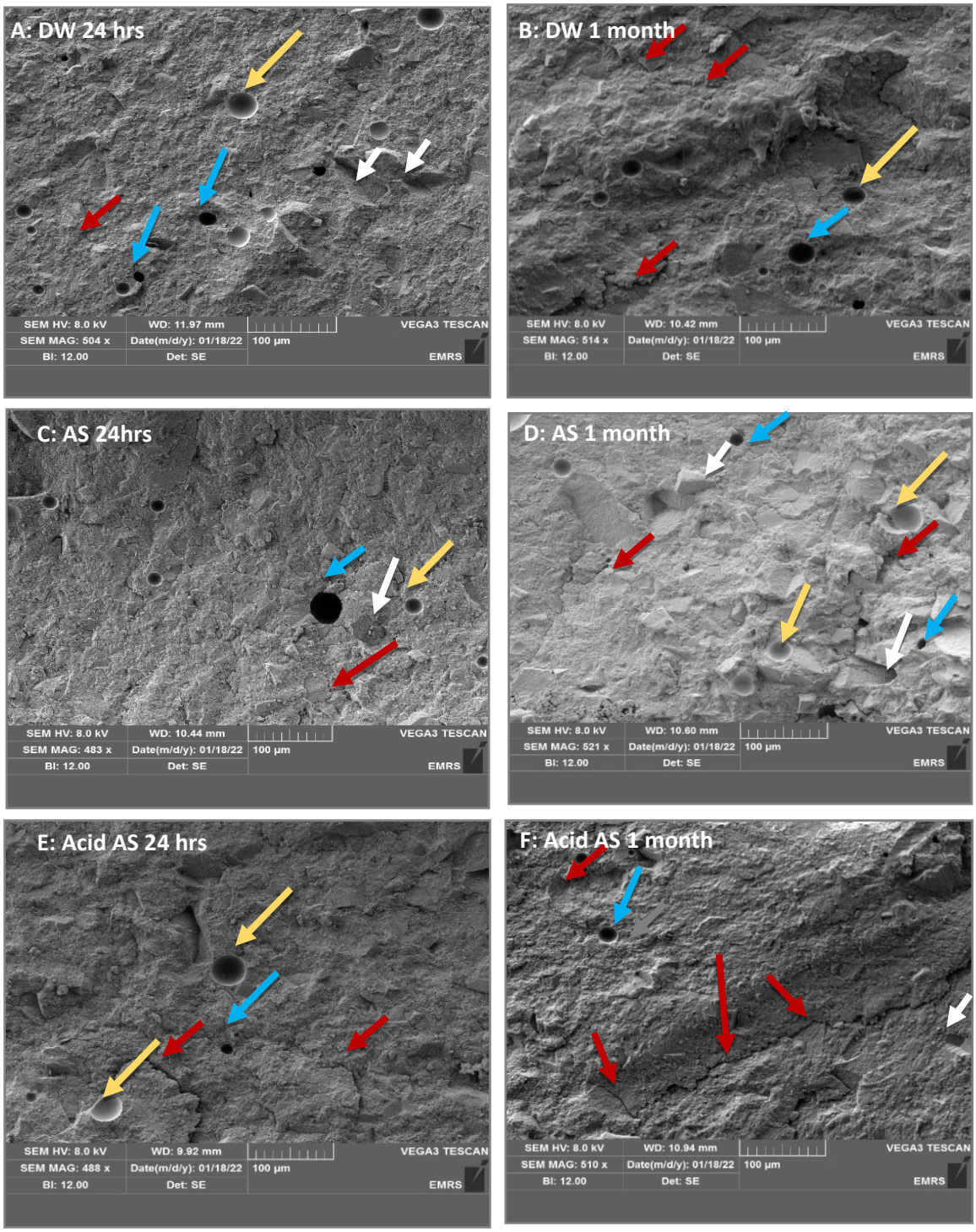

Figure 51: SEM micrographs of G-ænial composite. Specimen A & B aged in distilled water for 24 hours and one month, C & D aged in artificial saliva and E & F in acidified artificial saliva. The Red arrows display microcracks, blue arrows show micropores, white arrow, fillers plucking or plasticising effect and yellow arrows show spaces left after residual monomer leached out.

4.5 Discussion

In this chapter, two types of dental composite were used, these were developed in the lab with the same formula. Then, NanoFA fillers were added to one composite to test the effect of the addition of NanoFA fillers. Moreover, a commercially available composite material, G-ænial with the same main monomer, UDMA, and primary fillers was used as commercial comparator. In order to make a judgment whether the materials had satisfactory performance in the mouth, properties such as fluoride release, sorption, and flexural strength were investigated. The materials preparation method was described earlier in chapter 3, sections 3.2.2 and 3.2.3. The potential advantage of adding NanoFA to the composition of the dental composite is the release of fluoride. Fluoride release from dental restoratives has been shown to have anticariogenic effects, reduce demineralisation and increase remineralisation of dental tissues [369]. A fluoride releasing commercially available material, G-ænial, was used as a comparator. Fluoride release was measured under a range of storage solutions (distilled water, artificial saliva, and acidified artificial saliva, and for different time points. Distilled water was chosen as neutral condition [147]. The absence of ions in deionised distilled water makes it an appropriate solution to accurately estimate the fluoride release, in addition, it has been used as a baseline to measure fluoride release before [370] [371]. Moreover, in order to simulate an oral environment a solution such as human saliva could be used to gain a more accurate estimation of the fluoride release in a clinical setting. However, collecting human saliva is a time-consuming procedure and requires ethical approval. Therefore, artificial saliva was chosen to simulate an oral environment. The artificial saliva was prepared according to a previously published recipe [207]. Since the oral environment is dynamic with saliva pH affected by the consumption of different food and drink as well as in cariogenic conditions, an acidified artificial saliva was included, with a pH below the critical level, so that the influence of low pH could be measured on the performance of the composites [372] [206] [373].In order to explore the effect of fluoride release and storage on the materials, the weight changes and sorption process were examined. In addition, flexural strength tests were performed for all the restorative materials under all storage conditions.

In order to enhance bioactivity, NanoFA fillers have been incorporated in the materials formula. NanoFA fillers have been shown to improve bioactive behavior in glass ionomer cements [374]. Fluorapatite is found naturally in bone and teeth and fluoride content is

uniformly distributed within enamel and bones [375]. It has a structure similar to hydroxyapatite since the enamel consist of rod-like hydroxyapatite crystals. Fluorapatite is considered to have higher chemical and thermal stability than hydroxyapatite [376]. In addition, fluorapatite has been suggested as biomaterial for bone repair for its biocompatibility [377]. Hence, fluorapatite offers a suitable choice as compound to improve dental restorative materials with regard to bioactive behaviour and is considered to be biocompatible. The addition of bioactive glass has been used by researchers as a method to provide bioactivity [369]. While, bioactive glass can provide fluoride release, it has the same filler size and isotropic morphology as the conventional fillers in dental composite. Incorporating nano sized fillers such as NanoFA rather than bioactive glass in dental composite can improve mechanical properties due to differences in the particle anisotropy [378].

NanoFA composite showed higher fluoride release when compared to commercial G-ænial. In comparison to G-ænial, higher fluoride release was seen in distilled water and artificial saliva, while in acidified artificial saliva, G-ænial released a higher amount of fluoride. The pattern of fluoride release by $NanoF_A$ composite was similar in distilled water and acidified artificial saliva, where fluoride release increased in proportion to time. The release pattern was proportional to the square root of time, the nonlinear response shown in figure 45 indicating an early-burst phase release of $NanoF_A$ composite. In comparison, G-ænial fluoride release pattern in distilled water did not show initial burst release as demonstrated by the R^2 value of the linear model in figure 45. The pattern of an initial burst of fluoride release was frequently noticed with glass ionomer cements and compomers. The slow fluoride release following initial burst was attributed to dissolution of fluoride containing particles [379] [380] [381]. Both composites released higher fluoride in distilled water than in artificial saliva. Moreover, no initial burst release was seen in artificial saliva, rather a constant slow fluoride release increasing with time, this can be noted from the R^2 values of the linear model for both composite materials in figure 45. This can be explained by the effect of the ionic content and composition of artificial saliva that affected the solubility of fluoride containing particles [380]. The fluoride release is affected by the presence of ions in the medium it is being released into. The presence of calcium ion in the testing medium for instance has been shown to modify fluoride release due to the formation of CaF_2 [382]. Additionally, it has been shown that the higher viscosity of the artificial saliva retards the fluoride ion release from GIC [383]. Finally,

the presence of cations in artificial saliva that react with fluoride could have another role in retarding the release in artificial saliva [384]. Another explanation is that in artificial saliva the diffusion gradient between the composite material and ion enriched saliva is lower compared to the gradient between the composite and distilled water [155]. In a diffusion-controlled release process, the diffusion is dependent on the concentration gradient and diffusion constant according to Fick's law of diffusion, i.e. diffusion of the particles follow the concentration gradient [385]. Accordingly, reducing the concentration gradient between the specimen and the storage medium would reduce diffusion and allow equilibrium to be established in a shorter time.

The highest fluoride release by both composite materials in acidified artificial saliva (Figure 45) is indicative of an effect of storage medium on the pattern of fluoride release from the dental composite. The early phase of high fluoride release, 24 hours for NanoFA composite and 48hours for G-ænial (Figure 46) can be explained by the higher solubility of NanoFA in acidic solution. Previous studies have also reported that fluoride release is increased under acidic conditions [273] [372] [386]. The initial burst of fluoride release followed by gradual slow release is a common phenomenon of dental restoratives such as glass ionomer cements and due to the dissolution of fluoride containing particles in acidic medium [205] [387] [388]. G-ænial released a higher amount of fluoride in acidified artificial saliva than the NanoFA composite, most likely due to differences in the materials' compositions. In particular, G-ænial contains two sources of fluoride in its composition, which are not specified in the material safety data sheet. The product sheet states that the material contains pre-polymerized fillers containing strontium- and lanthanoid fluoride while the material safety data sheet lists ytterbium trifluoride as one of the components; though, material safety data sheets have been reported to be misleading [389]. Additionally, other researchers found that it is common for the MSDS of dental materials to be incomplete as manufacture are obliged to report only the main ingredients of material composition [390] [391] [392].

The addition of NanoFA fillers to the composite formula has clearly resulted in increased fluoride release. This is evident from fluoride measurement data (figure 46) as fluoride release was seen from early time points, i. e. in the first 30 minutes. The release of fluoride from the composite matrix into the surrounding environment has a downside. The dissolution of fluoridated particles from the material into the surrounding liquid lead to the formation of

voids in the material matrix [141]. These voids can be seen in SEM images (Fig 49-51). The porosity of composite materials will affect the mechanical properties. The diffusion of water and other molecules will be facilitated into the polymer network due to increased porosity of the material leading to swelling of the polymer network. Subsequently, this will aid hygroscopic/hydrolytic processes such as chain separation and silane bond degradation between the resin-phase and fillers [393] [394] [395]. Moreover, the porosity of dental composite is also related to incomplete monomer to polymer conversion [396]. Additionally, air trapped within the material during procedures such as specimen preparation or mechanical testing can contribute to voids formation.

One approach to achieve fluoride release from the experimental dental composite material, is by water diffusion through the polymer system to allow dissolution of fluoride containing particles within the material and subsequently outward migration of fluoride ions into the adjacent environment [397]. Therefore, the addition of HEMA to the monomer system of the experimental composite material would allow water diffusion due to the hydrophilicity of the monomer -in the hope that this approach would not significantly compromise the mechanical properties of the material. The dissolution of fluoride particles would result in void within the matrix and eventually weaken the materials structure. In addition, HEMA will increase the water sorption and increase the possibility of hydrolytic degradation [398].

In distilled water, G-ænial showed significant water sorption at the early time points: 30 minutes, 1 hour and 4 hours compared to NanoFA. In contrast, NanoFA water sorption was significant at week 1 of the storage. Moreover, the addition of NanoFA to the composite matrix increased water sorption as seen in Figure 47. All three materials showed water sorption during storage. The highest water sorption by NanoFA composite and G-ænial was noted by week 4. As discussed earlier, the fluoride release was detected until week 4 and the solubility of fluoride containing fillers will create space in the material's matrix and these spaces provide access to water. In addition, many other factors affect the water sorption by polymer network of composite materials. Initially, the main factor affecting the water sorption is the chemical structure of polymer network. All materials tested in this chapter contain UDMA as the main resin monomer. As discussed in chapter 2, UDMA is a less toxic alternative in dental composite matrices than Bis-GMA due to its Bisphenol A content. Improved mechanical properties and reduced water sorption was found with materials containing UDMA as the resin matrix [399].

Moreover, UDMA water uptake is 3.6-3.9 % less than Bis-GMA [400] [401]. UDMA contains urethane linkage that contribute to monomer hydrophilicity enabling water to easily penetrate the polymer network [402]. According to Benjamin (2018), water uptake and diffusion into an UDMA network follows Fick's law and is unavoidable due to the chemical nature of UDMA. Attempts to reduce water permeability by polymerization under high pressure aimed to improve resistance to water did not solve the problem [403]. Therefore, water sorption by UDMA based polymers is inevitable. The significant water sorption by G-ænial at the early time point can be explained by the more heterogenous structure of the material that contribute to the presence of micropores that can take larger amounts of water [396]. This also explains the higher water sorption by NanoFA composite compared to the control material (composite without NanoFA). An additional factor affecting the fluid sorption of dental materials is the degree of conversion. When composite materials are stored in liquid, residual unreacted monomers are released followed by diffusion of water or fluid into the polymer network to occupy the micropores. This process takes a few weeks to complete [117]. Therefore, the highest water sorption was seen by week 4.

In artificial saliva and acidified artificial saliva, NanoFA composite showed a higher sorption rate compared to the other groups, being significant for the most time points. It was interesting to find some degree of coincidence of fluoride release and fluid sorption. This potentially demonstrates the effect of NanoFA fillers and the immersion solution on the sorption pattern of composites in these experiments. For instance, in artificial saliva the highest fluoride release was seen by week 1 for G-ænial and week 2 for NanoFA (Figure 46, B), while the highest sorption values in artificial saliva were week 3 for G-ænial and week 4 for NanoFA composite (Figure 47, B). Moreover, the highest fluoride release by NanoFA composite in acidified artificial saliva was noted within the first 24hours whereas for G-ænial this was in the first 48 hours (Fig46, C). Similarly, the highest sorption value for NanoFA composite and G-ænial in acidified artificial saliva was measured at the 24-hour time point as shown in Figure 47, C. This early phase fluoride release in acidified artificial saliva (Figure 46) corresponds to the early sorption phase that was also noted in acidified artificial saliva (Figure 47). In addition, there was an initially high followed by steady lower sorption values of $NanoF_A$ and G-ænial composite in acidified artificial saliva. This indicates that once fluoride is released and nanofillers are dissolved in the storage medium, more fluid diffuses into the materials. In

support of our findings, sorption studies on commercial dental composites also demonstrated increased sorption by nanofilled composites [404] [252] [405] [406]. This was explained by poor impregnation of the nanofiller by resin matrix leading to the formation of micropores in the polymer network. The presence of these micropores facilitates fluid diffusion. Increased fluid uptake was attributed to the formation of pockets of clustered nanofillers, and irregular porous structure formed due to the increased surface area to volume ratio.

The three point-bending test data showed that the flexural strength of the experimental composite was significantly lower than the G-ænial composite. Designing dental composite material in the lab requires optimisation procedures to minimize the variability within the material. In addition, manufacture have larger batches of materials to reduce flaws within the final product. Moreover, silane coating of filler particles will improve the mechanical properties of the composite material. Silane coupling agents are responsible for good adhesion between the resin matrix and the filler phase [407]. Surface treatment of the nanofiller with a silane agent will allow adequate dispersion and binding of particles with the resin matrix [408]. However, in this occasion silane treatment of NanoFA particles would be detrimental to fluoride release. Silane coating would reduce the hydrophilicity of the medium and minimize water diffusion and thereby fluoride particle dissolution. Therefore, while non-silanization of the nanofillers resulted in fluoride release, eventually it affected the materials mechanical properties. On the other hand, silica fillers of G-ænial composite are hydrophobically treated with dimethyl constituent to ensure intimate contact with the resin-matrix phase. According to the manufacturer more stability and strength is provided by dimethyl-treated silica compared to silane coating.

Chapter 5: RNA Seq analysis of oral gingival fibroblasts treated with experimental and commercial composites.

5.1 Introduction

Dental composites are increasingly popular as restorative materials in modern dental practice. As tooth resembling materials, they are widely used as restorations to treat tooth decay, pit, and fissure sealant, crowns, veneers, and to cement a crown or a bridge. In addition, composites are used as cavity liners and endodontic sealers. They are a satisfying alternative to amalgam due to their aesthetic properties and adhesion to tooth structure. Their popularity became significant after the EU -wide phase-down of the use of amalgam in dental fillings aimed at reducing mercury release into the environment and calls for prevention, health promotion, and increasing the research for developing quality, mercury-free restorative dental materials. Consequently, academic research in the field of dental composite has increasingly focused on improving the performance of the materials in terms of mechanical properties, degree of polymerization, and optical properties with little consideration given to the safety of the materials at cellular levels. However, to provide dental professionals with the most suitable alternative restoratives with the best performance, research should be aimed at both mechanical properties and potentially toxic side effects of resin-based dental materials on the oral tissues.

In general, dental composites consist of the polymerized resin matrix, reinforcing fillers, and an initiator-activator system. Currently commercially available materials lack bioactive properties. Bioactive dental materials such as glass ionomer cement, resin-modified glass ionomer, and compomers are examples of products with bioactive behavior. However, these are not strong enough to be used as restorative materials. They are used as cavity liners or to restore primary teeth in children. The development of dental composites with bioactive fluoride release potentially helps to replace dental hard tissue and remineralize the remaining tooth structure. Therefore, this project aimed to develop composite materials containing Nanofluorapatite ($NanoF_A$) as secondary fillers. Here, NanoFA was added to enhance fluoride ion release, and fluoride ion release was confirmed by the ion-selective electrode. The release of fluoride ions from these materials has the advantage of making the restorative material anti-cariogenic, resisting caries formation, and strengthening the dental hard tissues. However, the effect of fluoride on oral gingival cells has not been extensively studied. Fluoride is known to be toxic at higher concentrations, especially in dental products such as toothpaste and mouth rinses. Upon contact with moisture, hydrofluoric acid will form and lead to harmful

effects due to low pH. According to the American Association of Poison Control (AAPC) children under the age of six are involved in 80% of reported fluoride toxicity cases [409].

The oral environment is harsh for resin-based materials as they are exposed to multiple factors such as moisture, salivary enzymes, the changing pH, and occlusion forces of mastication. All these factors can contribute to compromising the strength of the material and subsequent degradation of the polymer network. Degradation products can be either monomers or their by-products, additives, photoinitiator and ions such as fluoride. In addition, during polymerization monomer to polymer conversion is incomplete as the percentage of conversion is significantly less than 100%. Residual monomers make up 1-1.5% of the polymer network and this is enough to result in adverse effects [410]. Unreacted residual monomers leach into the oral environment due to the effect of solvents or degradation processes. Individual resin monomers have been shown to induce a toxic effect on oral tissues. For example Bis-GMA, a resin monomer widely used in composites is a highly toxic resin due to its ability to release Bisphenol A (BPA) into human saliva [339]. As a consequence, UDMA is preferably used in the composition of new materials to replace Bis-GMA. The potentially toxic effect of UDMA, fluoride, and other additives has not fully been investigated. Therefore, the consequences of the component release from these materials and their effect on oral tissue should be studied in detail to determine the cellular response in oral tissue to these chemicals.

To comprehensively address the effect of different components of resin-based dental composite materials, transcriptome modification of oral gingival fibroblasts was investigated. RNA seq analysis was performed with oral gingival fibroblasts cells incubated with polymerized novel dental composite and commercially available composites to reveal potential side effects on the cells. Recent advancement in high throughput next generation sequencing gives a detailed account of gene expression and enable researchers to investigate mechanisms of inflammation or toxicity.

5.2 Aim and Objectives

to analyse the effect of novel bioactive NanoFA dental composite and commercial G-ænial materials on gene expression changes in primary gingival fibroblasts using next-generation sequencing. Oral gingival fibroblasts were exposed to dental materials for 24hours. Total RNA

from primary gingival fibroblasts was extracted, purified, and quantified. Then, RNA seq was performed.

5.3 Method and materials

5.3.1 Materials preparation

The dental composite material was prepared from two monomers, 2-Hydroxyethyl methacrylate (HEMA; CAS-NO868-77-9) and Urethane methacrylate (UDMA; CAS-NO 72869-68-4), obtained from Sigma Aldrich, UK. The monomers UDMA: HEMA were used at a percentage of 80:20; the photoinitiator-system, camphorquinone (CQ) and accelerator 4-Ethyl dimethyl aminobenzoate EDAB (Sigma –Aldrich, UK), at a weight ratio of 1% of the weight of the monomers. The filler was silanized silica glass (First Scientific Dental Materials, Germany) used at a 63 % volume ratio. Initially, the two monomers were mixed for 20 minutes in amber glass bottles using a magnetic stirrer at 70 °C. After obtaining a homogenous mixture CQ and EDAB were added and mixed for another 20 minutes at 70 °C.

In a plastic container, the polymer portion was added first. Then, fillers were gradually added in four portions. A centrifugal mixer (Speed-Mixer™, DAC 150.1 FVZ, Hauschild Engineering, Germany) was used to mix the composite at a speed of 2000 rpm until a visibly homogenous mixture was obtained. Two types of composites were prepared at this stage, the first one containing Nanofluorapatite as a secondary filler (NanoFA composite) and another without NanoFA (-F composite).

Specimens of the two-model composite and commercial G-ænial Anterior (GC Europe) were prepared by pouring material into plastic PTFE molds (10mm diameter and 1mm thickness) using a plastic spatula. Plastic molds were placed on transparent polyethylene terephthalate (PET) film on top of a glass slide (Goodfellow Cambridge Ltd., Huntingdon, UK). A second PET strip was placed on top of the material and a glass slide was used to press the samples to a uniformly flat surface. All samples were polymerized for 20 seconds using a blue-light LED cure unit (EliparTM DeepCure-S, 3M ESPE, Germany). Light curing intensity ranged between 1100-1140 mW/cm^2 recorded with a Bluephase Meter II lightmeter. The specimens were sterilized with 70 % ethanol in a cell culture fume hood followed by UV light exposure for 15 minutes.

5.3.2 Cell Culture

Human gingival fibroblasts were obtained from ATCC (ATCC PCS -201-018), specifications of the cells were described in 2.3.1. Cells were grown in T175 flasks in fibroblasts basal medium (ATCC®PCS-201-030™). The medium was supplemented with a fibroblast growth kit-low serum (ATCC®PCS201-041™). The growth kit contains the following components added to the given final concentrations: Recombinant human basic FGF (5 ng/ml), L-glutamine (7.5 mM), ascorbic acid (50 µg/mL), hydrocortisone hemisuccinate (1 µg/mL), recombinant human insulin (5 µg/mL) and fetal bovine serum (2 %). When reaching 70-80 % confluency, cells were passaged and seeded in 6-well plates with a density of 3×10^5 cells per well. Cells were exposed to dental composite specimens after 24 hours and incubated for another 24 hours.

5.3.3 RNA extraction

For the RNA extraction, the RNeasy kit (Qiagen, #163029675) was used. Human gingival fibroblasts grown on 6-well plates were washed with PBS on ice. Then, 350 µl of cell lysis buffer (RLT buffer from Qiagen supplemented with 1 % β-mercaptoethanol) were added to each well. Cells were harvested using cell scrapers (Fisher scientific, #08-100-241). Then, the cell lysate was pipetted into QIAshredder spin columns placed in a 2 ml collection tube and centrifuged for 2 minutes at full speed. After homogenization, 1 volume of 70 % ethanol was added to the cleared cell lysate followed by pipetting up and down. 700 µl of the sample were transferred into RNeasy spin columns placed into 2 ml collection tubes and centrifuged for 30 seconds. The flow-through was discarded, after that, the RNeasy spin columns were washed with 700 µl of RW1 washing buffer (supplied in the RNeasy kit) and centrifuged for 30 seconds. Then, the spin columns were washed with 500 µl of RPE buffer and centrifuged for 30 seconds. This step was repeated followed by centrifugation for 2 minutes. The RNeasy spin columns were placed into new 1.5 ml collection tubes (supplied in the kit) and centrifuged for 1 minute. Finally, 20 µl of RNase-free water was used to elute the RNA from the spin columns. The samples were stored at -80 °C.

5.3.4 Qiazole extraction and DNase treatment

To obtain high quality RNA free of genomic DNA contamination, Qiazole extraction and DNase treatment was used. For each sample, 1 µl of DNase enzyme + 4 µl of DNase reaction buffer was added. Then, the samples were incubated for 15 minutes at 37 °C. QIAzol lysis reagent

(300 µl) was added to each sample and vortexed for 20 seconds. The samples were left on the bench for a few minutes. After that, 60 µl of chloroform was added and samples were centrifuged at 4 °C at 12000xg for 15 minutes. Later, the aqueous phase was taken out with a pipette and added to 150 µl of isopropanol. The samples were left at room temperature for 10 minutes, then centrifuged for 10 min at 4 °C 12000xg. The supernatant was discarded and 300 µl of 70 % ethanol were added and samples were centrifuged for 5 minutes at 4 °C. Finally, the samples were allowed to air dry for a few minutes. The RNA was dissolved in 20 µl of RNase-free water. The quantity and quality of RNA was evaluated by Nanodrop. Samples were stored at -80 °C.

5.3.5 RNA Sequencing

RNA sequencing was done at the Genomics Core Facility, Newcastle University (https://www.ncl.ac.uk/gcf/). First, RNA integrity was evaluated by RNA Tapestation (Agilent technology). For the depletion of ribosomal RNA, biotinylated target-specific oligos combined with Ribo-Zero rRNA removal beads were used according to the Illumina TruSeq standard guide. After rRNA depletion, RNA fragmentation was performed under elevated temperature. Then, adaptors were ligated using Index adaptors (IDT-ILMN TruSeq RNA UD Indexes (96 Indexes). The adaptor sequences are given in table 11:

Table 11: Adaptor sequences.

Adapter	AGATCGGAAGAGCACACGTCTGAACTCCAGTCA
AdapterRead2	AGATCGGAAGAGCGTCGTGTAGGGAAAGAGTGT

Paired-end RNA seq libraries were synthesized using Illumina NovaSeq technology. The raw data was obtained in FastQ format.

5.3.6 Quality control and read trimming.

Quality control aims to check the reliability of RNA seq data before proceeding to further analysis. As with any other technique, few limitations could exist due to issues such as library preparation, nucleotide composition, or GC% contents. Therefore, it is necessary to perform checks to eliminate reads with unreliably called nucleotides and trim primer sequences of each sample. Moreover, reads with low quality or incorrect PCR duplication rate are filtered out. The set cut-off point was a quality score of 20, below which reads were trimmed out. The quality scores are reported in Phred scale, which is a logarithmic measure of the probability of the base call accuracy. A base call with 20 quality score corresponds to an error rate of (1

in 100) and therefore reads with these scores were removed. The quality of the FASTQ files was assessed with FastQC (version 11.8).

5.3.7 Read Alignment and quantification.

After quality control, reads were mapped to the human reference genome and quantified. The human reference genome is available in a public database repository (https://www.gencodegenes.org/human/). The software used for this purpose was Salmon (version 0.12.0) and the reference genome file (Gencodeversion38) using the salmon index command.

Then quantification was run with Salmon by using the software salmon quant. This quantification algorithm uses the FASTQ file against the index file. Once quantification is accomplished, the R package tximport (version 1.18.0) was used to create the gene level counts (http://bioconductor.org/packages/release/bioc/html/tximport.html).

The next step was to annotate the structural and functional elements to these gene counts. The annotation file was obtained from the R package annotables (version 0.1.91, https://github.com/stephenturner/annotables).

5.3.8 Differential gene expression analysis

After obtaining the read counts, differential gene expression analysis was carried out with the R package DESeq2 (version 1.30.1). Internal normalization is required before quantification; this was done by DESeq2 to accommodate for the variation in the expression among samples to obtain comparable expression values. Two important factors are considered during normalization, sequencing depth, and gene length.

Statistical analyses determined whether differences in read counts for a given gene is significant between experimental conditions. Based on a Negative Binomial GLM (General Linear Model) and a logarithmic function, DESeq2 assesses the fold change and uses the logarithmic function to calculate the probability and carries out the Wald test on the resulting probability. The highest likelihood is divided by standard error to get test statistics which are then compared to the standard normal distribution.

5.3.9 Gene set enrichment analysis

After obtaining a list of differentially expressed genes, the genes were categorized into two groups using Microsoft excel. A list of upregulated genes (positive fold change) and down-

regulated genes (negative fold change) was generated. Filters were applied to generate tables of the top 20 most up/down regulated genes by each group. In addition, genes significantly expressed in the cells by all resin-based material were identified. The cut-off point was fold change >2 and a P-value <0.05. Differentially upregulated genes were submitted to a web-based gene set analysis toolkit (http://www.webgestalt.org/) to identify enriched functional pathways.

5.4 Results

5.4.1 RNA Samples QC

Table 12 summarizes the conditions of the experiment and the number of samples. Human gingival fibroblasts were treated with three resin based dental materials in three technical replicates (s1-s3) for each condition. Novel NanoFA based composite, dental composite without NanoFA fillers (-F composite) and commercial G-ænial (GC Europe) were used to compare the effect of the three materials on gene expression in oral gingival fibroblasts. After treatment with dental materials for 24 hours, RNA was extracted from the cells. Then, RNA was further treated with DNase to ensure no genomic DNA, or any contamination was present. Genomic DNA depletion is a necessary step before performing RNA sequencing as RNA purity is critical for obtaining reliable data. The presence of genomic DNA, even if in trace amounts in RNA samples will result in amplification of both DNA and RNA and skew quantification. The RNA quality for all samples was assessed by Agilent Tapestation. The table below shows an overall, high RNA quality with an RNA integrity number above 9 for each sample. A RIN number of 10 is considered ideal or least degraded. The quality of RNA for all samples was high enough for further processing.

Table 12: The quality of RNA from human gingival fibroblasts treated with dental composites.

Samples	GCF code	RIN	permission to process	Conc ng/µl
NanoFA composite (s1)	61_NanoFA_Positive F1	9.4	Yes	315
NanoFA composite (s2)	62_NanoFA Positive F2	9.4	Yes	153
NanoFA composite (s3)	63_NanoFA Positive F3	9.4	Yes	181
G-ænial (s1)	64_G-ænial	9.4	Yes	354
G-ænial (s2)	65_G-ænial	9.3	Yes	372
G-ænial (s3)	66_G-ænial	9.3	Yes	277
-F composite (s1)	67_ [-F composite]	9	Yes	213
-F composite (s2)	68_ [-F composite]	9.3	Yes	320
-F composite (s3)	69_ [-F composite]	9.2	Yes	375
Control1 (C1)	70_Control1_C1	9.3	Yes	331
control2 (C2)	71_Control2_C2	9.1	Yes	541
control3 (C3)	72_Control3_C3	9.4	Yes	266

5.4.2 Quality Scores

The quality control of raw reads was assessed by FastQC (version 11.8). This software aims to identify problems in the sequencing or initial library preparation. FastQC generates a report in the form of an HTML file with graphical summaries and tables to analyse the data. The FastQ file format obtained from Illumina sequencing is a text-based file that contains the sequences per sample with their corresponding quality score. This file has four lines, the first line is the read name. The second is the sequence of the bases (nucleotides) in the read. The third line contains the sequence identifier, or any other description proceeded by (+) character. Finally, the fourth line with ASCII characters (American Standard Code for Information Interchange) encodes the quality score of each base in the read. The quality scores, called Phred scores are a measure of the quality for each base, and they reflect the probability of base-calling error.

$Q = -10 \log_{10} P$

Q Phred score (Quality score)

P Base calling error probability

For example, a Phred score of 10 reflects a 1 in 10 probability of the base being wrong or 90% base call accuracy. A Phred score of 20 reflects 1 in 100 probability error or 99% base call accuracy and so on.

Figure 52 illustrates the mean quality scores for the raw reads of the RNA Seq data. The x-axis represents the location of each base along with the read sequence. The y-axis represents the Phred score for each base in the sequence read. The y-axis on the graph area is divided into three areas. The green area is an area of generally high-quality scores. The orange area contains, scores of reasonable qualities. Finally, in the red area, scores reflect poor quality reads. Overall, the quality was very high for all samples. All samples tested were in the green zone of the graph with Phred scores above 30. This score corresponds to 99.9% base calling accuracy. Therefore, no trimming or filtering of the reads was necessary as the quality scores were very high apart from called errors confined to the first ten bases. This is a common observation in RNA Seq data, due to the random priming process. A MultiQC tool (http://multiqc.info/) was used to aggregate the results into a single report and data were retained for further analysis.

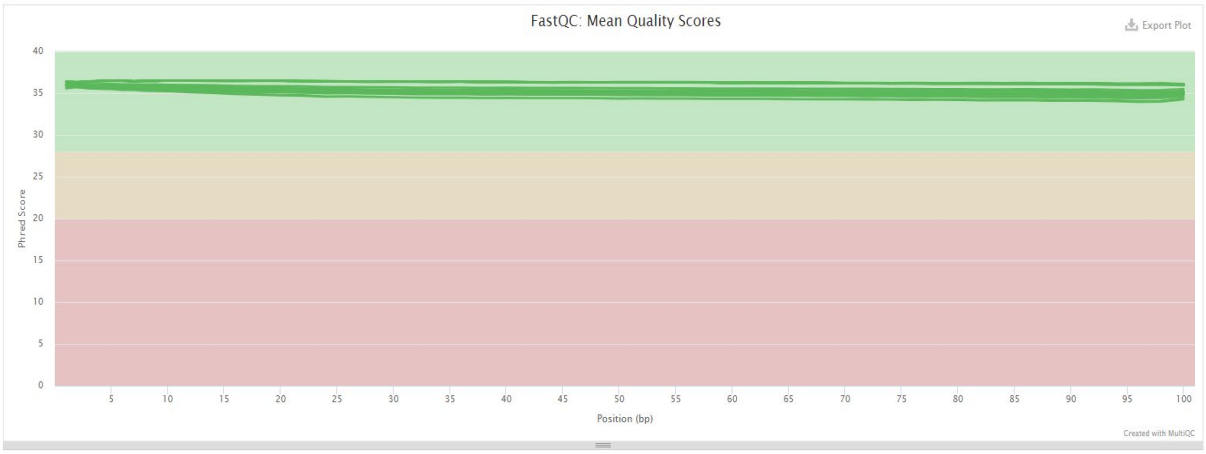

Figure 52: Mean quality scores of RNA Seq reads assessed with MultiQC showing the mean score distribution.

5.4.3 Read counts

The first step in the analysis of RNA Seq data is the normalization of the read counts. This is done to allow an accurate comparison of the level of RNA expression between the samples. The read count normalization process eliminates some factors that significantly affect the accuracy of the comparison such as reads mapped to the intron area of the gene. These reads don't reflect the accurate sequence depth as introns are not considered a gene coding area. The second factor is the gene length of a gene as the number of reads mapped to a long gene may seem that it has a higher expression level than a short gene, while in reality, they have the same expression level. The third factor is the RNA composition or the presence of

contamination. For example, the reads mapped to one differentially expressed gene in a sample can potentially skew the counts for this sample compared to another samples. Therefore DESeq2 adjusts for differences in sequencing depth and RNA composition by using the (log base e) values of the reads. Then, the geometric means which are defined as the average of these log values, are calculated. This will eliminate outliers, genes that are expressed at a high level due to sequence depth issues. In addition, genes with zero read counts (log value= infinity) are filtered out to focus on genes expressed at a similar level. In the next step, DESeq2 estimates the ratio of the counts in each sample to the average counts in all samples by subtracting the geometric means from the log (counts). This step will identify the significant differentially expressed genes. Finally, the median of the counts' ratio across each sample is calculated. The median values prevent the data from being skewed in one direction.

For better visualization, the data complexity is reduced with a principal component analysis (PCA) graph that aims to reduce dimensionality. In addition, PCA emphasizes the variations in sample composition reflected by clustering in the graph below. The principal component analysis and samples distances (Figure 53) demonstrate the variations in experimental conditions. The X-axis represents the PCA1 which shows significant variation of the expression profiles among the clustered groups. PCA1 indicates a 35% variation between the control cluster and dental composite materials clusters. The Y-axis PCA2 shows the second highest variation of gene expression between the groups (20%). Therefore, the graph illustrates a clear difference among the clusters indicating a distinct expression profile in human gingival fibroblasts resulting from exposure to different resin-based composites.

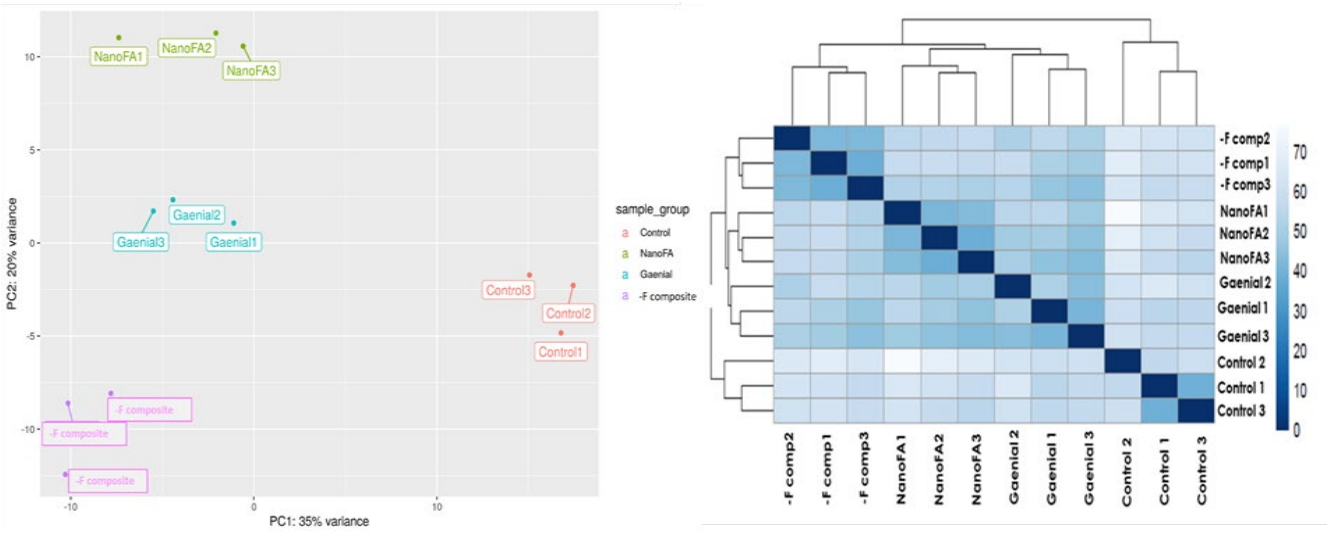

Figure 53: PCA and sample distance graph. A) PCA plot with colour coded samples. B) Heatmap showing the distance between the samples.

5.4.4 Differential gene expression analysis

To gain insights into the effect of resin-based dental composites on oral gingival tissue differentially expressed genes were identified. The expression changes are expected to reflect the impact of monomers and additives such as fillers and fluoride particles on tissue at molecular level. RNA seq data was assessed initially by Principal Component analysis to estimate how closely the replicates clustered and to test the variations between the experimental conditions. The PCA and sample distance analysis (Figure 54) emphasized distinct differences in the expression profile between the control cells and cells exposed to resin-based composites. Therefore, the next step was to assess the differential gene expression. Based on the negative binomial generalized linear model (GLM), the fold change and P value were estimated using DESeq2 with the R package. Genes with a log2 fold change larger than 1 and a Benjamini-Hochberg adjusted p-value of less than 0.05 were classified as significantly differentially expressed. The following comparisons between experimental conditions was assessed:

- NanoFA composite vs Control
- G-ænial composite vs Control
- -F composite vs Control

- NanoFA composite vs G-ænial composite
- NanoFA composite vs -F composite
- -F composite vs G-ænial composite

The figures below illustrate heatmaps of highly expressed genes in the three experimental conditions. The comparisons are -F composite vs control, NanoFA composite vs control, and G-ænial composite vs control. The heatmaps represent hierarchical clustering of similar expression patterns of genes within the same group. The rows represent the genes, while the columns represent the samples. The color-coded bar corresponds to the fold change. The heatmaps show the differentially expressed genes between the three dental composite materials and the control. The gene expression is ranked by fold change and p-value. Therefore, the top differentially expressed genes by the respective materials are represented in the heatmaps.

Overall, different composite materials affected different genes set. For instance, some of the top upregulated genes by -F composite were: *FLT* encodes proteins for vascular endothelial growth factor receptors; *SRXN1*, sulfiredoxin1 enables oxideoreductase activity, and *STAT1* encodes a protein of the STAT family of transcription activators in response to receptor associated kinases. Some of the top upregulated genes by NanoFA composite are *PLPP3* which codes for phospatidic acid phosphatase with a role in glycerolipid synthesis, and *NNMT* codes for proteins responsible for N-methylation with a role in detoxification. While some of the top regulated genes by Gænial composite include *FTL*, a gene that encodes for ferrtin protein subunits which have a role in iron storage in prokaryotic cells and *MMP1* or matrix metalloproteinase 1, a protein that is involoved in the breakdown of extracellular matrix.

Remarkably, *AKR1C1* or aldeoketo reductase family 1 member C is one of the top significantly upregulated genes in HGF cells exposed to all materials, indicating that all composites have induced a similar stress response. Addtionally, the gene *AGTR1* (Angiotensin II Receptor Type 1) was found to be significantly upregulated by all three composite materials in comparison to the control. Two genes, *KRT34* and *KRT19*, (Keratin 34 and Keratin 19) were differentially expressed in all three materials vs control. The gene *A0C90673.1* was significantly induced by both -F composite and NanFA composite. Moreover, *SLC40A1* (Solute Carrier Family 40 member 1, an Iron-Regulated Transporter) was significantly upregulated by both -F composite

and Gaenial, while in response to NanoFA a member of another SLC family gene, SLC2A6 (Solute Carrier Family 2 member 6, a facilitated glucose transporter) was upregulated.

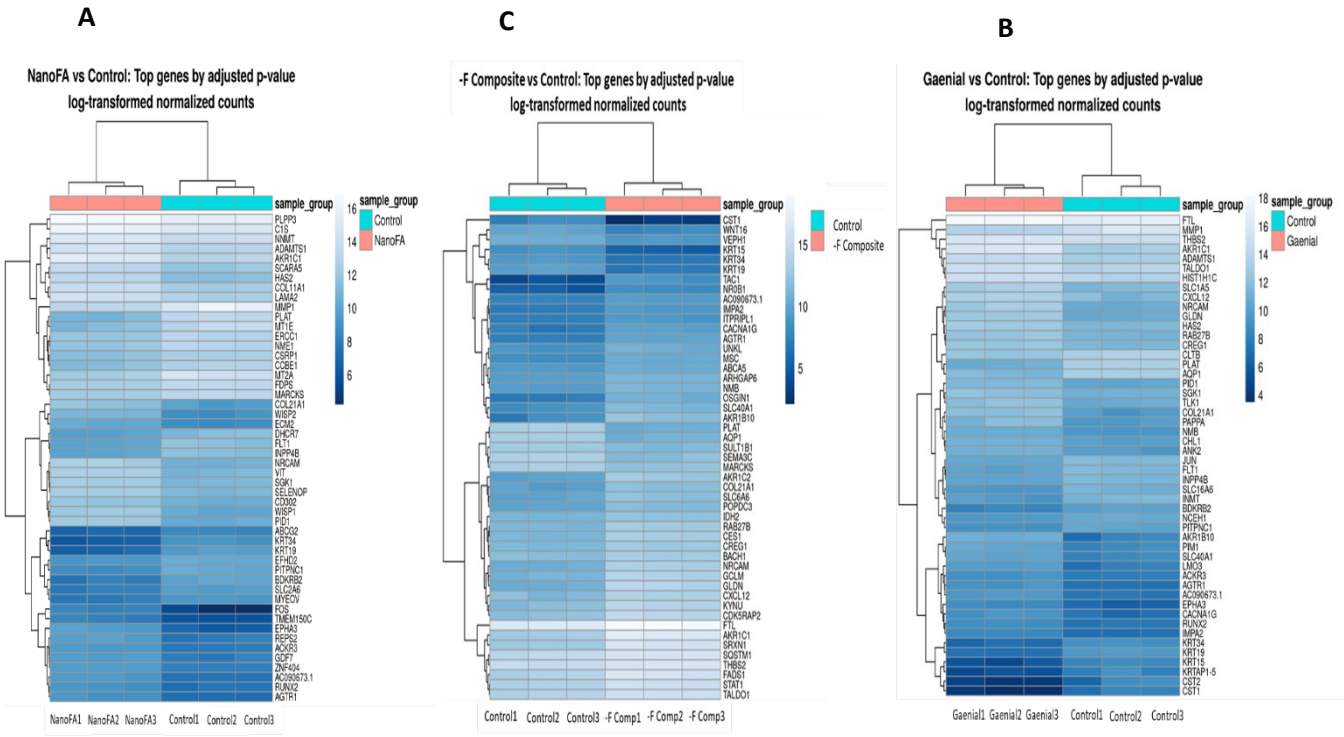

Figure 54: Heatmaps of statistically significant, differentially expressed genes for each treatment condition. A) HGF treated with (-F composite). B) HGF treated with NanoFA composite. C) HGF treated with G-ænial composite.

An alternative way of visualizing differentially expressed genes are volcano plots. The plots for the three comparisons demonstrate differences in highly expressed genes caused by each condition versus the control, differentially expressed genes are highlighted in red (Figure 55). The x-axis of the volcano plot represents the fold change or the magnitude of gene expression. The fold change for a specific gene is the ratio of the mean in the test group compared to the mean of the control. A fold change of 2 is considered significant. The upregulated genes are plotted along the positive scale (right), while the downregulated genes are towards the negative scale of the graph. The y-axis represents the significance (*P* value) of the expression differences of the genes. The –log10 (padj) is used, therefore the smaller the p-value the higher the –log 10 (Padj). Points high up in the graph represent the most statistically significant gene expression changes.

Differential gene expression analysis showed that for oral gingival fibroblasts treated with -F composite 124 genes were significantly upregulated ($P<0.05$, fold change >2). In addition, 133

genes were significantly downregulated. In gingival fibroblasts treated with NanoFA composite, 118 genes were significantly over expressed compared to 107 genes that were downregulated. For the G-ænial composite, 78 genes were significantly upregulated, while 46 genes were downregulated. Moreover, when the cells treated with NanoFA composite were compared to G-ænial six genes were upregulated, while eleven genes were downregulated. All composite materials resulted in significant upregulation of oxideoreductase activity as indicated by the upregulation of the *AKR1C1* gene. The following steps will involve gene set enrichments analysis to identify the specific pathways upregulated in the cells in response to each composite material.

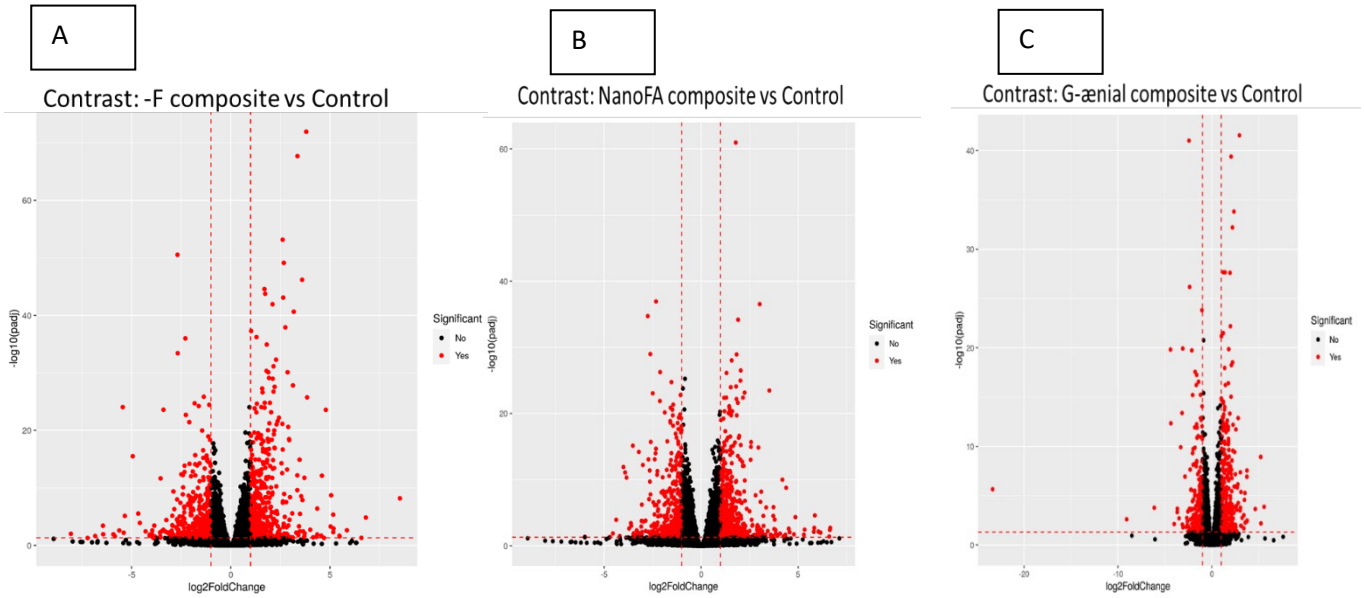

Figure 55: Heatmaps showing log transformed normalised counts of the 50 most significant differentially expressed genes in HGF cells in each treatment condition. A) HGF treated with (-F composite). B) HGF treated with NanoFA composite. C) HGF treated with G-ænial composite.

5.4.5 Gene Set Enrichment Analysis

Differentially expressed genes were submitted to a web-based gene set analysis toolkit (http://www.webgestalt.org/) to perform functional enrichment analysis. The cut-off criteria were a fold change ≥2 and a p-value ≤ 0.05. The goal of the pathway analysis was to infer a biological function to a series of differentially expressed genes in RNA seq data. This will help to understand the mechanism of disease or potential toxicity by identifying the pathways associated with the aetiology of the damage to the cells and tissues. The graphs below (Figures 56, 57 and 58) show the top 10 upregulated pathways by the dental composite

materials. Among these top 10 pathways, the pathway associated with the metabolism of xenobiotics was enriched in cells treated with all dental material composites. The ferroptosis pathway was enriched in both -F composite and NanoFA composite. The chemical carcinogenesis pathway was enriched in both -F composite and G-ænial composite.

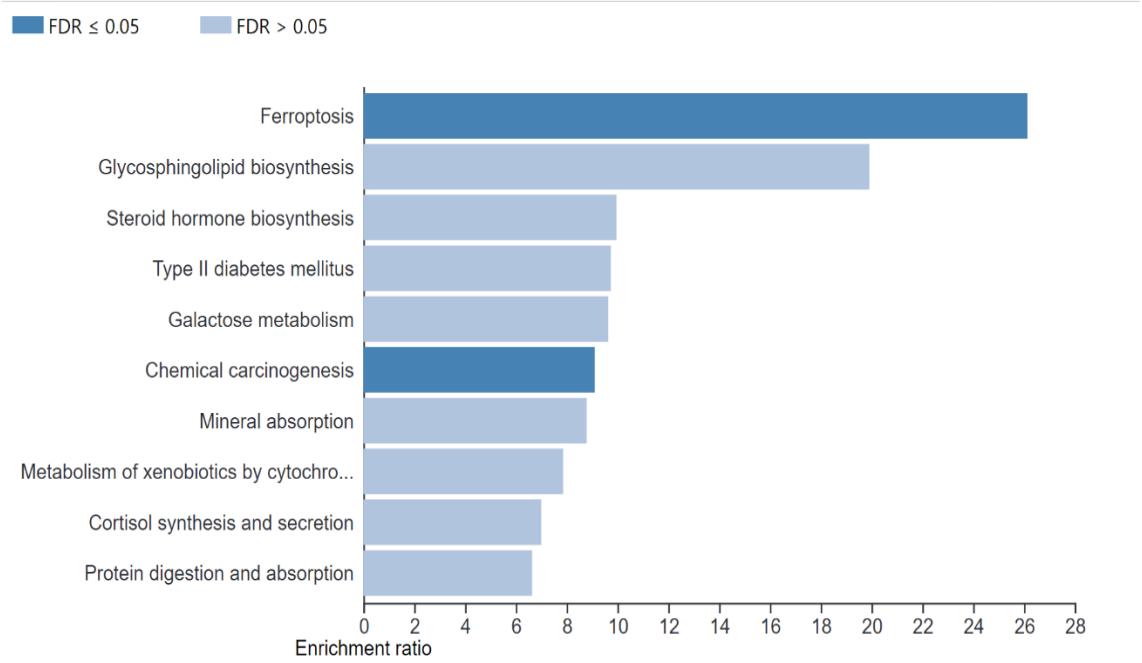

Figure 56: Bar chart demonstrating gene set enrichment in HGF in order from highest to the lowest enrichment ratio of HGF treated with -F composite. FDR stands for false discovery rate, which is a statistical measure used to control the number of false positive results in multiple hypothesis testing. Gene sets with higher FDR are considered more significant and are highlighted in the polts.

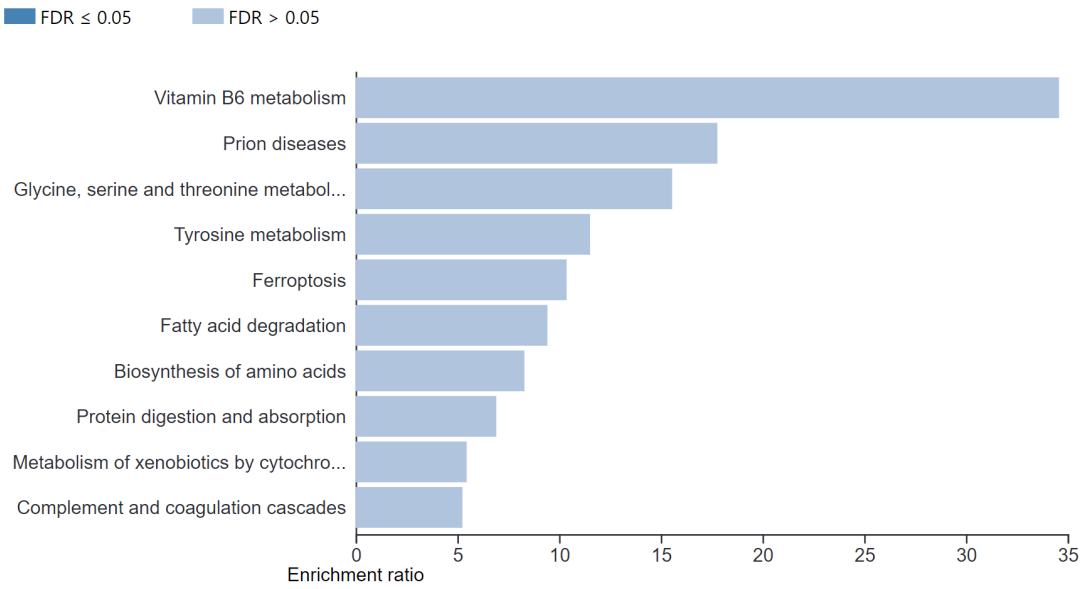

Figure 57: Bar chart demonstrating gene set enrichment in HGF in order from highest to the lowest enrichment ratio of HGF treated with NanoFA composite.

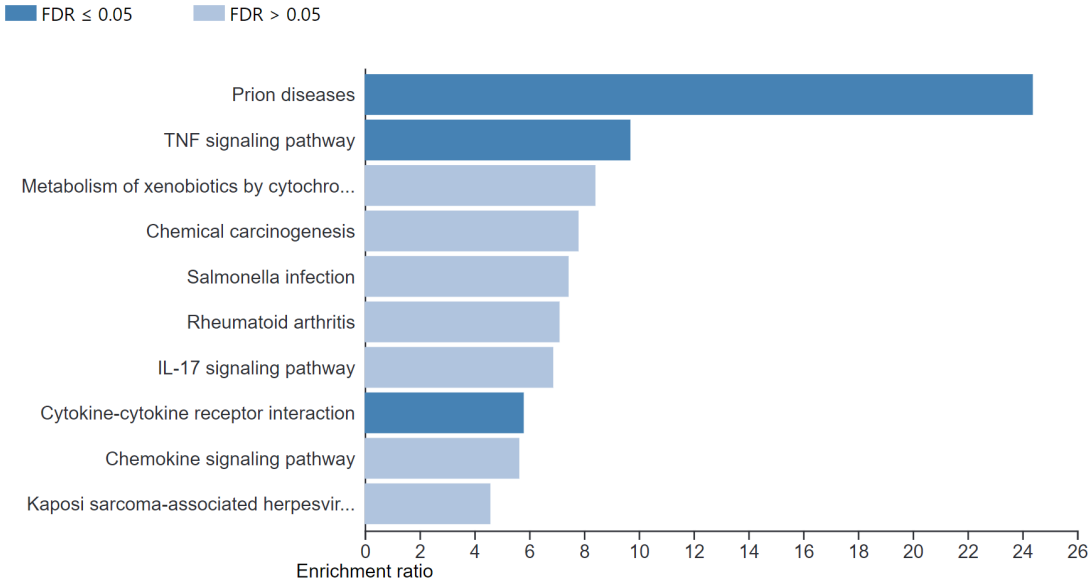

Figure 58: Bar chart demonstrating gene set enrichment in HGF in order from highest to the lowest enrichment ratio of HGF treated with G-ænial composite.

The following tables 13, 14, 15 demonstrate the list of top 20 significantly upregulated genes in HGF cells exposed to dental composite materials. Moreover, a detailed overview of the shared upregulated pathways in the cells by all composite materials are listed in table 16. The genes were filtered in Microsoft excel using cut-off criteria of $P<0.05$ and fold change >2.

Table 13: Top 20 differentially expressed upregulated genes in HGF cells treated with (-F composite) compared to control cells. The highlighted gene is also upregulated by other treatments.

Ensembl-gene-id	HGNC symbol	Description	log2Fold Change	pvalue	padj	chromosome
ENSG00000259132	AL132780.3	A protein coding gene. An important paralog of this gene is HAUS4.	8.53	1.16E-10	6.38E-09	14
ENSG00000236136	ADORA2BP1	adenosine A2b receptor pseudogene 1	6.81	5.52E-07	1.40E-05	1
ENSG00000274049	INO80B-WBP1	INO80B-WBP1 readthrough (NMD candidate)	6.58	0.00816	0.047751	2
ENSG00000226754	AL606760.1	A novel transcript, antisense to MAGOH.	5.85	1.87E-04	0.002271	1
ENSG00000268173	AC007192.1	Protein coding, member of CCDS.	5.49	0.003944	0.027359	19
ENSG00000260114	AC120114.2	No description found.	5.48	0.002778	0.020729	16
ENSG00000184106	TREML3P	triggering receptor expressed on myeloid cells like 3, pseudogene	5.18	8.39E-05	0.001159	6
ENSG00000163485	ADORA1	adenosine A1 receptor	5.17	4.75E-04	0.004947	1
ENSG00000137491	SLCO2B1	solute carrier organic anion transporter family member 2B1	5.16	1.50E-07	4.39E-06	11
ENSG00000123689	G0S2	G0/G1 switch 2	5.06	3.08E-11	1.92E-09	1
ENSG00000267321	LINC02001	long intergenic non-protein coding RNA 2001	5.03	3.21E-05	5.10E-04	17
ENSG00000006128	TAC1	tachykinin precursor 1	4.79	6.70E-27	2.69E-24	7
ENSG00000139985	ADAM21	ADAM metallopeptidase domain 21	4.70	0.008348	0.048493	14
ENSG00000227471	AKR1B15	aldo-keto reductase family 1 member B15	4.59	7.23E-15	7.56E-13	7
ENSG00000117069	ST6GALNAC5	ST6 N-acetylgalactosaminide alpha-2,6-sialyltransferase 5	4.56	0.002648	0.020004	1
ENSG00000229261	AL596223.1		4.36	1.05E-08	3.94E-07	10
ENSG00000116701	NCF2	neutrophil cytosolic factor 2	4.36	0.001497	0.012598	1
ENSG00000176928	GCNT4	glucosaminyl (N-acetyl) transferase 4, core 2	4.32	0.004709	0.031382	5
ENSG00000226091	LINC00937	long intergenic non-protein coding RNA 937	4.15	0.00635	0.039374	12
ENSG00000164142	FAM160A1	family with sequence similarity 160 member	4.01	1.45E-04	0.001843	4

Table 14: Top 20 differentially expressed upregulated genes in HGF cells treated with NanoFA composite compared to control cells. The highlighted gene is also upregulated by other treatments.

Ensembl-gene-id	HGNC symbol	Description	log2Fold Change	pvalue	padj	chromosome
ENSG00000188037	CLCN1	chloride voltage-gated channel 1	6.66	1.93E-04	0.001984	7
ENSG00000268173	AC007192.1		6.64	4.46E-04	0.003993	19
ENSG00000274049	INO80B-WBP1	INO80B-WBP1 readthrough (NMD candidate)	6.61	0.007892	0.039678	2
ENSG00000203685	STUM	stum, mechanosensory transduction mediator homolog	6.16	0.001409	0.010133	1
ENSG00000260114	AC120114.2		6.05	9.04E-04	0.007102	16
ENSG00000267321	LINC02001	long intergenic non-protein coding RNA 2001	5.87	1.22E-06	2.56E-05	17
ENSG00000226754	AL606760.1		5.84	1.94E-04	0.00199	1
ENSG00000139985	ADAM21	ADAM metallopeptidase domain 21	5.81	9.48E-04	0.007398	14
ENSG00000117069	ST6GALNAC5	ST6 N-acetylgalactosaminide alpha-2,6-sialyltransferase 5	5.34	3.94E-04	0.003607	1
ENSG00000243627	AP000322.1		5.30	0.003645	0.021548	21
ENSG00000128165	ADM2	adrenomedullin 2	4.86	2.52E-06	4.74E-05	22
ENSG00000164684	ZNF704	zinc finger protein 704	4.79	0.003032	0.018655	8
ENSG00000236136	ADORA2BP1	adenosine A2b receptor pseudogene 1	4.56	0.001142	0.008556	1
ENSG00000280800	FP671120.3		4.52	2.64E-04	0.002581	21
ENSG00000176826	FKBP9P1	FK506 binding protein 9 pseudogene 1	4.39	2.69E-11	1.71E-09	7
ENSG00000226091	LINC00937	long intergenic non-protein coding RNA 937	4.35	0.003678	0.021693	12
ENSG00000137558	PI15	peptidase inhibitor 15	4.35	0.005305	0.028912	8
ENSG00000254303	AC037486.1		4.26	0.006756	0.035109	8
ENSG00000227471	AKR1B15	aldo-keto reductase family 1 member B15	4.19	1.28E-12	1.02E-10	7
ENSG00000227141	AL160286.1		4.07	0.002219	0.014641	1

Table 15: Top 20 differentially expressed upregulated genes in HGF cells treated with (G-ænial composite) compared to control cells. The highlighted gene is also upregulated by other treatments.

Ensembl-gene-id	HGNC symbol	Description	log2Fold Change	pvalue	padj	chromosome
ENSG00000267321	LINC02001	long intergenic non-protein coding RNA 2001	5.56	4.33E-06	1.34E-04	17
ENSG00000226091	LINC00937	long intergenic non-protein coding RNA 937	5.23	4.80E-04	0.006524	12
ENSG00000123689	G0S2	G0/G1 switch 2	5.20	8.83E-12	1.18E-09	1
ENSG00000128165	ADM2	adrenomedullin 2	4.62	8.03E-06	2.25E-04	22
ENSG00000163823	CCR1	C-C motif chemokine receptor 1	3.75	2.13E-04	0.003382	3
ENSG00000227471	AKR1B15	aldo-keto reductase family 1 member B15	3.73	3.09E-10	2.82E-08	7
ENSG00000213648	SULT1A4	sulfotransferase family 1A member 4	3.72	1.47E-09	1.20E-07	16
ENSG00000213648	SULT1A4	sulfotransferase family 1A member 4	3.72	1.47E-09	1.20E-07	16
ENSG00000267272	LINC01140	long intergenic non-protein coding RNA 1140	3.68	2.92E-04	0.00436	1
ENSG00000137491	SLCO2B1	solute carrier organic anion transporter family member 2B1	3.55	3.74E-04	0.005296	11
ENSG00000176826	FKBP9P1	FK506 binding protein 9 pseudogene 1	3.51	1.09E-07	5.34E-06	7
ENSG00000165959	CLMN	calmin	3.47	6.70E-07	2.67E-05	14
ENSG00000140807	NKD1	naked cuticle homolog 1	3.40	4.50E-05	9.46E-04	16
ENSG00000196208	GREB1	growth regulation by estrogen in breast cancer 1	3.40	0.002244	0.020878	2
ENSG00000261279	ULK4P1	ULK4 pseudogene 1	3.22	9.62E-05	0.001783	15
ENSG00000210195	MT-TT	mitochondrially encoded tRNA threonine	3.14	0.00108	0.011987	MT
ENSG00000140600	SH3GL3	SH3 domain containing GRB2 like 3, endophilin A3	3.10	8.35E-08	4.23E-06	15
ENSG00000150594	ADRA2A	adrenoceptor alpha 2A	3.08	9.58E-04	0.011034	10
ENSG00000196517	SLC6A9	solute carrier family 6 member 9	3.04	5.49E-06	1.63E-04	1
ENSG00000174697	LEP	leptin	3.03	4.83E-10	4.29E-08	7

Table 16: Common overexpressed genes in HGF cells in all treatment conditions (-F composite, NanoFA and G-ænial composite).

Ensembl-gene-id	HGNC symbol	Description	log2Fold Change	chromosome
ENSG00000151012	SLC7A11	solute carrier family 7-member 11	>2	4
ENSG00000187134	AKR1C1	aldo-keto reductase family 1 member C1	>2	10
ENSG00000198074	AKR1B10	aldo-keto reductase family 1 member B10	>2	7
ENSG00000196616	ADH1B	alcohol dehydrogenase 1B (class I), beta polypeptide	>2	4
ENSG00000163823	CCR1	C-C motif chemokine receptor 1	>2	3
ENSG00000267321	LINC02001	long intergenic non-protein coding RNA 2001	>2	17
ENSG00000226091	LINC00937	long intergenic non-protein coding RNA 937	>2	12
ENSG00000123689	G0S2	G0/G1 switch 2	>2	1
ENSG00000196208	GREB1	growth regulation by estrogen in breast cancer 1	>2	2
ENSG00000164112	TMEM155	transmembrane protein 155	>2	4
ENSG00000140807	NKD1	naked cuticle homolog 1	>2	16
ENSG00000261279	ULK4P1	ULK4 pseudogene 1	>2	15
ENSG00000140600	SH3GL3	SH3 domain containing GRB2 like 3, endophilin A3	>2	15
ENSG00000143125	PROK1	prokineticin 1	>2	1
ENSG00000009950	MLXIPL	MLX interacting protein like	>2	7

Table 17: Common pathways significantly upregulated in HGF cells by all treatment conditions.

Pathway	ID	Description	Materials	status
D-threo-aldose 1-dehydrogenase activity	GO:0047834	Molecular function: oxidoreductase activity acting on CH-OH group.	All three	UP
Alcohol dehydrogenase (NADP+) activity	GO:0008106	Molecular function: oxidoreductase activity acting on CH-OH group.	All three	UP
Indanol dehydrogenase activity	GO:0047718	Molecular function: oxidoreductase activity acting on CH-OH group.	All three	UP
Phenanthrene 9,10-monooxygenase activity	GO:0018636	Catalysis of redox-reaction, oxidoreductase activity.	All three	UP
Cellular response to chemical stimulus	GO:0070887	Alteration of cellular activities due to Chemical stimulus. (Gene expression, enzymes production or secretion)	All three	UP
Multicellular organismal process	GO:0032501	Biological processes, this is a parent term as this involves different pathways associated with physiological processes at multicellular organism level.	All three	UP
Homeostatic process	GO:0042592	Processes involved in maintain homeostatic cellular state.	All three	UP
Chemical homeostasis	GO:0048878	Parent term involves processes associated with maintaining homeostasis of different molecules such as ion, carbon dioxide, gas…etc.	All three	UP
Response to xenobiotic stimulus	GO:0009410	Processes that alter cellular activities due to exposure to foreign compound or toxin.	All three	UP
Regulation of multicellular organismal process	GO:2000026	Processes such as growth and development.	All three	UP
Ferroptosis	GO:0097707	Programmed cell death due to lipid peroxidation and ROS production.	All three	UP
Ferritin complex	GO:0070288	Regulation of iron storage.	All three	UP
Intrinsic component of plasma membrane	GO:0031226	Protein complexes in the hydrophobic region of plasma membrane.	All three	Down
Integral component of plasma membrane	GO:0005887	Protein complexes such as interleukin-6,13,12 receptors and others.	All three	Down

5.5 Discussion

The objective of this study was to investigate the effect of resin-based dental composites on oral gingival fibroblasts. These materials contain resin monomers, fillers, and initiator-activator chemicals. Two types of the resin-based composites were developed in this project with comparable formulas, though one material contained NanoFA to release fluoride. These materials, in combination with commercial G-ænial, were examined to explore potential adverse effects on gingival tissues. To understand the mechanism of a disease and biological changes induced in tissues by potentially toxic chemicals, RNA Seq technology gives a comprehensive account of gene expression changes. The technique was applied for the first time to examine cells treated with resin-based dental restorative materials. Quantification of messenger RNA which carries the information for protein translation will reveal perturbation in biological pathways, therefore, understanding and quantifying the changes in protein-coding RNA is crucial to investigate the effect of internal or external stimuli on the cells [411]. RNA Seq data analysis showed 867 genes were differentially expressed in cells treated with (-F dental composite), cells treated with NanoFA composite, 971 genes were differentially expressed, while in cells treated with G-ænial composite 568 genes were differentially expressed. To clearly understand the mechanism of disease or side effects of these resin-based materials on the cells, considerations to the significantly upregulated genes were given. These were 124 genes with -F composite, 118 genes with NanoFA, and 78 genes with G-ænial ($P<0.05$, $FC>2$). In addition, 15 genes were significantly over expressed after treatment with all materials ($P<0.05$, $FC>2$), shown in table 16. These genes point to common mechanisms to mitigate resin-based composite toxicity. Table17 summarises the common pathways significantly upregulated in HGF cells by all treatment conditions with the three materials, when in direct contact with resin-based dental materials. The table shows a common trend towards stress-related pathways. Both resin monomers and fluoride have previously been shown to induce stress to cells in the oral environment. The published research, however, has investigated the toxic effect of fluoride and resin monomers individually [412] [271] [292]. BisGMA monomer, a material used in manufacturing earlier types of resin composites is a major conceren for dentists and patients. BisGMA toxicity is attributed to the fact that it is a bisphenol A (BPA) derivative, a material who's toxicity has been extensively reported in the literature [413] [414] [415]. Therefore, newer types of dental composite are made from the

UDMA monomer. Morever, HEMA that is also used in composite formulas in a smaller concentration and in dental adhesives, has been shown to induce harmful effects. On the other hand, significant fluoride release from resin-glass ionomer cements has been shown to be directly correlated with toxicity on human dental pulp cells [416]. However, the effect of the entire resin-based composite formula on oral tissue has not been investigated. Therefore, RNA Seq is a powerful technique to provide a detailed analysis of the mechanism and type of stress resin-based composite materials might induce at the transcriptomic level, giving clear insights into their potential toxicity.

The RNA Seq analysis of human gingival fibroblasts incubated with the dental materials tested in this project showed that dental resin-based composite materials have an adverse effect on the cells. The effect can be seen in the table summarising the shared pathways, table 17. Gene set enrichment analysis (Figures 56, 57 and 58) demonstrated an upregulation of pathways associated with disruption of the cellular redox balance, oxidative stress, reactive oxygen species production, ferroptosis and response to xenobiotics among other shared pathways.

Urethane dimethacrylate, UDMA, is a resin monomer extensively used as an alternative for Bis-GMA for fabrication of polymers used in restorative dental materials and bone reinforcement. Upon light activation of the monomers, polymerization is induced and a crosslinked network is formed [417]. Trace amounts of unbound UDMA and other resin monomers can be released from the polymer network to the peripherial environment [418]. Investigating potential harmful reactions to the released UDMA is essential and has been of increasing interset to dental material researchers. UDMA has been shown to result in reduced cell viability, apoptosis and reactive oxygen species production in chinese hamster cells (CHO), lymphocytes and macrophages [419] [420] [421]. Morever, investigations into UDMA chemical toxicity in human dental pulp cells showed a disturbed cellular redox balance and an increased expression of markers for ROS production and glutathione depletion [314]. These markers involve oxidative stress response genes such as hemeoxygenase-1 (HO-1), cyclooxygenase-2 (COX-2) and carboxylesterase (CES). The expression of these genes is manditory for cell survival, maintains homeostasis and resolves inflammation. However, the mechanism underlying UDMA toxicity has not been fully examined in gingival fibroblasts. Therefore, in this project we first examined the expression of stress genes in response to UDMA exposure by quantitive real-time polymerase chain reaction (RT-qPCR). The qPCR

results demonstrated overexpression of HO-1, COX-2 and CES1. These findings are in line with RNA Seq data, where analysis showed upregulation of these genes in addtion to many other mediators of oxidureductase and heme metabolism pathways.

2-hydroxymethylmethacrylate (HEMA), is a hydrophilic methacrylic acid based resin monomer used in dental adhesive and resin composite polymers. The hydrophilicity of HEMA enables its release into dentinal tubules and subsequentley penetration into the circulation [323]. Therefore, concerns arose regarding HEMA's toxicity as resin monomers can be detected in patient's saliva after dental treatment. In addition, dental professionals handle unreacted methacrylate monomers on a daily basis. Research compiled considerable evidence demonstrating the toxicity of HEMA. Several studies showed that HEMA bound to cysteine residues of glutathione (GSH) resulting in oxidative stress as the main mechanism of toxicity [422] [423] [424]. Another study suggested increased proinflammatory mediators as the result of HEMA exposure to dental pulp cells [425]. Conversely, Morisbak et al. argued that ROS production and glutathione depletion were not the main reason for HEMA toxicity but HEMA could affect the DNA [426]. Ansteinsson et al, examined DNA damage in human bronchial epithelial BEAS 2B cells. Their finding demonstrated that HEMA inhibits BEAS 2B cell proliferation as a result of ATM activation leading to p53 dependant apotosis. ATM activates cell cycle check point kinases in a complex network of histone H2AX and DNA repair pathways [427]. We have examined the expression of DNA repair transcripts in human gingival fibroblasts after exposure to HEMA. The qPCR data showed significant upregulation of DDX11, XRCC2, IPPK, and RAD50 when gingival fibroblasts were treated with HEMA, while UDMA treatment of the cells resulted in supression of these genes. RNA seq data, confirmed the downregulation of these DNA repair genes, as UDMA is the main monomer in the new material that we developed with 80% UDMA and 20% HEMA. The findings suggest that the released concentrations of HEMA from the new composites was too low to induce DNA damage after 24 hours of exposure. The HPLC experiments detected 0.11 mM/h, 0.037 mM/h of HEMA released from (-F composite) and (NanoFA composite), respectively. The cell viability experiments demonstrated that at 1mM HEMA showed no signs of toxicity. The upregulation of DNA repair genes at 1mM of HEMA was not significant.

Resin monomer toxicity has been tested as individual components in many studies. Evidence for a contribution of monomers to ROS production by depletion of intracellular resources for

glutathione synthesis and subsequent oxidation exist [428] [429] [430]. Reactive oxygen species (ROS) are normally generated in the body due to metabolism and environmental exposure. The controlled production of ROS is beneficial for processes such as cell division, inflammation, and immunological functions. Uncontrolled ROS generation leads to oxidative stress in the cells, lipid peroxidation in the cell membrane, disruption of homeostatic processes, and contributes to the development of toxicity, chronic illnesses and cancer [431] [432].

The upregulation of oxidoreductase and mitochondrial superoxide dismutase are indicative of chemical toxicity. The expression of catalase and glutathione peroxide help to mitigate the resulting oxidative stress induced by UDMA, HEMA and fluoride in the resin-based materials. This is evidenced by ROS generation, glutathione depletion and subsequent overexpression of mediators such as aldo-keto reductase family 1 member B15 (AKR1B15), and superoxide activity to counterbalance the oxidative stress in the cells [433]. The proteins encoded by these mediators function to reduce superoxides generated as byproducts of oxidative phosphorylation and converting them to hydrogen peroxide and oxygen. The exact mechanism of how fluoride contributes to oxidative stress has not been fully investigated. RNA Seq analysis in this project illustrates upregulation of superoxide dismutase (SOD) in ginginval fibroblasts exposed to fluoride containing composites such as G-ænial and NanoFA composite. The upregulation of SOD by gingival fibroblasts appears to be a mechanism to cope with and eliminate the oxidants generated due to fluoride exposure. Accordingly, SOD upregulation has been shown previously in response to fluoride exposure [434]. In agreement with a role of SOD in detoxification of fluoride, the -F composite resulted in downregulation of SOD in gingival fibroblasts.

Another example of impaired redox balance in gingival fibroblasts, represents the induction of NADPH synthesis and activation of the NERF2 pathway. NADPH oxidase was overexpressed in cells incubated with all resin-based dental composites in this experiment. NADPH has an important function in the metabolism of reactive oxygen species. It provides a reductive environment to eliminate generated ROS during the phosphorylation process that generates ATP [435]. Therefore, NADPH is essential for cell metabolism and proliferation, particularly in immunity. The redox state of NADPH is controlled by NERF2 signalling [436]. NERF2 signalling protects against chemical toxicity and oxidation related pathologies. The products generated

by this pathway enable cells to maintain redox homeostasis and increase intracellular antioxidant capacity for detoxification [437] [438].

In addition to disturbed redox balance, the cells treated with resin-based materials displayed additional signs of a stress response. This is illustrated by the expression of biomarkers involved in inflammation and altered iron homeostasis such as ferroptosis and hyperferritinemia. RNA Seq data shows significant expression of cytokines that regulate inflammatory processes [439]. Cytokine inflammatory mediator C-C motif chemokine receptor 1, CCR1, was overexpressed by gingival fibroblasts treated with composites reflecting signs of inflammation. Cytokine expression was identified as a response to xenobiotic exposure leading to post inflammatory gingival hyperplasia in an earlier study [440]. Moreover, elevated cytokine levels directly affected ferritin complex expression. For example, hyperferritinemia is triggered by elevated cytokine levels, considered as diagnostic criteria for several pathological states including macrophage activation, viral or bacterial sepsis, and systemic inflammatory response syndrome [441]. Furthermore, expression of proteins that contribute to elevated ferritin levels were found to decrease free radical generation and were associated in some cases with autoimmune diseases [442].

Ferroptosis describes programmed non-apoptotic cell death driven by redox imbalance and reactive oxygen species (ROS) production. This pathway is characterized by iron accumulation and lipid peroxidation leading to the disruption of various metabolic pathways and homeostasis. The result is ROS build-up due to the imbalance between free radical production and diminished antioxidant defence mechanisms [443] [444], subsequently leading to cell stress and death due to cysteine depletion, GPX4 inactivation and iron overload [445]. *SLC7A11* was found to be upregulated by the three dental composite materials. The *SLC40A1* gene has a significant role in ferroptosis. *SLC40A1* (solute carrier family 40 member 1) encodes ferroportin (FPN1), also known as iron-regulated transporter1 (IREG1) which is the only protein in the cell membrane responsible for iron transport [446]. Overexpression of *SLC40A1* was found to induce iron overload and hereditary hemochromatosis [447, 448]. On the other hand, SLC4A11 functions to import cystine for glutathione biosynthesis and antioxidant defence [449].

The aim of this study was to assess the transcriptome of oral gingival fibroblasts after 24 hours of exposure to resin composites. The data analysis has identified an early stress response

manifested by disturbance of the cells redox balance and expression of cellular signalling pathways such as oxidoreductase activity, NADPH activity, ferroptosis and response to xenobiotics or signs of chemical toxicity to reinstall redox balance in oral tissues. Biomarkers of DNA damage were not detected in the gene set enrichment analysis for this treatment time point. The amount of the released monomers from resin composites was measured by HPLC analysis, chapter 3. For that experiment dental composite without NanoFA filler (-F composite) released concentrations of monomers of 0.11 mM/h HEMA and 0.08 mM of UDMA in a solution of 75% ethanol. NanoFA composite released 0.03 mM/h UDMA and 0.04 mM/h mM of HEMA, chapter 3. Concentrations of 1 mM HEMA and UDMA did not show significant reduction in gingival cell viability. The stress response detected by RNA seq analysis is the effect of smaller concentrations released in cell culture medium than the ones measured by HPLC. Future experiments should determine the concentration of resin monomers released into the cell culture media to identify concentrations responsible for upregulation of the stress response pathways. In clinical settings, released monomers are continuously washed away by human saliva resulting in a dilution of monomers. RNA seq analysis from patient biopsies 24 hours after treatment with dental composites may confirm a potential stress response. Furthermore, the findings here represent an acute response of oral gingival fibroblasts. Studies should be designed to determine a chronic response of oral tissue to resin-based materials at transcriptional level as resin composites are subjected to degradation in oral environment which leads to the release of unbound monomers and other inorganic particles.

The findings of this project clearly suggest that regardless of the small concentrations of resins and other fillers in dental composite formula, signs of a toxic effect exist at an early stage. These results are relevant not only for patients but most importantly for dental professionals due to their daily handling of resin-based restoratives. Clinical considerations and protocols to follow can be applied to minimise the unbound resin in composite polymer networks. Some of these include the use of dental rubber dams during treatment to avoid contact of the oral tissue with unreacted monomer during dental procedures [450]. Moreover, the placement of several restorations at one time of treatment should be avoided. Finishing and polishing of dental restorations was found to be associated with minimizing the residual monomer release [451]. Another preventive measure that could be applied is the use of mouth wash after

restoration placement [452]. Alternatively, dental restorative materials are fabricated in the laboratory by computer aided design such as CAD\CAM systems which utilize material blocks where restorations are milled in a machine. Thereafter, fillings are prepared under high temperature and pressure resulting in high a degree of conversion and thus significantly reduced amounts of unreacted monomer [453]. Despite these alternatives, more research should be targeted toward developing materials with an improved biocompatible formula.

Chapter 6: General discussion and summary

6.1 General discussion and Summary

Resin-based composites also termed dental composites are known in restorative dentistry for their aesthetics and good mechanical performance. They are composed of active organic phase or resin matrix and inactive or inorganic fillers. The importance and popularity of composites increased in recent years, more specifically with regards to calls aimed at the reduction of amalgam restorations use. The resin phase contains multifunctional monomers and photoinitiator. While the filler phase contains nanoscale and micro-scale fillers that provide the material with strength and reinforcements. The advanced technology in the material science provided the possibility to synthesize materials with smaller filler size to improve the mechanical properties. These materials have come a long way in term of development that included the resin phase, fillers size and curing modification [14].

Bis-GMA composites were introduced to the dental market in the mid-1960s [29]. The Bis-GMA added the advantages of being polymerized by carbon-carbon double bond conversion. The monomer's characteristics were higher molecular weight, difunctional groups and higher viscosity. Moreover, it was superior to the previously used methylmethacrylate as it provided the crossed linked polymers upon polymerization that were stronger and stiffer. The higher viscosity of the resin was mitigated by mixing with other lower molecular weight dimethacrylate monomers [25], which made possible increasing the filler content that, in turn, resulted in materials that were stronger, stiffer, had lower polymerization shrinkage and lower thermal expansion coefficient. Therefore, Bis-GMA composites became a significant dental innovation. The use of these materials together with acid-etch adhesive techniques improved treatment options for patients. More carious lesions were prevented, bonding orthodontic brackets was facilitated and use of preventive fissure sealants became popular. Overall, the clinical success in dental profession was experienced due to increased longevity of restorations provided from the use of Bis-GMA composites compared to previous filling materials [454].

Bis-GMA-based composites, however, had certain shortcomings associated with them. From a biological point of view, impurities such as bisphenol A released from Bis-GMA containing restorations have been reported to be cytotoxic, genotoxic, and estrogenic. While some reports suggest these impurities are released in a small amount and can only be toxic under

extreme [454], other researchers suggested that these materials are biologically active and replacement of the resin Bis-GMA with more biocompatible resins should be considered. Pulgar and others studied the cytotoxic and mutagenic potential of biphenolic content of 7 commercially available dental composite materials. They confirmed the release of biphenolic component form the commercial composites in toxic range-concentrations from samples maintained under range of pH and controlled temperature conditions [413]. Schweikl and others, have also confirmed the cytotoxicity and mutagenicity of Bis-GMA containing commercial composites V79 fibroblasts[455]. An *in vitro* evolution of the cytotoxicity of Bis-GMA containing dental composites such as Clearfil DC Core Automix and Clearfil Majesty posterior compared to Clearfil Majesty Flow, which has no Bis-GMA, showed a non-significant increase in cell death [456]. The higher cytotoxicity was explained by the higher Bis-GMA content in other materials. In a clinical study involving human subjects, bisphenol A content were detected in human saliva and urine as degradation products from resin-based composites used for orthodontic retainer placement [457]. A meta-analysis on the amount of bisphenol A released from restorative composites and dental adhesives demonstrated that the amount released might be relevant in patient and can induce adverse effect especially in cases of large crown prosthesis and multiple restorations [458].

Another limitation of the currently available restorative composite materials is restoration failure. Systematic reviews on the most common reasons for restorations failure demonstrated that recurrent caries is more significant in primary teeth and fracture is most common reason in posterior teeth [459] [460] [461] [462] [234]. In another systematic review on overall failure rate of the composite restorations from 2006-2016, the secondary caries accounted for 26% compared to 39% failure due to restoration fracture [463]. Therefore, attempts to develop effective antimicrobial restorative composite has taken place. Several approaches have been implemented by research to develop such material, these included modification of the fillers phase, resin matrix or the use of antibacterial polymers [464]. Since the observation of reduced secondary caries in an area adjacent to fluoride containing dental material, an increased attention to the role of fluoride in development of bioactive dental restorative with antimicrobial properties [465]. While fluoride containing dental restoratives are available in dental profession today [147]. Most of these materials are not suitable as permeant restoration under load bearing occlusal areas. One strategy to develop fluoride

releasing restorative, is the inclusion of bioactive glass fillers to develop experimental composite [466] [467]. While bioactive glasses exhibit promising bioactive properties, the mechanical properties of experimental materials with these formulations are still under investigation [184]. Therefore, the development of novel bioactive dental composite with satisfactory mechanical and physical properties is essential to increase the longevity of restoration and improve the clinical performance.

The aim of this study was to develop a novel bioactive dental composite as an alternative to Bis-GMA composites with nanofluorapatite as secondary fillers to add antimicrobial and remineralisation properties. In addition, to investigate the mechanical properties of the new composites. The new composite materials were tested for tissue cytocompatibility and therefore, the effect of the individual resin monomers on human gingival fibroblasts plus the overall material effect on the modification of the cells transcriptional profile was investigated.

A novel bioactive dental composite was successfully designed, the material achieved high degree of conversion. Dental resin monomers are toxic to human gingival fibroblasts, HEMA resulted in significant reduction of the cells viability at 2mM and resulted in significant upregulation of DNA repair genes. UDMA significantly reduced the cells viability at 1mM, and induced stress response manifested by upregulation stress response genes. The amount of the monomers UDMA and HEMA released from composites were below the toxic concentrations for gingival fibroblasts detected by XTT viability assay and qPCR. The residual monomers within these materials and commercial Gænial showed modification of transcriptional profile of the cells in RNA seq analysis after 24hours of exposure.

An ideal restorative dental material for replacement of missing oral tissues including bone, teeth and soft tissues is still missing. The research is moving at rapid pace in attempt to develop better alternatives to restore oral, dental, and craniofacial tissues with efficient clinical performance and sufficient tissues biocompatibility. The new approaches for synthesis and production of novel and potential bioactive materials are abundant and well documented in the literature [468] [467] [466] [184] .

According to the world health organization, caries is the most common chronic disease of the oral cavity and lead to decalcification of the dental hard tissues, decomposition of the enamel and dentine and subsequently cavities and potential loss of teeth when untreated [469]. The

consequences of teeth loss include compromise of functions such as speech, chewing and quality of patient life. Most of the currently available restorative dental composites are considered to be inert materials. A bioactive dental composite will function not to only to restore teeth cavities, but instead to stimulate the regeneration dental tissues once placed in intimate contacts with the tissues.

On the other hand, while the approach for designing of bioactive fluoride releasing material was successful, low concentrations of residual monomers have affected the mechanical properties and showed evidence of changes in gene expression in HGF. Maintaining the health of oral tissues is an important aspect of restorative dentistry. This includes not only the dental hard tissue remineralization, but also maintenance of the dental soft tissues health. The assessment of new materials cytotoxicity to gingival tissues is crucial. The use of oral gingival fibroblasts as a model is based on several considerations: the proximity of restorative materials to these cells and their clinical relevance. Cytotoxicity of resin monomers to dental pulp fibroblasts has been has considered in several studies [269] [470] [471]. However, the extrapolation of dental restorative cytotoxicity based on pulp fibroblasts as a model cannot be made as these cells have dentine barrier [472]. Gingival fibroblasts can be obtained as tissue biopsy from patients easily and be grown in large quantities.

An additional important consideration in the evaluation of cytotoxicity is the overall effect of the complete formulation of dental composites. Most of the research investigated the cytotoxicity of resin monomers alone using primary and cell lines such as pulp fibroblasts, 3T3 mouse fibroblasts, lymphocytes and macrophages [269] [473] [474] [475] [476]. In this study the cytoxicity of polymerized composite specimens of new material and commercial Gænial specimens were exposed to primary gingival fibroblasts to extrapolate the adverse effect in more clinically relevant situation. The application of RNA seq technology provide a sensitive method for the analysis of the mechanism of toxicity. The resultant stress response in human gingival fibroblasts in response to commercial and experimental materials manifested by upregulation of genes to mitigate chemical toxicity is alarming. While cellular mechanism could potentially respond to a chemically toxic agent by operating defensive mechanisms as cell cycle arrest, repair or removal of damaged DNA, apoptosis or activation of checkpoint proteins [287] [288]. The results of this study confirmed that the prescence of even low concentrations of residual monomers results in adverse effects on gingival tissues. The

application of RNA Seq technology in investigating these adverse effects can be extremely helpful to understand the underlying mechanisms. Considerations to the application of such techniques to investigate lesions, irritations and oral lichenoid reactions developed in patients specifically after restorations placement can confirm the aetiology of these reactions.

6.2 Limitation of the study

1) The experimental and novel NanoFA containing composites achieved high degree of conversion. However, the degree of conversion does not reflect the depth of cure of dental composite. The depth of cure of the material might be affected due to the differences in the refractive indexes between the silica, $NanoF_A$ fillers and the monomers.
2) The amount of residual monomers measured by HPLC experiments represent a worst-case scenario to mimic harsh conditions in oral environment as in alcohol consumption. The residual monomers were extracted in a solvent of 75% ethanol, 25% water. In the oral environment, less residual monomers might be released or can be washed away by saliva.
3) While the addition of NanoFA increased the novel materials bioactivity, the absence of silane coupling agent of NanoFA resulted in reduced mechanical properties and therefore, future investigations for silanization effect on mechanical properties and fluoride release should be considered.
4) While the addition of the resin monomer HEMA to the material formulation assisted the fluoride release and improved degree of conversion. it has also resulted in reduction of the mechanical properties.
5) Due to the COIVD pandemic the supply of NanoFA fillers was limited. Therefore, optimization of the best mixing procedure for the preparation of dental composite was not possible.
6) The tissue model to investigate the cytotoxicity of the resin monomers and dental composites in this study was primary human gingival fibroblasts (HGF). The study demonstrated evidence of toxicity to HGF. While HGF are clinically more relevant and are in close proximity to monomers released from restorative materials, they should not be the only model of tissues used to investigate the cytotoxicity. Further considerations to investigate the cytotoxicity of dental restorative materials in epithelial cells. Moreover, comparisons of the cells sensitivity from different tissues and same cells type from

different patients would provide more comprehensive analysis of how different tissues react to the monomers, fillers, and other components in the composite material.

7) The cytotoxicity of resin monomers and dental composites was investigated after 24hours of exposure to HGF. While this gives an indication of short-term exposure effect, the cytotoxicity in instances of long-term exposure to resin monomers and dental composite should be considered.
8) The COVID-19 pandemic has affected the project progress due to the University closure and delayed delivery of materials and reagent necessary for the lab work.

6.3 Future work

1) Investigations of the depth of cure for these composite formulation and comparison to commercial materials.
2) Investigation of the effect of silanization of NanoFA fillers for these formulation on the fluoride release and mechanical performance.
3) Measure fluoride release in human saliva taken from patients.
4) Measurement of residual monomers released in human saliva.
5) Investigation of the effect of different mixing procedure of these materials formulation on the mechanical and physical properties.
6) Reducing HEMA concentrations to improve the mechanical properties and investigating the effect of this reduction on the fluoride release.
7) Investigation of other mechanical and physical properties of these restorative materials such as hardness and mechanical wear.
8) Testing the cytotoxicity of the resin monomers in HGF after longer exposure time and comparing these results to the cytotoxicity after 24 hours exposure.
9) Using human tissue models as in 3D models to investigate the cytotoxicity of the monomers and dental composites.
10) Consideration of further use of RNA Seq technology to assess the side effect of dental resin monomers and other xenobiotics from restorative dental materials. In addition to the use of this technology to assess these potential side effect on the modification of transcriptome in other epithelial cells in oral tissues. The public availability of such data will provide further understanding and facilitate metanalysis.

6.4 Concluding Summary

A novel bioactive dental composite was successfully produced. The experimental dental composite achieved high degree of conversion ranging from 82.98%-84.61%. The addition of NanoFA did not affect the degree of conversion. This degree of conversion is considered sufficient for a material to be used as occlusal restoration. Most commercially available composites materials have degree of conversion ranging from 50%-75% [16]. Bulk fill composite degree of conversion ranges from 67%-84 [477]. The degree of conversion for some experimental composites materials such as amorphous calcium phosphate can reach up to 87% [478].

The bioactivity of the composite material was provided by the addition of remineralizing NanoFA as secondary fillers. A statistically significant amount of fluoride was released ($P<0.05$) compared to the control. The cumulative fluoride released range from 2.51-3.55μg/cm^2. There is no agreement on the amount of fluoride released from restorative material that is sufficient for remineralization. However, it has been shown that a restorative material can be effective to remineralize the tooth structure when fluoride released in the adjacent tooth demineralized zone rather than elevation of salivary fluoride concentration. Localized small concentration in the range from 0.63-1.3 μg/cm^2 /day has been reported to be sufficient to induce tooth tissue remineralization [479] [147].

The mechanical properties of novel composite materials were significantly lower than Gænial composite ($P<0.01$). The mechanical performance testing was measured under different storage solutions DW, AS and acid AS. Several factors affected the flexural strength of the experimental composite such as the mixing procedure. The SEM showed the prescence of air bubbles and voids within the material. The addition of hydrophilic NanFA particles, intended to improve the bioactive fluoride releasing properties of the composite also led to an increase voids and porosity after the dissolution of NanoFA fillers. Additionally, these NanoFA fillers were not silane coated. The composite material are significantly affected by the prescence of silane bond between the resin phase and filler particles , silane coating is responsible for good adhesion of resin matrix-filler phase[407]. Surface treatment of the nanofillers with a silane agent will allow adequate dispersion and binding of particles with the resin matrix [408]. However, in this occasion this would be detrimental to fluoride release.

The potential cytotoxicity has been assessed by more than one parameter. More individual monomers cytotoxicity and the overall material effect on the transcriptional profile changes on gingival fibroblasts has been investigated. The XTT viability assay showed significant reduction of cell proliferation ($P<0.01$) at 2mM HEMA concentration and 1mMUDMA. The qPCR data indicated HEMA results in statistically significant, dose-dependent upregulation of DNA repair genes by HEMA and stress response genes by UDMA. The viability assays and qPCR results findings reflect toxicity by resin monomers to HGF. The resin monomers induce apoptosis, DNA damage and inflammation in their monomeric state. In the polymeric state, RNA seq data showed signs of chemical toxicity to HGF by both experimental and commercial dental composites reflected by the number of differentially expressed genes in the cells. The number of significantly expressed genes in the cells treated with experimental composite without NanoFA filers was 124 genes, NanoFA composite 118 and Gænial 78 genes. The genes set enrichment analysis showed these genes are enriched in pathways of inflammation such as ferroptosis, chemical carcinogenesis, impaired redox balance, and inflammation. The addition of NanoFA filler didn't significantly result in an additional sign of toxicity. These effects are highly likely to be caused by the residual monomers as the stress response in cells was identified by qPCR data.

The results of this study indicate that residual resin monomers within dental composite material have adverse effect on the connective oral tissues as they affect oral gingival fibroblasts. These finding are alarming when considering situation of material use in multiple restorations or even in worse scenarios as in non-ideal humidity control or insufficient curing. In an ideal situation, the availability of restorative composite material with complete monomer to polymer conversion might significantly reduce these side effects. However, increasing attention should be given to further improve the current degree of conversion and improve the materials rein-filler interphase bond to minimize the release of even the smallest amounts of residual monomers. Additional attention to dentist to strictly adhere with commercial material manufacturer's instruction to obtain highest degree of polymerization when using these materials.

Chapter 7: References

References:

1. Platt, J., *Performance standards for competitive dental materials.* OPERATIVE DENTISTRY, 2001. **26**: p. 81-86.
2. Singh, H., et al., *Evolution of restorative dentistry from past to present.* Indian Journal of Dental Sciences, 2017. **9**(1): p. 38.
3. Charles, A.D., *The story of dental amalgam.* Bull Hist Dent, 1982. **30**(1): p. 2-7.
4. Hyson, J.M., Jr., *Amalgam: Its history and perils.* J Calif Dent Assoc, 2006. **34**(3): p. 215-29.
5. Soler, J.I., et al., *A history of dental amalgam.* J Hist Dent, 2002. **50**(3): p. 109-16.
6. Ring, M., *What was happening in dentistry exactly 100 years ago?* Illinois Dental Journal, 1987. **56**(6): p. 542-544.
7. Joseph, R., *The Father of Modern Dentistry-Dr. Greene Vardiman Black (1836-1915).* Journal of Conservative Dentistry, 2005. **8**(2): p. 5.
8. Duke, E.S., et al., *Laboratory Profiles of 30 High Copper Amalgam Alloys.* The Journal of the American Dental Association, 1982. **105**(4): p. 636-640.
9. Schulein, T.M., *Significant events in the history of operative dentistry.* J Hist Dent, 2005. **53**(2): p. 63-72.
10. Baum, L., R.W. Phillips, and M.R. Lund, *Textbook of operative dentistry*. 1985: WB Saunders Company.
11. Lye, K.W., et al., *Bone cements and their potential use in a mandibular endoprosthesis.* Tissue Engineering Part B: Reviews, 2009. **15**(4): p. 485-496.
12. Rueggeberg, F.A., *From vulcanite to vinyl, a history of resins in restorative dentistry.* The Journal of Prosthetic Dentistry, 2002. **87**(4): p. 364-379.
13. Buonocore, M.G., *A simple method of increasing the adhesion of acrylic filling materials to enamel surfaces.* Journal of dental research, 1955. **34**(6): p. 849-853.
14. Miletic, V. and SpringerLink, *Dental Composite Materials for Direct Restorations*. 2018: Cham : Springer International Publishing : Imprint: Springer.
15. Anusavice, K.J., *Phillips' science of dental materials*. Twelfth edition.. ed. Science of dental materials, ed. R.W. Phillips, C. Shen, and H.R. Rawls. 2013, St. Louis, Mo.: St. Louis, Mo. : Elsevier/Saunders.
16. Tarle, Z. and M. Par, *Degree of Conversion*. Dental Composite Materials for Direct Restorations, ed. V. Miletic. 2018: Springer International Publishing.
17. Ferracane, J.L., *Current Trends in Dental Composites.* Critical Reviews in Oral Biology & Medicine, 1995. **6**(4): p. 302-318.

18. McCabe, J.F. and A. Walls, *Applied dental materials*. 9th ed.. ed. 2008, Oxford: Oxford : Blackwell.
19. Vidnes-Kopperud, S., et al., *Factors influencing dentists' choice of amalgam and tooth-colored restorative materials for Class II preparations in younger patients.* Acta Odontol Scand, 2009. **67**(2): p. 74-9.
20. Mitchell, R.J., M. Koike, and T. Okabe, *Posterior amalgam restorations--usage, regulation, and longevity.* Dent Clin North Am, 2007. **51**(3): p. 573-89, v.
21. Burke, F.J., *Amalgam to tooth-coloured materials--implications for clinical practice and dental education: governmental restrictions and amalgam-usage survey results.* J Dent, 2004. **32**(5): p. 343-50.
22. Tryfon, B., et al., *Economic Impact of Regulating the Use of Amalgam Restorations.* Public health reports (1974), 2007. **122**(5): p. 657-663.
23. Mitra, S.B., D. Wu, and B.N. Holmes, *An application of nanotechnology in advanced dental materials.* J Am Dent Assoc, 2003. **134**(10): p. 1382-90.
24. Sakaguchi, R.L., J.L. Ferracane, and J.M. Powers, *Craig's restorative dental materials*. Fourteenth edition.. ed. Restorative dental materials. 2019: St. Louis, Missouri : Elsevier.
25. Chen, M.H., *Update on dental nanocomposites.* J Dent Res, 2010. **89**(6): p. 549-60.
26. Grassie, N., *Developments in Polymer Degradation—7*. 2012: Springer Science & Business Media.
27. Zafar, M.S., *Prosthodontic Applications of Polymethyl Methacrylate (PMMA): An Update.* Polymers (Basel), 2020. **12**(10).
28. Anusavice, K.J., C. Shen, and H.R. Rawls, *Phillips' science of dental materials. St. Louis.* Missouri Saunders, 2003.
29. Peutzfeldt, A., *Resin composites in dentistry: the monomer systems.* Eur J Oral Sci, 1997. **105**(2): p. 97-116.
30. Moszner, N., et al., *A partially aromatic urethane dimethacrylate as a new substitute for Bis-GMA in restorative composites.* Dental Materials, 2008. **24**(5): p. 694-699.
31. Stansbury, J.W., *Dimethacrylate network formation and polymer property evolution as determined by the selection of monomers and curing conditions.* Dental Materials, 2012. **28**(1): p. 13-22.
32. Söderholm, K.J. and A. Mariotti, *BIS-GMA--based resins in dentistry: are they safe?* J Am Dent Assoc, 1999. **130**(2): p. 201-9.
33. Ahovuo-Saloranta, A., et al., *Pit and fissure sealants for preventing dental decay in permanent teeth.* The Cochrane database of systematic reviews, 2017. **7**(7): p. CD001830-CD001830.

34. Barszczewska-Rybarek, I.M., M.W. Chrószcz, and G. Chladek, *Novel urethane-dimethacrylate monomers and compositions for use as matrices in dental restorative materials.* International journal of molecular sciences, 2020. **21**(7): p. 2644.
35. Alrahlah, A., et al., *A Low-Viscosity BisGMA Derivative for Resin Composites: Synthesis, Characterization, and Evaluation of Its Rheological Properties.* Materials, 2021. **14**(2): p. 338.
36. Feilzer, A. and B. Dauvillier, *Effect of TEGDMA/BisGMA ratio on stress development and viscoelastic properties of experimental two-paste composites.* Journal of dental research, 2003. **82**(10): p. 824-828.
37. Asmussen, E. and A. Peutzfeldt, *Influence of UEDMA, BisGMA and TEGDMA on selected mechanical properties of experimental resin composites.* Dental Materials, 1998. **14**(1): p. 51-56.
38. Barszczewska-Rybarek, I.M., *Structure–property relationships in dimethacrylate networks based on Bis-GMA, UDMA and TEGDMA.* Dental Materials, 2009. **25**(9): p. 1082-1089.
39. Cho, K., et al., *Dental resin composites: A review on materials to product realizations.* Composites Part B: Engineering, 2022. **230**: p. 109495.
40. Srivastava, R., et al., *BisGMA analogues as monomers and diluents for dental restorative composite materials.* Materials Science and Engineering: C, 2018. **88**: p. 25-31.
41. Sideridou, I., V. Tserki, and G. Papanastasiou, *Effect of chemical structure on degree of conversion in light-cured dimethacrylate-based dental resins.* Biomaterials, 2002. **23**(8): p. 1819-1829.
42. Cornelio, R.B., et al., *The influence of bis-EMA vs bis GMA on the degree of conversion and water susceptibility of experimental composite materials.* Acta Odontologica Scandinavica, 2014. **72**(6): p. 440-447.
43. Moszner, N. and T. Hirt, *New polymer-chemical developments in clinical dental polymer materials: enamel–dentin adhesives and restorative composites.* Journal of Polymer Science Part A: Polymer Chemistry, 2012. **50**(21): p. 4369-4402.
44. Sidhu, S.K. and J.W. Nicholson, *A review of glass-ionomer cements for clinical dentistry.* Journal of functional biomaterials, 2016. **7**(3): p. 16.
45. Carvalho, R.M., et al., *Effects of HEMA/solvent combinations on bond strength to dentin.* Journal of dental research, 2003. **82**(8): p. 597-601.
46. Tauscher, S., et al., *Evaluation of alternative monomers to HEMA for dental applications.* Dental materials, 2017. **33**(7): p. 857-865.

47. Szczesio-Wlodarczyk, A., et al., *The Influence of Low-Molecular-Weight Monomers (TEGDMA, HDDMA, HEMA) on the Properties of Selected Matrices and Composites Based on Bis-GMA and UDMA.* Materials, 2022. **15**(7): p. 2649.
48. Collares, F.M., et al., *Influence of 2-hydroxyethyl methacrylate concentration on polymer network of adhesive resin.* J Adhes Dent, 2011. **13**(2): p. 125-9.
49. Ilie, N. and R. Hickel, *Resin composite restorative materials.* Aust Dent J, 2011. **56 Suppl 1**: p. 59-66.
50. Willems, G., et al., *A classification of dental composites according to their morphological and mechanical characteristics.* Dental Materials, 1992. **8**(5): p. 310-319.
51. Chan, D., et al., *Radiopacity of tantalum oxide nanoparticle filled resins.* Dental Materials, 1999. **15**(3): p. 219-222.
52. Miletic, V., *Development of Dental Composites*, in *Dental Composite Materials for Direct Restorations*, V. Miletic, Editor. 2018, Springer International Publishing: Cham. p. 3-9.
53. Raptis, C.N., P.L. Fan, and J.M. Powers, *Properties of microfilled and visible light-cured composite resins.* J Am Dent Assoc, 1979. **99**(4): p. 631-3.
54. Powers, J.M., P.L. Fan, and C.N. Raptis, *Color stability of new composite restorative materials under accelerated aging.* J Dent Res, 1980. **59**(12): p. 2071-4.
55. Dennison, J.B., P.L. Fan, and J.M. Powers, *Surface roughness of microfilled composites.* J Am Dent Assoc, 1981. **102**(6): p. 859-62.
56. Ferracane, J.L., *Current trends in dental composites.* Crit Rev Oral Biol Med, 1995. **6**(4): p. 302-18.
57. Blackham, J.T., K.S. Vandewalle, and W. Lien, *Properties of hybrid resin composite systems containing prepolymerized filler particles.* Oper Dent, 2009. **34**(6): p. 697-702.
58. Kumari, R.V., et al., *Evaluation of the Effect of Surface Polishing, Oral Beverages and Food Colorants on Color Stability and Surface Roughness of Nanocomposite Resins.* Journal of international oral health : JIOH, 2015. **7**(7): p. 63-70.
59. Alawjali, S.S. and J.L. Lui, *Effect of one-step polishing system on the color stability of nanocomposites.* Journal of Dentistry, 2013. **41**: p. e53-e61.
60. Dos Santos, P.A., et al., *Chemical and morphological features of dental composite resin: influence of light curing units and immersion media.* Microsc Res Tech, 2010. **73**(3): p. 176-81.
61. Van Noort, R. and M. Barbour, *Introduction to dental materials-e-book*. 2014: Elsevier Health Sciences.
62. Asmussen, E., *Quantitative analysis of peroxides in restorative resins.* Acta Odontologica Scandinavica, 1980. **38**(5): p. 269-272.

63. Talib, R., *Dental composites: a review.* The Journal of Nihon University School of Dentistry, 1993. **35**(3): p. 161-170.
64. Park, Y.-J., K.-H. Chae, and H. Rawls, *Development of a new photoinitiation system for dental light-cure composite resins.* Dental materials, 1999. **15**(2): p. 120-127.
65. Kamoun, E.A., et al., *Carboxylated camphorquinone as visible-light photoinitiator for biomedical application: Synthesis, characterization, and application.* Arabian Journal of Chemistry, 2016. **9**(5): p. 745-754.
66. Ogunyinka, A., et al., *Photoinitiation chemistry affects light transmission and degree of conversion of curing experimental dental resin composites.* Dental Materials, 2007. **23**(7): p. 807-813.
67. Yoshida, K. and E. Greener, *Effect of photoinitiator on degree of conversion of unfilled light-cured resin.* Journal of dentistry, 1994. **22**(5): p. 296-299.
68. Jan, C.M., et al., *The relationship between leachability of polymerization initiator and degree of conversion of visible light-cured resin.* Journal of Biomedical Materials Research: An Official Journal of The Society for Biomaterials, The Japanese Society for Biomaterials, and The Australian Society for Biomaterials, 2001. **58**(1): p. 42-46.
69. Schroeder, W.F. and C.I. Vallo, *Effect of different photoinitiator systems on conversion profiles of a model unfilled light-cured resin.* dental materials, 2007. **23**(10): p. 1313-1321.
70. Kowalska, A., J. Sokolowski, and K. Bociong, *The photoinitiators used in resin based dental composite—a review and future perspectives.* Polymers, 2021. **13**(3): p. 470.
71. Rueggeberg, F.A., J.W. Ergle, and P.E. Lockwood, *Effect of photoinitiator level on properties of a light-cured and post-cure heated model resin system.* Dental Materials, 1997. **13**(5-6): p. 360-364.
72. Ludovichetti, F.S., et al., *Depth of Cure, Hardness, Roughness and Filler Dimension of Bulk-Fill Flowable, Conventional Flowable and High-Strength Universal Injectable Composites: An In Vitro Study.* Nanomaterials, 2022. **12**(12): p. 1951.
73. Taira, M., et al., *Analysis of photo-initiators in visible-light-cured dental composite resins.* Journal of dental research, 1988. **67**(1): p. 24-28.
74. Mehta, P., et al., *Dental Light Curing Units-A Review.* Indian Journal of Dental Sciences, 2014. **6**(4).
75. Liu, H., et al., *Probing the origins and control of shrinkage stress in dental resin composites. Part II. Novel method of simultaneous measurement of polymerization shrinkage stress and conversion.* J Biomed Mater Res B: Appl Biomater B, 2004. **71**: p. 206-13.

76. Oréfice, R.L., et al., *In situ evaluation of the polymerization kinetics and corresponding evolution of the mechanical properties of dental composites.* Polymer Testing, 2003. **22**(1): p. 77-81.
77. Altintas, S.H. and A. Usumez, *Evaluation of monomer leaching from a dual cured resin cement.* Journal of Biomedical Materials Research Part B: Applied Biomaterials, 2008. **86B**(2): p. 523-529.
78. *Step-Growth Polymers—Condensation Polymers*. 2019.
79. Flory, P.J., *Fundamental principles of condensation polymerization.* Chemical Reviews, 1946. **39**(1): p. 137-197.
80. Odian, G., *Principles of polymerization*. 2004: John Wiley & Sons.
81. Lovelh, L., S. Newman, and C. Bowman, *The effects of light intensity, temperature, and comonomer composition on the polymerization behavior of dimethacrylate dental resins.* Journal of Dental Research, 1999. **78**(8): p. 1469-1476.
82. Pfeifer, C.S., et al., *Delayed gelation through chain-transfer reactions: mechanism for stress reduction in methacrylate networks.* Polymer, 2011. **52**(15): p. 3295-3303.
83. Fonseca, A.S.Q., et al., *Effect of monomer type on the CC degree of conversion, water sorption and solubility, and color stability of model dental composites.* Dental materials, 2017. **33**(4): p. 394-401.
84. Ferracane, J.L., *Developing a more complete understanding of stresses produced in dental composites during polymerization.* Dental Materials, 2005. **21**(1): p. 36-42.
85. Park, H.Y., et al., *Novel dental restorative materials having low polymerization shrinkage stress via stress relaxation by addition-fragmentation chain transfer.* Dental Materials, 2012. **28**(11): p. 1113-1119.
86. Eick, J.D., et al., *Properties of silorane-based dental resins and composites containing a stress-reducing monomer.* Dental Materials, 2007. **23**(8): p. 1011-1017.
87. Giachetti, L., et al., *A review of polymerization shrinkage stress: current techniques for posterior direct resin restorations.* J Contemp Dent Pract, 2006. **7**(4): p. 79-88.
88. Moraes, L.G.P., et al., *Infrared spectroscopy: a tool for determination of the degree of conversion in dental composites.* Journal of Applied Oral Science, 2008. **16**: p. 145-149.
89. Imazato, S., et al., *Degree of conversion of composites measured by DTA and FTIR.* Dental Materials, 2001. **17**(2): p. 178-183.
90. Alshaafi, M.M., *Factors affecting polymerization of resin-based composites: A literature review.* The Saudi Dental Journal, 2017. **29**(2): p. 48-58.

91. Calheiros, F.C., et al., *Degree of conversion and mechanical properties of a BisGMA:TEGDMA composite as a function of the applied radiant exposure.* J Biomed Mater Res B Appl Biomater, 2008. **84**(2): p. 503-9.
92. Ferracane, J.L., et al., *Wear and Marginal Breakdown of Composites with Various Degrees of Cure.* Journal of Dental Research, 1997. **76**(8): p. 1508-1516.
93. Collares, F.M., et al., *Discrepancies in degree of conversion measurements by FTIR.* Braz Oral Res, 2013. **27**(6): p. 453-454.
94. Moldovan, M., et al., *Evaluation of the degree of conversion, residual monomers and mechanical properties of some light-cured dental resin composites.* Materials, 2019. **12**(13): p. 2109.
95. Ferracane, J.L., *Buonocore Lecture. Placing dental composites--a stressful experience.* Oper Dent, 2008. **33**(3): p. 247-57.
96. Krifka, S., et al., *Oxidative stress and cytotoxicity generated by dental composites in human pulp cells.* Clin Oral Investig, 2012. **16**(1): p. 215-24.
97. Alshali, R.Z., et al., *Analysis of long-term monomer elution from bulk-fill and conventional resin-composites using high performance liquid chromatography.* Dent Mater, 2015. **31**(12): p. 1587-98.
98. Marovic, D., et al., *Degree of conversion and microhardness of dental composite resin materials.* Journal of Molecular Structure, 2013. **1044**: p. 299-302.
99. Sarosi, C., et al., *Effects of Monomer Composition of Urethane Methacrylate Based Resins on the C= C Degree of Conversion, Residual Monomer Content and Mechanical Properties.* Polymers, 2021. **13**(24): p. 4415.
100. AlShaafi, M.M., *Factors affecting polymerization of resin-based composites: A literature review.* Saudi Dent J, 2017. **29**(2): p. 48-58.
101. Imazato, S., et al., *Degree of conversion of composites measured by DTA and FTIR.* Dent Mater, 2001. **17**(2): p. 178-83.
102. Peutzfeldt, A., A. Sahafi, and E. Asmussen, *Characterization of resin composites polymerized with plasma arc curing units.* Dent Mater, 2000. **16**(5): p. 330-6.
103. Ali, F., et al., *N-Acetyl cysteine protects diabetic mouse derived mesenchymal stem cells from hydrogen-peroxide-induced injury: A novel hypothesis for autologous stem cell transplantation.* J Chin Med Assoc, 2016. **79**(3): p. 122-9.
104. Tarle, Z., *Degree of conversion.* Dental Composite Materials for Direct Restorations, 2018: p. 63-85.

105. Sobrinho, L.C., et al., *Correlation between light intensity and exposure time on the hardness of composite resin.* Journal of Materials Science: Materials in Medicine, 2000. **11**(6): p. 361-364.
106. Rueggeberg, F., W.F. Caughman, and J. Curtis, *Effect of light intensity and exposure duration on cure of resin composite.* Operative dentistry, 1994. **19**: p. 26-26.
107. Minguez, N., et al., *Advances in the history of composite resins.* J Hist Dent, 2003. **51**(3): p. 103-5.
108. Rueggeberg, F.A., *State-of-the-art: dental photocuring—a review.* Dental materials, 2011. **27**(1): p. 39-52.
109. Tirtha, R., et al., *In vitro depth of cure of photo-activated composites.* Journal of dental research, 1982. **61**(10): p. 1184-1187.
110. Main, C., et al., *An assessment of new dental ultraviolet sources and uv-polymerized fissure sealants.* Journal of oral rehabilitation, 1983. **10**(3): p. 215-227.
111. Craig, R.G., *Chemistry, composition, and properties of composite resins.* Dental Clinics of North America, 1981. **25**(2): p. 219-239.
112. Santini, A., I.T. Gallegos, and C.M. Felix, *Photoinitiators in dentistry: a review.* Prim Dent J, 2013. **2**(4): p. 30-3.
113. Rueggeberg, F., *Contemporary issues in photocuring.* Compendium of continuing education in dentistry.(Jamesburg, NJ: 1995). Supplement, 1999(25): p. S4-15; quiz S73.
114. Nagel, R., *Snap-on light shield for a dental composite light curing gun*. 2000, Google Patents.
115. Davidson, C.L. and A.J. De Gee, *Light-curing units, polymerization, and clinical implications.* Journal of adhesive dentistry, 2000. **2**(3).
116. Palin, W.M., et al., *Monomer conversion versus flexure strength of a novel dental composite.* J Dent, 2003. **31**(5): p. 341-51.
117. Ferracane, J.L., *Hygroscopic and hydrolytic effects in dental polymer networks.* Dent Mater, 2006. **22**(3): p. 211-22.
118. Ferracane, J.L., H.X. Berge, and J.R. Condon, *In vitro aging of dental composites in water--effect of degree of conversion, filler volume, and filler/matrix coupling.* J Biomed Mater Res, 1998. **42**(3): p. 465-72.
119. Halvorson, R.H., R.L. Erickson, and C.L. Davidson, *The effect of filler and silane content on conversion of resin-based composite.* Dent Mater, 2003. **19**(4): p. 327-33.
120. Daronch, M., et al., *Polymerization kinetics of pre-heated composite.* J Dent Res, 2006. **85**(1): p. 38-43.
121. Geurtsen, W., *Substances released from dental resin composites and glass ionomer cements.* Eur J Oral Sci, 1998. **106**(2 Pt 2): p. 687-95.

122. Ferracane, J.L., et al., *Academy of Dental Materials guidance-Resin composites: Part II-Technique sensitivity (handling, polymerization, dimensional changes).* Dent Mater, 2017. **33**(11): p. 1171-1191.
123. Feng, L., R. Carvalho, and B.I. Suh, *Insufficient cure under the condition of high irradiance and short irradiation time.* Dent Mater, 2009. **25**(3): p. 283-9.
124. Polydorou, O., et al., *Long-term release of monomers from modern dental-composite materials.* Eur J Oral Sci, 2009. **117**(1): p. 68-75.
125. Sideridou, I.D. and D.S. Achilias, *Elution study of unreacted Bis-GMA, TEGDMA, UDMA, and Bis-EMA from light-cured dental resins and resin composites using HPLC.* J Biomed Mater Res B Appl Biomater, 2005. **74**(1): p. 617-26.
126. Gezgin, O., et al., *HPLC analysis of eluted monomers released from dental composites containing bioactive glass.* Journal of Adhesion Science and Technology, 2018. **32**(15): p. 1724-1731.
127. Smith, B.C., *Fundamentals of Fourier transform infrared spectroscopy*. 2011: CRC press.
128. Woods, O.N., *EXPLORE!*
129. Mirabella Jr, F., *Practical spectroscopy series.* Internal Reflection Spectroscopy: Theory and Applications. New York, USA: Marcel Dekker, Inc, 1993: p. 17-52.
130. Ruyter, I.E. and S.A. Svendsen, *Remaining methacrylate groups in composite restorative materials.* Acta Odontol Scand, 1978. **36**(2): p. 75-82.
131. Alshali, R.Z., N. Silikas, and J.D. Satterthwaite, *Degree of conversion of bulk-fill compared to conventional resin-composites at two time intervals.* Dental Materials, 2013. **29**(9): p. e213-e217.
132. Marovic, D., et al., *Monomer conversion and shrinkage force kinetics of low-viscosity bulk-fill resin composites.* Acta Odontologica Scandinavica, 2015. **73**(6): p. 474-480.
133. Ruyter, I.E. and S.A. Svendsen, *Remaining methacrylate groups in composite restorative materials.* Acta odontologica scandinavica, 1978. **36**(2): p. 75-82.
134. Life, P.E., *Analytical Sciences (2005) FT-IR Spectroscopy, Attenuated Total Reflectance (ATR)*. Technical Report.
135. Sonarkar, S. and R. Purba, *Bioactive materials in conservative dentistry.* Int J Contemp Dent Med Rev, 2015. **2015**: p. 1-4.
136. Farhad, A. and Z. Mohammadi, *Calcium hydroxide: a review.* International Dental Journal, 2005. **55**(5): p. 293-301.
137. Fava, L.R. and W.P. Saunders, *Calcium hydroxide pastes: classification and clinical indications.* Int Endod J, 1999. **32**(4): p. 257-82.

138. Rehman, K., et al., *Calcium ion diffusion from calcium hydroxide-containing materials in endodontically-treated teeth: an in vitro study.* Int Endod J, 1996. **29**(4): p. 271-9.
139. Cohen, S., et al., *Pathways of the Pulp (1).* Learning, 1998. **30**(10).
140. Pitt Ford, T., *Apexification and apexogenesis.* Principles and practice of endodontics, 1996: p. 373-384.
141. Wiegand, A., W. Buchalla, and T. Attin, *Review on fluoride-releasing restorative materials—Fluoride release and uptake characteristics, antibacterial activity and influence on caries formation.* Dental Materials, 2007. **23**(3): p. 343-362.
142. Hamilton, I., *Fluoride effects on oral bacteria, Fejerskov O, Ekstrand.* J: Fluoride in dentistry, 1996: p. 230-251.
143. Ten Cate, J., *Physicochemical aspects of fluoride-enamel interactions.* Fluoride in dentistry, 1996.
144. Verbeeck, R., et al. *The fluoride release process of glass ionomer cements versus resin-modified glass ionomer cements and polyacid-modified composite resins*. in *Abstract book*. 1996.
145. Dutra, P.B., G. Iazzetti, and D. Vaitsman, *Fluoride Releasing from Dental Composites Resin and Glass Ionomer Cement Using a Fluoride Ion-Selective Electrode and Ion Chromatography.* Science Direct Working Paper, 2000(S1574-0331): p. 04.
146. Wilson, A.D., *Glass-ionomer cement.* The setting reaction and its clinical consequences, 1988.
147. Wiegand, A., W. Buchalla, and T. Attin, *Review on fluoride-releasing restorative materials--fluoride release and uptake characteristics, antibacterial activity and influence on caries formation.* Dent Mater, 2007. **23**(3): p. 343-62.
148. Smith, D.C., *Development of glass-ionomer cement systems.* Biomaterials, 1998. **19**(6): p. 467-478.
149. Tay, W.M. and M. Braden, *Fluoride ion diffusion from polyalkenoate (glass-ionomer) cements.* Biomaterials, 1988. **9**(5): p. 454-6.
150. Verbeeck, R.M., et al., *Fluoride release process of (resin-modified) glass-ionomer cements versus (polyacid-modified) composite resins.* Biomaterials, 1998. **19**(6): p. 509-19.
151. Davidson, C.L., *Advances in glass-ionomer cements.* Journal of Applied Oral Science, 2006. **14**: p. 3-9.
152. De Moor, R.J., R.M. Verbeeck, and E.A. De Maeyer, *Fluoride release profiles of restorative glass ionomer formulations.* Dental Materials, 1996. **12**(2): p. 88-95.
153. Xu, X. and J.O. Burgess, *Compressive strength, fluoride release and recharge of fluoride-releasing materials.* Biomaterials, 2003. **24**(14): p. 2451-2461.

154. Behrend, B. and W. Geurtsen, *Long-term effects of four extraction media on the fluoride release from four polyacid-modified composite resins (compomers) and one resin-modified glass-ionomer cement.* Journal of Biomedical Materials Research: An Official Journal of The Society for Biomaterials, The Japanese Society for Biomaterials, and The Australian Society for Biomaterials and the Korean Society for Biomaterials, 2001. **58**(6): p. 631-637.

155. Williams, J.A., R.W. Billington, and G.J. Pearson, *A long term study of fluoride release from metal-containing conventional and resin-modified glass-ionomer cements.* J Oral Rehabil, 2001. **28**(1): p. 41-7.

156. Dhondt, C.L., E.A. De Maeyer, and R.M. Verbeeck, *Fluoride release from glass ionomer activated with fluoride solutions.* J Dent Res, 2001. **80**(5): p. 1402-6.

157. Berg, J.H., *Glass ionomer cements.* Pediatric dentistry, 2002. **24**(5): p. 430-438.

158. Bowen, R.L. and W.A. Marjenhoff, *Dental composites/glass ionomers: the materials.* Advances in dental research, 1992. **6**(1): p. 44-49.

159. Nicholson, J. and H. Anstice, *The physical chemistry of light-curable glass-ionomers.* Journal of Materials Science: Materials in Medicine, 1994. **5**(3): p. 119-122.

160. Wright, A.B., et al., *Clinical and microbiologic evaluation of a resin modified glass ionomer cement for orthodontic bonding.* American journal of orthodontics and dentofacial orthopedics, 1996. **110**(5): p. 469-475.

161. Pameijer, C.H., *Crown retention with three resin-modified glass ionomer luting agents.* The Journal of the American Dental Association, 2012. **143**(11): p. 1218-1222.

162. Sidhu, S.K., *Clinical evaluations of resin-modified glass-ionomer restorations.* Dental Materials, 2010. **26**(1): p. 7-12.

163. Ruse, N.D., *What is a "compomer"?* Journal (Canadian Dental Association), 1999. **65**(9): p. 500-504.

164. Meyer, J., M. Cattani-Lorente, and V. Dupuis, *Compomers: between glass-ionomer cements and composites.* Biomaterials, 1998. **19**(6): p. 529-539.

165. Meyer, J.M., M.A. Cattani-Lorente, and V. Dupuis, *Compomers: between glass-ionomer cements and composites.* Biomaterials, 1998. **19**(6): p. 529-539.

166. KrÄMer, N. and R. Frankenberger, *Compomers in restorative therapy of children: a literature review.* International Journal of Paediatric Dentistry, 2007. **17**(1): p. 2-9.

167. Mjör, I.A., *The reasons for replacement and the age of failed restorations in general dental practice.* Acta Odontol Scand, 1997. **55**(1): p. 58-63.

168. Skartveit, L., et al., *Clinical assessment of a fluoride-containing amalgam.* Scand J Dent Res, 1986. **94**(1): p. 72-6.

169. Dionysopoulos, P., et al., *Secondary caries formation in vitro around fluoride-releasing restorations.* Oper Dent, 1994. **19**(5): p. 183-8.
170. Chadwick, R.G. and C.H. Lloyd, *Dental amalgam: the history and legacy you perhaps never knew?* British Dental Journal, 2022. **232**(9): p. 633-637.
171. Blum, I.R., et al., *The effect of surface conditioning on the bond strength of resin composite to amalgam.* Journal of dentistry, 2012. **40**(1): p. 15-21.
172. Chan, K.H.S., et al., *Review: Resin Composite Filling.* Materials, 2010. **3**(2): p. 1228-1243.
173. Jones, D., *A Scandinavian tragedy.* British Dental Journal, 2008. **204**(5): p. 233-234.
174. Brownawell, A.M., et al., *The potential adverse health effects of dental amalgam.* Toxicol Rev, 2005. **24**(1): p. 1-10.
175. German, M.J., *Developments in resin-based composites.* British Dental Journal, 2022. **232**(9): p. 638-643.
176. Liu, C., et al., *Evaluation of the biocompatibility of a nonceramic hydroxyapatite.* Journal of endodontics, 1997. **23**(8): p. 490-493.
177. Leinfelder, K.F., *Composite resins.* Dental Clinics of North America, 1985. **29**(2): p. 359-371.
178. Arcís, R.W., et al., *Mechanical properties of visible light-cured resins reinforced with hydroxyapatite for dental restoration.* Dental Materials, 2002. **18**(1): p. 49-57.
179. Domingo, C., et al., *Hydrolytic stability of experimental hydroxyapatite-filled dental composite materials.* Dental Materials, 2003. **19**(6): p. 478-486.
180. Dana, J.D., *Manual of Mineralogy*. 1864: Wiley.
181. Youness, R.A., M.A. Taha, and M. Ibrahim, *Dense alumina-based carbonated fluorapatite nanobiocomposites for dental applications.* Materials Chemistry and Physics, 2021. **257**: p. 123264.
182. Anastasiou, A., et al., *Antibacterial properties and regenerative potential of Sr2+ and Ce3+ doped fluorapatites; a potential solution for peri-implantitis.* Scientific reports, 2019. **9**(1): p. 1-11.
183. Chen, H., et al., *Acellular synthesis of a human enamel-like microstructure.* Advanced Materials, 2006. **18**(14): p. 1846-1851.
184. Altaie, A., et al., *Development and characterisation of dental composites containing anisotropic fluorapatite bundles and rods.* Dental Materials, 2020. **36**(8): p. 1071-1085.
185. Van der Laan, H., et al., *Biological and mechanical evaluation of novel prototype dental composites.* Journal of dental research, 2019. **98**(1): p. 91-97.
186. Hench, L.L., *The story of Bioglass®.* Journal of Materials Science: Materials in Medicine, 2006. **17**(11): p. 967-978.

187. Gillam, D., et al., *The effects of a novel Bioglass® dentifrice on dentine sensitivity: a scanning electron microscopy investigation.* Journal of Oral Rehabilitation, 2002. **29**(4): p. 305-313.

188. Greenspan, D.C., *NovaMin® and tooth sensitivity—an overview.* Journal of Clinical Dentistry, 2010. **21**(3): p. 61.

189. Earl, J., et al., *Physical and chemical characterization of the surface layers formed on dentin following treatment with a fluoridated toothpaste containing NovaMin.* The Journal of clinical dentistry, 2011. **22**(3): p. 68-73.

190. Tiskaya, M., et al., *The use of bioactive glass (BAG) in dental composites: A critical review.* Dental Materials, 2021. **37**(2): p. 296-310.

191. Williams, J., R. Billington, and G. Pearson, *The influence of sample dimensions on fluoride ion release from a glass ionomer restorative cement.* Biomaterials, 1999. **20**(14): p. 1327-1337.

192. Lucas, M.E., K. Arita, and M. Nishino, *Toughness, bonding and fluoride-release properties of hydroxyapatite-added glass ionomer cement.* Biomaterials, 2003. **24**(21): p. 3787-3794.

193. Osinaga, P.W., et al., *Zinc sulfate addition to glass-ionomer-based cements: influence on physical and antibacterial properties, zinc and fluoride release.* Dental Materials, 2003. **19**(3): p. 212-217.

194. De Maeyer, E.A.P., R.M.H. Verbeeck, and C.W.J. Vercruysse, *Stoichiometry of the Leaching Process of Fluoride-containing Aluminosilicate Glass-ionomer Glasses.* Journal of Dental Research, 1999. **78**(7): p. 1312-1318.

195. Nicholson, J. and B. Czarnecka, *The release of ions by compomers under neutral and acidic conditions.* Journal of oral rehabilitation, 2004. **31**(7): p. 665-670.

196. Brooks, E., et al., *Manipulation effects on fluoride release from chemically-cured and resin-modified glass ionomers.* American Journal of Dentistry, 1997. **10**(3): p. 120-122.

197. Miller, B., et al., *Effect of glass ionomer manipulation on early fluoride release.* American journal of dentistry, 1995. **8**(4): p. 182-186.

198. Nicholson, J.W., B. Czarnecka, and H. Limanowska-Shaw, *A preliminary study of the effect of glass-ionomer and related dental cements on the pH of lactic acid storage solutions.* Biomaterials, 1999. **20**(2): p. 155-158.

199. Levallois, B., et al., *In vitro fluoride release from restorative materials in water versus artificial saliva medium (SAGF).* Dental Materials, 1998. **14**(6): p. 441-447.

200. McKenzie, M., R. Linden, and J. Nicholson, *The physical properties of conventional and resin-modified glass-ionomer dental cements stored in saliva, proprietary acidic beverages, saline and water.* Biomaterials, 2003. **24**(22): p. 4063-4069.

201. Garcez, R.M.V.d.B., M.A.R. Buzalaf, and P.A.d. Araújo, *Fluoride release of six restorative materials in water and pH-cycling solutions.* Journal of Applied Oral Science, 2007. **15**: p. 406-411.

202. McNeill, C.J., et al., *Fluoride release from new light-cured orthodontic bonding agents.* American Journal of Orthodontics and Dentofacial Orthopedics, 2001. **120**(4): p. 392-397.

203. Garcia-Godoy, F., et al., *Fluoride release from fissure sealants.* The Journal of clinical pediatric dentistry, 1997. **22**(1): p. 45-49.

204. Ozmen, B., *ANALYSIS OF ANION AND CATION RELEASE FROM GLASS IONOMER CEMENTS USING ION CHROMATOGRAPHY.* Fluoride, 2020. **53**(3): p. 447-456.

205. Attin, T., et al., *Fluoride release/uptake of polyacid-modified resin composites (compomers) in neutral and acidic buffer solutions.* J Oral Rehabil, 1999. **26**(5): p. 388-93.

206. Moreau, J.L. and H.H. Xu, *Fluoride releasing restorative materials: Effects of pH on mechanical properties and ion release.* Dent Mater, 2010. **26**(11): p. e227-35.

207. Al-eesa, N.A., et al., *Fluoride containing bioactive glass composite for orthodontic adhesives — Apatite formation properties.* Dental Materials, 2018. **34**(8): p. 1127-1133.

208. Bell, A., et al., *The effect of saliva on fluoride release by a glass–ionomer filling material.* Journal of oral rehabilitation, 1999. **26**(5): p. 407-412.

209. Rezk-Lega, F., B. Ogaard, and G. Rölla, *Availability of fluoride from glass-ionomer luting cements in human saliva.* Scand J Dent Res, 1991. **99**(1): p. 60-3.

210. Potts, P., *Ion-selective electrodes*, in *A Handbook of Silicate Rock Analysis*. 1987, Springer. p. 213-225.

211. McCabe, J.F., T.E. Carrick, and S.K. Sidhu, *Determining low levels of fluoride released from resin based dental materials.* European journal of oral sciences, 2002. **110**(5): p. 380-384.

212. Itota, T., et al., *Determination of fluoride ions released from resin-based dental materials using ion-selective electrode and ion chromatograph.* J Dent, 2004. **32**(2): p. 117-22.

213. Chadwick, S.M. and P.H. Gordon, *An investigation to estimate the fluoride uptake adjacent to a fluoride-releasing bonding agent.* Br J Orthod, 1995. **22**(2): p. 113-22.

214. Michalski, R., *Ion chromatography as a reference method for determination of inorganic ions in water and wastewater.* Critical Reviews in Analytical Chemistry, 2006. **36**(2): p. 107-127.

215. Duggal, M., H. Chawla, and M. Curzon, *A study of the relationship between trace elements in saliva and dental caries in children.* Archives of oral biology, 1991. **36**(12): p. 881-884.

216. Sjögren, K. and D. Birkhed, *Factors related to fluoride retention after toothbrushing and possible connection to caries activity.* Caries research, 1993. **27**(6): p. 474-477.

217. Featherstone, J., *Laboratory and human studies to elucidate the mechanism of action of fluoride-containing dentifrices, in.* Clinical and Biological Aspects of dentifrices, 1992: p. 41-50.

218. Fritzsche, T. and U. Saxer, *Fluoride retention and clearance after rinsing with fluoridated mouthwashes.* Schweizer Monatsschrift fur Zahnmedizin= Revue Mensuelle Suisse D'odonto-stomatologie= Rivista Mensile Svizzera di Odontologia e Stomatologia, 1989. **99**(3): p. 299-306.

219. Duckworth, R., S. Morgan, and A. Murray, *Fluoride in saliva and plaque following use of fluoride-containing mouthwashes.* Journal of dental research, 1987. **66**(12): p. 1730-1734.

220. Bruun, C., H. Givskov, and A. Thylstrup, *Whole saliva fluoride after toothbrushing with NaF and MFP dentifrices with different F concentrations.* Caries research, 1984. **18**(3): p. 282-288.

221. Attin, T. and E. Hellwig, *Salivary fluoride content after toothbrushing with a sodium fluoride and an amine fluoride dentifrice followed by different mouthrinsing procedures.* The Journal of Clinical Dentistry, 1996. **7**(1): p. 6-8.

222. Koch, G. and S. Hatibović-Kofman, *Glass ionomer cements as a fluoride release system in vivo.* Swedish dental journal, 1990. **14**(6): p. 267-273.

223. Hatibović-Kofman, S. and G. Koch, *Fluoride release from glass ionomer cement in vivo and in vitro.* Swedish dental journal, 1991. **15**(6): p. 253-258.

224. Benelli, E., et al., *In situ anticariogenic potential of glass lonomer cement.* Caries research, 1993. **27**(4): p. 280-284.

225. Moura, J., et al., *Effect of luting cement on dental biofilm composition and secondary caries around metallic restorations in situ.* OPERATIVE DENTISTRY-UNIVERSITY OF WASHINGTON-, 2004. **29**: p. 509-514.

226. Hamilton, I., *Biochemical effects of fluoride on oral bacteria.* Journal of dental research, 1990. **69**(2_suppl): p. 660-667.

227. Ten Cate, J., J. Damen, and M. Buijs, *Inhibition of dentin demineralization by fluoride in vitro.* Caries Research, 1998. **32**(2): p. 141-147.

228. Buzalaf, M.A.R., et al., *Mechanisms of action of fluoride for caries control.* Fluoride and the oral environment, 2011. **22**: p. 97-114.

229. Ten Cate, J. and J. Featherstone, *Mechanistic aspects of the interactions between fluoride and dental enamel.* Critical Reviews in Oral Biology & Medicine, 1991. **2**(3): p. 283-296.

230. Peroš, K. and I. Šutej, *The cariostatic mechanisms of fluoride.* Acta medica academica, 2013. **42**(2): p. 179.

231. Moreno, E. and K. Varughese, *Crystal growth of calcium apatites from dilute solutions.* Journal of Crystal Growth, 1981. **53**(1): p. 20-30.

232. Cate, J.T., *In vitro studies on the effects of fluoride on de-and remineralization.* Journal of dental research, 1990. **69**(2_suppl): p. 614-619.

233. Wang, L., et al., *Mechanical properties of dental restorative materials: relative contribution of laboratory tests.* Journal of Applied Oral Science, 2003. **11**: p. 162-167.

234. Beck, F., et al., *Survival of direct resin restorations in posterior teeth within a 19-year period (1996–2015): A meta-analysis of prospective studies.* Dental Materials, 2015. **31**(8): p. 958-985.

235. Karimi, A. and M. Navidbakhsh, *An experimental study on the mechanical properties of rat brain tissue using different stress–strain definitions.* Journal of Materials Science: Materials in Medicine, 2014. **25**(7): p. 1623-1630.

236. Vaidya, A. and K. Pathak, *Mechanical stability of dental materials*, in *Applications of Nanocomposite Materials in Dentistry*. 2019, Elsevier. p. 285-305.

237. Chung, S.M., et al., *Flexural strength of dental composite restoratives: Comparison of biaxial and three-point bending test.* Journal of Biomedical Materials Research Part B: Applied Biomaterials, 2004. **71B**(2): p. 278-283.

238. Lambrechts, P., M. Braem, and G. Vanherle, *Buonocore memorial lecture. Evaluation of clinical performance for posterior composite resins and dentin adhesives.* Oper Dent, 1987. **12**(2): p. 53-78.

239. Ilie, N., et al., *Academy of dental materials guidance—Resin composites: Part I—Mechanical properties.* Dental materials, 2017. **33**(8): p. 880-894.

240. Peutzfeldt, A. and E. Asmussen, *Modulus of resilience as predictor for clinical wear of restorative resins.* Dental Materials, 1992. **8**(3): p. 146-148.

241. Kim, K.-H., J.L. Ong, and O. Okuno, *The effect of filler loading and morphology on the mechanical properties of contemporary composites.* The Journal of Prosthetic Dentistry, 2002. **87**(6): p. 642-649.

242. Willems, G., et al., *A classification of dental composites according to their morphological and mechanical characteristics.* Dental Materials, 1992. **8**(5): p. 310-319.

243. Randolph, L.D., et al., *Filler characteristics of modern dental resin composites and their influence on physico-mechanical properties.* Dental Materials, 2016. **32**(12): p. 1586-1599.

244. Daronch, M., et al., *Polymerization kinetics of pre-heated composite.* Journal of Dental Research, 2006. **85**(1): p. 38-43.

245. Ferracane, J. and E. Greener, *The effect of resin formulation on the degree of conversion and mechanical properties of dental restorative resins.* Journal of biomedical materials research, 1986. **20**(1): p. 121-131.

246. ASMUSSEN, E., *Restorative resins: hardness and strength vs. quantity of remaining double bonds.* European Journal of Oral Sciences, 1982. **90**(6): p. 484-489.

247. Ilie2, M.P.Z.T.R.H.N., *Mechanical properties of experimental composites containing bioactive glass after artificial aging in water and ethanol.* 2018.

248. Momoi, Y. and J. McCabe, *Hygroscopic expansion of resin based composites during 6 months of water storage.* British dental journal, 1994. **176**(3): p. 91-96.

249. Martin, N. and N. Jedynakiewicz, *Measurement of water sorption in dental composites.* Biomaterials, 1998. **19**(1): p. 77-83.

250. Pearson, G. and C. Longman, *Water sorption and solubility of resin-based materials following inadequate polymerization by a visible-light curing system.* Journal of Oral Rehabilitation, 1989. **16**(1): p. 57-61.

251. Soderholm, K.-J. and M. Roberts, *Influence of water exposure on the tensile strength of composites.* Journal of Dental Research, 1990. **69**(12): p. 1812-1816.

252. Curtis, A.R., et al., *Water uptake and strength characteristics of a nanofilled resin-based composite.* J Dent, 2008. **36**(3): p. 186-93.

253. Santerre, J.P., L. Shajii, and B.W. Leung, *Relation of Dental Composite Formulations To Their Degradation and the Release of Hydrolyzed Polymeric-Resin-Derived Products.* Critical Reviews in Oral Biology & Medicine, 2001. **12**(2): p. 136-151.

254. MUNKSGAARD, E.C. and M. FREUND, *Enzymatic hydrolysis of (di) methacrylates and their polymers.* European Journal of Oral Sciences, 1990. **98**(3): p. 261-267.

255. Fotos, P., A. Diaz-Arnold, and V. Williams, *The effect of microbial contamination and pH changes in storage solutions during in vitro assays of bonding agents.* Dental Materials, 1990. **6**(3): p. 154-157.

256. Prati, C., et al., *Early marginal leakage and shear bond strength of adhesive restorative systems.* Dental Materials, 1990. **6**(3): p. 195-200.

257. Hadis, M., et al., *High irradiance curing and anomalies of exposure reciprocity law in resin-based materials.* Journal of dentistry, 2011. **39**(8): p. 549-557.

258. Asmussen, E. and A. Peutzfeld, *Influence of pulse-delay curing on softening of polymer structures.* Journal of Dental Research, 2001. **80**(6): p. 1570-1573.

259. Sideridou, I.D. and D.S. Achilias, *Elution study of unreacted Bis-GMA, TEGDMA, UDMA, and Bis-EMA from light-cured dental resins and resin composites using HPLC.* Journal of Biomedical

Materials Research Part B: Applied Biomaterials: An Official Journal of The Society for Biomaterials, The Japanese Society for Biomaterials, and The Australian Society for Biomaterials and the Korean Society for Biomaterials, 2005. **74**(1): p. 617-626.

260. Unemori, M., et al., *Composite resin restoration and postoperative sensitivity: clinical follow-up in an undergraduate program.* Journal of Dentistry, 2001. **29**(1): p. 7-13.
261. de Souza Costa, C.A., et al., *Short-term evaluation of the pulpo-dentin complex response to a resin-modified glass-ionomer cement and a bonding agent applied in deep cavities.* Dental Materials, 2003. **19**(8): p. 739-746.
262. Jontell, M., et al., *Effects of unpolymerized resin components on the function of accessory cells derived from the rat incisor pulp.* Journal of dental research, 1995. **74**(5): p. 1162-1167.
263. Blomgren, J., et al., *Adverse reactions in the oral mucosa associated with anterior composite restorations.* Journal of oral pathology & medicine, 1996. **25**(6): p. 311-313.
264. Janke, V., et al., *TEGDMA causes apoptosis in primary human gingival fibroblasts.* Journal of Dental Research, 2003. **82**(10): p. 814-818.
265. Kanerva, L., et al., *Occupational allergic contact dermatitis from 2-hydroxyethyl methacrylate and ethylene glycol dimethacrylate in a modified acrylic structural adhesive.* Contact Dermatitis, 1995. **33**(2): p. 84-89.
266. Lindström, M., et al., *Dentist's occupational asthma, rhinoconjunctivitis, and allergic contact dermatitis from methacrylates.* Allergy, 2002. **57**(6): p. 543-545.
267. Ratanasathien, S., et al., *Cytotoxic interactive effects of dentin bonding components on mouse fibroblasts.* J Dent Res, 1995. **74**(9): p. 1602-6.
268. Yoshii, E., *Cytotoxic effects of acrylates and methacrylates: Relationships of monomer structures and cytotoxicity.* Journal of Biomedical Materials Research, 1997. **37**(4): p. 517-524.
269. Geurtsen, W., et al., *Cytotoxicity of 35 dental resin composite monomers/additives in permanent 3T3 and three human primary fibroblast cultures.* Journal of Biomedical Materials Research: An Official Journal of The Society for Biomaterials, The Japanese Society for Biomaterials, and the Australian Society for Biomaterials, 1998. **41**(3): p. 474-480.
270. Reichl, F.X., et al., *Cell death effects of resin-based dental material compounds and mercurials in human gingival fibroblasts.* Arch Toxicol, 2006. **80**(6): p. 370-7.
271. Moharamzadeh, K., et al., *Cytotoxicity of resin monomers on human gingival fibroblasts and HaCaT keratinocytes.* Dental Materials, 2007. **23**(1): p. 40-44.
272. Moharamzadeh, K., et al., *Cytotoxicity of resin monomers on human gingival fibroblasts and HaCaT keratinocytes.* Dent Mater, 2007. **23**(1): p. 40-4.

273. Geurtsen, W., et al., *Effects of extraction media upon fluoride release from a resin-modified glass-ionomer cement.* Clinical Oral Investigations, 1998. **2**(3): p. 143-146.
274. Chan, F.K.-M., K. Moriwaki, and M.J. De Rosa, *Detection of necrosis by release of lactate dehydrogenase activity.* Methods in molecular biology (Clifton, N.J.), 2013. **979**: p. 65-70.
275. Walther, U., et al., *Antioxidative vitamins decrease cytotoxicity of HEMA and TEGDMA in cultured cell lines.* Archives of oral biology, 2004. **49**(2): p. 125-131.
276. Mosmann, T., *Rapid colorimetric assay for cellular growth and survival: application to proliferation and cytotoxicity assays.* J Immunol Methods, 1983. **65**(1-2): p. 55-63.
277. Issa, Y., et al., *Resin composite monomers alter MTT and LDH activity of human gingival fibroblasts in vitro.* Dental Materials, 2004. **20**(1): p. 12-20.
278. Volk, J., et al., *Effects of three resin monomers on the cellular glutathione concentration of cultured human gingival fibroblasts.* Dent Mater, 2006. **22**(6): p. 499-505.
279. Samuelsen, J.T., et al., *The dental monomer HEMA causes proteome changes in human THP-1 monocytes.* J Biomed Mater Res A, 2019. **107**(4): p. 851-859.
280. Bouillaguet, S., et al., *In vitro cytotoxicity and dentin permeability of HEMA.* J Endod, 1996. **22**(5): p. 244-8.
281. Teti, G., et al., *HEMA down-regulates procollagen α1 type I in human gingival fibroblasts.* Journal of Biomedical Materials Research Part A, 2009. **90**(1): p. 256-262.
282. Engelmann, J., et al., *Effect of TEGDMA on the intracellular glutathione concentration of human gingival fibroblasts.* J Biomed Mater Res, 2002. **63**(6): p. 746-51.
283. Devasagayam, T.P., et al., *Free radicals and antioxidants in human health: current status and future prospects.* J Assoc Physicians India, 2004. **52**: p. 794-804.
284. Ferracane, J.L., *Elution of leachable components from composites.* J Oral Rehabil, 1994. **21**(4): p. 441-52.
285. Stanislawski, L., et al., *TEGDMA-induced toxicity in human fibroblasts is associated with early and drastic glutathione depletion with subsequent production of oxygen reactive species.* J Biomed Mater Res A, 2003. **66**(3): p. 476-82.
286. Sandberg, E., et al., *HEMA bound to self-protein promotes auto-antibody production in mice.* J Dent Res, 2002. **81**(9): p. 633-6.
287. Sancar, A., et al., *Molecular mechanisms of mammalian DNA repair and the DNA damage checkpoints.* Annu Rev Biochem, 2004. **73**: p. 39-85.
288. Shiloh, Y., *ATM and related protein kinases: safeguarding genome integrity.* Nat Rev Cancer, 2003. **3**(3): p. 155-68.

289. Eckhardt, A., et al., *TEGDMA-induced oxidative DNA damage and activation of ATM and MAP kinases.* Biomaterials, 2009. **30**(11): p. 2006-14.

290. Samuelsen, J.T., et al., *HEMA reduces cell proliferation and induces apoptosis in vitro.* Dent Mater, 2008. **24**(1): p. 134-40.

291. Sedelnikova, O.A., et al., *Quantitative detection of (125)IdU-induced DNA double-strand breaks with gamma-H2AX antibody.* Radiat Res, 2002. **158**(4): p. 486-92.

292. Urcan, E., et al., *Induction of DNA double-strand breaks in primary gingival fibroblasts by exposure to dental resin composites.* Biomaterials, 2010. **31**(8): p. 2010-4.

293. Bakopoulou, A., T. Papadopoulos, and P. Garefis, *Molecular toxicology of substances released from resin-based dental restorative materials.* Int J Mol Sci, 2009. **10**(9): p. 3861-99.

294. Kleinsasser, N.H., et al., *Cytotoxic and genotoxic effects of resin monomers in human salivary gland tissue and lymphocytes as assessed by the single cell microgel electrophoresis (Comet) assay.* Biomaterials, 2006. **27**(9): p. 1762-70.

295. Kleinsasser, N.H., et al., *Genotoxicity and cytotoxicity of dental materials in human lymphocytes as assessed by the single cell microgel electrophoresis (comet) assay.* J Dent, 2004. **32**(3): p. 229-34.

296. Di Nisio, C., et al., *Transcriptome modifications in human gingival fibroblasts exposed to 2-hydroxyethyl methacrylate.* Gene, 2016. **582**(1): p. 38-46.

297. Moharamzadeh, K., I.M. Brook, and R. Van Noort, *Biocompatibility of Resin-based Dental Materials.* Materials, 2009. **2**(2): p. 514-548.

298. Wang, Z., M. Gerstein, and M. Snyder, *RNA-Seq: a revolutionary tool for transcriptomics.* Nature reviews genetics, 2009. **10**(1): p. 57-63.

299. Metzker, M.L., *Sequencing technologies—the next generation.* Nature reviews genetics, 2010. **11**(1): p. 31-46.

300. Corchete, L.A., et al., *Systematic comparison and assessment of RNA-seq procedures for gene expression quantitative analysis.* Scientific reports, 2020. **10**(1): p. 1-15.

301. Chen, M., et al., *Diagnostic biomarker candidates for pulpitis revealed by bioinformatics analysis of merged microarray gene expression datasets.* BMC Oral Health, 2020. **20**(1): p. 1-13.

302. Zhang, Y.-Y., M.-H. Mao, and Z.-X. Han, *Identification of a gene prognostic signature for oral squamous cell carcinoma by RNA sequencing and bioinformatics.* BioMed research international, 2021. **2021**.

303. Weissmann, R., et al., *Transcriptome alterations in X-irradiated human gingiva fibroblasts.* Health Physics, 2016. **111**(2): p. 75.

304. Tang, X.-H., et al., *Gene expression profiling signatures for the diagnosis and prevention of oral cavity carcinogenesis-genome-wide analysis using RNA-seq technology.* Oncotarget, 2015. **6**(27): p. 24424.

305. Murray, P.E., C. García Godoy, and F. García Godoy, *How is the biocompatibilty of dental biomaterials evaluated?* Medicina Oral, Patología Oral y Cirugía Bucal (Internet), 2007. **12**(3): p. 258-266.

306. Schmalz, G. and F.-X. Reichl, *Regulation of Dental Materials 83.* Regulatory Toxicology, 2021: p. 1153.

307. Schmalz, G. and K.M. Galler, *Biocompatibility of biomaterials–Lessons learned and considerations for the design of novel materials.* Dental Materials, 2017. **33**(4): p. 382-393.

308. Pratap, B., et al., *Resin based restorative dental materials: characteristics and future perspectives.* Japanese Dental Science Review, 2019. **55**(1): p. 126-138.

309. Lovell, L.G., S.M. Newman, and C.N. Bowman, *The effects of light intensity, temperature, and comonomer composition on the polymerization behavior of dimethacrylate dental resins.* J Dent Res, 1999. **78**(8): p. 1469-76.

310. Goldberg, M., *In vitro and in vivo studies on the toxicity of dental resin components: a review.* Clin Oral Investig, 2008. **12**(1): p. 1-8.

311. Kuan, Y.-H., et al., *Proinflammatory activation of macrophages by bisphenol A-glycidyl-methacrylate involved NFκB activation via PI3K/Akt pathway.* Food and chemical toxicology, 2012. **50**(11): p. 4003-4009.

312. Kuan, Y.-H., et al., *Bisgma stimulates prostaglandin E2 production in macrophages via cyclooxygenase-2, cytosolic phospholipase A2, and mitogen-activated protein kinases family.* PLoS One, 2013. **8**(12): p. e82942.

313. Huang, F.M., et al., *BisGMA-induced cytotoxicity and genotoxicity in macrophages are attenuated by wogonin via reduction of intrinsic caspase pathway activation.* Environmental Toxicology, 2016. **31**(2): p. 176-184.

314. Chang, H.H., et al., *Urethane dimethacrylate induces cytotoxicity and regulates cyclooxygenase-2, hemeoxygenase and carboxylesterase expression in human dental pulp cells.* Acta Biomater, 2014. **10**(2): p. 722-31.

315. Squier, C.A. and M.J. Kremer, *Biology of Oral Mucosa and Esophagus.* JNCI Monographs, 2001. **2001**(29): p. 7-15.

316. Altman, F.P., *Tetrazolium salts and formazans.* Prog Histochem Cytochem, 1976. **9**(3): p. 1-56.

317. Szep, S., et al., *Cytotoxicity of modern dentin adhesives--in vitro testing on gingival fibroblasts.* J Biomed Mater Res, 2002. **63**(1): p. 53-60.

318. Saxena, I., S. Srikanth, and Z. Chen, *Cross Talk between H2O2 and Interacting Signal Molecules under Plant Stress Response.* Frontiers in Plant Science, 2016. **7**.

319. Wang, S., H. Yu, and J.K. Wickliffe, *Limitation of the MTT and XTT assays for measuring cell viability due to superoxide formation induced by nano-scale TiO2.* Toxicology in Vitro, 2011. **25**(8): p. 2147-2151.

320. Drozdz, K., et al., *Bisphenol A-glycidyl methacrylate induces a broad spectrum of DNA damage in human lymphocytes.* Arch Toxicol, 2011. **85**(11): p. 1453-61.

321. Shahi, S., et al., *A review on potential toxicity of dental material and screening their biocompatibility.* Toxicology Mechanisms and Methods, 2019. **29**(5): p. 368-377.

322. Teti, G., et al., *HEMA down-regulates procollagen alpha1 type I in human gingival fibroblasts.* J Biomed Mater Res A, 2009. **90**(1): p. 256-62.

323. Van Landuyt, K.L., et al., *How much do resin-based dental materials release? A meta-analytical approach.* Dent Mater, 2011. **27**(8): p. 723-47.

324. Finer, Y., F. Jaffer, and J.P. Santerre, *Mutual influence of cholesterol esterase and pseudocholinesterase on the biodegradation of dental composites.* Biomaterials, 2004. **25**(10): p. 1787-93.

325. Finer, Y. and J. Santerre, *The influence of resin chemistry on a dental composite's biodegradation.* Journal of Biomedical Materials Research Part A: An Official Journal of The Society for Biomaterials, The Japanese Society for Biomaterials, and The Australian Society for Biomaterials and the Korean Society for Biomaterials, 2004. **69**(2): p. 233-246.

326. Schweikl, H., G. Schmalz, and T. Spruss, *The induction of micronuclei in vitro by unpolymerized resin monomers.* J Dent Res, 2001. **80**(7): p. 1615-20.

327. Schweikl, H., G. Schmalz, and K. Rackebrandt, *The mutagenic activity of unpolymerized resin monomers in Salmonella typhimurium and V79 cells.* Mutat Res, 1998. **415**(1-2): p. 119-30.

328. Janssen, K., et al., *DNA repair activity of 8-oxoguanine DNA glycosylase 1 (OGG1) in human lymphocytes is not dependent on genetic polymorphism Ser326/Cys326.* Mutation Research/DNA Repair, 2001. **486**(3): p. 207-216.

329. Furda, A.M., et al., *Analysis of DNA damage and repair in nuclear and mitochondrial DNA of animal cells using quantitative PCR.* Methods in molecular biology (Clifton, N.J.), 2012. **920**: p. 111-132.

330. Ferenbach, D.A., D.C. Kluth, and J. Hughes, *Hemeoxygenase-1 and Renal Ischaemia-Reperfusion Injury.* Nephron Experimental Nephrology, 2010. **115**(3): p. e33-e37.

331. Güven, G., et al., *Co-expression of cyclooxygenase-2 and vascular endothelial growth factor in inflamed human pulp: an immunohistochemical study.* J Endod, 2007. **33**(1): p. 18-20.

332. Imai, T., *Human carboxylesterase isozymes: catalytic properties and rational drug design.* Drug Metab Pharmacokinet, 2006. **21**(3): p. 173-85.

333. Moraes, L.G., et al., *Infrared spectroscopy: a tool for determination of the degree of conversion in dental composites.* J Appl Oral Sci, 2008. **16**(2): p. 145-9.

334. Skrtic, D. and J.M. Antonucci, *Dental Composites Based on Amorphous Calcium Phosphate — Resin Composition/Physicochemical Properties Study.* Journal of Biomaterials Applications, 2007. **21**(4): p. 375-393.

335. Gajewski, V.E., et al., *Monomers used in resin composites: degree of conversion, mechanical properties and water sorption/solubility.* Braz Dent J, 2012. **23**(5): p. 508-14.

336. Floyd, C.J.E. and S.H. Dickens, *Network structure of Bis-GMA- and UDMA-based resin systems.* Dental Materials, 2006. **22**(12): p. 1143-1149.

337. Kostoryz, E.L., et al., *Biocompatibility of hydroxylated metabolites of BISGMA and BFDGE.* J Dent Res, 2003. **82**(5): p. 367-71.

338. Kang, Y.G., et al., *Release of bisphenol A from resin composite used to bond orthodontic lingual retainers.* Am J Orthod Dentofacial Orthop, 2011. **140**(6): p. 779-89.

339. Lopes-Rocha, L., et al., *An integrative review on the toxicity of Bisphenol A (BPA) released from resin composites used in dentistry.* Journal of Biomedical Materials Research Part B: Applied Biomaterials, 2021. **109**(11): p. 1942-1952.

340. Morra, M., *Acid-base properties of adhesive dental polymers.* Dental Materials, 1993. **9**(6): p. 375-378.

341. Domingo, C., et al., *Hydrolytic stability of experimental hydroxyapatite-filled dental composite materials.* Dental Materials, 2003. **19**(6): p. 478-486.

342. Lovell, L.G., et al., *Effects of Composition and Reactivity on the Reaction Kinetics of Dimethacrylate/Dimethacrylate Copolymerizations.* Macromolecules, 1999. **32**(12): p. 3913-3921.

343. van Noort, R., *Clinical relevance of laboratory studies on dental materials: strength determination--a personal view.* J Dent, 1994. **22 Suppl 1**: p. S4-8.

344. Silikas, N. and D. Watts, *Rheology of urethane dimethacrylate and diluent formulations.* Dental Materials, 1999. **15**(4): p. 257-261.

345. Van Landuyt, K.L., et al., *Systematic review of the chemical composition of contemporary dental adhesives.* Biomaterials, 2007. **28**(26): p. 3757-3785.

346. Holmes, R.G., et al., *Effect of solvent type and content on monomer conversion of a model resin system as a thin film.* Dental materials, 2007. **23**(12): p. 1506-1512.

347. Lee, J.H., C.M. Um, and I.B. Lee, *Rheological properties of resin composites according to variations in monomer and filler composition.* Dent Mater, 2006. **22**(6): p. 515-26.

348. Chung, E.P., et al., *Dual Asymmetric Centrifugation Efficiently Produces a Poloxamer-Based Nanoemulsion Gel for Topical Delivery of Pirfenidone.* AAPS PharmSciTech, 2020. **21**(7): p. 265.

349. Al-Taie, A.M.B.J., *Development and characterisation of novel fluorapatite containing dental composite materials*. 2017, University of Leeds.

350. Leinfelder, K. and A. Prasad, *A new condensable composite for the restoration of posterior teeth.* Dent Today, 1998. **17**(2): p. 112-6.

351. Zanchi, C.H., et al., *Effect of the silane concentration on the selected properties of an experimental microfilled composite resin.* Applied Adhesion Science, 2015. **3**(1): p. 27.

352. Antonucci, J.M., W.F. Regnault, and D. Skrtic, *Polymerization shrinkage and stress development in amorphous calcium phosphate/urethane dimethacrylate polymeric composites.* Journal of composite materials, 2010. **44**(3): p. 355-355.

353. Pearce, E.M., *Principles of polymerization (third edition), by George Odian, Wiley-Interscience, New York, 1991, 768 pp. price: $59.95.* Journal of Polymer Science Part A: Polymer Chemistry, 1992. **30**(7): p. 1508-1508.

354. Skrtic, D. and J. Antonucci, *Effect of chemical structure and composition of the resin phase on vinyl conversion of amorphous calcium phosphate-filled composites.* Polymer International, 2007. **56**(4): p. 497-505.

355. Gonçalves, F., et al., *Influence of BisGMA, TEGDMA, and BisEMA contents on viscosity, conversion, and flexural strength of experimental resins and composites.* European Journal of Oral Sciences, 2009. **117**(4): p. 442-446.

356. Elliott, J.E., L.G. Lovell, and C.N. Bowman, *Primary cyclization in the polymerization of bis-GMA and TEGDMA: a modeling approach to understanding the cure of dental resins.* Dental Materials, 2001. **17**(3): p. 221-229.

357. Ilie, N. and K. Stark, *Curing behaviour of high-viscosity bulk-fill composites.* Journal of Dentistry, 2014. **42**(8): p. 977-985.

358. Emami, N. and K.J.M. Söderholm, *How light irradiance and curing time affect monomer conversion in light-cured resin composites.* European Journal of Oral Sciences, 2003. **111**(6): p. 536-542.

359. Halvorson, R.H., R.L. Erickson, and C.L. Davidson, *Energy dependent polymerization of resin-based composite.* Dental Materials, 2002. **18**(6): p. 463-469.

360. Leprince, J.G., et al., *Photoinitiator type and applicability of exposure reciprocity law in filled and unfilled photoactive resins.* Dental Materials, 2011. **27**(2): p. 157-164.

361. Ratanasathien, S., et al., *Cytotoxic Interactive Effects of Dentin Bonding Components on Mouse Fibroblasts.* Journal of Dental Research, 1995. **74**(9): p. 1602-1606.

362. Manojlovic, D., et al., *Monomer elution from nanohybrid and ormocer-based composites cured with different light sources.* Dent Mater, 2011. **27**(4): p. 371-8.

363. Łagocka, R., et al., *Elution study of unreacted TEGDMA from bulk-fill composite (SDR™ Dentsply) using HPLC.* Adv Med Sci, 2015. **60**(2): p. 191-8.

364. Moharamzadeh, K., et al., *HPLC analysis of components released from dental composites with different resin compositions using different extraction media.* J Mater Sci Mater Med, 2007. **18**(1): p. 133-7.

365. Szczesio-Wlodarczyk, A., et al., *The Influence of Low-Molecular-Weight Monomers (TEGDMA, HDDMA, HEMA) on the Properties of Selected Matrices and Composites Based on Bis-GMA and UDMA.* Materials (Basel, Switzerland), 2022. **15**(7): p. 2649.

366. Oysaed, H. and I.E. Ruyter, *Water sorption and filler characteristics of composites for use in posterior teeth.* J Dent Res, 1986. **65**(11): p. 1315-8.

367. Sonkaya, E., Z.G.B. Kürklü, and Ş. Bakır, *Effect of Polymerization Time on Residual Monomer Release in Dental Composite: In Vitro Study.* International Journal of Polymer Science, 2021. **2021**: p. 8101075.

368. Taylor, D., et al., *Relationship between filler and matrix resin characteristics and the properties of uncured composite pastes.* Biomaterials, 1998. **19**(1-3): p. 197-204.

369. Francois, P., et al., *Commercially Available Fluoride-Releasing Restorative Materials: A Review and a Proposal for Classification.* Materials (Basel, Switzerland), 2020. **13**(10): p. 2313.

370. Preston, A.J., et al., *Fluoride release from aesthetic dental materials.* J Oral Rehabil, 1999. **26**(2): p. 123-9.

371. Lee, S.Y., et al., *Fluoride ion diffusion from a glass-ionomer cement.* J Oral Rehabil, 2000. **27**(7): p. 576-86.

372. Kiran, A. and V. Hegde, *A short term comparitive analysis of Fluoride release from a newly introduced Glass Ionomer Cement in deionised water and lactic acid.* Journal of International Oral Health, 2010. **2**(2).

373. Jingarwar, M.M., et al., *Quantitative assessment of fluoride release and recharge ability of different restorative materials in different media: an in vitro study.* Journal of clinical and diagnostic research : JCDR, 2014. **8**(12): p. ZC31-ZC34.

374. Moshaverinia, M., et al., *Effects of incorporation of nano-fluorapatite particles on microhardness, fluoride releasing properties, and biocompatibility of a conventional glass ionomer cement (GIC).* Dent Mater J, 2016. **35**(5): p. 817-821.

375. Pajor, K., L. Pajchel, and J. Kolmas, *Hydroxyapatite and fluorapatite in conservative dentistry and oral implantology—A review.* Materials, 2019. **12**(17): p. 2683.

376. Niu, Y., et al., *Development of a bioactive composite of nano fluorapatite and poly (butylene succinate) for bone tissue regeneration.* Journal of Materials Chemistry B, 2014. **2**(9): p. 1174-1181.

377. Liu, J., et al., *The stimulation of adipose-derived stem cell differentiation and mineralization by ordered rod-like fluorapatite coatings.* Biomaterials, 2012. **33**(20): p. 5036-46.

378. Altaie, A., et al., *Development and characterisation of dental composites containing anisotropic fluorapatite bundles and rods.* Dent Mater, 2020. **36**(8): p. 1071-1085.

379. Mousavinasab, S.M. and I. Meyers, *Fluoride release by glass ionomer cements, compomer and giomer.* Dental research journal, 2009. **6**(2): p. 75-81.

380. Okte, Z., et al., *Fluoride and aluminum release from restorative materials using ion chromatography.* Journal of applied oral science : revista FOB, 2012. **20**(1): p. 27-31.

381. Gururaj, M., et al., *Fluoride releasing and uptake capacities of esthetic restorations.* J Contemp Dent Pract, 2013. **14**(5): p. 887-91.

382. REZK-LEGA, F., *O8GAARD, B. & RO LLA, G.(1991) Availability of fluoride from glass–ionomer luting cements in human saliva.* Scandinavian Journal of Dental Research. **99**: p. 60.

383. El Mallakh, B. and N. Sarkar, *Fluoride release from glass-ionomer cements in de-ionized water and artificial saliva.* Dental Materials, 1990. **6**(2): p. 118-122.

384. Jingarwar, M.M., et al., *Quantitative assessment of fluoride release and recharge ability of different restorative materials in different media: an in vitro study.* J Clin Diagn Res, 2014. **8**(12): p. Zc31-4.

385. Khan, A.S., et al., *Synthesis and characterizations of a fluoride-releasing dental restorative material.* Mater Sci Eng C Mater Biol Appl, 2013. **33**(6): p. 3458-64.

386. Kumar, S.M., et al., *Comparative Evaluation of the Effect of Various Surface Coating Agents on Fluoride Release from Conventional Glass Ionomer Cement in Deionized Water, Artificial Saliva and Lactic Acid-An In-Vitro Study.*

387. Karantakis, P., et al., *Fluoride release from three glass ionomers, a compomer, and a composite resin in water, artificial saliva, and lactic acid.* Oper Dent, 2000. **25**(1): p. 20-5.

388. Czarnecka, B., H. Limanowska-Shaw, and J.W. Nicholson, *Buffering and ion-release by a glass-ionomer cement under near-neutral and acidic conditions.* Biomaterials, 2002. **23**(13): p. 2783-8.

389. Harhash, A.Y., I.I. ElSayad, and A.G.S. Zaghloul, *A comparative in vitro study on fluoride release and water sorption of different flowable esthetic restorative materials.* European journal of dentistry, 2017. **11**(2): p. 174-179.

390. Michelsen, V.B., et al., *Quantification of organic eluates from polymerized resin-based dental restorative materials by use of GC/MS.* J Chromatogr B Analyt Technol Biomed Life Sci, 2007. **850**(1-2): p. 83-91.

391. Vervliet, P., et al., *Qualitative analysis of dental material ingredients, composite resins and sealants using liquid chromatography coupled to quadrupole time of flight mass spectrometry.* J Chromatogr A, 2018. **1576**: p. 90-100.

392. Putzeys, E., et al., *Long-term elution of monomers from resin-based dental composites.* Dent Mater, 2019. **35**(3): p. 477-485.

393. Øysæd, H. and I. Ruyter, *Water sorption and filler characteristics of composites for use in posterior teeth.* Journal of dental research, 1986. **65**(11): p. 1315-1318.

394. Santerre, J., L. Shajii, and B. Leung, *Relation of dental composite formulations to their degradation and the release of hydrolyzed polymeric-resin-derived products.* Critical Reviews in Oral Biology & Medicine, 2001. **12**(2): p. 136-151.

395. Curtis, A., et al., *Water uptake and strength characteristics of a nanofilled resin-based composite.* Journal of dentistry, 2008. **36**(3): p. 186-193.

396. Sarna-Boś, K., et al., *Contemporary Approach to the Porosity of Dental Materials and Methods of Its Measurement.* International Journal of Molecular Sciences, 2021. **22**(16): p. 8903.

397. Glasspoole, E., R. Erickson, and C. Davidson, *A fluoride-releasing composite for dental applications.* Dental Materials, 2001. **17**(2): p. 127-133.

398. Tichy, A., et al., *Can a New HEMA-free Two-step Self-etch Adhesive Improve Dentin Bonding Durability and Marginal Adaptation?* J Adhes Dent, 2021. **23**: p. 505-12.

399. Sideridou, I., V. Tserki, and G. Papanastasiou, *Study of water sorption, solubility and modulus of elasticity of light-cured dimethacrylate-based dental resins.* Biomaterials, 2003. **24**(4): p. 655-65.

400. Bastioli, C., G. Romano, and C. Migliaresi, *Water sorption and mechanical properties of dental composites.* Biomaterials, 1990. **11**(3): p. 219-223.

401. Fonseca, A.S., et al., *Effect of monomer type on the CC degree of conversion, water sorption and solubility, and color stability of model dental composites.* Dent Mater, 2017. **33**(4): p. 394-401.

402. Kerby, R.E., et al., *Synthesis and evaluation of modified urethane dimethacrylate resins with reduced water sorption and solubility.* Dental Materials, 2009. **25**(3): p. 302-313.

403. Pomes, B., et al., *Water ageing of urethane dimethacrylate networks.* Polymer Degradation and Stability, 2018. **154**: p. 195-202.

404. Kalachandra, S. and T.W. Wilson, *Water sorption and mechanical properties of light-cured proprietary composite tooth restorative materials.* Biomaterials, 1992. **13**(2): p. 105-9.

405. da Silva, E.M., et al., *Relationship between the degree of conversion, solubility and salivary sorption of a hybrid and a nanofilled resin composite.* Journal of applied oral science : revista FOB, 2008. **16**(2): p. 161-166.

406. da Silva, E.M., et al., *The diffusion kinetics of a nanofilled and a midifilled resin composite immersed in distilled water, artificial saliva, and lactic acid.* Clin Oral Investig, 2011. **15**(3): p. 393-401.

407. Kumar, S.R., A. Patnaik, and I. Bhat, *Physical and thermo-mechanical characterizations of resin-based dental composite reinforced with silane-modified nanoalumina filler particle.* Proceedings of the Institution of Mechanical Engineers, Part L: Journal of Materials: Design and Applications, 2016. **230**(2): p. 504-514.

408. Mitra, S.B., et al., *Fluoride release and recharge behavior of a nano-filled resin-modified glass ionomer compared with that of other fluoride releasing materials.* American journal of dentistry, 2011. **24**(6): p. 372.

409. Martínez-Mier, E.A., *Fluoride: its metabolism, toxicity, and role in dental health.* Journal of Evidence-Based Complementary & Alternative Medicine, 2012. **17**(1): p. 28-32.

410. Stanislawski, L., et al., *Factors responsible for pulp cell cytotoxicity induced by resin-modified glass ionomer cements.* Journal of Biomedical Materials Research: An Official Journal of The Society for Biomaterials, The Japanese Society for Biomaterials, and The Australian Society for Biomaterials, 1999. **48**(3): p. 277-288.

411. Guo, Y., et al., *Functional genomic screen reveals genes involved in lipid-droplet formation and utilization.* Nature, 2008. **453**(7195): p. 657-61.

412. Whitford, G.M., *Acute and chronic fluoride toxicity.* Journal of dental research, 1992. **71**(5): p. 1249-1254.

413. Pulgar, R., et al., *Determination of bisphenol A and related aromatic compounds released from bis-GMA-based composites and sealants by high performance liquid chromatography.* Environmental health perspectives, 2000. **108**(1): p. 21-27.

414. Joskow, R., et al., *Exposure to bisphenol A from bis-glycidyl dimethacrylate–based dental sealants.* The Journal of the American Dental Association, 2006. **137**(3): p. 353-362.

415. Maserejian, N.N., et al., *Changes in urinary bisphenol A concentrations associated with placement of dental composite restorations in children and adolescents.* The Journal of the American Dental Association, 2016. **147**(8): p. 620-630.

416. Kanjevac, T., et al., *Cytotoxic effects of glass ionomer cements on human dental pulp stem cells correlate with fluoride release.* Med Chem, 2012. **8**(1): p. 40-5.

417. Panpisut, P., et al., *Polymerization kinetics stability, volumetric changes, apatite precipitation, strontium release and fatigue of novel bone composites for vertebroplasty.* PLoS One, 2019. **14**(3): p. e0207965.

418. Schulz, S.D., et al., *Elution of Monomers from Provisional Composite Materials.* International Journal of Polymer Science, 2015. **2015**: p. 617407.

419. Wisniewska-Jarosinska, M., et al., *Independent and combined cytotoxicity and genotoxicity of triethylene glycol dimethacrylate and urethane dimethacrylate.* Molecular biology reports, 2011. **38**(7): p. 4603-4611.

420. Poplawski, T., et al., *Genotoxicity of urethane dimethacrylate, a tooth restoration component.* Toxicol In Vitro, 2010. **24**(3): p. 854-62.

421. Chang, C.Y., et al., *Toxic Effects of Urethane Dimethacrylate on Macrophages Through Caspase Activation, Mitochondrial Dysfunction, and Reactive Oxygen Species Generation.* Polymers (Basel), 2020. **12**(6).

422. Samuelsen, J.T., et al., *Apoptosis induced by the monomers HEMA and TEGDMA involves formation of ROS and differential activation of the MAP-kinases p38, JNK and ERK.* Dent Mater, 2007. **23**(1): p. 34-9.

423. Samuelsen, J.T., et al., *Role of thiol-complex formation in 2-hydroxyethyl- methacrylate-induced toxicity in vitro.* J Biomed Mater Res A, 2011. **96**(2): p. 395-401.

424. Ansteinsson, V., et al., *Cell toxicity of methacrylate monomers-the role of glutathione adduct formation.* J Biomed Mater Res A, 2013. **101**(12): p. 3504-10.

425. Massaro, H., et al., *Solvent and HEMA Increase Adhesive Toxicity and Cytokine Release from Dental Pulp Cells.* Materials (Basel, Switzerland), 2019. **12**(17): p. 2750.

426. Morisbak, E., V. Ansteinsson, and J.T. Samuelsen, *Cell toxicity of 2-hydroxyethyl methacrylate (HEMA): the role of oxidative stress.* European Journal of Oral Sciences, 2015. **123**(4): p. 282-287.

427. Ansteinsson, V., et al., *DNA-damage, cell-cycle arrest and apoptosis induced in BEAS-2B cells by 2-hydroxyethyl methacrylate (HEMA).* Mutat Res, 2011. **723**(2): p. 158-64.

428. Schweikl, H., G. Spagnuolo, and G. Schmalz, *Genetic and cellular toxicology of dental resin monomers.* J Dent Res, 2006. **85**(10): p. 870-7.

429. Singh, R., et al., *Oxidative Stress Evokes a Metabolic Adaptation That Favors Increased NADPH Synthesis and Decreased NADH Production in Pseudomonas fluorescens.* Journal of Bacteriology, 2007. **189**(18): p. 6665-6675.

430. Jo, S.H., et al., *Control of mitochondrial redox balance and cellular defense against oxidative damage by mitochondrial NADP+-dependent isocitrate dehydrogenase.* J Biol Chem, 2001. **276**(19): p. 16168-76.

431. Kensler, T.W., N. Wakabayashi, and S. Biswal, *Cell survival responses to environmental stresses via the Keap1-Nrf2-ARE pathway.* Annu Rev Pharmacol Toxicol, 2007. **47**: p. 89-116.

432. Ma, Q., *Transcriptional responses to oxidative stress: pathological and toxicological implications.* Pharmacol Ther, 2010. **125**(3): p. 376-93.

433. Penning, T.M., *Aldo-Keto Reductase Regulation by the Nrf2 System: Implications for Stress Response, Chemotherapy Drug Resistance, and Carcinogenesis.* Chemical research in toxicology, 2017. **30**(1): p. 162-176.

434. Li, W., et al., *Protective effect of lycopene on fluoride-induced ameloblasts apoptosis and dental fluorosis through oxidative stress-mediated Caspase pathways.* Chem Biol Interact, 2017. **261**: p. 27-34.

435. Panday, A., et al., *NADPH oxidases: an overview from structure to innate immunity-associated pathologies.* Cellular & molecular immunology, 2015. **12**(1): p. 5-23.

436. Kovac, S., et al., *Nrf2 regulates ROS production by mitochondria and NADPH oxidase.* Biochimica et Biophysica Acta (BBA) - General Subjects, 2015. **1850**(4): p. 794-801.

437. Walters, D.M., H.Y. Cho, and S.R. Kleeberger, *Oxidative stress and antioxidants in the pathogenesis of pulmonary fibrosis: a potential role for Nrf2.* Antioxid Redox Signal, 2008. **10**(2): p. 321-32.

438. Ma, Q., *Role of nrf2 in oxidative stress and toxicity.* Annual review of pharmacology and toxicology, 2013. **53**: p. 401-426.

439. Yoshida, R., et al., *Molecular Cloning of a Novel Human CC Chemokine EBI1-ligand Chemokine That Is a Specific Functional Ligand for EBI1, CCR7*.* Journal of Biological Chemistry, 1997. **272**(21): p. 13803-13809.

440. Candotto, V., et al., *Gabapentin affects the expression of inflammatory mediators on healthy gingival cells.* International journal of immunopathology and pharmacology, 2019. **33**: p. 2058738419827765-2058738419827765.

441. Tang, Y., et al., *Early diagnostic and prognostic significance of a specific Th1/Th2 cytokine pattern in children with haemophagocytic syndrome.* Br J Haematol, 2008. **143**(1): p. 84-91.

442. Kernan, K.F. and J.A. Carcillo, *Hyperferritinemia and inflammation.* International immunology, 2017. **29**(9): p. 401-409.

443. Tang, D., et al., *Ferroptosis: molecular mechanisms and health implications.* Cell Research, 2021. **31**(2): p. 107-125.

444. Lu, B., et al., *The Role of Ferroptosis in Cancer Development and Treatment Response.* Frontiers in pharmacology, 2018. **8**: p. 992-992.

445. Hao, S., et al., *Metabolic networks in ferroptosis.* Oncology letters, 2018. **15**(4): p. 5405-5411.

446. Lakhal-Littleton, S., et al., *Cardiac ferroportin regulates cellular iron homeostasis and is important for cardiac function.* Proceedings of the National Academy of Sciences of the United States of America, 2015. **112**(10): p. 3164-3169.

447. McKie, A.T., et al., *A Novel Duodenal Iron-Regulated Transporter, IREG1, Implicated in the Basolateral Transfer of Iron to the Circulation.* Molecular Cell, 2000. **5**(2): p. 299-309.

448. Zhu, B., et al., *Reduced expression of ferroportin1 and ceruloplasmin predicts poor prognosis in adrenocortical carcinoma.* J Trace Elem Med Biol, 2019. **56**: p. 52-59.

449. Choi, M., *Role of Mitochondrial SLC4A11 in Corneal Endothelium*. 2021, Indiana University.

450. Zou, H., et al., *[An overview on rubber dam application in dental treatments].* Zhonghua Kou Qiang Yi Xue Za Zhi, 2016. **51**(2): p. 119-23.

451. Bezgin, T., C. Cimen, and N. Ozalp, *Evaluation of Residual Monomers Eluted from Pediatric Dental Restorative Materials.* BioMed Research International, 2021. **2021**: p. 6316171.

452. Paula, A.B., et al., *Once Resin Composites and Dental Sealants Release Bisphenol-A, How Might This Affect Our Clinical Management?-A Systematic Review.* International journal of environmental research and public health, 2019. **16**(9): p. 1627.

453. Ayman, A.-D., *The residual monomer content and mechanical properties of CAD\CAM resins used in the fabrication of complete dentures as compared to heat cured resins.* Electronic physician, 2017. **9**(7): p. 4766-4772.

454. SÖDERHOLM, K.-J. and A. Mariotti, *BIS-GMA–based resins in dentistry: are they safe?* The Journal of the American Dental Association, 1999. **130**(2): p. 201-209.

455. Schweikl, H., et al., *Cytotoxic and mutagenic effects of dental composite materials.* Biomaterials, 2005. **26**(14): p. 1713-1719.

456. Ausiello, P., et al., *Cytotoxicity of dental resin composites: an in vitro evaluation.* Journal of Applied Toxicology, 2013. **33**(6): p. 451-457.

457. Kang, Y.-G., et al., *Release of bisphenol A from resin composite used to bond orthodontic lingual retainers.* American journal of orthodontics and dentofacial orthopedics, 2011. **140**(6): p. 779-789.

458. Van Landuyt, K., et al., *How much do resin-based dental materials release? A meta-analytical approach.* Dental Materials, 2011. **27**(8): p. 723-747.

459. Bernardo, M., et al., *Survival and reasons for failure of amalgam versus composite posterior restorations placed in a randomized clinical trial.* The Journal of the American Dental Association, 2007. **138**(6): p. 775-783.

460. Soncini, J.A., et al., *The longevity of amalgam versus compomer/composite restorations in posterior primary and permanent teeth: findings From the New England Children's Amalgam Trial.* The Journal of the American Dental Association, 2007. **138**(6): p. 763-772.

461. Sunnegårdh-Grönberg, K., et al., *Selection of dental materials and longevity of replaced restorations in Public Dental Health clinics in northern Sweden.* Journal of dentistry, 2009. **37**(9): p. 673-678.

462. Demarco, F.F., et al., *Longevity of posterior composite restorations: not only a matter of materials.* Dental materials, 2012. **28**(1): p. 87-101.

463. Alvanforoush, N., et al., *Comparison between published clinical success of direct resin composite restorations in vital posterior teeth in 1995–2005 and 2006–2016 periods.* Australian dental journal, 2017. **62**(2): p. 132-145.

464. Beyth, N., et al., *Antibacterial dental resin composites.* Reactive and Functional Polymers, 2014. **75**: p. 81-88.

465. Eichmiller, F. and W. Marjenhoff, *Fluoride-releasing dental restorative materials.* Operative Dentistry, 1998. **23**: p. 218-228.

466. Hyun, H.-K., S. Salehi, and J.L. Ferracane, *Biofilm formation affects surface properties of novel bioactive glass-containing composites.* Dental Materials, 2015. **31**(12): p. 1599-1608.

467. Alania, Y., et al., *Bioactive composites containing TEGDMA-functionalized calcium phosphate particles: degree of conversion, fracture strength and ion release evaluation.* Dental Materials, 2016. **32**(12): p. e374-e381.

468. Khvostenko, D., et al., *Mechanical performance of novel bioactive glass containing dental restorative composites.* Dental Materials, 2013. **29**(11): p. 1139-1148.

469. Organization, W.H., *Sugars and dental caries*. 2017, World Health Organization.

470. Schweikl, H., G. Spagnuolo, and G. Schmalz, *Genetic and cellular toxicology of dental resin monomers.* Journal of dental research, 2006. **85**(10): p. 870-877.

471. Tadin, A., et al., *Composite-induced toxicity in human gingival and pulp fibroblast cells.* Acta Odontologica Scandinavica, 2014. **72**(4): p. 304-311.

472. Caughman, W.F., et al., *Correlation of cytotoxicity, filler loading and curing time of dental composites.* Biomaterials, 1991. **12**(8): p. 737-740.

473. Kleinsasser, N.H., et al., *Cytotoxic and genotoxic effects of resin monomers in human salivary gland tissue and lymphocytes as assessed by the single cell microgel electrophoresis (Comet) assay.* Biomaterials, 2006. **27**(9): p. 1762-1770.

474. Schweikl, H., G. Schmalz, and T. Spruss, *The Induction of Micronuclei in vitro by Unpolymerized Resin Monomers.* Journal of Dental Research, 2001. **80**(7): p. 1615-1620.

475. Ginzkey, C., et al., *Assessment of HEMA and TEGDMA induced DNA damage by multiple genotoxicological endpoints in human lymphocytes.* Dental Materials, 2015. **31**(8): p. 865-876.

476. Chang, C.-Y., et al., *Toxic Effects of Urethane Dimethacrylate on Macrophages Through Caspase Activation, Mitochondrial Dysfunction, and Reactive Oxygen Species Generation.* Polymers, 2020. **12**(6): p. 1398.

477. Par, M., et al., *Raman spectroscopic assessment of degree of conversion of bulk-fill resin composites–changes at 24 hours post cure.* Operative dentistry, 2015. **40**(3): p. E92-E101.

478. Par, M., et al., *Conversion and temperature rise of remineralizing composites reinforced with inert fillers.* Journal of Dentistry, 2016. **48**: p. 26-33.

479. Rawls, H.R., *Evaluation of fluoride-releasing dental materials by means of in vitro and in vivo demineralization models: reaction paper.* Advances in Dental Research, 1995. **9**(3): p. 324-331.

Chapter 8: Appendices

A) Poster presented at the (IADR) International association of dental research health congress 15 September, Marseille 2022.

Characteristics and biological considerations of a newly developed bioactive NanoFA-based dental composite

W. Al-Omairi[1], A. Werner[1], A. Altaie[2], D. Wood[2], M. J. German[1]

P124

Introduction:

Dental composites are becoming the main direct tooth restorative materials. The currently available composites lack bioactive properties. The development of bioactive composites with bacteriostatic and remineralizing properties due to fluoride release will reduce restoration failure due secondary caries. Any new material has to be thoroughly tested for cytocompatibility.

Objectives:

- To develop fluoride releasing model dental composites incorporating nano-fluorapatite (nanoFA) as secondary fillers and to measure fluoride ion release.
- To investigate the toxicity of the monomers UDMA, HEMA as well as the effect of the new composite material on gene expression in gingival fibroblasts by RNA-Seq analysis.

Methods:

- Composites containing UDMA: HEMA (4:1) as resin were made either with 62.1 vol % silica fillers (control) or with 42.1 vol % silica fillers and 20 vol% nanoFA. G-ænial Anterior (GC Europe) was used as comparator.
- An ion-selective electrode was used to measure fluoride release over a period of three months.
- Monomer toxicity was tested by XTT viability assay and gene expression analysis using RT-qPCR.
- RNA-Seq with gingival fibroblasts exposed for 24 hours to the dental composites was performed followed by standard differential expression analysis.

Results:

- NanoFA composite showed significant fluoride release, figure 1.
- A significant reduction in cell viability occurred at 2 mM of HEMA and 1 mM of UDMA. RT-qPCR showed a dose-dependent expression increase of DNA repair genes (*DDX11*, *IPPK*, *XRCC2* and *RAD50*) in gingival fibroblasts treated with HEMA. Significant upregulation of stress response genes (*COX-2*, *CES2* and *HO-1*) was found after 3 mM and 4 mM treatment of UDMA, figure 2.
- RNA-Seq analysis identified an early stress response and disturbed cellular redox balance manifested by an increased expression of cellular signalling pathways such as oxidoreductase activity, NADPH activity, ferroptosis in response to composite materials, figure 3.

Figure 1: Cumulative Fluoride release from NanoFA and Gænial composites measured by ISE.

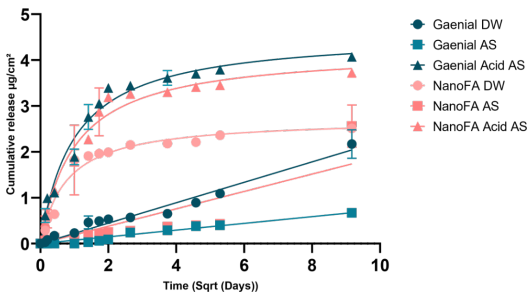

Figure 2: Effect of the resin monomers (HEMA & UDMA) on cell viability and genes expression in Human gingival fibroblasts. (P value <0.05 = *, P value < 0.01= ** . P value < 0.001= ***).

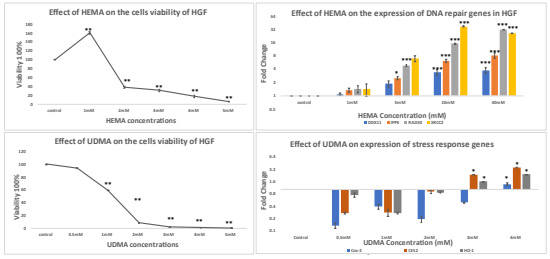

Figure 3: Volcano plots demonstrating the RNA Seq results of HGF cells treated with dental composites.

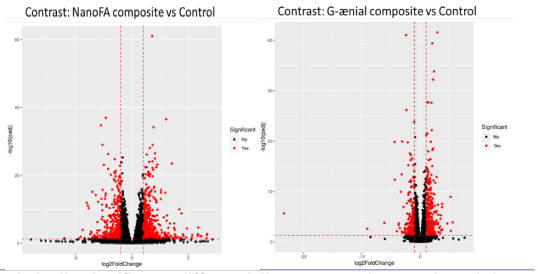

Statistically significant, differentially expressed genes in red dots vs non-significant genes in black dots for each treatment condition. A) HGF treated with NanoFA-containing composite. B) HGF treated with G-ænial composite.

Figure 4: Bar charts demonstrating the enriched pathways in HGF treated with NanoFA and Gænial composites.

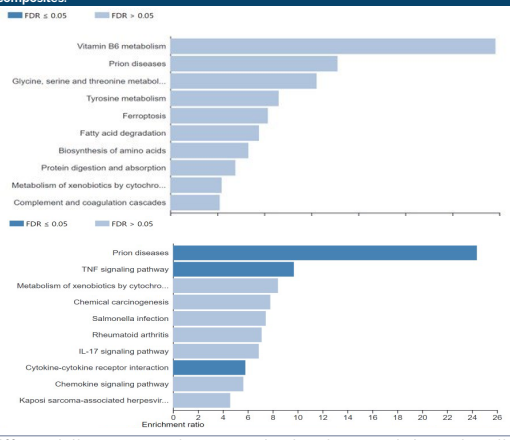

Differentially expressed genes submitted to a web-based toolkit to perform functional annotation enrichment analysis. The graphs above show the biological functions of the set of differentially expressed genes in HGF treated with NanoFA and Gænial composites. Enriched categories identified with FDR (False discovery rate) correction

Conclusions:

- The amount of fluoride released was comparable to G-ænial dental composites.
- Dental composite material induced signs of chemical toxicity such as impaired redox balance in oral tissues.

Newcastle University
1: FMS Biosciences Institute & School of Dental Science Newcastle Upon Tyne NE2 4HH, United Kingdom.
2: School of Dentistry, University of Leeds Leeds LS2 9LU, United Kingdom

Funded by:
Iraqi Ministry of Higher education & scientific research

Widad AL-Omairi
W.Al-Omairi2@ncl.ac.uk

B)

Table 1: Median values of fluoride release(=Interquartile ranges) from experimental and commercial dental composites in distilled water.

Median Fluoride release in distilled water (µg/cm²/day)												
Groups	**30 min**	**60 min**	**4 hours**	**24 hours**	**48 hours**	**72 hours**	**96 hours**	**1 week**	**2weeks**	**3 weeks**	**weeks 4**	**12 weeks**
Control	(0)^{a}	(0)^{a}	(0)^{a}	(0)^{a}	(0)^{a}	(0)^{a}	(0)^{a}	(0)^{a}	(0)^{a}	(0)^{a}	(0)^{a}	(0)^{a}
G-ænial	(0.034)^{ab}	(0.051)^{ab}	(0.048)^{ab}	(0.058)^{ab}	(0.175)^{b}	(0.029)^{ab}	(0.039)^{b}	(0.028)^{ab}	(0.074)^{b}	(0.251)^{b}	(0.152)^{b}	(1.148)^{b}
NanoFA	(0.278)^{b}	(0.155)^{b}	(0.082)^{b}	(0.940)^{b}	(0.070)^{ab}	(0.045)^{b}	(0.037)^{ab}	(0.137)^{b}	(0.027)^{ab}	(0.035)^{ab}	(0.127)^{ab}	(0.145)^{ab}

Table 2: Median values of fluoride release (=Interquartile ranges) from experimental and commercial dental composites in artificial saliva.

Median Fluoride release in artificial Saliva (µg/cm²/day)												
Groups	**30 min**	**60 min**	**4 hours**	**24 hours**	**48 hours**	**72 hours**	**96 hours**	**1 week**	**2weeks**	**3 weeks**	**weeks 4**	**12 weeks**
Control	(0)^{a}	(0)^{a}	(0)^{a}	(0)^{a}	(0)^{a}	(0)^{a}	(0)^{a}	(0)^{a}	(0)^{a}	(0)^{a}	(0)^{a}	(0)^{a}
G-ænial	(0)^{a}	(0)^{a}	(0)^{a}	(0)^{a}	(0.036)^{b}	(0.024)^{ab}	(0.036)^{b}	(0.134)^{b}	(0.050)^{ab}	(0.083)^{b}	(0.021)^{ab}	(0.273)^{ab}
NanoFA	(0.041)^{b}	(0.024)^{b}	(0.04)^{b}	(0.035)^{b}	(0.026)^{ab}	(0.034)^{b}	(0.024)^{ab}	(0.029)^{ab}	(0.096)^{b}	(0.037)^{ab}	(0.029)^{b}	(1.628)^{b}

Table 3: Median values of fluoride release(=Interquartile ranges) from experimental and commercial dental composites in acidified artificial saliva.

Median Fluoride release in Acidified Artificial Saliva (µg/cm²/day)												
Groups	**30 min**	**60 min**	**4 hours**	**24 hours**	**48 hours**	**72 hours**	**96 hours**	**1 week**	**2weeks**	**3 weeks**	**weeks 4**	**12 weeks**
Control	(0)^{a}	(0)^{a}	(0)^{a}	(0)^{a}	(0)^{a}	(0)^{a}	(0)^{a}	(0)^{a}	(0)^{a}	(0)^{a}	(0)^{a}	(0)^{a}
G-ænial	(0.694)^{b}	(0.392)^{b}	(0.109)^{ab}	(0.763)^{b}	(0.962)^{b}	(0.288)^{ab}	(0.337)^{b}	(0.050)^{ab}	(0.087)^{b}	(0.061)^{ab}	(0.075)^{b}	(0.277)^{b}
NanoFA	(0.432)^{ab}	(0.174)^{ab}	(0.533)^{b}	(0.668)^{cb}	(0.406)^{ab}	(0.370)^{b}	(0.308)^{cb}	(0.065)^{b}	(0.038)^{ab}	(0.095)^{b}	(0.030)^{ab}	(0.270)^{cb}

Table 4: Median sorption values (=Interquartile ranges) of experimental and commercial dental composites in distilled water.

Median Sorption in Distilled Water (μg)												
Groups	**30 min**	**60 min**	**4 hours**	**24 hours**	**48 hours**	**72 hours**	**96 hours**	**1 week**	**2weeks**	**3 weeks**	**weeks 4**	**12 weeks**
Control	(0)^{ab}	(0)^{ab}	(0.005)^{ab}	(0.017)^{a}	(0.017)^{a}	(0.043)^{a}	(0.040)^{ab}	(0.036)^{a}	(0.031)^{a}	(0.023)^{a}	(0.047)^{a}	(0.058)^{a}
G-ænial	(0.052)^{a}	(0.082)^{a}	(0.027)^{a}	(0.045)^{a}	(0.081)^{a}	(0)^{b}	(0.012)^{a}	(0.059)^{a}	(0.070)^{a}	(0.069)^{a}	(0.102)^{a}	(0.023)^{a}
NanoFA	(0)^{b}	(0)^{b}	(0)^{b}	(0.035)^{a}	(0.021)^{a}	(0.010)^{ab}	(0.056)^{b}	(0.117)^{b}	(0.065)^{a}	(0.086)^{a}	(0.100)^{a}	(0.048)^{a}

Table 5: Median sorption values (=Interquartile ranges) of experimental and commercial dental composites in artificial saliva.

Median Sorption in Artificial Saliva (μg)												
Groups	**30 min**	**60 min**	**4 hours**	**24 hours**	**48 hours**	**72 hours**	**96 hours**	**1 week**	**2weeks**	**3 weeks**	**weeks 4**	**12 weeks**
Control	(0.003)^{a}	(0.004)^{a}	(0.025)^{a}	(0.02)^{ab}	(0.021)^{a}	(0.017)^{a}	(0.023)^{ab}	(0.020)^{ab}	(0.017)^{a}	(0.017)^{a}	(0.021)^{ab}	(0.010)^{a}
G-ænial	(0.002)^{a}	(0.004)^{a}	(0)^{a}	(0)^{a}	(0.008)^{a}	(0.008)^{a}	(0.008)^{a}	(0.177)^{a}	(0.019)^{ab}	(0.018)^{ab}	(0.019)^{a}	(0.019)^{a}
NanoFA	(0.073)^{b}	(0.100)^{a}	(0.087)^{a}	(0.15)^{b}	(0.125)^{a}	(0.124)^{a}	(0.139)^{b}	(0.087)^{b}	(0.127)^{b}	(0.206)^{b}	(0.292)^{b}	(0.053)^{a}

Table 6: Median sorption values (=Interquartile ranges) of experimental and commercial dental composites in acidified artificial saliva.

Median Sorption in Acidified Artificial Saliva (μg)												
Groups	**30 min**	**60 min**	**4 hours**	**24 hours**	**48 hours**	**72 hours**	**96 hours**	**1 week**	**2weeks**	**3 weeks**	**weeks 4**	**12 weeks**
Control	(0.02)^{a}	(0.02)^{a}	(0.02)^{a}	(0.03)^{ab}	(0.03)^{ab}	(0.02)^{a}	(0.03)^{ab}	(0.03)^{a}	(0.03)^{a}	(0.02)^{a}	(0.02)^{a}	(0.02)^{a}
G-ænial	(0.02)^{a}	(0.02)^{a}	(0.03)^{a}	(0.02)^{a}	(0.02)^{a}	(0.05)^{a}	(0.02)^{a}	(0.02)^{a}	(0.02)^{a}	(0.02)^{a}	(0.02)^{a}	(0.02)^{a}
NanoFA	(0.02)^{a}	(0.01)^{a}	(0.01)^{a}	(0.06)^{b}	(0.04)^{b}	(0.04)^{a}	(0.04)^{b}	(0.06)^{a}	(0.05)^{a}	(0.05)^{a}	(0.06)^{a}	(0.05)^{a}

Table *7*: Median weight changes values (=Interquartile ranges) of experimental and commercial dental composites in distilled water.

Median Weight Changes in distilled water (µg)												
Groups	**30 min**	**60 min**	**4 hours**	**24 hours**	**48 hours**	**72 hours**	**96 hours**	**1 week**	**2weeks**	**3 weeks**	**weeks 4**	**12 weeks**
Control	0	0.10	0.70	1.90	1.90	5.20	4.50	4.00	3.50	2.60	5.70	6.60
G-ænial	7.40	11.60	4.00	6.50	10.90	0	1.60	7.90	9.40	9.50	17.00	3.30
NanoFA	0	0	0	4.20	2.50	13.00	6.70	13.50	7.00	8.30	11.00	6.00

Table *8*: Median weight changes values (=Interquartile ranges) of experimental and commercial dental composites in artificial saliva.

Median Weight Changes in Artificial Saliva (µg)												
Groups	**30 min**	**60 min**	**4 hours**	**24 hours**	**48 hours**	**72 hours**	**96 hours**	**1 week**	**2weeks**	**3 weeks**	**weeks 4**	**12 weeks**
Control	0.50	O.50	2.90	2.80	2.50	2.00	2.70	2.40	2.00	2.00	2.50	1.20
G-ænial	0.40	0.60	0	0.10	1.30	1.40	1.40	2.60	2.80	2.70	3.10	2.90
NanoFA	10.40	13.90	12.20	19.00	15.90	17.40	17.60	12.10	20.30	32.20	37.00	6.80

Table9: Median weight changes values (=Interquartile ranges) of experimental and commercial dental composites in acidified artificial saliva.

Median Weight Changes in Acidified Artificial Saliva (µg)												
Groups	**30 min**	**60 min**	**4 hours**	**24 hours**	**48 hours**	**72 hours**	**96 hours**	**1 week**	**2weeks**	**3 weeks**	**weeks 4**	**12 weeks**
Control	2.40	3.20	2.00	3.90	3.60	2.70	3.40	3.60	3.60	3.10	2.53	1.80
G-ænial	2.30	2.30	4.70	2.80	2.50	7.20	3.00	2.70	3.50	3.50	3.80	2.80
NanoFA	4.55	1.25	1.25	10.05	6.90	5.15	6.40	8.30	7.25	8.30	8.45	6.70

C)

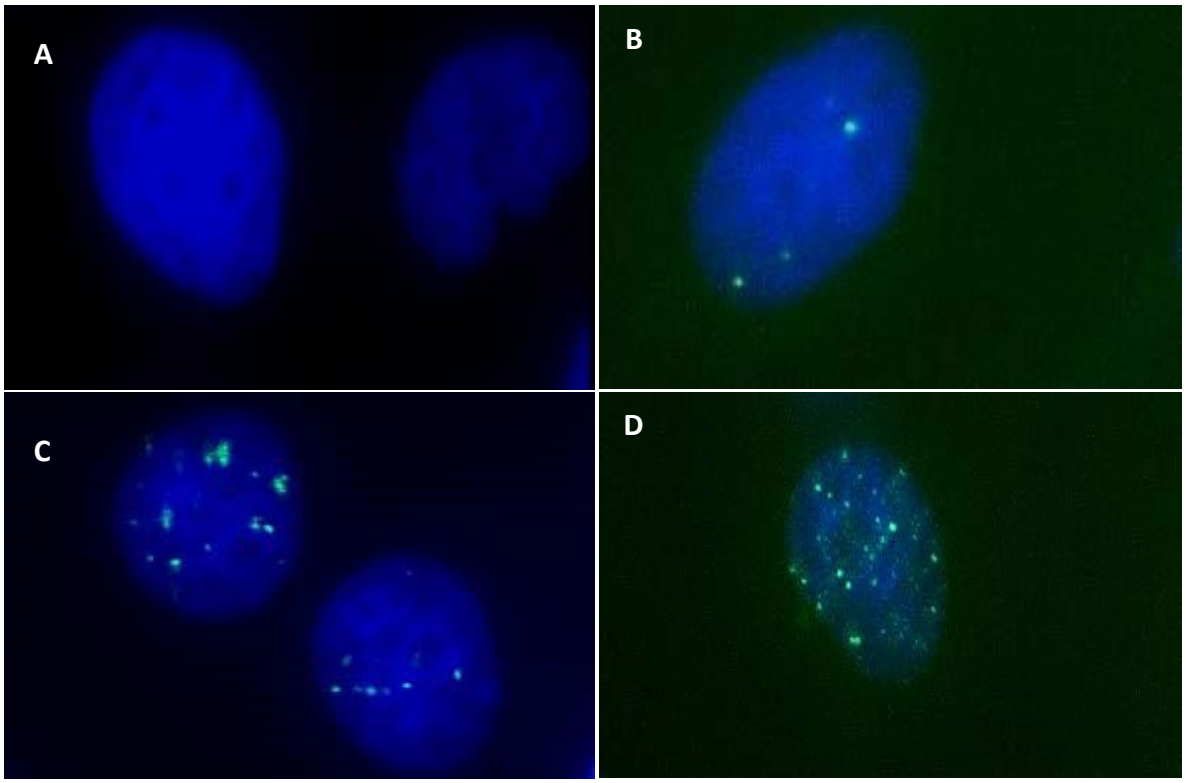

Figure1: Immunofluorescence staining of H2AX phosphorylation in MCF7 cells treated with dental resin monomers HEMA and UDMA. A) Nuclei of untreated MCF7 cells. B) Nucleus treated with 10mM UDMA. C) Nucleus treated with 40mM HEMA. D) Nucleus

D) Figures showing the primers efficiency for qPCR.

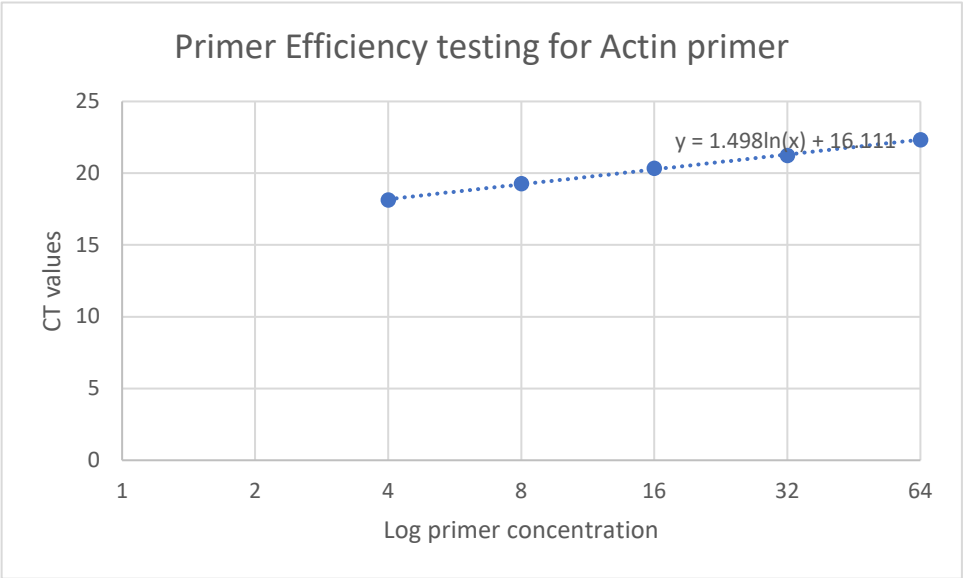

Figure1: Primer efficiency testing for RT-qPCR (Actin primer for the reference gene) to determine the efficiency of the primer in amplifying a target RNA. Serial dilutions of cDNA amplified by RT-qPCR to validate the Actin primer efficiency. The X-axis represent the log concentrations of the primers and Y-axis represent the threshold cycle or CT values.

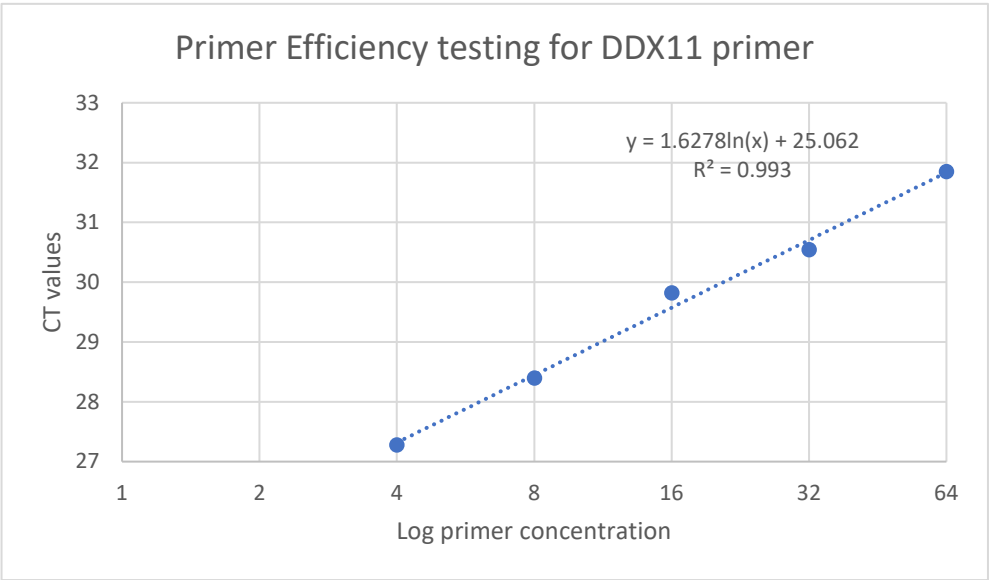

Figure 2: Primer efficiency testing for RT-qPCR (DDX11 primer for the DDX11gene) to determine the efficiency of the primer in amplifying a target RNA. Serial dilutions of cDNA amplified by RT-qPCR to validate the DDX11 primer efficiency. The X-axis represent the log concentrations of the primers and Y-axis represent the threshold cycle or CT values.

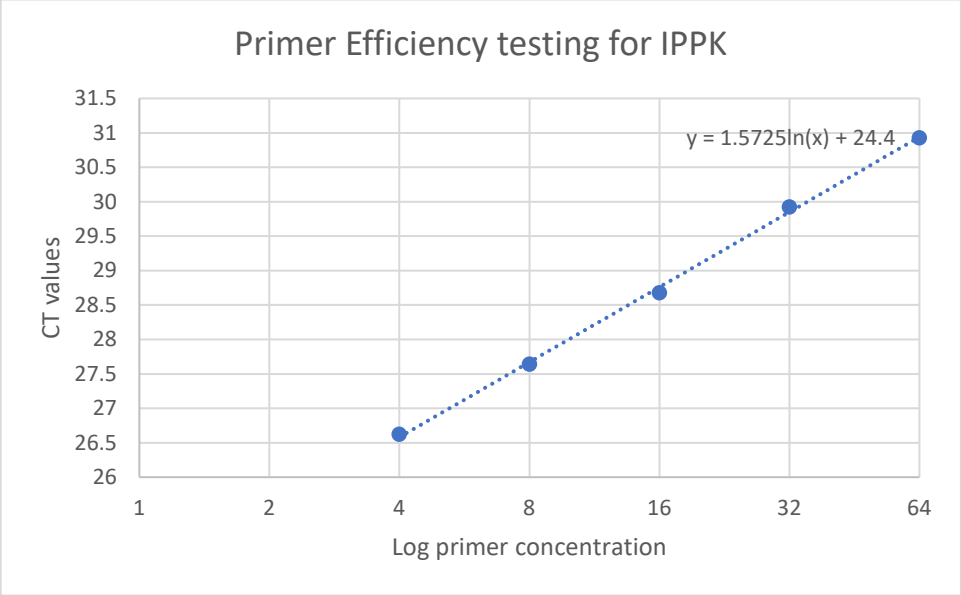

Figure 3: Primer efficiency testing for RT-qPCR (IPPK primer for the IPPK gene) to determine the efficiency of the primer in amplifying a target RNA. Serial dilutions of cDNA amplified by RT-qPCR to validate the IPPK primer efficiency. The X-axis represent the log concentrations of the primers and Y-axis represent the threshold cycle or CT values.

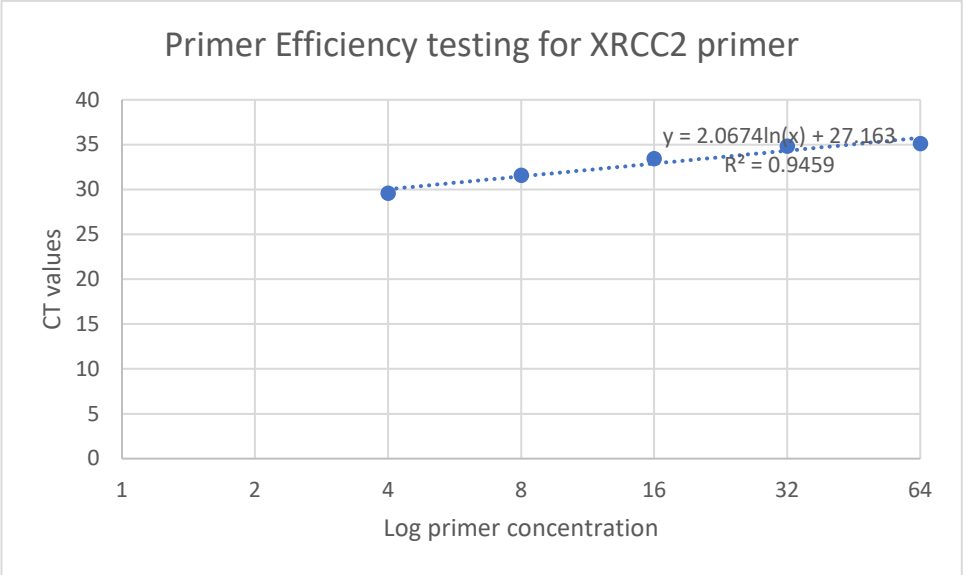

Figure 5: Primer efficiency testing for RT-qPCR (XRCC2 primer for the XRCC2 gene) to determine the efficiency of the primer in amplifying a target RNA. Serial dilutions of cDNA amplified by RT-qPCR to validate the XRCc2 primer efficiency. The X-axis represent the log concentrations of the primers and Y-axis represent the threshold cycle or CT values.

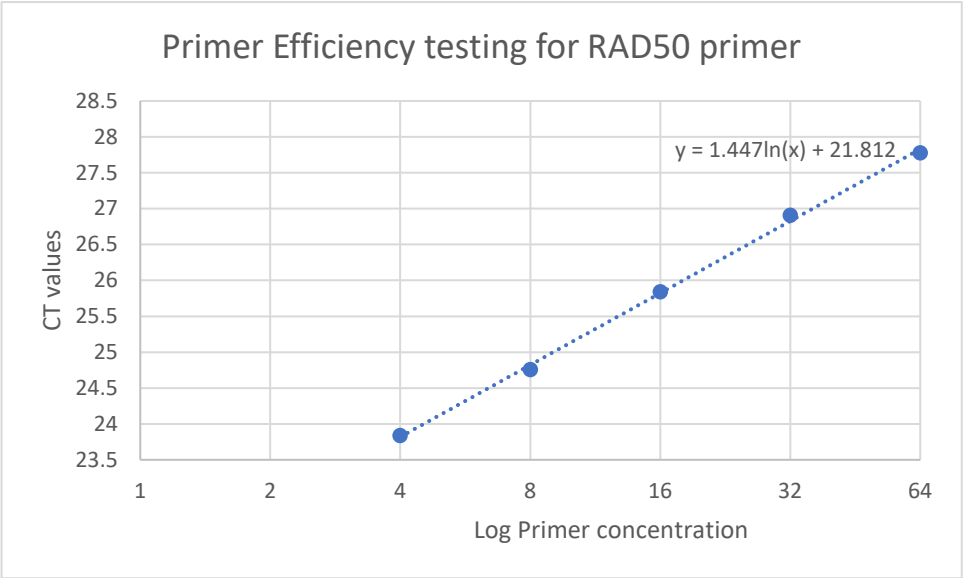

Figure5: Primer efficiency testing for RT-qPCR (RAD50 primer for the RAD50 gene) to determine the efficiency of the primer in amplifying a target RNA. Serial dilutions of cDNA amplified by RT-qPCR to validate the RAD50 primer efficiency. The X-axis represent the log

E) ANOVA (Post Hoc) Results for 100% UDMA group 1, Top surface of the specimens:

ANOVA					
DC					
	Sum of Squares	df	Mean Square	F	Sig.
Between Groups	687.717	4	171.929	3.615	0.028
Within Groups	760.950	16	47.559		
Total	1448.667	20			

Multiple Comparisons						
Dependent Variable:						
Tukey HSD						
(I) CT		Mean Difference (I-J)	Std. Error	Sig.	95% Confidence Interval	
					Lower Bound	Upper Bound
5 sec	10 sec	1.50000	4.87644	0.998	-13.4398	16.4398
	20 sec	-4.40000	4.62620	0.873	-18.5732	9.7732
	40sec	6.25000	4.87644	0.706	-8.6898	21.1898
	60 sec	-11.00000	4.87644	0.210	-25.9398	3.9398
10 sec	5 sec	-1.50000	4.87644	0.998	-16.4398	13.4398
	20 sec	-5.90000	4.62620	0.709	-20.0732	8.2732
	40sec	4.75000	4.87644	0.863	-10.1898	19.6898
	60 sec	-12.50000	4.87644	0.125	-27.4398	2.4398
20 sec	5 sec	4.40000	4.62620	0.873	-9.7732	18.5732
	10 sec	5.90000	4.62620	0.709	-8.2732	20.0732
	40sec	10.65000	4.62620	0.195	-3.5232	24.8232
	60 sec	-6.60000	4.62620	0.620	-20.7732	7.5732
40sec	5 sec	-6.25000	4.87644	0.706	-21.1898	8.6898
	10 sec	-4.75000	4.87644	0.863	-19.6898	10.1898
	20 sec	-10.65000	4.62620	0.195	-24.8232	3.5232
	60 sec	-17.25000*	4.87644	0.020	-32.1898	-2.3102
60 sec	5 sec	11.00000	4.87644	0.210	-3.9398	25.9398
	10 sec	12.50000	4.87644	0.125	-2.4398	27.4398
	20 sec	6.60000	4.62620	0.620	-7.5732	20.7732
	40sec	17.25000*	4.87644	0.020	2.3102	32.1898
*. The mean difference is significant at the 0.05 level.						

Bottom:

ANOVA					
DC					
	Sum of Squares	df	Mean Square	F	Sig.
Between Groups	784.252	4	196.063	2.914	0.055
Within Groups	1076.700	16	67.294		
Total	1860.952	20			

Post Hoc Tests						
Multiple Comparisons						
Dependent Variable:						
Tukey HSD						
(I) CT		Mean Difference (I-J)	Std. Error	Sig.	95% Confidence Interval	
					Lower Bound	Upper Bound
5 sec	10 sec	12.25000	5.80059	0.262	-5.5211	30.0211
	20 sec	1.60000	5.50293	0.998	-15.2592	18.4592
	40sec	7.25000	5.80059	0.724	-10.5211	25.0211
	60 sec	-6.00000	5.80059	0.836	-23.7711	11.7711
10 sec	5 sec	-12.25000	5.80059	0.262	-30.0211	5.5211
	20 sec	-10.65000	5.50293	0.339	-27.5092	6.2092
	40sec	-5.00000	5.80059	0.907	-22.7711	12.7711
	60 sec	-18.25000*	5.80059	0.043	-36.0211	-0.4789
20 sec	5 sec	-1.60000	5.50293	0.998	-18.4592	15.2592
	10 sec	10.65000	5.50293	0.339	-6.2092	27.5092
	40sec	5.65000	5.50293	0.839	-11.2092	22.5092
	60 sec	-7.60000	5.50293	0.648	-24.4592	9.2592
40sec	5 sec	-7.25000	5.80059	0.724	-25.0211	10.5211
	10 sec	5.00000	5.80059	0.907	-12.7711	22.7711
	20 sec	-5.65000	5.50293	0.839	-22.5092	11.2092
	60 sec	-13.25000	5.80059	0.200	-31.0211	4.5211
60 sec	5 sec	6.00000	5.80059	0.836	-11.7711	23.7711
	10 sec	18.25000*	5.80059	0.043	0.4789	36.0211
	20 sec	7.60000	5.50293	0.648	-9.2592	24.4592
	40sec	13.25000	5.80059	0.200	-4.5211	31.0211
*. The mean difference is significant at the 0.05 level.						

Combined:

ANOVA					
DC					
	Sum of Squares	df	Mean Square	F	Sig.
Between Groups	1322.868	4	330.717	6.098	0.001
Within Groups	2006.775	37	54.237		
Total	3329.643	41			

Post Hoc Tests						
Multiple Comparisons						
Dependent Variable:						
Tukey HSD						
(I) CT		Mean Difference (I-J)	Std. Error	Sig.	95% Confidence Interval	
					Lower Bound	Upper Bound
5 sec	10 sec	6.87500	3.68229	0.352	-3.6815	17.4315
	20 sec	-1.40000	3.49333	0.994	-11.4148	8.6148
	40sec	6.75000	3.68229	0.371	-3.8065	17.3065
	60 sec	-8.50000	3.68229	0.165	-19.0565	2.0565
10 sec	5 sec	-6.87500	3.68229	0.352	-17.4315	3.6815
	20 sec	-8.27500	3.49333	0.147	-18.2898	1.7398
	40sec	-0.12500	3.68229	1.000	-10.6815	10.4315
	60 sec	-15.37500*	3.68229	0.002	-25.9315	-4.8185
20 sec	5 sec	1.40000	3.49333	0.994	-8.6148	11.4148
	10 sec	8.27500	3.49333	0.147	-1.7398	18.2898
	40sec	8.15000	3.49333	0.157	-1.8648	18.1648
	60 sec	-7.10000	3.49333	0.271	-17.1148	2.9148
40sec	5 sec	-6.75000	3.68229	0.371	-17.3065	3.8065
	10 sec	0.12500	3.68229	1.000	-10.4315	10.6815
	20 sec	-8.15000	3.49333	0.157	-18.1648	1.8648
	60 sec	-15.25000*	3.68229	0.002	-25.8065	-4.6935
60 sec	5 sec	8.50000	3.68229	0.165	-2.0565	19.0565
	10 sec	15.37500*	3.68229	0.002	4.8185	25.9315
	20 sec	7.10000	3.49333	0.271	-2.9148	17.1148
	40sec	15.25000*	3.68229	0.002	4.6935	25.8065
*. The mean difference is significant at the 0.05 level.						

90% UDMA: 10% HEMA Top:

ANOVA					
DC					
	Sum of Squares	df	Mean Square	F	Sig.
Between Groups	545.260	4	136.315	2.898	0.056
Within Groups	752.550	16	47.034		
Total	1297.810	20			

Post Hoc Tests						
Multiple Comparisons						
Dependent Variable:						
Tukey HSD						
(I) CT		Mean Difference (I-J)	Std. Error	Sig.	95% Confidence Interval	
					Lower Bound	Upper Bound
5 sec	10 sec	0.50000	4.84945	1.000	-14.3571	15.3571
	20 sec	10.30000	4.60059	0.215	-3.7947	24.3947
	40sec	12.75000	4.84945	0.112	-2.1071	27.6071
	60 sec	7.50000	4.84945	0.549	-7.3571	22.3571
10 sec	5 sec	-0.50000	4.84945	1.000	-15.3571	14.3571
	20 sec	9.80000	4.60059	0.255	-4.2947	23.8947
	40sec	12.25000	4.84945	0.134	-2.6071	27.1071
	60 sec	7.00000	4.84945	0.610	-7.8571	21.8571
20 sec	5 sec	-10.30000	4.60059	0.215	-24.3947	3.7947
	10 sec	-9.80000	4.60059	0.255	-23.8947	4.2947
	40sec	2.45000	4.60059	0.983	-11.6447	16.5447
	60 sec	-2.80000	4.60059	0.972	-16.8947	11.2947
40sec	5 sec	-12.75000	4.84945	0.112	-27.6071	2.1071
	10 sec	-12.25000	4.84945	0.134	-27.1071	2.6071
	20 sec	-2.45000	4.60059	0.983	-16.5447	11.6447
	60 sec	-5.25000	4.84945	0.813	-20.1071	9.6071
60 sec	5 sec	-7.50000	4.84945	0.549	-22.3571	7.3571
	10 sec	-7.00000	4.84945	0.610	-21.8571	7.8571
	20 sec	2.80000	4.60059	0.972	-11.2947	16.8947
	40sec	5.25000	4.84945	0.813	-9.6071	20.1071

Bottom:

ANOVA					
DC					
	Sum of Squares	df	Mean Square	F	Sig.
Between Groups	924.010	4	231.002	5.092	0.008
Within Groups	725.800	16	45.363		
Total	1649.810	20			

Post Hoc Tests						
Multiple Comparisons						
Dependent Variable:						
Tukey HSD						
(I) CT		Mean Difference (I-J)	Std. Error	Sig.	95% Confidence Interval	
					Lower Bound	Upper Bound
5 sec	10 sec	2.50000	4.76248	0.983	-12.0907	17.0907
	20 sec	11.05000	4.51809	0.153	-2.7919	24.8919
	40sec	12.50000	4.76248	0.112	-2.0907	27.0907
	60 sec	18.50000*	4.76248	0.010	3.9093	33.0907
10 sec	5 sec	-2.50000	4.76248	0.983	-17.0907	12.0907
	20 sec	8.55000	4.51809	0.360	-5.2919	22.3919
	40sec	10.00000	4.76248	0.267	-4.5907	24.5907
	60 sec	16.00000*	4.76248	0.028	1.4093	30.5907
20 sec	5 sec	-11.05000	4.51809	0.153	-24.8919	2.7919
	10 sec	-8.55000	4.51809	0.360	-22.3919	5.2919
	40sec	1.45000	4.51809	0.997	-12.3919	15.2919
	60 sec	7.45000	4.51809	0.490	-6.3919	21.2919
40sec	5 sec	-12.50000	4.76248	0.112	-27.0907	2.0907
	10 sec	-10.00000	4.76248	0.267	-24.5907	4.5907
	20 sec	-1.45000	4.51809	0.997	-15.2919	12.3919
	60 sec	6.00000	4.76248	0.718	-8.5907	20.5907
60 sec	5 sec	-18.50000*	4.76248	0.010	-33.0907	-3.9093
	10 sec	-16.00000*	4.76248	0.028	-30.5907	-1.4093
	20 sec	-7.45000	4.51809	0.490	-21.2919	6.3919
	40sec	-6.00000	4.76248	0.718	-20.5907	8.5907
*. The mean difference is significant at the 0.05 level.						

Combined:

ANOVA					
DC					
	Sum of Squares	df	Mean Square	F	Sig.
Between Groups	1289.108	4	322.277	6.836	0.000
Within Groups	1744.225	37	47.141		
Total	3033.333	41			

Post Hoc Tests						
Multiple Comparisons						
Dependent Variable:						
Tukey HSD						
(I) CT		Mean Difference (I-J)	Std. Error	Sig.	95% Confidence Interval	
					Lower Bound	Upper Bound
5 sec	10 sec	1.50000	3.43297	0.992	-8.3418	11.3418
	20 sec	10.67500*	3.25680	0.018	1.3383	20.0117
	40sec	12.62500*	3.43297	0.006	2.7832	22.4668
	60 sec	13.00000*	3.43297	0.005	3.1582	22.8418
10 sec	5 sec	-1.50000	3.43297	0.992	-11.3418	8.3418
	20 sec	9.17500	3.25680	0.056	-0.1617	18.5117
	40sec	11.12500*	3.43297	0.020	1.2832	20.9668
	60 sec	11.50000*	3.43297	0.015	1.6582	21.3418
20 sec	5 sec	-10.67500*	3.25680	0.018	-20.0117	-1.3383
	10 sec	-9.17500	3.25680	0.056	-18.5117	0.1617
	40sec	1.95000	3.25680	0.974	-7.3867	11.2867
	60 sec	2.32500	3.25680	0.952	-7.0117	11.6617
40sec	5 sec	-12.62500*	3.43297	0.006	-22.4668	-2.7832
	10 sec	-11.12500*	3.43297	0.020	-20.9668	-1.2832
	20 sec	-1.95000	3.25680	0.974	-11.2867	7.3867
	60 sec	0.37500	3.43297	1.000	-9.4668	10.2168
60 sec	5 sec	-13.00000*	3.43297	0.005	-22.8418	-3.1582
	10 sec	-11.50000*	3.43297	0.015	-21.3418	-1.6582
	20 sec	-2.32500	3.25680	0.952	-11.6617	7.0117
	40sec	-0.37500	3.43297	1.000	-10.2168	9.4668
*. The mean difference is significant at the 0.05 level.						

80% UDMA: 20% HEMA (Top):

ANOVA					
DC					
	Sum of Squares	df	Mean Square	F	Sig.
Between Groups	222.750	4	55.688	1.907	0.158
Within Groups	467.250	16	29.203		
Total	690.000	20			

Multiple Comparisons						
Dependent Variable:						
Tukey HSD						
(I) CT		Mean Difference (I-J)	Std. Error	Sig.	95% Confidence Interval	
					Lower Bound	Upper Bound
5 sec	10 sec	4.50000	3.82120	0.764	-7.2069	16.2069
	20 sec	8.25000	3.62511	0.203	-2.8561	19.3561
	40sec	3.75000	3.82120	0.860	-7.9569	15.4569
	60 sec	9.00000	3.82120	0.178	-2.7069	20.7069
10 sec	5 sec	-4.50000	3.82120	0.764	-16.2069	7.2069
	20 sec	3.75000	3.62511	0.836	-7.3561	14.8561
	40sec	-0.75000	3.82120	1.000	-12.4569	10.9569
	60 sec	4.50000	3.82120	0.764	-7.2069	16.2069
20 sec	5 sec	-8.25000	3.62511	0.203	-19.3561	2.8561
	10 sec	-3.75000	3.62511	0.836	-14.8561	7.3561
	40sec	-4.50000	3.62511	0.728	-15.6061	6.6061
	60 sec	0.75000	3.62511	1.000	-10.3561	11.8561
40sec	5 sec	-3.75000	3.82120	0.860	-15.4569	7.9569
	10 sec	0.75000	3.82120	1.000	-10.9569	12.4569
	20 sec	4.50000	3.62511	0.728	-6.6061	15.6061
	60 sec	5.25000	3.82120	0.652	-6.4569	16.9569
60 sec	5 sec	-9.00000	3.82120	0.178	-20.7069	2.7069
	10 sec	-4.50000	3.82120	0.764	-16.2069	7.2069
	20 sec	-0.75000	3.62511	1.000	-11.8561	10.3561
	40sec	-5.25000	3.82120	0.652	-16.9569	6.4569

Bottom:

ANOVA					
DC					
	Sum of Squares	df	Mean Square	F	Sig.
Between Groups	860.860	4	215.215	3.264	0.039
Within Groups	1054.950	16	65.934		
Total	1915.810	20			

Post Hoc Tests						
Multiple Comparisons						
Dependent Variable:						
Tukey HSD						
(I) CT		Mean Difference (I-J)	Std. Error	Sig.	95% Confidence Interval	
					Lower Bound	Upper Bound
5 sec	10 sec	4.00000	5.74171	0.954	-13.5907	21.5907
	20 sec	10.90000	5.44706	0.309	-5.7880	27.5880
	40sec	-0.75000	5.74171	1.000	-18.3407	16.8407
	60 sec	16.00000	5.74171	0.084	-1.5907	33.5907
10 sec	5 sec	-4.00000	5.74171	0.954	-21.5907	13.5907
	20 sec	6.90000	5.44706	0.714	-9.7880	23.5880
	40sec	-4.75000	5.74171	0.918	-22.3407	12.8407
	60 sec	12.00000	5.74171	0.271	-5.5907	29.5907
20 sec	5 sec	-10.90000	5.44706	0.309	-27.5880	5.7880
	10 sec	-6.90000	5.44706	0.714	-23.5880	9.7880
	40sec	-11.65000	5.44706	0.252	-28.3380	5.0380
	60 sec	5.10000	5.44706	0.879	-11.5880	21.7880
40sec	5 sec	0.75000	5.74171	1.000	-16.8407	18.3407
	10 sec	4.75000	5.74171	0.918	-12.8407	22.3407
	20 sec	11.65000	5.44706	0.252	-5.0380	28.3380
	60 sec	16.75000	5.74171	0.066	-0.8407	34.3407
60 sec	5 sec	-16.00000	5.74171	0.084	-33.5907	1.5907
	10 sec	-12.00000	5.74171	0.271	-29.5907	5.5907
	20 sec	-5.10000	5.44706	0.879	-21.7880	11.5880
	40sec	-16.75000	5.74171	0.066	-34.3407	0.8407

Combined:

ANOVA					
DC					
	Sum of Squares	df	Mean Square	F	Sig.
Between Groups	937.805	4	234.451	4.775	0.003
Within Groups	1816.600	37	49.097		
Total	2754.405	41			

Post Hoc Tests						
Multiple Comparisons						
Dependent Variable:						
Tukey HSD						
(I) CT		Mean Difference (I-J)	Std. Error	Sig.	95% Confidence Interval	
					Lower Bound	Upper Bound
5 sec	10 sec	4.25000	3.50347	0.744	-5.7939	14.2939
	20 sec	9.57500*	3.32369	0.048	0.0465	19.1035
	40sec	1.50000	3.50347	0.993	-8.5439	11.5439
	60 sec	12.50000*	3.50347	0.008	2.4561	22.5439
10 sec	5 sec	-4.25000	3.50347	0.744	-14.2939	5.7939
	20 sec	5.32500	3.32369	0.505	-4.2035	14.8535
	40sec	-2.75000	3.50347	0.933	-12.7939	7.2939
	60 sec	8.25000	3.50347	0.151	-1.7939	18.2939
20 sec	5 sec	-9.57500*	3.32369	0.048	-19.1035	-0.0465
	10 sec	-5.32500	3.32369	0.505	-14.8535	4.2035
	40sec	-8.07500	3.32369	0.130	-17.6035	1.4535
	60 sec	2.92500	3.32369	0.902	-6.6035	12.4535
40sec	5 sec	-1.50000	3.50347	0.993	-11.5439	8.5439
	10 sec	2.75000	3.50347	0.933	-7.2939	12.7939
	20 sec	8.07500	3.32369	0.130	-1.4535	17.6035
	60 sec	11.00000*	3.50347	0.026	0.9561	21.0439
60 sec	5 sec	-12.50000*	3.50347	0.008	-22.5439	-2.4561
	10 sec	-8.25000	3.50347	0.151	-18.2939	1.7939
	20 sec	-2.92500	3.32369	0.902	-12.4535	6.6035
	40sec	-11.00000*	3.50347	0.026	-21.0439	-0.9561
*. The mean difference is significant at the 0.05 level.						